

***In Vitro* Studies Comparing Activities of Antimicrobial  
Photodynamic Therapy and Electrochemically Activated  
Solutions**

**Zeeniya Hassan Kamil**

**A thesis submitted in partial fulfilment of the requirements of the  
University of the West of England, Bristol for the degree of  
Doctor of Philosophy**

**Faculty of Health and Applied Sciences, University of the West of England,  
Bristol**

**December 2014**

## Abstract

There is a need for alternative “treatments” for killing microbes in wound and other body surfaces. Antimicrobial Photodynamic Therapy (APDT) and Electrochemically Activated Solutions (ECAS) are two recent developments in the field of biocide research that in the future may have widespread applications, replacing conventional antibiotics or disinfectants. The aims of the work described in this thesis are 5-fold. (1) Develop an *in vitro* model and determine the kill rates of bioluminescent species using bioluminescence light output (2) Measure the comparative effects of heavy water and reactive oxygen species (ROS) inhibitory agents against appropriate controls for both APDT and ECAS treatment and gain insight into general killing mechanisms (3) Develop methods to compare kill rates of target microbe (prokaryotic cells) against mammalian eukaryotic cells, by comparison of kill rates under the same treatment conditions and thus, assess the likelihood of cytotoxic damage to the host (4) Measure the potential of treatments to induce genotoxic damage to mammalian cells using a COMET assay (5) Measure the effects of treatments when the target is growing in biofilm mode (using a continuous matrix perfusion model) and compare standard treatments for fast and slow growing cells.

A standard assay was developed containing target cell suspensions with killing agent ECAS or APDT (methylene blue (MB) combined with polychromatic light) and bioluminescence was measured using luminometer and viable count methods. For mechanistic study, the assay was repeated in the presence of ROS scavenger molecules. Fluorescence responses by probes singlet oxygen sensor green (SOSG), 3<sup>2</sup>-(*p*-aminophenyl) fluorescein (APF), 3<sup>2</sup>-(*p*-hydroxyphenyl) fluorescein (HPF) were measured using a fluorimeter to detect ROS in the presence or absence of specific ROS inhibitory agents. The potential cytotoxicity of APDT and ECAS against keratinocytes (H103) and lymphocytes (Jurkat cell) was measured using the neutral red test (for keratinocytes) and MTS assay (for lymphocytes). Trevigen’s comet assay kit was used to measure genotoxicity produced by ECAS and APDT towards lymphocytes, DNA damage was determined using epifluorescence microscopy. An *in vitro* flat-bed perfusion biofilm model was used to compare the effects of ECAS and APDT against biofilms, using a low light camera to measure bioluminescence within the biofilm. All data were compared using appropriate statistical analyses.

The light output from the bioluminescent target species was highly proportional to the viable counts with high correlation ( $R^2 > 0.9$ ). Order of killing susceptibility was *S. aureus* > *E. coli* > *P. aeruginosa* > MRSA. Kill rates measured using luminescent light output from lux-modified target species are more accurate than conventional viable count. The rapid assay method, coupled with the use of D<sub>2</sub>O, ROS-scavengers and fluorescent probes provided key insights into mechanisms of APDT and ECAS. It was confirmed that singlet oxygen is the main cytotoxic species for ADPT whilst a mixed system (hydroxyl radical plus singlet oxygen, and possibly other species) was involved for ECAS. APDT and ECAS are not particularly cytotoxic to mammalian cells (keratinocytes or lymphocytes); therefore a large safety margin of dose may exist to reduce the microbial cells without harm to mammalian cells. APDT is more genotoxic to lymphocytes than is ECAS but both are less toxic compared to H<sub>2</sub>O<sub>2</sub> positive control. The *in vitro* flat-bed perfusion biofilm model was suitable to study both APDT and ECAS against biofilm cells. The results showed that biofilm was resistant compared to planktonic cells, and was able to recover easily post treatment. Slower growing cells take longer to recover following APDT.

## **Acknowledgement**

I would like to express my sincere gratitude to Professor John Greenman, my director of studies for his guidance and support throughout my studies. In particular, I would like to express my deepest appreciation for his generous support and encouragement in the final stages of completing my thesis.

My thanks to all my supervisory team: Professor John Greenman, Professor Vyv Salisbury, Dr. Shona Nelson who all helped me complete this thesis.

I am grateful for Dr. Saliha Saad for her support, encouragement and friendship.

I would like to thank Professor Darren Reynolds for his permission to use ECAS in my work.

I am grateful for the assistance given by Dr. Robin Thorn and Dr. Gareth Robinson.

I would like to thank everyone in the microbiology research laboratory for the technical support throughout my studies.

I would like to thank Dave Corry for his kind support with cell culture work.

Lastly I would like to thank my family for their loving support throughout my studies, and especially my dad for always encouraging me to continue with further studies.

## Table of Contents

<b>Chapter 1: Introduction .....</b>	<b>1</b>
1.1 Overview.....	2
1.2 Photodynamic Therapy (PDT).....	3
1.3 Antimicrobial Photodynamic Therapy (APDT).....	4
1.4 Photosensitizers.....	8
1.5 Light Sources.....	13
1.6 Mechanism of Antimicrobial Photodynamic therapy.....	17
1.7 Methods used to study the mechanism of APDT .....	21
1.8 Mechanism of APDT damage to bacteria .....	23
1.9 Photodynamic Inactivation of Microbial Cells.....	24
1.10 Electrochemically Activated Solutions (ECAS) .....	33
1.11 Comparison of APDT and ECAS .....	36
1.12 Rapid bioluminescence method to evaluate activities of APDT and ECAS .....	37
1.13 Aims of the investigation:.....	51
<b>Chapter 2: General Materials and Methods.....</b>	<b>52</b>
2.1 Bioluminescent bacteria and growth conditions .....	53
2.2 Growth and maintenance of micro-organisms.....	53
2.3 Bacterial growth curve.....	54
2.4 Photosensitizer .....	55
2.5 Light source .....	55
2.6 APDT Studies: Development of standard bioluminescent assay to study photodynamic effects.....	56
2.7 ECAS assay: preparation of inoculum .....	57
2.8 Preparation of ECAS .....	57
2.9 ECAS single tube luminometric assay.....	57
2.10 Photodynamic and ECAS mediated effects on bioluminescence output in the presence of reactive oxygen species inhibitors/enhancer.....	58
2.11 The evaluation of the role of ROS and <sup>1</sup> O <sub>2</sub> in APDT by detection of formation by SOSG, APF and HPF Assay .....	59
2.12 Methods to determine the cytotoxic effects of APDT on keratinocytes and lymphocytes .....	60
2.13 Methods for genotoxic effects of APDT and ECAS on T lymphocytes (Comet assay).....	66
2.14 Flat-bed biofilm perfusion model.....	69

<b>Chapter 3: Development of bioluminescent target based assay to study kill kinetics of APDT and ECAS .....</b>	<b>75</b>
3.1 Introduction.....	76
3.2 Aims of the chapter.....	77
3.3 Results.....	77
3.5 Discussion.....	94
<b>Chapter 4: Comparative mechanistic study of APDT and ECAS using bioluminescent rapid assay and ROS specific fluorescent probes.....</b>	<b>101</b>
4.1. Introduction.....	101
4.4 Aims and objectives of this chapter.....	110
4.5 Results.....	111
4.6 Discussion.....	153
<b>Chapter 5: Cytotoxicity of APDT and ECAS on mammalian cells.....</b>	<b>160</b>
5.1 Introduction.....	161
5.2 Aims of this chapter.....	166
5.3 Results.....	167
5.4 Discussion.....	185
<b>Chapter 6: Genotoxicity effects of APDT and ECAS on lymphocytes.....</b>	<b>192</b>
6.1. Introduction.....	193
6.2 Aims of this chapter.....	196
6.3 Results.....	197
6.4 Discussion.....	208
<b>Chapter 7: Application of APDT and ECAS against biofilm .....</b>	<b>212</b>
7.1 Introduction.....	213
7.2 Aims of the investigation.....	218
7.3 Results.....	218
7.4 Discussion.....	229
<b>Chapter 8: General Discussion .....</b>	<b>235</b>
8.1 Discussion.....	236
8.2 Conclusions and further study.....	241

**References ..... 243**

**Appendix ..... 266**

## List of figures

<b>Figure 1-1</b> Applications of APDT .....	7
<b>Figure 1-2</b> Chemical formula of MB .....	10
<b>Figure 1- 3</b> Commonly used phenothiazinium and related PSs.....	11
<b>Figure 1- 4</b> Structure—function relationships for phenothiazinium PSs.....	13
<b>Figure 1-5</b> Schematic illustration of photophysical and photochemical mechanisms of APDT.....	18
<b>Figure 1- 6</b> The Gram-positive (a) and Gram-negative (b) cell envelope.....	26
<b>Figure 1- 7:</b> Ideal first order kill kinetic survival curve with examples of non-ideal behaviour .....	31
<b>Figure 1-8</b> Applications of ECAS .....	33
<b>Figure 1-9</b> (a) Image showing growth of bioluminescent <i>E. coli</i> Nissle pGLITE on the surface of nutrient agar plate (b) bioluminescent <i>E. coli</i> Nissle pGLITE expressing the <i>lux</i> gene coding for the emission of light image captured ICCD photon-counting camera.....	38
<b>Figure 1-10</b> The stages of biofilm formation .....	44
<b>Figure 2-1</b> (a) Schematic of the flat-bed perfusion biofilm model. (b) Photograph of the biofilm growth chamber. (c) Photograph of three flat-bed units running in parallel.....	74
<b>Figure 3-1</b> Growth curves of <i>P. aeruginosa</i> MCS5-lite followed by bioluminescence and viable count. ....	79
<b>Figure 3-2</b> Correlation between bioluminescence of <i>P. aeruginosa</i> MCS5-lite and viable count of bacteria in exponential phase of growth .....	80
<b>Figure 3-3</b> Correlation between bioluminescence and viable counting in bacteria in exponential phase of growth of a suspension of series of log fold dilutions of <i>P. aeruginosa</i> MCS5-lite. ....	81
<b>Figure 3-4</b> Growth curves of <i>E. coli</i> Nissle 1917 pGLITE followed by bioluminescence and viable count.. ....	82
<b>Figure 3-5</b> Correlation between bioluminescence of <i>E. coli</i> Nissle 1917 pGLITE and viable count of bacteria in exponential phase of growth .....	83
<b>Figure 3-6</b> Correlation between bioluminescence and viable counting in bacteria in exponential phase of growth of a suspension of series of log fold dilutions of <i>E. coli</i> Nissle 1917 pGLITE.....	84
<b>Figure 3- 7</b> Kill rates of <i>E. coli</i> Nissle 1917 pGLITE exposed to APDT with different concentrations of MB. ....	87
<b>Figure 3- 8</b> Reduction of bioluminescence and viable count of <i>E. coli</i> Nissle 1917 pGLITE exposed to APDT compared to controls. ....	88

<b>Figure 3- 9</b> Reduction bioluminescence and viable count of <i>P. aeruginosa</i> MCS5-lite exposed to APDT compared to controls.....	89
<b>Figure 3- 10</b> Reduction in viable count of MRSA exposed to APDT compared to controls.....	90
<b>Figure 3- 11</b> Reduction in viable count of <i>S. aureus</i> exposed to APDT compared to controls.....	90
<b>Figure 3- 12</b> Reduction in bioluminescence of <i>E. coli</i> Nissle 1917 pGLITE when exposed to ECAS at different concentrations for 2 minutes.....	92
<b>Figure 3- 13</b> Initial reduction (first 10 seconds) in bioluminescence of <i>E. coli</i> Nissle 1917 pGLITE when exposed to ECAS at different concentrations. ....	92
<b>Figure 4- 1</b> Changes in bioluminescence of <i>P. aeruginosa</i> MCS5-lite treated with APDT compared to APDT in the presence of 10 mM DMTU .....	112
<b>Figure 4- 2</b> Changes in bioluminescence of <i>P. aeruginosa</i> MCS5-lite treated with APDT compared to APDT in the presence of 10 mM mannitol .....	112
<b>Figure 4- 3</b> Changes in bioluminescence of <i>P. aeruginosa</i> MCS5-lite treated with APDT compared to APDT in the presence of D <sub>2</sub> O.....	113
<b>Figure 4- 4</b> Changes in bioluminescence of <i>P. aeruginosa</i> MCS5-lite treated with APDT compared to APDT in the presence of 10 mM tryptophan.....	113
<b>Figure 4- 5</b> Changes in bioluminescence of <i>S. aureus</i> treated with APDT compared to APDT in the presence of tryptophan, mannitol and DMTU .....	115
<b>Figure 4-6</b> Changes in bioluminescence of <i>E. coli</i> Nissle 1917 pGLITE treated with APDT compared to controls.....	118
<b>Figure 4-7</b> Changes in bioluminescence of <i>E. coli</i> Nissle 1917 pGLITE treated with APDT compared to in the presence of 0.1 mM or 10 mM tryptophan .....	118
<b>Figure 4-8</b> Changes in bioluminescence of <i>E. coli</i> Nissle 1917 pGLITE treated with APDT compared to assay in the presence of 10 mM mannitol.....	119
<b>Figure 4-9</b> Changes in bioluminescence of <i>E. coli</i> Nissle 1917 pGLITE treated with APDT compared to in the presence of 10 mM DMTU .....	119
<b>Figure 4-10</b> Changes in bioluminescence of <i>E. coli</i> Nissle 1917 pGLITE treated with APDT compared to assay in the presence of D <sub>2</sub> O.....	120
<b>Figure 4-11</b> Changes in bioluminescence of <i>E. coli</i> Nissle 1917 pGLITE treated with ECAS at 50, 25, 10, 5 and 1% (v/v of neat).....	123
<b>Figure 4-12</b> Changes in bioluminescence of <i>E. coli</i> Nissle 1917 pGLITE treated with ECAS: effects of tryptophan (10 mM).....	123
<b>Figure 4-13</b> Changes in bioluminescence of <i>E. coli</i> Nissle 1917 pGLITE treated with ECAS: effects of sodium azide (100 mM).....	124
<b>Figure 4-14</b> Changes in bioluminescence of <i>E. coli</i> Nissle 1917 pGLITE treated with ECAS: effects of D <sub>2</sub> O .....	124

<b>Figure 4-15</b> Changes in bioluminescence of <i>E. coli</i> Nissle 1917 pGLITE treated with ECAS: effects of mannitol (100 mM) .....	125
<b>Figure 4-16</b> Changes in bioluminescence of <i>E. coli</i> Nissle 1917 pGLITE treated with ECAS: effects of DMSO (128mM) .....	125
<b>Figure 4-17</b> Effects of APDT on fluorescence response by SOSG probe at 5 $\mu$ M	128
<b>Figure 4-18</b> Effects of APDT on fluorescence response by SOSG probe at 5 $\mu$ M in D <sub>2</sub> O .....	129
<b>Figure 4-19</b> Effects of APDT on fluorescence response by SOSG probe at 5 $\mu$ M in the presence of tryptophan (10 mM).....	130
<b>Figure 4-20</b> Effects of APDT on fluorescence response by SOSG probe at 5 $\mu$ M in the presence of mannitol (10 mM).....	131
<b>Figure 4-21</b> Fluorescence response by 5 $\mu$ M SOSG probe with ECAS at 1 % and 5% (v/v of neat .....	132
<b>Figure 4-22</b> Fluorescence response by 5 $\mu$ M APF to control conditions .....	135
<b>Figure 4-23</b> Effects of APDT on fluorescence response by 5 $\mu$ M APF.....	136
<b>Figure 4-24</b> Effects of APDT on fluorescence response by 5 $\mu$ M APF in the presence of D <sub>2</sub> O .....	137
<b>Figure 4-25</b> Effects of APDT on fluorescence response by 5 $\mu$ M APF in the presence Histidine (10 mM) .....	138
<b>Figure 4-26</b> Effects of APDT on fluorescence response by 5 $\mu$ M APF in the presence tryptophan (1 mM and 10 mM).....	139
<b>Figure 4-27</b> Effects of APDT on fluorescence response by 5 $\mu$ M APF in the presence sodium azide (10 mM and 100 mM).....	140
<b>Figure 4-28</b> Effects of APDT on fluorescence response by 5 $\mu$ M APF in the presence of mannitol (10 mM and 100 mM).....	141
<b>Figure 4-29</b> Fluorescence by APF probe with ECAS and in the presnce of ROS scavengers (tryptophan, Azide, DMSO and Mannitol) or enhancer (D <sub>2</sub> O) incubated for 5 minutes .....	143
<b>Figure 4-30</b> Effects of APDT on fluorescence emission by HPF probe at 5 $\mu$ M...	147
<b>Figure 4-31</b> Effects of APDT on fluorescence emission by HPF probe at 10 $\mu$ M	148
<b>Figure 4-32</b> Effects of APDT on fluorescence emission by HPF probe at 5 $\mu$ M compared to APDT in the presence of tryptophan (10 mM).....	149
<b>Figure 4-33</b> Effects of APDT on fluorescence emission by HPF probe at 5 $\mu$ M compared to APDT in the presence of mannitol (10mM) .....	150
<b>Figure 4-34</b> Fluorescence by HPF (5 $\mu$ M) probe with ECAS at 0.2, 0.5 and 1 % (v/v of neat).....	152
<b>Figure 5-1</b> Viability of keratinocytes after immedaite exposure to APDT compared to viability following 24h recovery period after exposure to APDT .....	169

<b>Figure 5-2</b> Viability of keratinocytes exposed to APDT in the presence of different concentrations of FBS.....	170
<b>Figure 5-3</b> Viability of co-mixture of mammalian and bacterial cells exposed to APDT.....	172
<b>Figure 5-4</b> Viability of keratinocytes after immediate exposure to ECAS compared to viability following 24h recovery period after exposure to ECAS.....	174
<b>Figure 5-5</b> Viability of keratinocytes exposed to ECAS at 5, 10, 25 and 50 % v/v in the presence of 0, 1, 5 and 10% (v/v) FBS. ....	175
<b>Figure 5-6</b> Viability of lymphocytes after immediate exposure to APDT compared to viability following 24h recovery period after exposure to APDT .....	177
<b>Figure 5-7</b> Viability of lymphocytes after immediate exposure to ECAS compared to viability following 24h recovery period after exposure to ECAS.....	178
<b>Figure 6-1</b> Comet image of lymphocytes not exposed to treatment (negative control). ....	199
<b>Figure 6-2</b> Comet image of lymphocytes treated with 100 $\mu$ M of hydrogen peroxide (positive control). ....	199
<b>Figure 6-3</b> Comet image of lymphocytes exposed to light only and no incubation after treatment. ....	200
<b>Figure 6-4</b> Comet image of lymphocytes exposed to MB in the dark and no incubation after treatment. ....	200
<b>Figure 6-5</b> Comet image of lymphocytes incubated for 6 hours after exposure to MB in the dark.....	201
<b>Figure 6-6</b> Comet image of lymphocytes incubated for 24 hours after exposure to exposed to MB in dark .....	201
<b>Figure 6-7</b> Comet image of lymphocytes treated with APDT without incubation after treatment .....	202
<b>Figure 6-8</b> Comet image of lymphocytes incubated for 6 hours after APDT .....	202
<b>Figure 6-9</b> Comet image of lymphocytes incubated for 24 hours after APDT.....	203
<b>Figure 6-10</b> Comet image of lymphocytes treated with 5% ECAS for 30 minutes without incubation after treatment.....	204
<b>Figure 6-11</b> Comet image of lymphocytes incubated for 6 hours after treatment with 5% ECAS for 30 minutes .....	204
<b>Figure 6-12</b> Comet image of lymphocytes incubated for 24 hours after treatment with 5% ECAS for 30 minutes .....	205
<b>Figure 6-13</b> Box-Whiskers plot of data collected for each comet assay for lymphocytes treated with APDT.....	206
<b>Figure 6-14</b> Box-Whiskers plot of data collected for each comet assay for lymphocytes treated with 5% v/v ECAS for 30 minutes.. ....	207

<b>Figure 7-1</b> Development from inoculation /colonization to steady state growth of <i>E. coli</i> Nissle 1917 pGLITE biofilm within an in vitro flat-bed perfusion biofilm model.....	219
<b>Figure 7-2</b> Development quasi-steady state of <i>E. coli</i> Nissle 1917 pGLITE biofilm .....	220
<b>Figure 7-3</b> Development of <i>E. coli</i> Nissle 1917 pGLITE biofilms perfused with growth media at fast (50 ml/h), intermediate (15 ml/h) and slow (1 ml/h) flow rates, followed by bioluminescence output by the biofilm matrix.....	222
<b>Figure 7-4</b> <i>E. coli</i> Nissle 1917 pGLITE biofilm after 1ml PBS as a control treatment .....	223
<b>Figure 7-5</b> Change in photon count by bioluminescent <i>E. coli</i> Nissle (low growth rate) following ECAS treatments .....	224
<b>Figure 7-6</b> Change in photon count by bioluminescent <i>E. coli</i> Nissle (intermediate growth rate) following ECAS treatments .....	224
<b>Figure 7-7</b> Change in photon count by bioluminescent <i>E. coli</i> Nissle (fast growth rate) following ECAS treatments.....	225
<b>Figure 7-8</b> Change in photon count by bioluminescent <i>E. coli</i> Nissle1917 pGLITE biofilm (low growth rate) following APDT treatments .....	226
<b>Figure 7-9</b> Change in photon count by bioluminescent <i>E. coli</i> Nissle1917 pGLITE biofilm (intermediate growth rate) following APDT treatments .....	227
<b>Figure 7-10</b> Change in photon count by bioluminescent <i>E. coli</i> Nissle 1917 pGLITE biofilm (fast growth rate) following APDT treatments .....	227
<b>Figure 7-11</b> of <i>E. coli</i> Nissle 1917 biofilm as a function of recovery time in hours following APDT treatment for each biofilm compared to control .....	228

## List of tables

<b>Table 1-1</b> Use of photosensitizers and light to inactivate micro-organisms.....	28
<b>Table 1-2</b> APDT for biofilms .....	47
<b>Table 3-1</b> Rate of change in bioluminescence or viable count of target organisms when exposed to APDT.....	91
<b>Table 3-2</b> Rate of change in bioluminescence of <i>E. coli</i> Nissle 1917 pGLITE when exposed to ECAS at different concentrations.....	93
<b>Table 4-1</b> Indirect method of detecting ROS using specific scavengers.....	106
<b>Table 4-2</b> Showing the APDT kill rate over 20-30 minutes assay of <i>P. aeruginosa</i> MCS5-lite in the presence or absence of singlet oxygen scavengers or hydroxyl radical scavengers.....	114
<b>Table 4-3</b> Showing the APDT kill rate of <i>P. aeruginosa</i> MCS5-lite in the presence or absence of singlet oxygen scavengers or hydroxyl radical scavengers (Kill rate calculations based on the first (8min).....	114
<b>Table 4-4</b> Showing the APDT kill rate of <i>S. aureus</i> in the presence or absence of singlet oxygen scavengers or hydroxyl radical scavengers.....	116
<b>Table 4-5</b> Showing the APDT kill rate of <i>E. coli</i> Nissle 1917 pGLITE in the presence or absence of singlet oxygen scavengers and/or hydroxyl radical scavengers (summary of rate data from figures 4.6 to 4.10).....	121
<b>Table 4-6</b> Showing the APDT kill rate of <i>E. coli</i> Nissle 1917 pGLITE in the presence or absence of singlet oxygen scavengers and/or hydroxyl radical scavengers (summary of rate data from figures 4.6 to 4.10) Kill rate calculations based on the first (8min) of data points .....	121
<b>Table 4-7</b> The effects free radicals and singlet oxygen scavengers on the kill rate of bioluminescent <i>E. coli</i> Nissle 1917 by ECAS (calculations based on the total assay times 2 minutes).....	126
<b>Table 4-8</b> The effects free radicals and singlet oxygen scavengers on the kill rate of bioluminescent <i>E. coli</i> Nissle 1917 by ECAS (calculations based on the first 1 minute- Initial kill rate).....	126
<b>Table 4-9</b> Summary of rate change in fluorescence following APDT in the presence or absence of ROS inhibitors or enhancers ( $D_2O$ ) using APF (5 $\mu M$ ) ...	142
<b>Table 4-10</b> Summarises the data obtained from testing APF fluorescence against ECAS.....	144
<b>Table 4-11</b> Summary of rate change in fluorescence following APDT in the presence or absence of ROS inhibitors using HPF probe.....	151

<b>Table 5-1</b> Significance level comparison of keratinocytes exposed to APDT or control conditions in the presence or absence of FBS.....	171
<b>Table 5-2</b> Kill rates of mammalian cells compared to bacterial cells after APDT	173
<b>Table 5-3</b> Kill rates of mammalian cells compared to bacterial cells after ECAS treatment .....	173
<b>Table 5-4</b> Significance level comparison of keratinocytes exposed to ECAS and/ or control conditions in the presence and absence of FBS .....	176
<b>Table 5-5</b> Reduction in percentage viability of keratinocytes after exposure to APDT and ECAS .....	180
<b>Table 5-6</b> Reduction in percentage viability of lymphocytes after exposure to APDT and ECAS.....	181
<b>Table 5-7</b> Influence of FBS on the viability of keratinocytes after exposure to APDT .....	182
<b>Table 5-8</b> Influence of FBS on the viability of keratinocytes after exposure to ECAS treatment .....	183
<b>Table 5-9</b> Comparison keratinocytes and lymphocytes cytotoxicity levels of APDT and ECAS .....	184

## List of abbreviations

ALA 5-aminolevulinate

APDT Antimicrobial photodynamic therapy

APF 3-*p*-(aminophenyl) fluorescein

ATP – Adenosine triphosphate

CFU colony forming units

CLSM – confocal laser scanning microscopy

D<sub>2</sub>O Deuterium oxide

DABCO 1,4-diazabicyclo- 2,2,2-octane

DMTU N,N'-dimethylthiourea

DNA deoxyribonucleic acid

ECAS Electrochemically activated solution

EPS – extracellular polymeric substances

FBS Foetal bovine serum

HPF hydroxyphenyl fluorescein

ICCD Intensified charge coupled device

LED light emitting diode

LPS lipopolysaccharide

M molar

MAL methyl aminolevulinate

MB methylene blue

MIC – minimum inhibitory concentration

MRSA methicillin resistant *Staphylococcus aureus*

NB nutrient broth

OD optical density

ORP – Oxidation-reduction potential

PDT photodynamic therapy

Photosensitizer PS

PI photodynamic inactivation

RLU Relative light units

ROS Reactive oxygen species

SEM – Scanning electron microscopy

SOSG Singlet oxygen sensor green

TBO Toluidine blue O

EMRSA Epidemic methicillin-resistant *Staphylococcus aureus*

TYE Tryptone yeast extract

v/v Volume/volume

W Watt

## **Chapter 1: Introduction**

## 1.1 Overview

Antimicrobial resistance across a wide range of micro-organisms, most of which can cause a wide spectrum of diseases is now considered to be a growing public health threat (Spellberg *et al.*, 2008). This has led major research efforts to develop alternative antimicrobial therapeutics (Dai *et al.*, 2009). Infections caused by antibiotic resistant bacteria lead to increased morbidity and mortality causing a considerable burden on the healthcare systems (de Kraker *et al.*, 2011). Therefore, it is essential to develop and apply novel antimicrobial strategies to which pathogens will not easily develop resistance. Antimicrobial Photodynamic Therapy (APDT) (Hamblin and Hassan, 2004) and Electrochemically Activated Solutions (ECAS) are now considered to be possible alternative biocide/disinfectant therapies (Thorn *et al.*, 2012). APDT is the application of a non-toxic compound, termed a photosensitizer (PS), which can be activated by light of appropriate wavelength to produce reactive oxygen species (ROS) (i.e. singlet oxygen and free radicals), which can then exert antimicrobial effects (Hamblin *et al.*, 2002, Embleton *et al.*, 2005). ECAS is a highly oxidative (OPR 1,170 to 1,180 mV) and fast acting biocidal solution, generated from electrolysis of a dilute salt solution (Robinson *et al.*, 2010). Both agents have a broad-spectrum of activity against a wide range of microbial species. The ROS generated by these agents react with multiple components within the bacterial cell structure, leading to cell death (Thorn *et al.*, 2012; Hamblin and Hassan, 2004). The general mechanisms of these two agents involve multiple target sites, in contrast to antibiotics, which generally involve a single target site. Therefore bacteria are less likely to develop resistance against these agents. In order to study the efficacy and understand the mechanisms of both APDT and ECAS activities, rapid methods of data acquisition are required to monitor survivors at any time point and allow calculation of death rate (K) as the basic “unit” of comparison between different conditions, including different species, different biocide or different physicochemical factors.

## 1.2 Photodynamic Therapy (PDT)

Photodynamic therapy (PDT) utilizes the combination of non-toxic dyes known as photosensitizers and harmless visible light of the correct wavelength to excite the PS. In the presence of oxygen, the excited PS transfers energy or electrons to the ground state molecular oxygen producing reactive oxygen species (ROS) such as singlet oxygen and hydroxyl radical that are able to kill both mammalian and microbial cells (Ochsner, 1997). PDT targets cells (whether microbial or mammalian) based on the phenomenon that PS accumulate preferentially in the target species or, for mammalian systems, hyperproliferative cell populations (Hamblin and Newman, 1994). The term PDT is generally used when treatment is targeted at cancers.

Photodynamic anti-tumour therapy (PDT) is based on the fact that photosensitive substance administered systematically are preferentially incorporated into rapidly proliferating tumorous tissue, and after its irradiation the cell structures are damaged due to the development of reactive cytotoxic products and subsequent apoptosis of tumorous cells. The first successful application of PDT was in skin tumour therapy by local application of eosin, which accumulates quickly in the proliferating neoplastic cells (Ryskova *et al.*, 2010). Currently PDT is used for the treatment of superficial malignancies and localised cancer of the skin (Zhao and He, 2010). Various PS have been approved for clinical use, including porfimer sodium (photofrin) (chemical structure shown in appendix 1) for treatment of lung cancer in USA, Japan and Europe (Brown *et al.*, 2004).

PDT initially has been mainly studied and developed as a cancer treatment, but now numerous investigations demonstrates possible applications in diverse conditions such as dermatological areas such as psoriasis (Boehnche *et al.*, 2000) and acne vulgaris (Hongcharu *et al.*, 2000), rheumatoid arthritis (Hansch *et al.*, 2008), atherosclerosis (Peng *et al.*, 2011) and re-stenosis (Mansfield *et al.*, 2001). One of the most successful applications of PDT developed so far is for an (ophthalmological) treatment of age related macular degeneration, now a Foods and Drugs Authority (USA) approved treatment (Bressler and Bressler, 2000).

### 1.3 Antimicrobial Photodynamic Therapy (APDT)

Similar to PDT, APDT utilizes PS activated by visible light to produce cytotoxic reactive oxygen species (ROS) that damage microbial cells via oxidative damage. When the cells to be killed are pathogenic micro-organisms the procedure is termed APDT. In the literature different terms are used to describe APDT. APDT is also known as photodynamic inactivation (PDI), lethal photosensitization (LPS), photo activated disinfection (PAD) or photodynamic antimicrobial chemotherapy (PACT).

The first demonstration of lethal photosensitization of microbial cells was recorded over a century ago by Raab (1900) who showed that low concentrations of methylene blue (MB), which does not have any toxicity in the absence of light towards *Paramecium caudatum*, could lead to cessation of motility (that is presumption of the killing of the organism) by exposure to ordinary daylight (Ryskova *et al.*, 2010). Furthermore, Raab showed that acridine and light were also toxic to *Paramecium* (Daniel and Hill, 1991). The term photodynamic therapy was coined by Von Tappeiner in 1904 to describe the involvement of light and oxygen in the photodynamic reactions (Tappeiner and Jodlbauer, 1904).

Since the discovery of APDT, applications in this area largely came to an end because of the discovery of antibiotics raising the belief that infectious diseases would be eradicated (Coates and Hu, 2007). However, because of the overuse of antibiotics combined with the ability of micro-organisms to evolve and overcome the antimicrobial properties of antibiotics, these drugs are becoming increasingly ineffective in treating microbial infections (Levy, 2002).

In a recent report published by the World Health Organisation (WHO) the seriousness of the antibiotic resistance problem was stated; “A post-antibiotic era—in which common infections and minor injuries can kill—far from being an apocalyptic fantasy, is instead a very real possibility for the 21st century”, based on a recent survey (Antimicrobial resistance: global report on surveillance, WHO, 2014). WHO report that antimicrobial resistance now pose serious threat to

effective prevention and treatment of infections caused by bacteria, fungi, parasites and viruses. This is the first time a comprehensive survey has been carried out to find the current status of antimicrobial resistance worldwide based on surveillance data submitted by 114 countries. The findings of the report showed that for *E. coli*, *K. pneumoniae* and *S. aureus* the proportion resistant to commonly used specified antibacterial drugs exceeded 50% in many settings. The report highlighted the increase of *K. pneumoniae* resistance to carbapenems, usually the last line of available treatment, from all regions. In addition, high rates of methicillin-resistant *Staphylococcus aureus* (MRSA) mean that treatments of these infections must rely upon second line drugs in many countries. Second-line drugs for *S. aureus* may have severe side-effects and are more expensive; further increasing the burden on the healthcare systems especially in under-developed countries where resources are limited.

Regarding the real threat of antibiotic resistant micro-organisms to the public health in general, it is more urgent than ever to develop alternative therapies. In this case both APDT and ECAS can target skin and wound infections (localised infections) by *S. aureus* or MRSA. In recent years research in APDT has been stimulated, due to the emergence of antibiotic resistant strains, such as MRSA and vancomycin-resistant *Enterococcus faecalis* (Jori and Brown, 2004).

The use of APDT against infectious disease is now recognised as a highly important emerging area of research (Jori and Brown, 2004; Hamblin and Hassan, 2004). The most accepted use of APDT is in the sterilization of blood products from potential microbial agents and it is approved for this purpose in Germany (Mohr *et al.*, 1997; Wainwright, 2000). APDT has been recognised as a new form of treatment for infectious agents (Hassan and Hamblin, 2004) and its development has been compared to that of the discovery of antibiotics (McCaughan, 1999).

There are several advantages of using APDT to treat microbial diseases. The main favourable features of APDT can be summarized as follows:

- Broad spectrum of action, since one photosensitizer can act on bacteria, fungi, yeasts and parasitic protozoa.
- Efficacy is independent of the antibiotic resistance pattern of the given microbial strain.
- Lack of selection of photoresistant strains after multiple treatments.
- Use of low cost light sources for activation of photosensitizing agent.

Because of these favourable features, APDT has the potential to be the treatment of choice especially for localised infection and oral cavity conditions (Dai *et al.*, 2009).

Figure 1.1 shows the general applications of APDT in localised infections. Recent research findings strongly supports the hypothesis that APDT can represent a viable alternative to antibiotics since the mechanism of action of APDT against microbial cells are different from the typical action of most antibiotics (Wainwright, 1998). Conventional antibiotics kill bacteria through single site/mode of action and may be specific to single species or groups given sufficient exposure to the drug: therefore most microbes are able to evolve resistance to a single specific point of attack. Unlike conventional antibiotics, biocides, disinfectants and APDT act on a broad spectrum of targets and species (Wainwright, 1998).

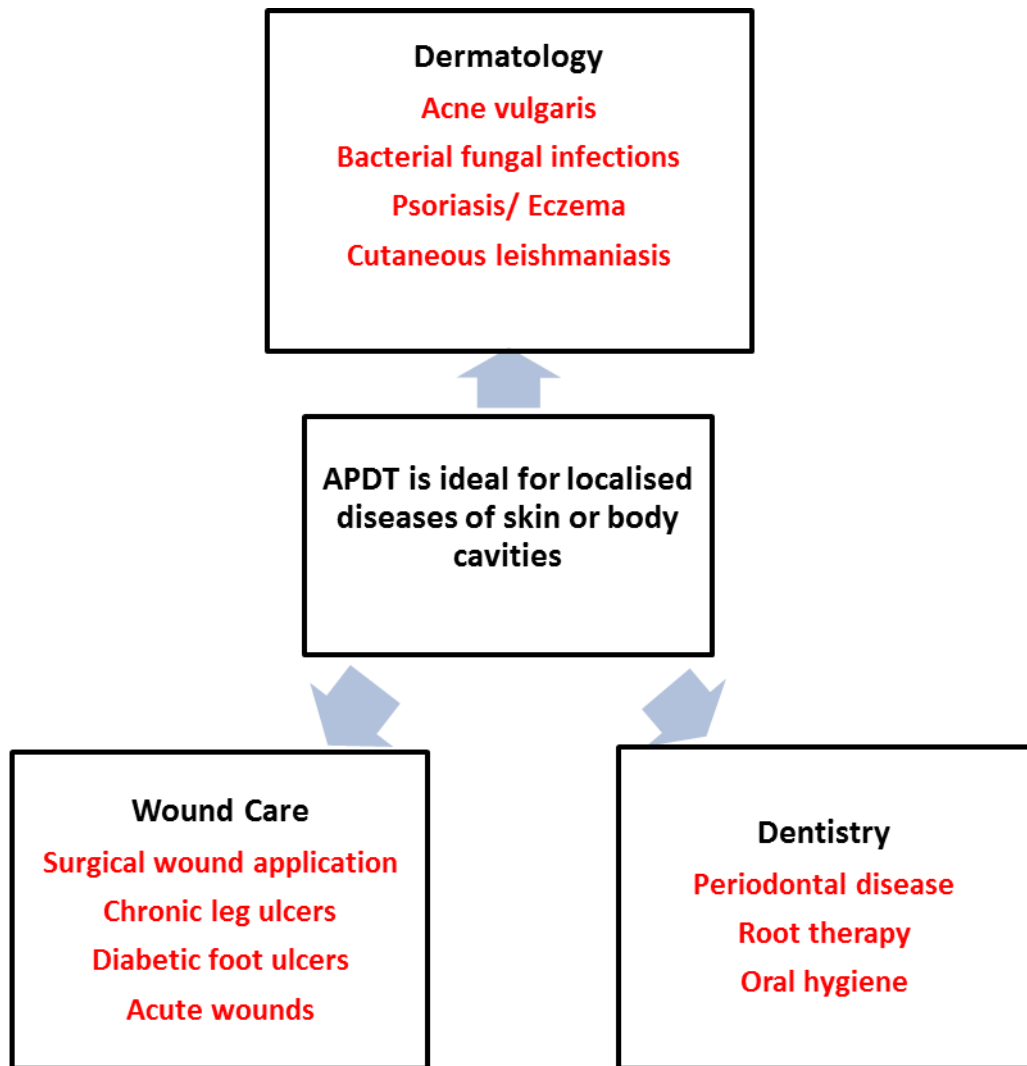


**Figure 1-1 Applications of APDT**

The technology of APDT may be developed to eradicate pathogens under mild irradiation conditions, such as short interaction times or low fluence rates, with limited damages to host tissue (Jori *et al.*, 2006). However there are some limitations of APDT including the need for external energy from a specific radiation source to activate the PS. APDT requires sufficient oxygenation of the target in addition to sufficient concentration of photosensitizer drug. Target cells must be accessible for the activating radiation energy. Penetration depth of the activating radiation is a limiting factor. Thus surfaces can easily be treated but deeper layers need longer wavelengths or special delivery systems. The activating wavelength must be sufficiently different from the absorption characteristics of

surrounding tissue to avoid energy loss and possible side effects from high intensity irradiation and APDT may have detrimental effects on mammalian cells (cytotoxic or genotoxic).

#### **1.4 Photosensitizers (PS)**

PS are usually aromatic molecules, which are efficient in the formation of long-lived triplet excited states. The most frequently used PSs in APDT studies to kill micro-organisms are activated by light within the visible part of the spectrum (400-700 nm). Photosensitizing agents should have specific features. The ideal properties are:

1. Chemically pure, water soluble, stable in solutions at physiological pH for ease of application and rapidly cleared from the body (Sharman *et al.*, 1999).
2. Minimal skin sensitivity (Sharman *et al.*, 2000).
3. High yield for generation of long-lived triplet state and the cytotoxic singlet oxygen species are both important features, which influence the efficiency of PS (Castano *et al.*, 2004). High absorption of light at longer wavelengths (600-950 nm) is important; they should ideally absorb light in the red wavelength (630 nm), which has greater tissue penetration than shorter wavelengths. Therefore PS that absorbs in the region of 600-800nm are preferred (Castano *et al.*, 2004).
4. Selective uptake by the target pathogens (Lyon *et al.*, 2011; Wainwright *et al.*, 2007).
5. Possession of a broad spectrum of action against bacteria, fungi, yeasts, viruses, and parasitic protozoa especially those resistant to conventional antibiotics (Wainwright *et al.*, 2007).
6. Non-specific in terms of biomolecular targeting (Wainwright *et al.*, 2007).
7. Efficacy, independent of the antibiotic-susceptibility of the target organism.
8. Ability to cause extensive reduction in pathogens with low dark toxicity (PS toxicity in the absence of light) to human cells and absence of production of toxic by-products. Low mutagenic potential in mammalian cells (Lyon *et al.*, 2011).
9. Photostable during application (Wainwright *et al.*, 2007).

Currently available PSs do not meet all of the above-mentioned properties; however with chemical modifications many give active derivatives with properties closer to the ideal. There are several groups of PSs that are in current use in PDT cancer and, with some modifications can be applied to treat infectious diseases. The photosensitizer classes employed to date in APDT include phenothiaziniums, acridines, porphyrins, phthalocyanines, cyanines chlorins, psoralens and fullerenes. Increasing numbers of studies are now carried out to assess effectiveness of these PSs and to increase specificity to micro-organism over mammalian cells. Phenothiazinium PSs are close to ideal for APDT since they possess many of the ideal properties required of a PS (Wainwright *et al.*, 2007). The PS employed in this current research is the phenothiazinium PS MB and is discussed in section 1.4.3.

### **1.4.3 Phenothiaziniums**

Phenothiaziniums are a class of positively charged, aromatic photosensitizing molecules. Phenothiaziniums have a core structure consisting of a planar tricyclic heteroaromatic ring, with an absorption wavelength range of 600-660 nm (Phoenix and Harris, 2003). These ranges of light absorption properties of the phenothiazinium dyes are excellent for the local therapy of microbial disease. The intense long wavelength absorption in this region 600-660 nm lies outside the light absorption by endogenous pigments such as haem that might otherwise interfere with the photosensitization process. Several compounds in this group have been shown to possess antibacterial properties (Wainwright *et al.*, 2007).

The lead compound of phenothiaziniums is MB. With the increase in research in PDT there was a great need for the development of novel analogues. A large variety of phenothiazines have been synthesized, of which MB, toluidine blue O (TBO), azure A-C and thionin are the most commonly used (Wainwright *et al.*, 2007). These novel photosensitizers are now routinely tested against different micro-organisms.

MB structure is shown in Figure 1.2. Among the most widely used phenothiazinium dyes are MB and TBO. They are efficient producers of singlet

oxygen (Wainwright *et al.*, 2007) and the maximum absorption wavelength in water is 656nm for MB and 625nm for TBO, respectively (Wainwright *et al.*, 2007)

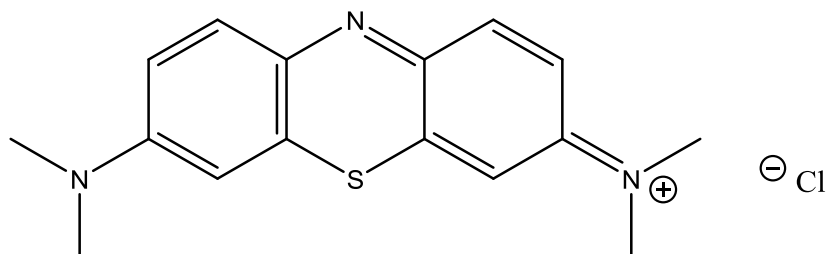


**Figure 1-2: Chemical formula of MB**

One of the most important features for a drug is its selectivity towards the target organism and cytotoxicity and genotoxicity towards mammalian cells. Research has shown no detectable cytotoxic or genotoxic effects of MB on keratinocytes. (Zeina *et al.*, 2002; Zeina *et al.*, 2003).

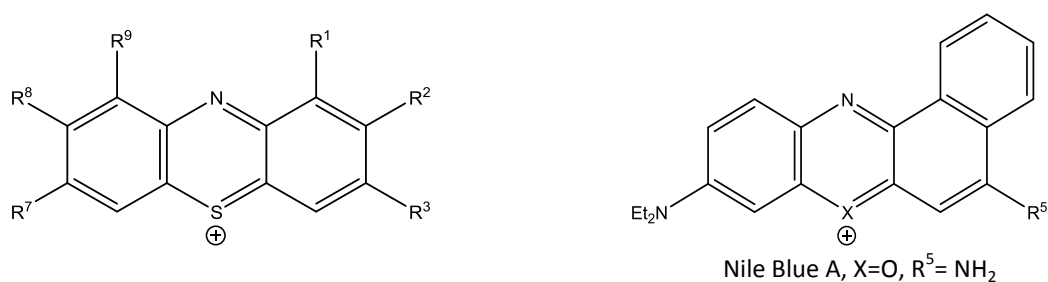
MB was initially synthesised in 1876 for use in the textile industry, and was first employed in medicine in 1891 as a successful treatment for malaria (Wainwright, 2005). MB has been used in histology for over a century. MB was reported for its photodynamic action against bacteriophages as early as 1930 (Wainwright, 1998). The oxidized phenothiaziniums may be reduced by biological systems. MB is utilized as an indicator of bacterial activity in the testing of milk, microbial reduction of the MB causing decolorization (Wainwright, 1998). MB is used in surgical identification of organs or tissue structures at a concentration of 1% w/v without causing human toxicity (Creagh *et al.*, 1995).

Cationic PSs are more selective for bacterial cells compared with mammalian cells as cationic molecules are taken up comparatively slowly by mammalian cells, and thus damage to host cells may be limited by carrying out APDT within a short time of applying the photosensitizer (Demidova and Hamblin, 2004; Dai *et al.*, 2009).

MB combination with light has been shown to cause damage to membrane lipids, essential proteins, DNA and other cellular components, usually leading to

bacterial cell death (Phoenix and Harris, 2003). At increasing concentrations, MB may aggregate and form dimers, which may cause a shift in the absorption maximum of the photosensitizer. It has been proposed that dimerization is further induced at the bacterial cell surface due to electrostatic interactions between MB and negatively charged polymers on the bacterial cell surface, and that these dimers are also involved in cell photo damage, as well as monomeric species (Usacheva *et al.*, 2003).

Figure 1.3 shows commonly used phenothiazinium and related PSs. MB and TBO are the most extensively studied phenothiazinium based PSs for their antibacterial activity. The minimal toxicity of these dyes to human cells, plus their ability to produce high quantum yields of singlet oxygen, has evolved a great interest in testing the potential of these PSs as photoactivated antimicrobial agents.



	R <sup>1</sup>	R <sup>2</sup>	R <sup>3</sup>	R <sup>7</sup>	R <sup>8</sup>	R <sup>9</sup>
MB	H	H	NMe <sub>2</sub>	NMe <sub>2</sub>	H	H
Azure A	H	H	NMe <sub>2</sub>	NH <sub>2</sub>	H	H
Azure B	H	H	NMe <sub>2</sub>	NHMe	H	H
Azure C	H	H	NHMe	NH <sub>2</sub>	H	H
Thionin	H	H	NH <sub>2</sub>	NH <sub>2</sub>	H	H
1-MMB	Me	H	NMe <sub>2</sub>	NMe <sub>2</sub>	H	H
1,9 DMMB	Me	H	NMe <sub>2</sub>	NMe <sub>2</sub>	H	Me
NMB	H	Me	NHEt	NHEt	Me	H

**Figure 1- 3: Commonly used phenothiazinium and related PSs (source: Wainwright, 2005).**

At physiological pH, these molecules are generally cationic. Most of these molecules are also lipophilic ( $\log P > 0$ ) which support partitioning into the membrane environment, and have amphiphilic properties (i.e. chemical compound possessing both hydrophilic and lipophilic properties). These properties are important for interaction with the membrane and enable the molecules to become internalized into the cell (Phoenix & Harris, 2003).

Numerous studies carried out so far have shown antimicrobial activities of these commercially available phenothiaziniums is high against both Gram-positive and Gram-negative bacteria (Wainwright *et al.*, 2007) including MRSA (Wainwright *et al.*, 1998) and vancomycin-resistant *Enterococcus* spp. (Wainwright *et al.*, 1998) thus indicating clinical potential in localised infections. The phenothiazinium PS TBO has been shown to eliminate of periodontopathogenic bacteria confirming its application in oral cavity infections (Kömerik *et al.*, 2003). Phenothiazinium dyes are the only PS that has been applied in the clinical settings: in the photo-decontamination of blood plasma (Mohr *et al.*, 1997; Wainwright, 2000).

Currently there are only a relatively small number of analogues, which have been prepared to allow proper structure—function and activity properties. Figure 1.4 shows the relationship between structure function and improved activity of PS. It is important to study these PSs in terms of function and structure activity to improve their efficacy as PSs while limiting their phototoxicity to healthy cells. This is a major part of on-going research, which will allow increased photosensitizer screening both in the antimicrobial and oncological fields. As with conventional drug discovery, the use of the substitutions/alterations will lead to development of optimized PSs (Wainwright, 2005).

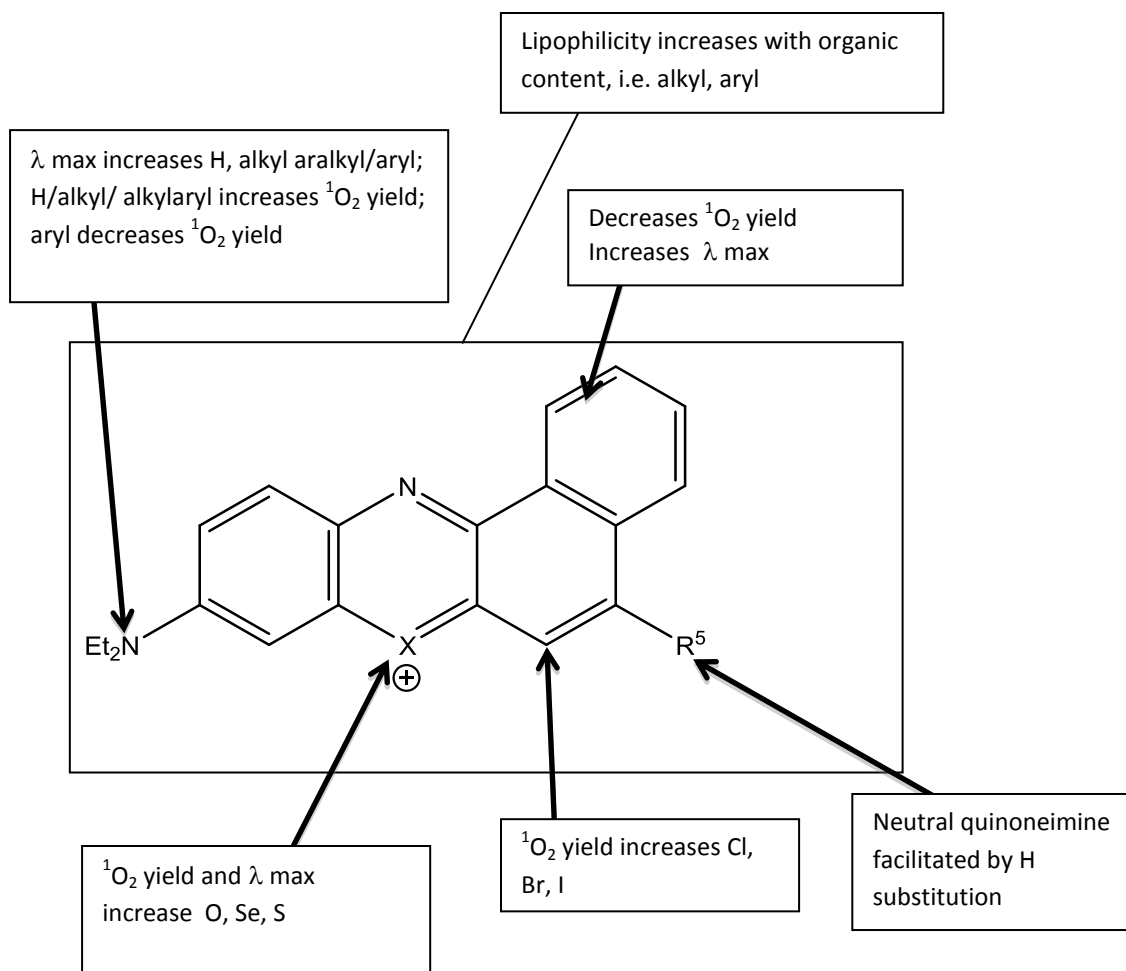


**Figure 1- 4: Structure—function relationships for phenothiazinium PSs (source: Wainwright, 2005).**

### 1.5 Light Sources

The use of light and light-sensitive compounds to treat diseases goes back thousands of years since the healing properties of sunlight were known (Daniell and Hill, 1991). In Egypt, India and China therapeutic effect of the sunlight was used to treat diverse diseases including vitiligo, rickets and psoriasis (Ackroyd *et al.*, 2001).

The application of light for the treatment of diseases is known as heliotherapy or phototherapy. The ancient Greeks used sunlight as treatment of disease in the second century BC (Moan and Peng, 2003). At the end of the 19<sup>th</sup> century the Danish physician, Neils Finsen (Nobel prize, 1903) used red light to treat

smallpox and ultraviolet light to treat cutaneous tuberculosis (Moan and Peng, 2003). Another well-known application of phototherapy is the treatment of hyperbilirubinemia (jaundice) in new born babies using blue light. The light converts the overproduced bilirubin to isomers that can be more readily excreted by the liver (Moan and Peng, 2003).

In PDT, the photosensitizer will only be activated by the correct wavelength and once the photosensitizer gets activated the photosensitization reaction is initiated in the presence of oxygen. The PSs used in PDT are activated by visible light. Visible light has a wavelength range of 400-760nm. Therefore the choice of light to use in PDT is dependent on the photosensitizer used and the depth of the targeted tissue into which light should penetrate. The depth of light penetration increases in the visible and near- Infrared (NIR) spectral regions. For clinical applications of PDT it is very important for sufficient light to reach the target area in order to activate enough photosensitizer molecules. The penetration of light is limited due to both absorption and scattering that occur in tissue structures (Dougherty and Marcus, 1992). In human tissue, water and oxygenated haemoglobin are two important absorbers. Below 600nm the absorption coefficient for haemoglobin increases strongly while above 1100 nm the absorption for water becomes quite large. Therefore for these reasons wavelength regions that can be used for the clinical application in PDT roughly lies between 600 and 1100 nm. This is called the phototherapeutic window, which is a trade-off between sufficient energy (i.e. lower wavelengths) and sufficient penetration depths (i.e. longer wavelengths). Moreover the beam of longer wavelength is less scattered than that of a shorter one (Niemz, 2007).

There are different types of light sources that have been used to photo-activate the photosensitizing agents in use. For APDT, coherent and non-coherent light and ultraviolet light sources have been used. In PDT a wavelength ranging from 600-800nm is widely used (Wainwright, 1998). APDT like PDT uses mainly low power light rather than laser light (Wainwright, 1998). Microbial photodynamic killing also have been shown with natural sunlight (Zeina *et al.*, 2001).

Research into improving the light technology is important to increase the efficiency of both PDT and APDT. In this regard developments in optical fibre technology promise to be a more targeted approach to delivering the light to nearly all body cavities and foci of infection (abscesses). Optical fibre technology can benefit both PDT and APDT.

The characteristic of light source on the efficacy of both PDT and APDT is essential and therefore requires development for its use in clinical applications. Comparative studies are devised to show efficiency on both Gram positive and Gram negative bacteria using the same photosensitizer and different light sources, along with knowledge of the killing behaviour across a wide range of target physiochemical condition. The majority of these studies can be most usefully developed *in vitro*.

The light source is measured by power density, which is normally given in  $\text{mWcm}^{-2}$  whereas the light dose is  $\text{mJ cm}^{-2}$  which is the total energy received. The total energy is calculated as the power density multiplied by the illumination time (in seconds) that is  $\text{mWcm}^{-2} \times \text{s} = \text{mJcm}^{-2}$ . The power density, the illumination time or both can be varied to give the same light dose. Despite the equivalent dose the microbial kill from the exposure to low power density over a long time compared to high power density over a short time period is not equivalent (Wainwright 1998).

### **Incoherent light**

Natural light is incoherent, polychromatic consisting of light of different wavelengths and is divergent, typically radiating in all directions (Wilson, 1993). Sunlight has been used in APDT as source of light to activate PSs. Zeina *et al.* (2001) showed sunlight with photosensitizer MB (100  $\mu\text{g/ml}$ ) was highly effective in killing *S. aureus* and *S. epidermidis*. In a study carried out to show inactivation of micro-organisms in the environment it was shown that *V. fischeri* in aquaculture water was inactivated by sunlight (Alves *et al.*, 2011). The use of

solar energy as an alternative to the other illumination systems could be economically viable for regions with a high degree of sunlight radiation and could be used for the treatment of contaminated wastewaters as well as for the disinfection of drinking water and of aquaculture water (Alves *et al.*, 2011).

Incoherent light sources include lamps with continuous spectrum (incandescent lamps, xenon arc lamps) or sources with the spectrum in discrete bands (gas discharge lamps or metallic vapour lamps) (Calin and Parasca, 2009). Photodynamic inactivation of micro-organisms has been demonstrated using incoherent light sources such as (some) light-emitting diodes and tungsten, halogen and xenon lamps (Calin and Parasca, 2009). Incoherent light sources are easy to use and comparatively cheap (Ackroyd *et al.*, 2001). Incoherent light has several advantages as a light source for PDT: the polychromatic nature of the light means that different PSs with different absorption maxima may be used, and large illumination fields may be achieved for use over large areas, which is particularly relevant to dermatological indications. Incoherent light sources are also relatively cheap, easy to operate and are readily available (Pervaiz and Olivo, 2006). However, the disadvantages of incoherent light are low intensity of the required wavelengths, difficulties in management of light dose, and significant thermal effects (Pervaiz and Olivo, 2006). The low intensity of incoherent light means that long exposure times are generally required for a therapeutic effect to be achieved (Wilson, 1993). However, incandescent lamps have proven useful in APDT, especially for *Staphylococcus aureus* and *Escherichia coli* (Calin and Parasca, 2009).

### **Ultraviolet**

Light with wavelength less than 300 nm is absorbed by proteins and nucleic acids and induces bacterial killing due to dimerization of DNA (Wilson, 1993). However ultraviolet (UV) is rarely used as a source of light in killing of micro-organism in human infections due to its potential to cause mutagenic effects (Wilson, 1993).

## **Coherent Light (Laser)**

Laser is an acronym of light amplification by stimulated emission of radiation. Lasers produce high-energy monochromatic light. Monochromaticity permits irradiation with the exact wavelength at which a certain PS has its absorption maximum (Pervaiz and Olivo, 2006). Laser is seen as an ideal light source for the photodynamic inactivation of bacteria, due to its monochromaticity and coherence (Calin and Parasca, 2009). The high power of laser light makes it ideal since shorter exposure times can be employed to kill microbes by APDT (Wilson, 1993). In addition the laser light is easily coupled into fibers for highly controlled delivery of light to the location of treatment (Calin and Parasca, 2009). These characteristics make laser light an appropriate candidate for clinical applications. In addition to activation of PS by the laser light, laser light alone may have other photobiological effects within the body tissue such as bactericidal, regenerative and vasodilative effects (Vladimirov *et al.*, 2004).

A variety of lasers have been used over the years; these are described in terms of the lasing medium used to generate the beam, which may be a gas, dye, and crystal or semiconductor diode. Examples include the helium/neon (He-Ne), carbon dioxide, gallium aluminium arsenide (GaAlAs), Argon dye and neodymium yttrium aluminium garnet (Nd : YAG) lasers (Wilson, 1993). For APDT studies the most frequently used lasers are the helium–neon (He-Ne) laser and the semiconductor laser (diode laser). These have the advantage of being relatively cheap, of smaller size, portable and reliable. The use of He-Ne laser light has been well documented in APDT in particular inactivation of *S. aureus* and *P. aeruginosa* (Calin and Parasca, 2009).

### **1.6 Mechanism of APDT**

The antimicrobial photo damage at the molecular level in many cases is well established (Wainwright, 1998). The PDT or APDT reaction starts when a light of appropriate wavelength to activate the PS molecule to the excited singlet state that ultimately leads to production of cytotoxic species damaging bacterial cells (Wainwright, 1998). Figure 1.5 shows diagrammatic illustration of the light absorption and energy transfer processes that takes place during APDT.

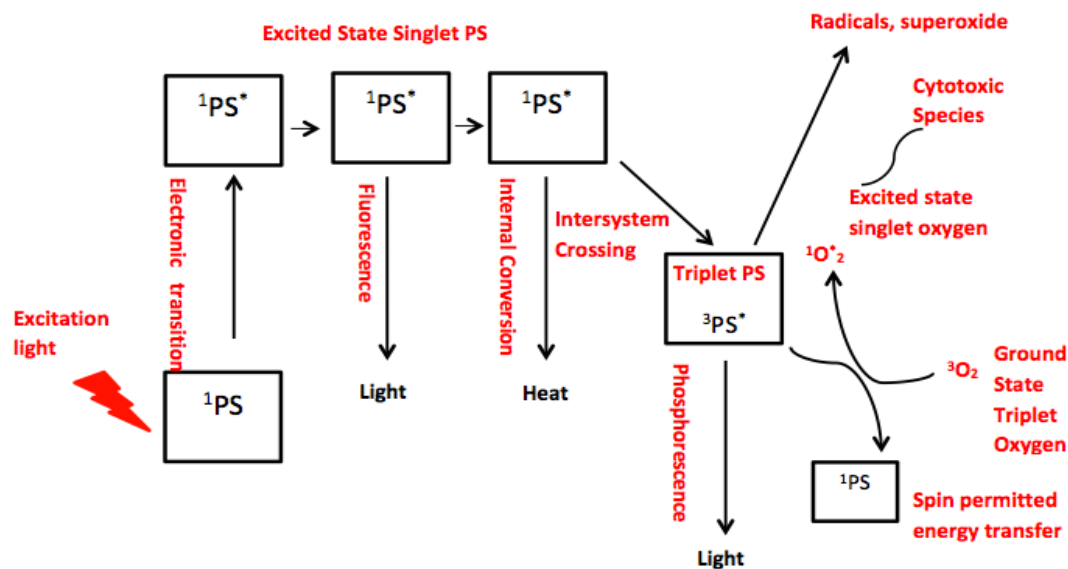


**Figure 1-5: Schematic illustration of photophysical and photochemical mechanisms of APDT (adapted from Castano *et al.*, 2004).**

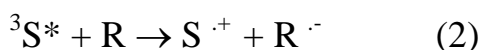
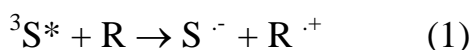
Mechanisms of ROS generation by combination of light, photosensitizer (PS) and ground state triplet oxygen ( $^3\text{O}_2$ ). Ground state photosensitizer ( $^1\text{PS}$ ) is irradiated with visible light generating excited singlet state PS ( $^1\text{PS}^*$ ).  $^1\text{PS}^*$  can relax back to excited triplet state photosensitizer ( $^3\text{PS}^*$ ) generating superoxide radical (type I mechanism) and/or excited state singlet oxygen ( $^1\text{O}_2$ ) (type II mechanism).

A photodynamic reaction starts with the absorption of light (photons) by the ground state PS. The ground state PS has two electrons with opposite spins (this is known as singlet state) in the low energy molecular orbital. Following the absorption of light, one of these electrons is boosted into a high energy orbital but keeps its spin (first excited singlet state). This is a short-lived species, lasting nano seconds (Phillips, 1997), which is a very short time for any significant interaction to take place with the surrounding molecules. The excited singlet species therefore loses its energy by emitting light (fluorescence) or by internal conversion to heat. The excited singlet state PS may also undergo the process known as intersystem crossing whereby the spin of the excited electron inverts to form the relatively

long-lived (microsecond) excited triplet-state that has parallel electron spins (Castano *et al.*, 2004). The long lifetime of the triplet state PS is due to the fact that loss of energy by emission of light (Phosphorescence) is a spin-forbidden process. This triplet state is long lived enough to take part in chemical reactions and therefore most of the photodynamic reactions take place when in triplet state. Therefore it is recognized that triplet state of the photosensitizer is responsible for the generation of cytotoxic species produced during PDT and APDT (Jori and Spikes, 1990). Interaction of the triplet excited PS with surrounding molecules results in two types of photo-oxidative reaction, type I and type II (Foote, 1991; Castano *et al.*, 2004).

### **Type I reaction**

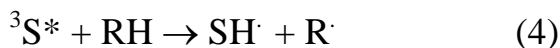
In type I reactions the excited triplet state PS ( $S^*$ ) reacts directly with a local substrate R, via electron or hydrogen transfer. This leads to the production of radicals or ion radicals (Sharman *et al.*, 2000). Equation 1 and 2 shows the two possible electron transfer reactions between an excited photosensitizer and substrate R. Subsequent redox reactions and oxygenation products rely on close proximity of the photosensitizer and the biomolecular target. A type I reaction with water in the microbial milieu can give rise to hydroxyl radicals ( $HO\bullet$ ) which can also react with biomolecules or combine to give hydrogen peroxide in situ with subsequent cytotoxic results (Wainwright, 1998).



The PS and substrate radicals produced in turn react with other substrate molecules. If PS reacts with ground state oxygen it leads to formation of cytotoxic oxidation products (Wainwright, 1998). Type I reactions frequently involve initial production of superoxide anion by electron transfer from the triplet PS to molecular oxygen (Castano *et al.*, 2004). PS radicals ideally react in a way that regenerates the ground state PS to enable another reaction cycle continuing the process. The excited PS ( $S^*$ ) can also directly transfer an electron to molecular oxygen producing superoxide (Sharman *et al.*, 2000) (equation 3).

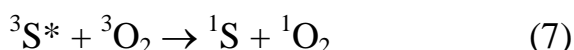


Equation 4 to 6 shows chain reaction induced by hydrogen transfer (Sharman *et al.*, 2000).



### Type II reaction

A type II photodynamic reaction is an energy transfer reaction where the excited triplet state PS ( ${}^3\text{S}^*$ ) transfers its energy directly to a ground state oxygen molecule ( ${}^3\text{O}_2$ ), generating the reactive oxygen species, singlet oxygen ( ${}^1\text{O}_2$ ) (Sharman *et al.*, 2000) equation 7, that in turns react with various substrates (Sharman *et al.*, 2000).



Singlet oxygen is thought to play the key role in APDT (Maisch *et al.*, 2007). Singlet oxygen is electrophilic and is able to oxidise a variety of electron rich substrate molecules, such as polyunsaturated lipids, cholesterol, proteins and nucleic acid bases, especially guanine (Agnéz-Lima *et al.*, 2012). Singlet oxygen readily reacts with amino acids containing double bonds (Wainwright, 1998).

The type-I and type-II reactions shown above are described as the primary processes in PDT and APDT. Superoxide ( $\text{O}_2^{\cdot-}$ ), singlet oxygen ( ${}^1\text{O}_2$ ) and hydroxyl radical ( $\text{HO}^{\cdot}$ ) interact to produce peroxy-radical ( $\text{RO}^*_{\cdot 2}$ ) alkoxy-radical ( $\text{RO}^*$ ), hydroperoxides and peroxide ( $\text{ROOR}$ ) (Singh, 1982). Superoxide can react with a variety of compounds including hydroxyl radical to form singlet oxygen, or nitric oxide radical to produce peroxynitrite, another highly reactive oxidising molecule.

One of the important reactions of superoxide is the production of hydrogen peroxide in the presence of the enzyme superoxide dismutase that catalyses this reaction; also known as dismutation. Hydrogen peroxide is important in biological systems because it can readily pass through cell membranes (Gutteridge and

Halliwell 1990). Another important reaction is the Fenton reaction, which occurs in the presence of  $\text{Fe}^{2+}$  ions. In this reaction  $\text{Fe}^{2+}$  ions acts as a catalyst to convert hydrogen peroxide into hydroxyl radical. This reaction is important in biological systems because most cells have some significant levels of iron and is an important source of highly reactive species such as superoxide, hydroxyl and alkoxy radical. The highly reactive hydroxyl radicals undergo three main types of reactions. The first is addition to double bonds to give secondary radicals. There are many types of molecules in the cell containing double bonds such as an unsaturated fatty acid could form hydroxylated adduct. The second type of reaction is where hydroxyl radical can oxidize a substrate by abstraction of an electron from it, for example it could react with oxygen to produce peroxy radical. The third type of reaction is the transfer of electrons where hydroxyl radical can cause electron transfer reactions with organic and inorganic compounds. This type of reaction produces highly reactive species, resulting in chain reactions responsible for oxidative damage of fatty acids and lipids. This demonstrates why radicals such as hydroxyl radicals can cause so much damage (Wainwright, 1998).

These further reactions are free radical secondary processes, which depend on the particular chemical environment in which the reactions are occurring. All these species have the potential to cause cellular damage. Hence both type I and type II pathways can lead to damage to cellular proteins or cell death (Wainwright, 1998). Both type I and II can occur simultaneously and which pathway is dominant depends on the concentration of PS and on environmental factors such as oxygen supply. A low oxygen concentration or more polar environments will favour a type I reaction (Wainwright, 1998; Sharman *et al.*, 1999).

### **1.7 Methods used to study the mechanism of APDT**

The evidence supporting the involvement of singlet oxygen in APDT by detection of singlet oxygen is confirmed using different techniques. The evidence to support the formation of singlet oxygen in a system is obtained when that system produces light (distinctive monomol luminescence) at approximately 1270nm (Sharman *et al.*, 2000). The direct method of detecting singlet oxygen and free radicals include

electron spin paramagnetic resonance (ESR or EPR) and spin-trapping methods (Hadjur *et al.*, 1997). Singlet oxygen is not commonly studied with the electron spin resonance (ESR) technique in biological systems; because there are few suitable detecting agents and the detection of singlet oxygen *in vivo* is difficult due to its short lifetime in cells (Moan and Berg, 1991). Also because of the rapid rate of singlet oxygen consumption and low luminescent quantum yields of singlet oxygen (only 200 singlet oxygen molecules per billion undergo irradiative decay) luminescence emission cannot be detected from the cell (Gorman and Rodgers, 1992).

Other methods of evidence for involvement of singlet oxygen are obtained through indirect methods using competitive quenchers. Indirect method of using quenchers supports the hypothesis of involvement of singlet oxygen and other reactive oxygen species in APDT. Quenchers of singlet oxygen inhibit the photo-damage caused during APDT. There are a variety of scavengers and quenchers of specific reactive oxygen species, which provide protection against APDT cytotoxic effects. Reagents such as 1,4-diazabicyclo-2,2,2-octane (DABCO), methionine, tryptophan, propylgallate, mannitol and cysteine have proved to reduce the microbial killing due to quenching effects by these scavengers and quenchers under APDT conditions in the presence of PS and light (Nitzan *et al.*, 1989; Bhatti *et al.*, 1998).

Another method of testing the involvement of singlet oxygen is seen by the variation in the lifetime of singlet oxygen in heavy water ( $D_2O$ ). Singlet oxygen has normally a lifetime of 3  $\mu s$  which increases to 65  $\mu s$  in heavy water (Gorman and Rodgers, 1992). This increase in the lifetime of singlet oxygen results in more time for singlet oxygen to cause cytotoxic damage to the cell. Therefore in the presence of heavy water the kill rate by PDT and APDT is increased. Heavy water is considered a specific singlet oxygen identification substance. However, in the presence of  $D_2O$  the quantum yield of triplet state formation for the PS is also greater, which will favour both the type I and type II reaction pathways (Phillips, 1997; Rosenthal and Ben-Hur 1995). Moreover, structural variations in cell target

proteins may occur in presence of D<sub>2</sub>O environments compared to H<sub>2</sub>O, making proteins more susceptible to oxidative damage via type I and type II mechanism. Heavy water may also have a negative effect on the ability of the cell repair system, thus increasing the damaging effects of PDT (Rosenthal and Ben-Hur, 1995). The use of other quenchers to study the mechanism of APDT is also limited because these quenchers are not entirely specific to singlet oxygen and can cross react with other reactive oxygen species produced during PDT processes. For example, azide is an effective quencher of singlet oxygen but is also known to react with hydroxyl radical but at a much slower rate. Tryptophan is a quencher of singlet oxygen, but has been shown to react under certain circumstances via a mixed type I/type II mechanism (Shopova and Gantchev, 1990). Therefore identifying the mechanism of APDT processes with quenchers and D<sub>2</sub>O requires careful examination of the reaction products and understanding the limitations of each method.

### **1.8 Mechanism of APDT damage to bacteria**

The overall mechanism of photodynamic therapy takes place in two distinct steps. The first step is the photophysical and photochemical properties of the PS and its ability to generate cytotoxic agents. The second step is the biological response of the cell to the cytotoxic agents (Wainwright, 1998). The efficiency of step one is determined by the activity of the photosensitizing drug, which is governed by both the lifetime and yield of the triplet state of the PS, which in turn have an effect on the quantum yield of singlet molecular oxygen formation. Singlet molecular oxygen is regarded as the main mediator of phototoxicity in APDT (Wainwright, 1998). The ROS and singlet oxygen produced are oxidising agents that can directly react with many biological molecules. One of the damaging reactions is when radical species react with oxygen producing lipid hydroperoxide. Lipid hydroperoxide is detrimental to membrane integrity, leading to loss of fluidity allowing leakage of cellular contents and increased ion permeability (Wainwright, 1998) or inactivation of membrane transport systems and enzymes (Hamblin and Hassan, 2004).

Type II processes are known as the major pathways in photooxidative microbial cell damage. Singlet oxygen reacts with molecules involved in the maintenance and structure of cell wall membrane such as phospholipids, peptides and, for yeasts sterols (Wainwright, 1998). Reactions of other molecules with singlet oxygen also occur. Amino acids in proteins are known to be important targets and these include cysteine, methionine, tyrosine, histidine and tryptophan (Grune *et al.*, 2001; Midden and Dahl, 1992). Tryptophan undergoes cycloaddition with singlet oxygen. Also methionine reacts with singlet oxygen producing methionine sulphoxide (Bonnett, 1995; Wainwright, 1998).

The photodynamic processes can also damage DNA at both nucleic acid bases and sugars that link the DNA by oxidation or cross-linking of DNA to protein (Wainwright, 1998). One of the main reactions of nucleic acids is the reaction, which results in production of guanosine residue (Hamblin and Hassan, 2004). Of the four bases in the nucleic acid guanine is the most susceptible to oxidation by singlet oxygen (Foote, 1991). Cells are known to have some capability of fixing oxidative damage caused to proteins and DNA. However DNA cross-linking and strand breakage are particularly difficult for the cell to repair and excessive damage can cause mutations or cell death (Wainwright, 1998)

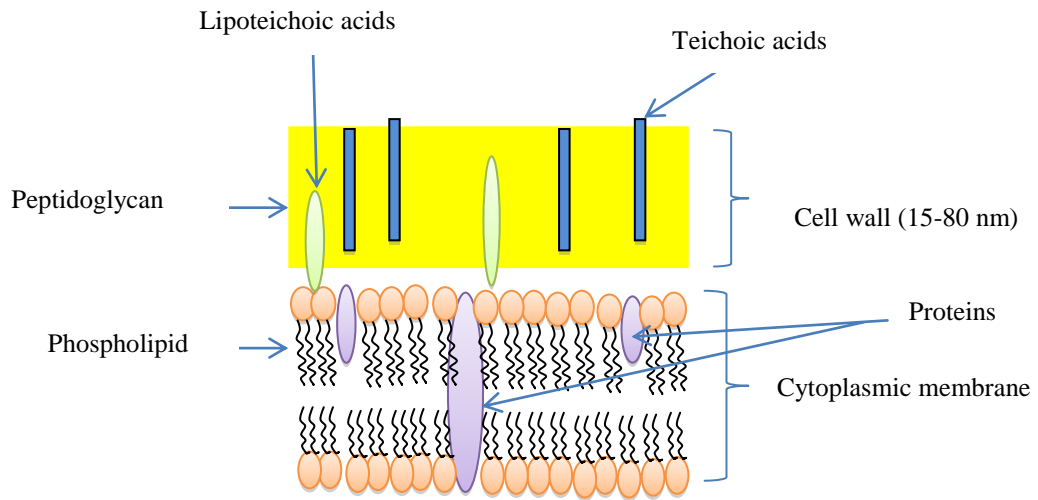
It has been shown that, although DNA damage occurs, it may not be the prime cause of bacterial cell death as *Deinococcus radiodurans*, which is known to have a very efficient DNA repair mechanism and is very tolerant to UV or  $\gamma$  radiation, is easily killed by APDT (Hamblin and Hassan, 2004). Photodynamic treatments have been shown to result in the alteration of cytoplasmic membrane proteins (Valduga *et al.*, 1999; Bertoloni *et al.*, 1990). Therefore APDT works by targeting multiple components of the cell.

### **1.9 Photodynamic Inactivation of Microbial Cells**

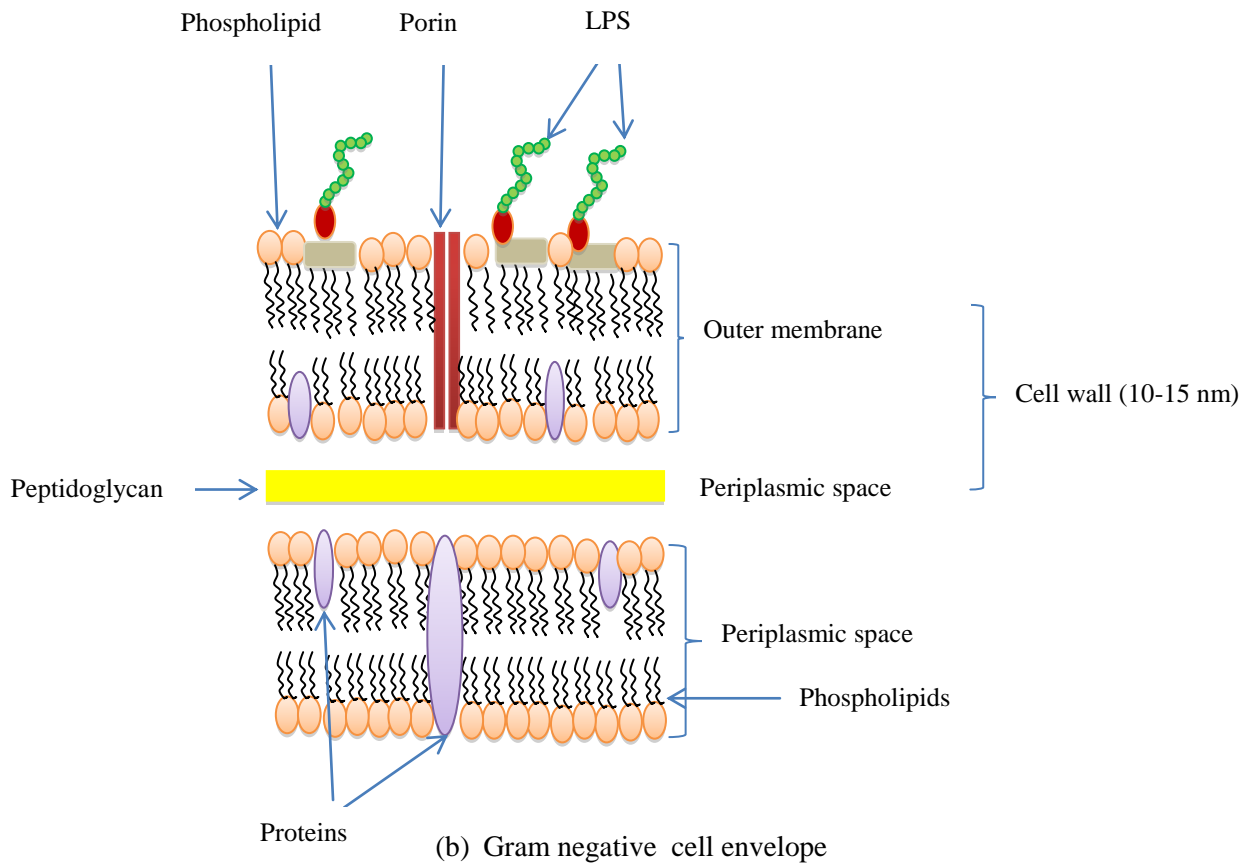
The cellular structural differences between different micro-organisms is an important factor affecting the way in which photosensitizing agent can interact with the cell targets and influence both the efficiency of photosensitizing agent

and the mechanism of action. Bacteria are grouped into two main categories Gram-positive and Gram-negative organisms, based on their cellular structure and organization. The main differences in these two groups are the differences in their outer cell wall structure as shown in Figure 1.6. This difference in structure influences the permeability of the cell wall of the targeted micro-organism to the PS which is an important factor that determines antimicrobial activity of photodynamic processes (Bertoloni *et al.*, 1992; Wainwright, 1998). Whilst the majority of the PSs are effective against Gram positive bacteria, many have exhibited low efficacy against Gram negative bacteria, due to the extra barrier posed by the negatively charged outer membrane of the Gram negative species (Minnock *et al.*, 2000; Nitzan *et al.*, 1992).

To overcome this intrinsic resistant feature of gram-negative organisms, different approaches have been used. These include administration of membrane permeabilising agents in conjugation with PS (Bertoloni *et al.*, 1990), stimulating the endogenous synthesis of bacterial porphyrins as endogenous PSs (Hamblin *et al.*, 2005) and the use of PSs chemically modified to possess a positive charge (Malik *et al.*, 1992), to target the outer membrane. In a study carried out on the Gram-negative species *E. coli* and *Klebsiella pneumonia*, pre-treatment of bacteria with EDTA allowed a significant concentration of the PS to penetrate to the cytoplasmic membrane killing the organisms; this supports the importance of the cytoplasmic membrane as a critical target for bacterial cell photo-inactivation (Bertoloni *et al.*, 1990). Using outer wall membrane disrupting agents such as EDTA allows PS to penetrate and to overcome the negative charge barrier of the Gram-negative cells. The cell wall structure of the target micro-organism is important to antimicrobial PDT. In order to efficiently inactivate a micro-organism, the PS has to reach the cytoplasmic membrane and thus has to pass through the cell wall. However, it is more desirable in a clinical setting to have an effective PS without a need for additional chemicals. Therefore, it is more favourable to use cationic PSs such as MB, which bind to a broad spectrum of microbial species and is light-active in itself without the addition of further chemicals (Jori *et al.*, 2006).



(a) Gram positive cell envelope



(b) Gram negative cell envelope

**Figure 1- 6: Diagrams illustrating differences in membrane structure between (a) The Gram-positive and (b) Gram-negative bacteria. (diagram adapted from Jori *et al.*, 2006)**

APDT has also been demonstrated to destroy virulence factors associated with bacterial infections. PDT with TBO were shown to affect the potency of two key bacterial virulence factors, lipopolysaccharide (LPS) and proteases (Komerik *et al.*, 2000). The target species for photoinactivation are mainly bacteria although other micro-organisms (yeasts, protozoan) are sensitive to APDT (Zeina *et al.*, 2001). The possibility of bacterial photoinactivation *in vitro* by APDT has been experimentally proven many times with various combinations of PSs and different light doses and table 1.1 shows a summary of previous research carried out against a number of different micro-organisms. From these studies it can be concluded that APDT may be effective in killing microbial organisms in infections, for sterilisation and as a disinfectant. Also these studies show the effectiveness of APDT is dependent on the concentration of PS, light dose and the microbial species. However from the APDT studies carried out so far, it is difficult to compare one study with the other since either may be carried out under different conditions even for the same combinations of PS and light.

**Table 1- 1 Use of PSs and light to inactivate micro-organisms**

Reference	Micro-organism and concentration (CFU/ml)	PS and PS concentration	Irradiation protocol	Fluence rate (W/cm <sup>2</sup> )	Radiation time (Minutes)	Total light dose (J/cm <sup>2</sup> )	Killing effect
Embleton <i>et al.</i> , 2002	Epidemic methicillin-resistant <i>Staphylococcus aureus</i> -16 (EMRSA) 1x10 <sup>9</sup> -1x10 <sup>10</sup>	SnCe6-IgG 4.2 mg/ml	Helium-neon laser Wavelength 632.8 nm (measure light output 35 mW)	-	5	21	Growth phase of bacteria lag-70% Exponential-99.9% Stationary phase-99.7%
Gross <i>et al.</i> , 1997	<i>S. aureus</i> Cowen 1x10 <sup>5</sup>		Bacteriochlorophyllide IgG conjugate (10 µM)	140	5	42	99.9%
Wilson and Yanni, 1995	<i>S. aureus</i> MRSA strain 1.3x10 <sup>10</sup>	TBO (12.5 µg ml <sup>-1</sup> )	Helium-neon laser 632.8 nm wavelength (light output 35 mW)	-	1	43	99.99%
Alves <i>et al.</i> , 2009	<i>Enterococcus faecalis</i> 10 <sup>7</sup>	5,10,15,20-tetrakis (1-methylpyridinium4-yl) porphyrin tetraiodide (Tetra-Py++-Me) 1 µM	White light (380-700 nm)	40	270	64.8	PS concentration- 1 µM 7.33 log reduction (99.7%) PS concentration- 0.5 µM 5.07 log reduction (93.23%)
Alves <i>et al.</i> , 2009	<i>E. coli</i> 10 <sup>7</sup>	5,10,15,20-tetrakis(1-methylpyridinium4-yl) -porphyrin tetraiodide (Tetra-Py++-Me) 1 µM	White light (380-700 nm)	40	270	64.8	> 7 log reduction of survivors (99.999%)

Banfi <i>et al.</i> , 2006	<i>Pseudomonas aeruginosa</i> 10 <sup>8</sup>	5,15-Di (N-(4-methoxybenzyl)-4-pyridyl) -10,20-di(4-pyridyl) porphyrin dichloride (dicationic porphyrin) 8 µM	Visible light		60	266	> 7 log reduction of survivors
Foschi <i>et al.</i> , 2007	<i>E. faecalis</i> (ATCC 29212) 10 <sup>9</sup>	MB 16.75 µM	Diode laser	100	10	60	77.5% reduction
Souza <i>et al.</i> , 2010	<i>C. albicans</i> 10 <sup>6</sup>	TBO, MB, malchite green (concentration 0.1 mg/ml)	Light source GaAlAs laser with a wavelength of 660 nm, output power 0.035 W Illuminated area 0.38 cm <sup>2</sup> .		428 sec (15 J)	39.5	TBO- 3-log reduction MB- 2.71-log reduction Malachite green-2.25 log reduction
Zolfaghari <i>et al.</i> , 2009	EMRSA-16 in excision wound model- wounds 6 mm (28 mm <sup>2</sup> ); 25 µl of cell suspension (10 <sup>8</sup> cfu) 25 mm <sup>2</sup> square shaped wounds by scarification. 10 µl of the suspension placed on wound (4×10 <sup>7</sup> cfu).	MB 100 µg ml <sup>-1</sup>	The light source used was a 665 nm diode laser	200	30	360	25-fold reduction in number of viable EMRSA- 16 (1.4 logCFU/ wound- in excision wounds) 4 fold reduction (1.15 log CFU/ wounds- in superficial scarified wounds

Zeina <i>et al.</i> , 2001	<i>S. aureus</i> , <i>S. epidermidis</i> , <i>Strep pyogenes</i> , <i>C. minutissimum</i> , <i>P. acnes</i> , <i>Candida albicans</i> Bacterial cells 10 <sup>8</sup> - 10 <sup>9</sup>  <i>C. albicans</i> 10 <sup>7</sup>	MB 100 µg ml <sup>-1</sup>	Polychromatic visible light	42	10-60	25.2- 151J	<i>Staphylococcus aureus</i> – kill rate 0.9 log cfu/ml, D value 72s  <i>Staphylococcus epidermidis</i> -kill rate 1log cfu/ml , D value 66s  <i>Streptococcus pyogenes</i> - kill rate 1.15 log cfu/ml, D value 48s  <i>Corynebacterium minutissimum</i> – kill rate 0.7log cfu/ml, D value 120s <i>Propionibacterium acnes</i> -kill rate 1.85log cfu/ml, D value 30s  <i>Candida albicans</i> -kill rate 0.09 log cfu/ml, D value 660s
-------------------------------	---	-------------------------------	--------------------------------	----	-------	---------------	---

To show the killing effect of antimicrobial agents, kill kinetics are derived and expressed as kill rate and corresponding D values which make it easier to understand the effectiveness of the agent and to compare it under different conditions. Figure 1.7 shows a model graph of ideal kill kinetics depicting a survival curve showing potential variations in pattern. In some studies, key information about the kill rate (K) is not given or presented; merely “before and after” measurements, thus making it difficult to accurately assess the efficacy of treatments or compare results from different studies.

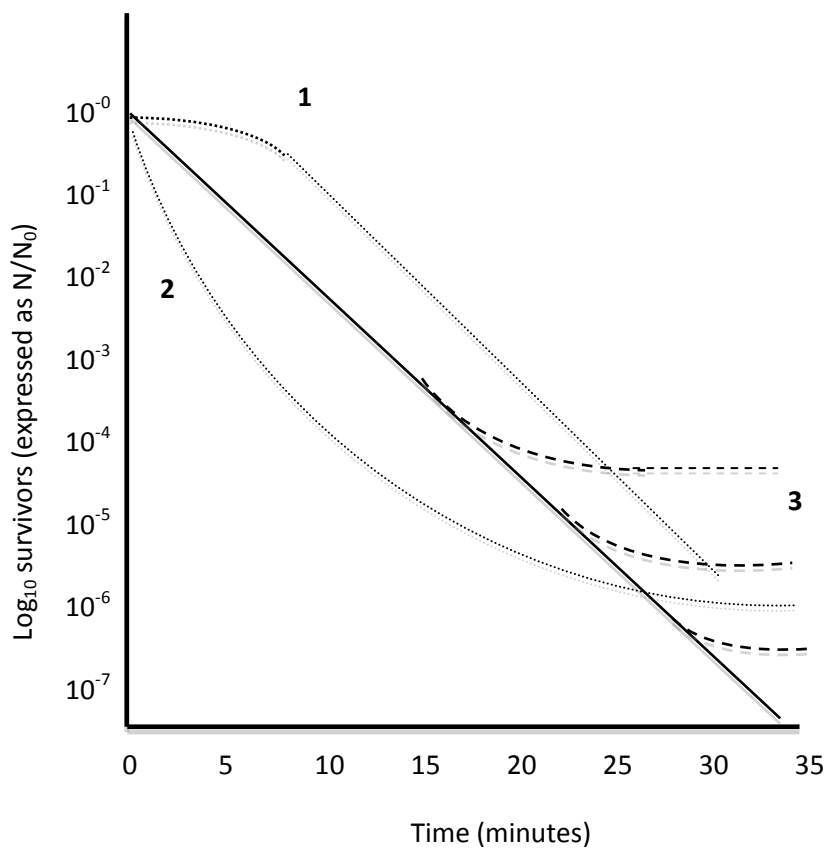


**Figure 1-7: Ideal first order kill kinetic survival curve with examples of non-ideal behaviour**The solid line shows an ideal representation of first order kill kinetics. Non-ideal curves commonly encountered include (1) Multi-phasic; there is an apparent delay and slow rate of kill before the reaction accelerates to maximum rate. (2) Multi-phasic; the reaction rate decelerates slowly with time. (3) Multi-phasic; the reaction abruptly ends, marking the end of the killing phase.

Figure 1.7 shows the ideal first order kill kinetics survival curve and non ideal multiphasic curves. Likely reasons for multiphasic curves include a multi-hit process, where agent molecules must hit many targets in the cell before killing commences. If the target cells are mixed species with a range of susceptibilities (e.g. *Bacillus* vegetative cells plus a proportion of endospores), then a rapid rate of kill will be followed by a much slower rate; depending on the ratio of vegetative cells to spores. Some killing agents at low concentrations can be neutralised by the chemical environment (especially with additions like serum), and if the target population is high, the agent rapidly runs out of killing power. This is true of agents that decay, or are specifically neutralised by other components. It should be noted that assay systems have a minimum level of detection, below which reductions of the target cells may still be occurring but cannot be detected. For viable count, the minimum detection level is typically  $10^2$  cfu ml<sup>-1</sup>. For bioluminescence, the background readings remain constant at the minimum detection level. An apparent deceleration will occur, but this is dependent on the detection system rather than the reality of the reactions.

If multiphasic, but without a significant shoulder, the initial kill rate is analogous to an initial reaction rate in enzyme kinetics, and (within limits) is proportional to the concentration or magnitude or flux of killing molecules or particles (photons) depending on the type of agent. A well-standardised assay system can thus be used to determine the strength or efficacy of the treatments in question.

Kill rates: A reduction of a population is equivalent to a negative growth rate ( $-\mu$ ). The specific growth rate in batch culture with unrestrained growth conditions is:

$$\mu = (\ln N_x - \ln N_0) / t_x - t_0 \dots\dots\dots \text{(Eq 1)}$$

Where  $\mu$  is the specific growth rate, and  $N_x$  and  $N_0$  are numbers of cells at zero time ( $t_0$ ) and later time ( $t_x$ ). The equivalent for kill rate ( $-\mu$ ) is given by:

$$-\mu = (\ln S_x - \ln S_0) / t_x - t_0 \dots\dots\dots \text{(Eq 2)}$$

Where  $S_x$  and  $S_0$  are numbers of survivors at zero time ( $t_0$ ) and later time ( $t_x$ ). However, in many studies kill rates are more often reported in log<sub>10</sub> units (log-fold reduction per time unit). This is given as:

$$K = (\log_{10}S_x - \log_{10}S_0)/t_x - t_0 \text{ (Eq 3)}$$

From this is derived the decimal reduction time (D)

$$D = 1/K = t_x - t_0 / (\log_{10}S_x - \log_{10}S_0) \text{ (Eq 4)}$$

In this thesis, all kill rates are reported as K or its reciprocal, D, the time it takes to achieve a 90% kill.

### 1.10 Electrochemically Activated Solutions (ECAS)

APDT and ECAS are proposed as alternative methods of clearing microbial load in both clinical and environmental settings. These treatments have the potential to be applied to various settings. Figure 1.8 shows possible applications of ECAS.

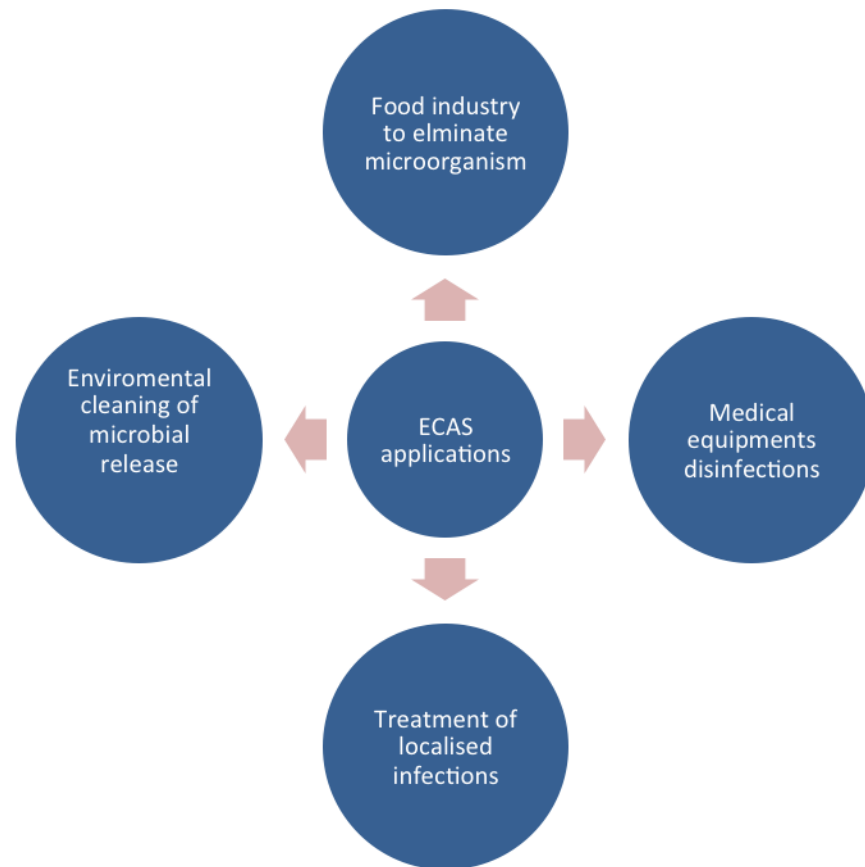


**Figure 1-8: Applications of ECAS (showing a broad spectrum)**

Electrochemically activated solutions (ECAS) are produced from tap water and low-concentration salt solutions (Bakhir *et al.*, 1999) using a flow through electrolytic module (FEM), comprising of coated titanium electrodes that are separated by electro-catalytic ceramic diaphragm. ECAS are known to exhibit high redox potential, contain free radical species and exist in a metastable state

(Robinson *et al.*, 2011). The metastable status of ECAS is not permanent. However it has been shown that by storing at low temperature the activity can be prolonged (Robinson *et al.*, 2012).

Electrochemical treatment of low concentration salt solution in the anode and cathode chambers results in synthesis of two types of solutions. Solutions produced at the cathode chamber are called catholyte and solution produced at the anode chamber is termed the anolyte (Shetty *et al* 1999; Selkon *et al.*, 1999). It is the solution produced at the anode that has bactericidal and sporicidal activity that is not toxic to human tissue and essentially non-corrosive for most metal surfaces (Shetty *et al* 1999; Selkon *et al.*, 1999). Anolyte solutions contain a mixture of oxidizing substances and it is this solution that is very effective at killing bacteria, viruses, fungi and protozoa (Prilutskii *et al.*, 1996; Bakhir *et al.*, 1999).

The microbicidal activity of ECAS (super oxidised water) have been demonstrated against *Escherichia coli* (including type 0157), *Pseudomonas aeruginosa*, *Bacillus subtilis* var. niger spores, methicillin-resistant *Staphylococcus aureus*, *Clostridium difficile* spores, *Helicobacter pylori*, vancomycin resistant *Enterococcus species*, *Candida albicans* (Shetty *et al* 1999; Selkon *et al.*, 1999). This microbicidal activity against a variety of organisms is very important as ECAS can be used as a very effective disinfectant or as a broad-spectrum biocide.

The main attractive feature of electrochemically-activated solution is it is highly active against micro-organisms killing 99.999% or greater, in 2 minutes or less (D values for example MRSA was 2.08s and 1.98 s for *P. aeruginosa*) (Robinson *et al.*, 2010). It is recognised that ECAS are potent microbiocidal agents (Selkon *et al.*, 1999, Shetty *et al.*, 1999). They are also non-toxic when in contact with vital biological tissues (Shraev *et al.*, 1993). Clinical applications of anolyte and catholyte have been reported to be effective (Malakhov *et al.*, 1994). ECAS has been used in dermatological washing, cleaning and dressing of wounds and disinfection of instruments (Leonov, 1997). It is also widely used as a disinfectant

in hospitals and dental clinics in Japan (Al-Haq *et al.*, 2002). ECAS has use in environmental decontamination (Marais and Williams, 2001) and within the food industry as a disinfectant (Koseki *et al.*, 2004). Therefore ECAS has been suggested to have wide range of application from health care setting to broad-spectrum disinfectant.

Biocides kill micro-organisms through the targeting of several structures or macromolecules or biochemical pathways (McDonnell and Russell 1999). It has been shown that ECAS anolyte cause bacterial death by complete destruction of proteins or by causing oxidative stress resulting in protein fragmentation (Cloete *et al.*, 2009), which is similar to APDT killing of microbial cells. Moreover, exposure of micro-organisms to the high oxidation reduction potential (ORP) environment in ECAS is known to create an unbalanced osmolarity between ion concentrations in the solution and that of the unicellular organisms, further damaging membrane structure (Thorn *et al.*, 2012).

Despite considerable research in electrochemical processes and its practical applications as a disinfectant and its use as a biocide in various environments, the killing mechanisms of electrochemically-activated solutions have not been fully identified. Some studies have attributed the high bactericidal capacity of electrochemical (EC) processes to electrochlorination (Rodgers *et al.*, 1999), destruction caused by electric field (Grahl and Markl 1996), and inactivation by production of energy rich short-lived intermediate products. Also research has shown the critical role of free radicals generated during electrolysis such as  $O_2^{\cdot-}$ ,  $OH^{\cdot}$ ,  $ClO_2^{\cdot-}$  and  $HClO^{\cdot}$  in exerting strong germicidal action (Patermarakis and Fountoukidis, 1990; Oturan, 2000). A study on electrochemical disinfection of saline wastewater effluent showed that electrochlorination is not the predominant disinfective means of EC process. This study concluded that the production of more powerful but short-lived killing substances, free radicals, occurs which are facilitated by chloride ions to provide the strong disinfecting action within short contact time. The study also showed the importance of  $Cl^-$  ions and with excess  $Cl^-$  the chain reaction produces more  $OH^{\cdot}$  radicals and extends the lifetime of  $OH^{\cdot}$  by

a factor of 10, thus making it more useful in the destruction of cells (Li *et al.*, 2002). Although these studies explain the mechanism of bactericidal capacity of electrochemical processes and ECAS, it does not explain fully how it can kill organisms in such a short contact time and therefore it is necessary to find evidence for this superior action and to find the predominant killing action.

### **1.10 Comparison of APDT and ECAS**

In this present study it is proposed that by using specific scavengers of free radicals and singlet oxygen scavengers and stabilisers, the mechanism of ECAS could be understood. It is known that the mode of action of APDT is mainly due to damage caused by singlet oxygen with an element of free radical damage. Singlet oxygen is known to be very potent to cells and is a short-lived reactive species. The killing action of ECAS also involves free radical species and may have similarities to APDT.

The approach in this thesis was to compare APDT to ECAS. It is anticipated that this approach of comparing and contrasting these two antimicrobial agents under the same standardized conditions will lead to comprehensive understanding of these two antimicrobial agents. Previously, different workers have made mechanistic studies of both APDT and ECAS but none have studied them in tandem together.

ECAS was chosen for comparison with APDT for several reasons. They are both known to damage micro-organism due to ROS and hydroxyl radical, and both agents can be applied to localised infections. Therefore the first aim of the study was to develop a rapid kill kinetic assay based on lux transformed bioluminescent species in order to compare the properties and mechanism of the two agents under standardised conditions.

## **1.11 Rapid bioluminescence method to evaluate activities of APDT and ECAS**

New methods of applying the bioluminescence approach for rapid and simple detection activities of bacteria are required for faster development of these alternative agents in order to understand their effectiveness and mechanisms of action.

### **1.11.1 Bacterial Bioluminescence**

Bioluminescence refers to the process of visible light emission, by the enzyme catalyzed chemical reactions, in living organisms (Meighen, 1993). Bioluminescent organisms are widely distributed in nature (Campbell, 1989). The phenomenon of bioluminescence has been observed among bacteria, dinoflagellates, fungi, fish, insects, shrimps and squids. This set of organisms includes terrestrial, freshwater and marine species (Meighen, 1993).

Almost all bioluminescent bacteria have been classified into the three genera *Vibrio*, *Photobacterium* and *Photorhabdus* (formally *Xenorhabdus*). Bioluminescent bacteria are the most abundant and widely distributed among the light emitting organisms and are found in marine, freshwater and terrestrial environments as free-living species, saprophytes, parasites, or as light organ symbionts in a number of aquatic species (Alves *et al.*, 2011). All naturally occurring bioluminescent bacteria that have been characterized are Gram-negative rods and can function as facultative anaerobes (Meighen, 1991). The most studied group of bioluminescent bacteria include *Vibrio harveyi*, *Aliivibrio fischeri*, *Photobacterium phosphoreum*, *Photobacterium leiognathi*, and *Photorhabdus luminescens*.

Light production by bacterial symbionts of higher organism may serve to attract prey, in intra species communication or to escape from predators (Martin *et al.*, 1989). *P. luminescens* has only been found infecting terrestrial organisms acting in symbiosis with nematodes in a parasitic infection of caterpillars (Meighen, 1991). This bacterium has been isolated from human wounds (Meighen, 1991).

### 1.11.2 Bioluminescence systems in bacteria

Bioluminescence is an enzyme catalyzed chemiluminescence reaction in which free energy released ultimately leads to the emission of a photon. The enzymes that catalyze the bioluminescent reaction are called luciferases and the substrates are known as a luciferin (Hasting, 1996). In all bioluminescence systems oxygen is required for light emission (Meighen, 1993). The structures of luciferases and luciferins are different from one bioluminescent organism to the other (Meighen, 1993). Consequently, the light-emitting reactions are quite distinct among different organisms.

The bacterial light emitting reactions catalyzed by luciferase, involves the oxidation of reduced riboflavin phosphate (FMNH<sub>2</sub>) and long chain fatty aldehyde (tetradecanal) with the subsequent emission of blue green light at 490 (Meighen, 1993). The natural aldehyde for the bioluminescence reaction is believed to be tetradecanal on the basis of identification of this compound in lipid extract.

The reaction involves reducing power (FMNH<sub>2</sub>) and adenylate energy, since it is dependent on the metabolic activity of the bacteria (Vesterlund *et al.*, 2004). Under conditions in which FMNH<sub>2</sub> and ATP is continually supplied in a *lux*-expressing bacterium, luminescence remains at a constant level (Meighen, 1993). Figure 1.9 shows the light emission by bioluminescent bacteria captured by ICCD photon counting camera. The reaction is as follows:

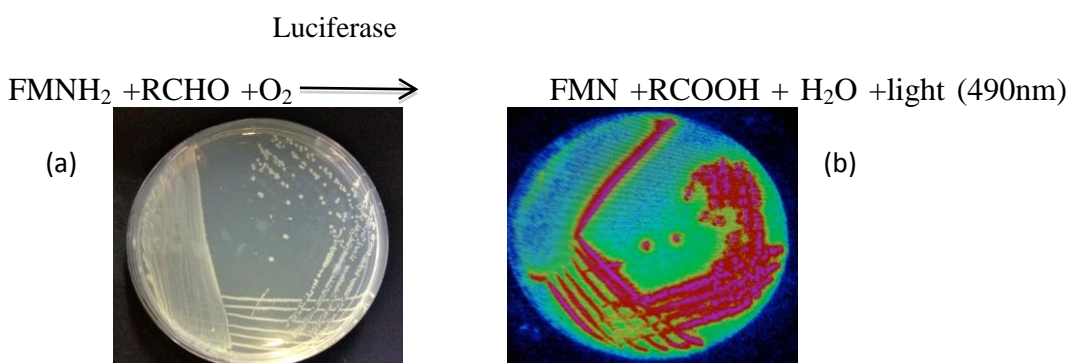


**Figure 1-9: (a) Image showing growth of bioluminescent *E. coli* Nissle pGLITE on the surface of nutrient agar plate (b) bioluminescent *E. coli* Nissle pGLITE expressing the *lux* gene coding for the emission of light image captured ICCD photon-counting camera: Red colour represents higher light emission and Green, low light emission**

The *lux* genes, required for bacterial bioluminescence are arranged in a single operon *luxCDABE*, encodes the luciferase and biosynthetic enzymes (for the synthesis of the aldehyde substrate) necessary for light production. Bacterial luciferase is a heterodimeric enzyme of 77kDa composed of  $\alpha$  and  $\beta$  subunits with molecular masses of 40 and 37 kDa, respectively (Meighen, 1993). The synthesis of aldehyde and recycling of fatty acid to aldehyde for bioluminescence reaction is catalyzed by a multienzyme fatty acid reductase complex containing three proteins, a reductase, a transferase and synthetase (Meighen, 1993). These three polypeptides are encoded by *luxC*, *luxD* and *luxE* respectively and found in the *lux* operon of all luminescent bacteria (Meighen, 1993). A number of additional *lux* genes have been identified, but only *luxCDABE* is essential for light production (Meighen, 1993).

### **1.11.3 Applications of bioluminescence**

The *lux* operons of *V. fischeri* and of *P. luminescens* (*luxCDABE* operon) have been expressed successfully in a wide range of Gram-negative bacteria and a redesigned operon has also been used to transform Gram-positive bacteria (Francis *et al.*, 2000). The luciferase gene from *P. luminescens* has very high thermal stability, making the *lux* operon of this organism ideal to use as a reporter system (Meighen 1993). When the luciferase was expressed in *E. coli* it was found to be stable at 42°C (Chatterjee and Meighen, 1995). Consequently, transformed organisms with the *lux* operon from *P. luminescens* are ideally suited for the study of pathogens in mammalian animal models as the enzyme retains significant activity at 37°C (Meighen 1993).

Though Gram-positive cells express bioluminescence the output compared to Gram-negative is low. Therefore in the current study Gram-negative bioluminescent organisms were used to study the efficacy of APDT and ECAS. In the efficacy testing of antimicrobials it is preferred to see at least a 3-log fold drop in bacterial number. Because of the low light output by the Gram-positive organism it is not possible to use this organism in the current study. Therefore traditional viable count methods were used to study the efficacy of APDT against Gram-positive organisms.

One of main advantages the bioluminescence systems is that when transfected the entire *lux* gene operon encoding both the bacterial luciferase and the biosynthetic enzymes for substrate synthesis, generate bioluminescence without the need for exogenous administration of luciferin or aldehyde (Rocchetta *et al.* 2001). Indicator strains used the full operon gene (*luxCDABE* or modified *luxABCDE*) as a consequence, allowing stable light production (Vasterlund *et al.*, 2004).

The bioluminescence output from bioluminescent bacteria is a highly sensitive reporter of metabolic activity (Marincs *et al.*, 2000) since it is directly dependent on the metabolic activity of the organism (Vasterlund *et al.*, 2004) and thus it can be used to monitor the real time effects of antimicrobials on bacterial killing (Salisbury *et al.*, 1999; Vasterlund *et al.*, 2004). Bacterial genes cloned into *Staphylococcus aureus*, *Escherichia coli* and *Salmonella enterica* serovar Typhimurium indicator strains have been used for detection of antimicrobial activity without the need for laborious plate counting and overnight incubation (Vasterlund *et al.*, 2004). Studies have shown quantifiable use of luminescence as a measure of cell viability and reported to show good correlation with standard recovery techniques such as viable counting under defined conditions (Jassim *et al.*, 1990). However, *in vitro* studies have shown that, although in general the relationship between bioluminescence and viable counts is closely correlated (Salisbury *et al.*, 1999; Thorn *et al.*, 2007), sometimes there are disagreements between the two methods. This is seen in the case where the given antibiotic inhibits multiplication (increase in viable number) or metabolism (Alloush *et al.*, 2003; Salisbury *et al.*, 1999). The *in vivo/in situ* detection of bioluminescent organism is non-invasive, allowing rapid monitoring of the infective state of cells both in culture and animal models (Alves *et al.*, 2011, Contag *et al.*, 1995; Francis *et al.*, 2000). Bioluminescence has been utilized to screen new PS and to investigate their efficacy of APDT against bacteria, and to evaluate their re-growth after APDT and to assess the toxicity of PS in the cells of the infected tissue (Alves *et al.*, 2011).

Bacterial bioluminescence has also been used in APDT studies focused on the application of water disinfection (Alves *et al.*, 2008). In this study a

bioluminescent *E. coli* was used to evaluate APDT by three cationic meso-substituted porphyrins under artificial ( $40 \text{ Wm/cm}^2$ ) and solar irradiation ( $\approx 620 \text{ Wm}^{-2}$ ) (Alves *et al.*, 2008; Alves *et al.*, 2011). Photoinactivation of *E. coli* was detected by a decrease of more than  $4 \log_{10}$  in bioluminescence (the detection limit of the method used) using the three porphyrins in 270 minutes of irradiation. The authors found that the inactivation patterns previously obtained for these PS using conventional methods of viable count (Alves *et al.*, 2008) were closely related to when the PS was assessed by the bioluminescence method. The authors concluded that the bioluminescence-based method is effective, sensitive, simpler, faster, more cost effective, and much less laborious than the conventional method as a screening for *in vitro* studies of photoinactivation (Alves *et al.*, 2008).

Bioluminescence methods of analysis have also been used in animal models to study APDT. In these studies wound infections (Hamblin *et al.*, 2002; Gad *et al.*, 2004; Demidova *et al.*, 2005) *Acinetobacter baumannii* infected burn infections in mice (Dai *et al.*, 2009) *Staphylococcus aureus* infected burn wounds in mice (Lambrechts *et al.*, 2005) were treated with APDT and the efficacy of the treatment was monitored with bioluminescence imaging. It was shown that there was a dose-dependent loss of luminescence upon illumination of treated cells with light that was related to bacterial killing (Hamblin *et al.*, 2002; Gad *et al.*, 2004; Lambrechts *et al.*, 2005). These investigations showed that monitoring bioluminescence is a successful method and allowed the monitoring of the infection progress in real time with low light imaging charge-coupled device (CCD) camera. These studies confirmed the important role of bioluminescence target organisms to monitor APDT effects under different conditions.

In a study to compare the effectiveness of APDT, bioluminescence imaging was used to study efficacy of standard endodontic treatment and the combined treatment to eliminate bacterial biofilms present in infected root canals (Garcez *et al.*, 2007). In this study single-rooted freshly extracted human teeth were inoculated with stable bioluminescent Gram-negative bacteria, *Proteus mirabilis* and *Pseudomonas aeruginosa* to form artificial 3-day biofilms in prepared root canals. Bioluminescence imaging was used to serially quantify bacterial burdens.

The PS employed in this study was a conjugate between polyethylenimine and chlorin(e6) as the photosensitizer (PS) and the light source was 660-nm diode laser light. Endodontic therapy alone reduced bacterial bioluminescence by 90% while APDT alone-reduced bioluminescence by 95%. The combination treatment reduced bioluminescence by more than 98%. Bioluminescence imaging is an efficient way to monitor endodontic therapy and antimicrobial PDT may be used to optimize endodontic therapy. However in this study the bioluminescent species are not oral periodontal pathogens. This study could be improved by carrying out the experiment with a bioluminescent strain of a periodontal pathogen. This will make the treatment more significant in periodontology.

### **1.12 Clinical applications of APDT and ECAS**

With the growing evidence of effectiveness of APDT against a wide range of micro-organisms by *in vitro* studies stimulated clinical applications *in vivo*. The main area of development of APDT is in dental applications, ophthalmology, dermatology and infectious diseases. APDT has been used to clinically treat bacterial infections in brain abscesses and non-healing ulcers (Kharkwal *et al.*, 2011). Clinical trials of APDT for gastric infections caused by *Helicobacter pylori* in 10 patients have been carried out which showed 99% reduction in bacterial load in some patients (Ganz *et al.*, 2005). Blue light alone was also tested for reduction in *Helicobacter pylori* infection (Lembo *et al.*, 2009) However, elimination of bacteria was not sustained as there was repopulation of bacteria days after treatment. In dermatological conditions such as acne, APDT has been used to eliminate *Propionibacterium acnes* using PS 5-aminolevulinate (ALA) and methyl aminolevulinate (MAL) (Kharkwal *et al.*, 2011). APDT for dental infections represents the largest growth of clinical application in APDT (Kharkwal *et al.*, 2011). Commercial application has developed a system called Periowave<sup>TM</sup> (Ondine Biopharma Corporation) marketed as a photodynamic disinfection system for use in dentistry. The evidence for clinical use of ECAS has also been shown in small scale case studies with positive results. ECAS used twice daily to wash infected ulcers (in 15 patients) was shown to reduce bacterial infections and aid debridement (Sekiya *et al.*, 1997). ECAS treatment of burn wounds infected with *P. aeruginosa* in rodents significantly improved their

survival rates (Nakae and Inaba, 2000). Furthermore one pilot study using extracted teeth showed that ECAS was more effective compared to sodium hypochlorite as a root canal cleaning solution (Solovyeva and Dummer, 2000). These results indicate the potential use of ECAS in sterilisation and disinfection in clinical settings.

### **1.13 Biofilm**

Bacteria occur in nature in two different growth forms, as planktonic cells (free-floating single cell organism) or as communities of cells known as biofilms (Costerton *et al.*, 1999). Biofilms constitute the predominant form of growth in nature (Costerton *et al.*, 2003). A microbial biofilm is defined as a structured community of bacterial cells enclosed in a self-produced polymeric matrix that is adherent to an inert or living surface and exhibiting phenotypic heterogeneity (Costerton *et al.*, 1999). The biofilm can consist of one or more type of species (bacterial or fungal) cells and the matrix, which consists of polysaccharides, proteins and extracellular DNA (Taraszkiwicz *et al.*, 2013). The structure that forms the biofilm contains channels in which nutrients can circulate and the cells in the different regions of the biofilm exhibit different patterns of gene expression (Costerton *et al.*, 1999). This complexity of biofilm structure and metabolism led to its comparison to tissue of higher organism (Costerton *et al.*, 1999). The biofilm formation is a complex process involving early, intermediate and mature stages (Taraszkiwicz *et al.*, 2013). Different species can form biofilms on different kinds of surfaces. Figure 1.10 shows stages in the formation of biofilm. The cell-to-cell communication is regulated in the biofilm by quorum sensing (QS) molecules that enable cell density “sensing” (Taraskiewicz *et al.*, 2013).

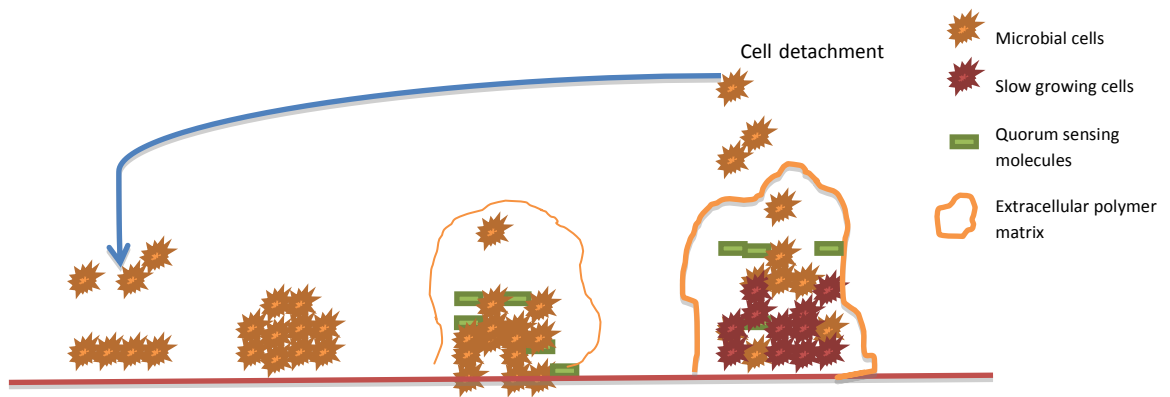


**Figure 1-10** The biofilm formation involves first attachment of planktonic cells to the surface followed by microcolony formation, during this stage quorum sensing molecule are produced and extracellular polymer matrix is formed around the microcolony. The final stage is the maturation of the biofilm to form mushroom shaped structures with expansion and dissemination. Microbial cells liberated from the mature biofilm can attach to another location or surface causing expansion of infection (diagram adapted from Taraszkievicz *et al.*, 2013).

The biofilm mode of growth allows the survival of bacteria in hostile environments and also protects the biofilm microbial cells against antimicrobial agents and from the host immune system (Costerton *et al.*, 1999; Bjarnsholt *et al.*, 2008). Biofilm infections are important clinically because bacteria in biofilms exhibit resistance to antimicrobial compounds and persistence in spite of sustained host defenses (Hall-Stoodley and Stoodley, 2009; Ammons, 2010). Multiple characteristics of the biofilm contribute to the resistance of biofilms to antimicrobial agents such as the growth status of the biofilm cells (Lewis, 2001). Most antibiotics target metabolically active cells. Therefore slow growing cells in the biofilm may contribute to resistance mechanisms. General stress response and resistance subpopulation also contribute to resistance (Lewis, 2001). Another contributing factor of biofilm resistance is restricted penetration. Biofilms are enclosed within an exopolymer matrix that can restrict the diffusion and bind antimicrobials thereby preventing the action of the antimicrobial on the biofilm cells (Mah and O'Toole, 2001). It is still not fully understood to what extent each of these factors contributes to biofilm resistance.

A recent study has shown that photodynamic therapy could be successful in combination with antibiotic action or host defence mechanisms on *S. aureus* biofilms (Di Pota *et al.*, 2009). This study showed that APDT combined with vancomycin or phagocytic activity from whole blood, successfully reduced the survival of staphylococcal cells within biofilms. This shows another method of using photodynamic therapy to treat superficial infections that are accessible to light. Moreover, this study describes that in addition to killing bacteria in the biofilms, PDT led to microbial cell detachment, and consequent disruption of biofilm architecture. In this study it was also shown that the thickness of a biofilm is not a hindrance to photosensitizer diffusion and light penetration. This may be an advantage because it is known that antibiotic action is hindered because of the slow diffusion of drug into the biofilm due to the presence of extracellular polymeric substances (EPS). Currently numerous studies have been carried out to test effects of APDT against biofilms. Table 1.2 shows a summary of the APDT studies carried out on biofilms using different biofilm models.

#### **Methods to study biofilms (*in vitro* Biofilm Models)**

A single standardised method to study biofilm is not available. To date various biofilm models have been developed. Biofilm *in vitro* models are grouped into two categories: closed or static systems or open or dynamic systems. In closed systems there are limited nutrients available. Closed systems are simple to use and may be sufficient to address basic questions about biofilm formation, physiology and architecture (Lebeaux *et al.*, 2013). They offer a number of advantages such as a low cost, easy set-up, and high throughput screens. This includes colony biofilm model and microtiter plates and Calgary biofilm device. However, all batch culture systems suffer from changes over time including changes in substrate concentration, product formation, pH, redox, O<sub>2</sub> partial pressure and production rate of new cells.

The principle of open or dynamic system models is similar to continuous cultures, in which spent culture consisting of wastes, metabolic byproducts, and dispersed and dead cells are constantly replaced by fresh medium (Lebeaux *et al.*, 2013). The advantage over the closed systems is that they generally allow the control of

environmental parameters such as shear forces, and have been therefore extensively used to study the physical and chemical resistance of biofilms and are also more comparable to biofilm formation *in vivo* (Lebeaux *et al.*, 2013).

**Table 1- 2 APDT for biofilms**

<b>Inoculum Microorganisms (Photosensitizer)</b>	<b>Treatment protocol</b>	<b>Killing effect</b>	<b>Model</b>
<p>Clinical isolates of multidrug-resistant <i>Pseudomonas aeruginosa</i> and methicillin-resistant <i>Staphylococcus aureus</i></p> <p>MB</p>	<p>Biofilm grown discs treated with 100 µL of the photosensitizer and incubated for 5 minutes in the dark. Two treatment groups.</p> <p>Group 1 300 µg/mL were exposed to 664 nm light at a dose rate of 150 mW/cm<sup>2</sup> and a light dose of 60 J/cm<sup>2</sup> for 400 seconds.</p> <p>Group 2 500 µg/mL group were exposed at a dose rate of 76 mW/cm<sup>2</sup> and two light doses of 55 J/cm<sup>2</sup> separated by a 5 minutes dark time between each light dose. Control groups of no treatment, light alone and MB alone were also performed</p>	<p>APDT reduced the CRS polymicrobial biofilm by &gt;99.9% after a single treatment.</p> <p>Group 1 300 µg/mL MB Mean log reduction of 6.67</p> <p>Group 2 500 µg/mL MB Mean log Reduction of 7.39</p>	<p>FC 270 dual flow system Biofilm grown Beil <i>et al.</i>, 2011 (a)</p>
<p><i>Enterococcus faecalis</i></p> <p>TBO</p> <p>MB</p>	<p>APDT commercial systems (Denfotex and Helbo)</p> <p>Denfotex system- each disc was placed in a well containing 1 mL of photosensitizer [i.e. TBO at 12.7 mg/L), pH 5]. After a 2min-pre-irradiation time), discs were uniformly irradiated for 150 s at 100 mW with a soft diode laser emitting at 635nm, The antimicrobial action of the second a PDT system (Helbo) (MB at a concentration of 10 mg/mL) After 3 min pre-incubation time, excess dye was removed and discs were irradiated for 2 min with a soft laser (Helbo Theralite Laser) with a wavelength of 660 nm, an output power of 75 mW</p>	<p>Denfotex system Mean log reduction 0.84</p> <p>Helbo system- Mean log reduction 1.9</p>	<p>biofilms were grown on dentine discs in a microtiter plate, Meire <i>et al.</i>, 2012</p>

<p>Clinical isolates of multidrug-resistant <i>Pseudomonas aeruginosa</i> and methicillin-resistant <i>Staphylococcus aureus</i></p> <p>MB</p>	<p>After the photosensitizer solution was sprayed into the lumen of the biofilm coated endotracheal tube, the photosensitizer pre-incubation was 5 minutes.</p> <p>Treatment parameters included: 500 µg/mL of MB, a fluence rate of 150 mW/cm of catheter length and a total light dose of 12 minutes on, 5 minutes off and 12 minutes on again.</p>	<p>Mean log reduction of 3</p>	<p>biofilm coated endotracheal tube Beil <i>et al.</i>, 2011 (b)</p>
<p><i>Candida spp. Trichosporon mucoides · Kodamaea ohmeri</i></p> <p>zinc 2,9,16,23- tetrakis (phenylthio)- 29H, 31H-phthalocyanine (ZnPc)</p>	<p>The biofilm formed by each strain was immersed in 250 µl of a solution of ZnPc for 5 min (pre-irradiation time) in an orbital shaker</p> <p>The light source used was a gallium-aluminum-arsenide (GaAlAs) laser (Easy Laser, Clean Line, Taubaté, SP, Brazil) with a wavelength of 660 nm, output power of 0.035 W, and illuminated area of 0.38 cm<sup>2</sup>. A fluence of 26.3 J cm<sup>2</sup> (energy of 10 J and time of 285 s) and a fluence rate of 92 mWcm<sup>2</sup> were used.</p>	<p>A mean reduction of 0.45 log was achieved for <i>Candida spp.</i> biofilms, and a reduction of 0.85 and 0.84, were achieved for biofilms formed by <i>T. mucoides</i> and <i>K. ohmeri</i>, respectively.</p>	<p>Biofilms formed by yeasts after 48 h in the bottom of 96-well microtiter plates Junqueira <i>et al.</i>, 2012</p>
<p><i>P. aeruginosa PAO1</i> 5,10,15,20-tetrakis(1-methyl- pyridino)-21H,23H-porphine, tetra-p-tosylate salt (TMP)</p>	<p>Exposing static biofilms to 5,10,15,20-tetrakis(1-methyl-pyridino)-21H,23H-porphine, tetra-p-tosylate salt (TMP) followed by irradiation. TMP concentrations of 100 µM (0.14 mg ml<sup>-1</sup>) and 225 µM (0.35 mg ml<sup>-1</sup>). Samples were irradiated for various exposure times at an intensity of 220– 240 Joules/cm<sup>2</sup>.</p> <p>Biofilms were visualized using confocal laser scanning microscopy (CLSM) and cell viability determined using the LIVE/DEAD BacLight viability assay and standard plate counts.</p>	<p>At a concentration of 100 µM TMP, there was substantial killing of <i>P. aeruginosa</i> PAO1 wild-type and pqsA mutant biofilms with little disruption of the biofilm matrix or structure.</p> <p>Exposure to 225 µM TMP resulted in almost complete killing as well as the detachment of wild-type PAO1 biofilms.</p> <p>4.1-log<sub>10</sub> and a 3.9-log<sub>10</sub> reduction in viable cells of wild-type PAO1 and pqsA mutant strains, respectively.</p>	<p>Static biofilm grown on glass slides Collins <i>et al.</i>, 2010</p>

Multi species oral bacteria grown from human saliva sample The biofilms consisted of 32.8% streptococci, 6.5% <i>Veillonella spp.</i> , 0.1% <i>Actinomyces spp.</i> , and 0.1% Gram- negative anaerobes. TBO	Biofilm was exposed to 25 µg/ml TBO and 31.5 J of laser light	97.4% bacteria killed	Multi-species biofilms were grown on 5-mm diameter discs prepared from cellulose nitrate  O'Neill <i>et al.</i> , 2002
Multi species bacterial biofilm developed from plaque samples MB	The light parameters used in this study for bacterial suspensions and biofilms were 100 mW/cm <sup>2</sup> (power density) and 30 J/cm <sup>2</sup> (energy fluence) at 665nm. The MB concentration at 25 µg/mL and 50 µg /mL exposed to light for 5 minutes	8.4% killed at 25 µg/mL and 31% killed at 50 µg/mL	96-well microtiter plates  Fontana <i>et al.</i> , 2009
<i>Streptococcus mutans</i> Erythrosine	Biofilms exposed to 20 µmolL <sup>-1</sup> erythrosine and light from dental halogen curing unit light intensity at 600mW/cm <sup>2</sup> for 30s energy dose 18J/cm <sup>2</sup>	74% bacteria killed	24 well cell culture plate Lee <i>et al.</i> , 2012
<i>Streptococcus sanguis</i> aluminium disulphonated phthalocyanine (AlPcS <sub>2</sub> )	Biofilms were grown on hydroxyapatite, irradiated with up to 12.2J of light from a gallium aluminium arsenide laser in the presence of aluminium disulphonated phthalocyanine (AlPcS <sub>2</sub> )	5 log kill	Biofilm grown on hydroxyapatite,  Wilson <i>et al.</i> , 1996
<i>S.aureus</i> and <i>E.coli</i> MB Toluidine blue (TBO) Malachite green	Biofilm subjected to PDT using a 600nm diode laser and PS concentration 37.5 to 300 µM	300 µM MB: 0.8log <i>E. coli</i> kill. <i>S. aureus</i> 1 log kill. 150 µM TBO 0.9 <i>E. coli</i> kill. <i>S. aureus</i> 1 log kill 3000 µM TBO <i>E. coli</i> 1.6 kill <i>S. aureus</i> 4 log kill	Biofilms grown on sample pieces of acrylic resin  Vilela <i>et al.</i> , 2011
<i>Pseudomonas aeruginosa</i> PAOI	350 µl of 0, 5, 10, 20, and 40 mM α-ALA, respectively, in the dark for 1 h. Four disks treated with different concentrations of δ-ALA were exposed to the LED. The	When treated with 20 and 40 mM µ-ALA, about 2-log reduction in biofilm density was observed. When exposed to	Rotating disc reactor with removable

	<p>fluence of light delivered was 100 mW cm<sup>2</sup> for 20 min. All of the samples exposed to either light or drug alone were put into test tubes containing 10 ml PBS. The test tubes were vortexed for 1 min in order to remove the biofilms from the disks. The resultant suspension was used for both viable and total cell count.</p>	<p>120 J cm<sup>2</sup>, the biofilm density decreased with increasing concentrations of δ-ALA treatment. No viable cells were detected when 20 and 40 mM of δ-ALA were applied. <i>P. aeruginosa</i> biofilm regrowth after δ- ALA-mediated PACT. After biofilm samples were treated with 20mM of δ-ALA and exposed to 120 J cm<sup>2</sup> light dose, No viable cell was detected on the PACT-treated disk until 24 h of regrowth. Biofilms appeared to re-accumulate thereafter. To completely eliminate the possibility of re-growth, the PACT treated biofilms were allowed for recover for 12 h, followed by another PACT treatment in a separate experiment. The biofilm was completely eradicated and not a single viable cell was found at the end of experiment.</p>	<p>stainless steel discs  Lee <i>et al.</i>, 2004</p>
--	--	---	---

### 1.13 Aims of the investigation:

**Aim 1: To develop reliable kill curve assays (based on bioluminescence) and measure the target microbial kill rate and final populations at the end of the treatment period.**

The traditional methods of measuring kill rates following antimicrobial treatments by recovering cell survivors (viable count) is impossible to apply when the kill kinetics are either rapid, or complex in nature (e.g. biphasic or multiphasic survival curves with “shoulders”).

**Aim 2: To use standardised assays to measure the killing effects of ROS-based biocide treatments**

The second aim was to use the methods and approaches developed in the first aim, and apply the developed assay to the study of two different types of ROS-based biocide treatments (APTD and ECAS) and compare treatments in terms of their likely mechanisms of ROS generation and killing.

**Aim 3: To compare kill rates of target microbes (prokaryotic) with mammalian (eukaryotic) cells**

The third aim was to compare the kill rates of target microbes with mammalian cells under the same treatment conditions and measure the equivalent of an *in vitro* therapeutic index, to help gauge the likelihood of treatment damaging the host *in vivo*.

**Aim 4: To measure the potential of biocides to induce genotoxic damage to mammalian cells by use of COMET assays and compare treatments**

It is insufficient to show that a particular treatment is (or is not) cytotoxic to mammalian cells if ROS agents can induce genotoxic damage.

**Aim 5: To measure the effects of treatments on target micro-organisms when growing in biofilm mode (using a continuous matrix perfusion model) and compare standard treatment on fast growing and slow growing cells.**

In addition to the concentration of ROS species being an important factor in determining the kill rate of target species there are also biological variables such as growth rate and physiological state of the organisms that must be considered, particularly when cells are growing in biofilm mode.

## **Chapter 2: General Materials and Methods**

## 2.1 Bioluminescent bacteria and growth conditions

The two bioluminescent target organism used in this investigation were a recombinant bioluminescent strain *Pseudomonas aeruginosa* MCS5-lite and a recombinant bioluminescent strain *E. coli* Nissle 1917 pGLITE kindly provided by UWE microbiology laboratory.

The *Pseudomonas aeruginosa* MCS5-lite strain was produced previously by transforming *Pseudomonas aeruginosa* PAO1 SEI (ATCC 15692) with a recombinant plasmid containing the *luxCDABE* gene cassette of *Photorhabdus luminescens* (Marques *et al.*, 2005).

*Pseudomonas aeruginosa* MCS5-lite was maintained on nutrient agar (Oxoid Ltd, Basingstoke, UK) containing gentamicin (10 mg/l) (Sigma-Aldrich, Dorset, UK), the selective agent for the recombinant plasmid.

*E. coli* Nissle 1917 was previously transformed with the recombinant plasmid pGLITE (method cited in Robinson *et al.*, 2011), encoding the *P. luminescens lux* operon from plasmid pLITE27 inserted into the broad-host-range plasmid PBBR1MCS-2.

The previously transformed *E. coli* pGLITE Nissle 1917 was cultured on nutrient agar (Oxoid Ltd, Basingstoke, UK) supplemented with 10 mg/liter kanamycin (Sigma-Aldrich, Dorset, UK), the selective agent for the recombinant plasmid.

## 2.2 Growth and maintenance of micro-organisms

Methicillin-resistant *Staphylococcus aureus* (MRSA) (methicillin-resistant Llewellyn strain SMH 22115) and *S. aureus* ATCC 6538 kindly provided by UWE were maintained from frozen stock on nutrient agar (Oxoid Ltd, Basingstoke, UK) and broth cultures were grown using 1% (w/v) tryptone, 0.5% (w/v) yeast extract (TYE) (Oxoid Ltd Basingstoke, UK).

Batch cultures of *Pseudomonas aeruginosa* MCS5-lite, *E. coli* Nissle 1917 pGLITE and *S. aureus* ATCC 6538 and MRSA (methicillin-resistant Llewellyn strain SMH 22115) were grown in 1% (w/v) tryptone, 0.5% (w/v) yeast extract

(TYE) (Oxoid Ltd Basingstoke, UK) with the selective antibiotic where appropriate.

For experiments on photodynamic killing, microbial cells were obtained from broth cultures. These were produced following inoculation and incubation of test species in 10 ml volume of appropriate liquid medium. All species were incubated in a shaking incubator (model S 150, Stuart shakers, UK) at 37 °C for up to 24 hours (stationary phase cultures) or for shorter periods of time (4 to 6 hours) to obtain mid- or late exponential phase.

## **2.3 Bacterial growth curve**

### **2.3.1 *P. aeruginosa* MCS5-lite**

Overnight cultures of *P. aeruginosa* MCS5-lite were grown in 1% tryptone-0.5% yeast extract (TYE) broth (with addition of gentamicin (10 mg/l) and used to inoculate 50ml of broth of the same composition within 250ml flask to a standardized OD<sub>540</sub> of 0.02. Flasks were then incubated at 32 °C with orbital shaking 200rpm (model S 150, Stuart shakers, UK) and 3 replicate cultures were used to follow the growth kinetics of both strains. Viable counts were performed as previously described. The optical density (OD<sub>540</sub>) was measured using a light photometer (Helios, Thermo Electron Corporation, UK), and bioluminescence measured using a single-tube luminometer (Junior LB9509, Bethhold Technologies UK Ltd., Harpenden, UK) (method adapted from Thorn, 2009).

### **2.3.2 *E. coli* Nissle 1917/pGLITE**

Overnight cultures of *E. coli* Nissle 1917/pGLITE were grown in 1% tryptone-0.5% yeast extract (TYE) broth (with addition of kanamycin (10 mg/l) and used to inoculate 50ml of broth of the same composition within a 250ml flask to a standardized OD<sub>600</sub> of 0.02. Flasks were then incubated at 37 °C with orbital shaking 250rpm (model S 150, Stuart shakers, UK) and 3 replicate cultures were used to follow the growth kinetics of both strains. Viable count, OD<sub>600</sub> and bioluminescence were measured as previously described (method adapted from Thorn, 2009).

### **2.3.3 Log-fold dilution standards**

An exponential phase cell suspension of *P. aeruginosa* MCS5-lite and *E. coli* Nissle 1917/pGLITE (broth cultures of organisms grown to known cell density) was used to prepare a series of log fold dilutions. The dilutions were used to measure both bioluminescence and viable count to assess the correlation between the two methods (method adapted from Thorn, 2009).

### **2.4 Photosensitizer**

MB (C.I. 52015; Sigma, Poole, U.K) dye content, 85% was used as the PS in all experiments. A stock solution was prepared by dissolving MB in deionized water to give a 2 mg/ml concentration. This stock solution was filter-sterilized using a 0.22- $\mu$ m-pore size membrane filter (Fisher Scientific) and stored in the dark at 4<sup>0</sup>C until use. The stock solution was diluted to obtain the test solutions of appropriate concentration and fresh stock solutions were prepared as required.

### **2.5 Light source**

The light source used in all APDT experiments were polychromatic light produced from a standard slide projector (Reflector Diamator 2500 AF, Portugal) equipped with a 250 W lamp and built-in infra red filters to produce white light (400-700nm). The emission spectrum of the projector light beam was previously measured with a diode array spectrophotometer (4851A, Hewlett Packard, Blacknell, Berks, UK) with a total power output (white light ) was 2.8 W with infrared power less than 1.0% of the total (Zeina, 2001). The standard distance (vertical distance) to target was 12.5 cm. The light intensity was measured using a light meter (Skye Instruments Ltd., Llandrindod Wells, Powys, UK) and shown to be 9.47 mW/cm<sup>2</sup> for planktonic cultures.

The light source used in all biofilm experiments (chapter 7) was white light via a fibre optic cable (Thorlabs Limited, Ely, Cambridgeshire) to give 16 mW/cm<sup>2</sup> for biofilm studies.

## **2.6 APDT Studies: Development of standard bioluminescent assay to study photodynamic effects**

A 1ml volume of cell culture suspension was prepared by taking 100  $\mu\text{l}$  of  $10^8$  cfu/ml log phase culture target organism (target organism grown as described in section 2.1), 50  $\mu\text{l}$  of MB to give a final assay concentration of 10  $\mu\text{g/ml}$  MB and 850 $\mu\text{l}$  of Phosphate Buffer Solution (PBS pH 7.4) (In APDT mechanism studies (section 2.12) scavenger/enhancer was added into the system). This cell mixture tube was exposed to polychromatic light produced by standard slide projector by keeping it under the projector at a measured distance of 12.5 cm (standard experiments). At each measured time interval the tube was loaded into the luminometer to measure the bioluminescence (for bioluminescence target organisms) and a 20 $\mu\text{l}$  sample was removed to enumerate the cells by viable count. After measuring bioluminescence and taking samples for viable count, the tube (borosilicate glass tube (12 by 75 mm; Fisher Scientific, Loughborough, United Kingdom) was put back under the projector to complete the irradiation time. For all the experiments bioluminescence was measured using the single-tube luminometer (Junior LB9509, Bethhold Technologies UK Ltd., Harpenden, UK) and viable counts were carried out by log serial dilutions ( $10^{-1}$ - $10^{-5}$ ) and plating the appropriate dilutions on nutrient agar count medium.

The standardised assay (total light dose of 11  $\text{J/cm}^2$  at light intensity of 9.4  $\text{mW/cm}^2$  and in the presence of MB (10  $\mu\text{g/ml}$ ) (when present) was used, and known concentrations of target organism for the treatment. The three controls (a) bacteria alone (culture diluted in PBS) (b) bacteria alone with light (light control) (c) bacteria and MB without light (Dark control).

The reduction in the number of survivors after APDT treatment was shown by reduction in bioluminescence. The data from these experiments (change in bioluminescence readings) were plotted on a graph to show reduction in bacterial bioluminescence after APDT together with data obtained for the controls.

### **2.6.1 APDT Data analysis**

To show the kill kinetics of APDT for different target organism a graph was constructed with log change in light output for bioluminescent species and for non-bioluminescent species log change in viable counts against time. For each kill curve linear regression analysis was performed. Statistical analyses were carried out to determine if the correlation was statistically different from control groups. Graph construction and statistical modelling was conducted with the use of GraphPad Prism version 5 for windows.

### **2.7 ECAS assay: preparation of inoculum**

An overnight culture of *E. coli* Nissle 1917/pGLITE was grown at 37 °C with shaking at 250 rpm in nutrient broth supplemented with 10 mg/liter kanamycin. This was subcultured with appropriate dilution into 10 ml fresh prewarmed nutrient broth supplemented with 10 mg/liter kanamycin and grown at 37 °C with shaking at 250 rpm until an OD<sub>600</sub> of 0.6 was achieved. The cells were then centrifuged for 20 min at 3000 g, washed twice in an equal volume of sterile Ringer's solution, and then resuspended in 10 ml sterile Ringer's solution to obtain a specified cell density (method adapted from Robinson *et al.*, 2011).

### **2.8 Preparation of ECAS**

ECAS was generated according to the manufacturer's instructions (Purest Solutions Ltd., London, United Kingdom) with a pH of 1.826 and a redox potential of 1139.3mV and diluted in deionized water where required.

### **2.9 ECAS single tube luminometric assay**

A 100 µl volume of *E. coli* Nissle 1917/pGLITE (final concentration 10<sup>7</sup> cfu/ml) and 900µl of Ringer's was added to a borosilicate glass tube (12 by 75 mm; Fisher Scientific, Loughborough, United Kingdom) and loaded into a Sirius luminometer (Berthold Detection Systems, Pforzheim, Germany). For ECAS mechanism studies (section 2.12) scavenger/enhancer was also added into the system). The bacterial bioluminescence of the cell culture suspension was recorded by automated protocol that was set up to record every 0.2 s for 15 s prior to automated injection of ECAS to allow light levels to equilibrate. ECAS (diluted

where appropriate) was injected by the automated injection system at 15 seconds (this time was recoded as time zero corresponding to the start of ECAS interaction with bacteria) and data collected every 0.2 s until the end of the experiment. Control light levels were established by replacing the ECAS with Ringer's solution, and background light levels were established by replacing the inoculum with Ringer's solution (modified method from Robinson *et al.*, 2011).

### **2.9.1 ECAS Data analysis**

To show the kill kinetics of ECAS for target organism a graph was constructed with log change in light output. For each kill curve linear regression analysis was performed. Graph construction and statistical modelling was conducted with the use of GraphPad Prism version 5 for windows.

### **2.10 Photodynamic and ECAS mediated effects on bioluminescence output in the presence of reactive oxygen species inhibitors/enhancer**

Stock solutions of the inhibitor were prepared immediately before use and filter sterilised using a 0.22- $\mu$ m-pore size membrane filter (Fisher Scientific) prior to their addition to the reaction mixture at the required concentration. All the inhibitors were obtained from Sigma Aldrich. The inhibitors used in the assays were DMTU, DMSO, mannitol, tryptophan, histidine, sodium azide. The enhancer D<sub>2</sub>O was substituted for H<sub>2</sub>O in buffers (PBS).

Into the standard APDT and ECAS assay (procedure described above were used for APDT (section 2.6) and ECAS (section 2.10) appropriate test inhibitors was added at the required concentration. In APDT the cell mixture was exposed to light from a standard slide projector by keeping it under the projector at a measured distance of 12.5 cm light and at set time intervals the tube was loaded into the single-tube luminometer (Junior LB9509, Bethhold Technologies UK Ltd., Harpenden, UK) and bioluminescence readings measured (for bioluminescence target organisms). For non-bioluminescent target cells a 20 $\mu$ l sample was removed to enumerate the surviving cells by viable count. After measuring bioluminescence and taking samples for viable count the tube

(borosilicate glass tube (12 by 75 mm; Fisher Scientific, Loughborough, United Kingdom) was put back under the projector to complete the irradiation time.

In ECAS assay the bioluminescence of bacterial suspension with or without the inhibitor was recorded by automated protocol every 0.2 s for 15 s prior to automated injection of ECAS for light levels to equilibrate, after this delay period ECAS (diluted where appropriate) was injected by the automated injection system (this time was recoded as time zero corresponding to the start of ECAS interaction with bacteria) and data collection every 0.2 s until the end of the experiment. Appropriate controls were carried out by replacing ECAS with the control solution.

## **2.11 The evaluation of the role of ROS and $^1\text{O}_2$ in APDT by detection of formation by SOSG, APF and HPF Assay**

### **2.11.1 Chemicals**

The fluorescent probes SOSG, HPF and APF were obtained from Invitrogen as solutions in methanol (SOSG) or dimethylformamide (APF and HPF).

### **2.11.2 Procedures for the fluorescent probe (SOSG, APF and HPF) assay in APDT**

To detect the generation of singlet oxygen in a cell-free system were carried out in  $1 \times 1 \times 3$  cm glass cuvettes. The cuvettes containing the solutions of MB and the probe was exposed to visible light from a projector placed at 12.5 cm vertically. The light intensity at this distance was measured to be  $9.4 \text{ mW/cm}^2$ . The total light dose applied to the samples was in the range of  $0\text{-}11 \text{ J/cm}^2$  (over 20 minutes period), by varying the irradiation time. The fluorescence was monitored by acquisition of the fluorescence signal by fluorimeter. The measurements were then expressed as fluorescence over time for solutions containing: APDT:  $5 \mu\text{M}$  SOSG and  $10 \mu\text{g/mL}$  MB exposed to light (light dose  $0\text{-}11 \text{ J/cm}^2$ ), dark control: SOSG and  $10 \mu\text{g/mL}$  MB in the dark for 20 minutes, control:  $5 \mu\text{M}$  SOSG on its own. To measure the fluorescence  $5 \mu\text{M}$  APF/HPF the same procedure was repeated replacing the SOSG probe with  $5 \mu\text{M}$  APF or HPF.

### **2.11.3 Procedures for the fluorescent probe (SOSG, APF, HPF) assay in ECAS**

In a  $1 \times 1 \times 3$  cm glass cuvettes fluorescent probe (5  $\mu$ M SOSG, APF, HPF) and a diluted solution of ECAS (1% v/v or 5% v/v) was mixed and was immediately loaded into fluorimeter and the fluorescence signal was measured 5 minutes.

### **2.11.5 Quenching studies with fluorescence probes (SOSG, APF, HPF)**

Using the procedure described in the above sections the interaction between fluorescent probes  $^1\text{O}_2$  and  $\bullet\text{OH}$  specific inhibitors or enhancers were assessed for APDT or ECAS in the presence of inhibitors (tryptophan, histidine,  $\text{NaN}_3$  mannitol, DMSO, enhancer ( $\text{D}_2\text{O}$ ) using SOSG, APF or HPF in the systems

## **2.12 Methods to determine the cytotoxic effects of APDT on keratinocytes and lymphocytes**

### **2.12.1 Keratinocytes culture conditions**

The human keratinocyte cell line, H103 (kindly donated by UWE, Bristol, UK) was cultured in  $75\text{cm}^2$  tissue flasks in 20 ml volumes DMEM:F12 (1:1) containing 2.5 mM L-glutamine, 0.5  $\mu\text{g}/\text{ml}$  hydrocortisone (all Sigma Aldrich) and heat inactivated 10% FBS (FBS Gold, PAA Laboratories Ltd. Termare Close, Houndstone Business Park, Yevil Sommerst). Cells were incubated at  $37^\circ\text{C}$ , 95% air, 5%  $\text{CO}_2$  in a humidified incubator for 3 days until the cell monolayer became confluent. The growth medium was replaced every 3 days as required if indicated by change in pH. Upon reaching 70% confluence, the cells were washed with phosphate buffered saline (PBS) and trypsinized for 3 minutes at  $37^\circ\text{C}$  with 0.25% trypsin. Cells were passaged and re-seeded at  $1.5 \times 10^5$  cells/ml.

### **2.12.2 T lymphocytes culture conditions**

The human T lymphocytes cells line Jurkat cells (cells in suspension), (kindly donated by CRIB, UWE, Bristol, UK) was cultured in  $75\text{cm}^2$  tissue flasks in 20ml volumes of RPMI 1640 medium supplemented with heat inactivated 10% FBS (FBS Gold, PAA Laboratories Ltd. Termare Close, Houndstone Business Park, Yevil Sommerst), 10U/ml penicillin (Sigma Aldrich) and  $100\mu\text{g}/\text{ml}$  streptomycin

(all Sigma Aldrich). When cells were 70% confluent ( $6 \times 10^5$  cells/ml), they were split 1:4 with fresh media.

### **2.12.3 Photosensitizer and light source**

MB (dye content approximately 85%, Sigma, UK) solution were prepared fresh for each experiment in sterile PBS (pH 7.4), filter-sterilized and kept in the dark. The source of light placed at 12.5cm giving  $9.47 \text{ mW/cm}^2$  (as described in section 2.5).

### **2.12.4 Antimicrobial Photodynamic treatment of keratinocytes**

Aliquots of 20 mL suspension containing  $1.5 \times 10^5$  cells/ml H103 culture were seeded in 96 well plates (100  $\mu\text{l}$  in each well) and incubated for 24 hours for the cells to attach to the bottom of the 96 well plates at  $37^\circ\text{C}$  in 95% air, 5%  $\text{CO}_2$ . After 24h of cell incubation, the growth medium was removed from all wells and the cells were washed with PBS. For APDT treatments into each well (n=6), 100  $\mu\text{l}$  MB to give a final concentration of 10  $\mu\text{g/mL}$  (diluted in PBS) was added and were irradiated with light (20 min). Following treatment the MB solution mixture was removed and washed cells 4 times in PBS to remove any residual MB solution; to test the immediate cytotoxicity effects of APDT on H103 cells, viability tests were carried out immediately. To test for the recovery of the cells after treatment the cells were re-supplied with growth medium and incubated overnight at  $37^\circ\text{C}$  for 24-hour recovery period before viability tests were carried out. For both immediate and following 24h recovery period, controls were included in the 96 well plate (for each condition n=6 was repeated 3 times): (a) cells not treated with MB or light (cells exposed to same procedure with PBS (the untreated control)), (b) cells treated with MB but not exposed to light (dark control cells incubated 10  $\mu\text{g/mL}$  MB (diluted in PBS) for 20 minutes in the dark), (c) cells exposed to light (20 min) in the absence of MB (light control cells in PBS exposed to light (same irradiation dose as the treatment). After treatment was completed the viability of cells were assessed using the neutral red method described in section 2.12.11.

### **2.12.5 Antimicrobial Photodynamic treatment of keratinocytes in the presence of FBS**

Aliquots of 20 mL suspension containing  $1.5 \times 10^5$  cells/ml H103 culture were seeded in 96 well plates (100  $\mu$ l in each well) and incubated for 24 hours for the cells to attach to the bottom of the 96 well plates at 37°C in 95% air, 5% CO<sub>2</sub>. After 24h of cell incubation, the growth medium was removed from all wells and the cells were washed with PBS. FBS (FBS Gold, PAA Laboratories Ltd. Termare Close, Houndstone Business Park, Yevil Sommerst) was added into the cell mixture in 96 well plate at different concentrations (10%, 25%, 50% v/v) for each treatment conditions. The conditions tested were (a) treatment MB final concentration 10  $\mu$ g/mL diluted in PBS with different concentration of FBS and exposed to light dose (total light dose 11 J/cm<sup>2</sup>) (b) dark control with MB final concentration 10  $\mu$ g/mL diluted in PBS with different concentration of FBS and incubated for 20 minutes (c) light control cells exposed to light only (total light dose 11 J/cm<sup>2</sup>) (d) untreated cell as control. After treatment was completed the viability of cells were assessed using the neutral red method described in section 2.12.11.

### **2.12.6 Antimicrobial Photodynamic treatment Co-mix assay**

The co-mix assay was carried out by first growing adherent keratinocytes in 96 well plate until 70% confluence ( $1.5 \times 10^5$  cells/ml) and the cell culture media was removed just before the treatment and *E. coli* Nissle 1917 pGLITE ( $1.5 \times 10^7$  cells/ml) added and the treatment containing the MB (10  $\mu$ g/mL) diluted in PBS was added in to the mammalian cell mixture and exposed to light for 20 minutes (total light dose 11 J/cm<sup>2</sup>). During the experiment, every 5 minutes, samples were taken to measure the light output by the bacterial cells using a bench luminometer. After treatment was completed, the bacterial cell mixture was removed and the adherent keratinocytes were washed twice with PBS and neutral red viability test was carried out as described in section 2.12.11.

### **2.12.7 ECAS treatment of keratinocytes**

Aliquots of H103 culture suspension ( $1.5 \times 10^5$  cells/ml) were seeded in 96 well plates (100  $\mu$ l in each well) and incubated for 24 hours for the cells to attach to the bottom of the 96 well plates at 37°C in 95% air, 5% CO<sub>2</sub>. After incubation from each well of 96 well plate the media was removed and different concentration of ECAS diluted (5%, 10%, 25%v/v) in ringers solutions was added and for the control wells the media was replaced by ringers solution and incubated for 30 minutes. After treatments the cells were washed twice with PBS. In one group of treated cells and controls the viability tests were carried out immediately and in the other group the fresh media was added and incubated for 24 hours before neutral red viability tests as described in (section 2.12.11) were carried out.

### **2.12.8 ECAS treatment of keratinocytes in the presence of FBS**

Aliquots of keratinocyte (H103) culture suspension ( $1.5 \times 10^5$  cells/ml) were seeded in 96 well plates (100  $\mu$ l in each well) and incubated for 24 hours for the cells to attach to the bottom of the 96 well plates at 37°C in 95% air, 5% CO<sub>2</sub>. After incubation the media from each well was removed and different concentration of ECAS (diluted 5%, 10%, 25%v/v) in ringers solutions and supplemented with different concentration of FBS (final concentration 1%, 5, 10% v/v) was added. For the control well the media was replaced by ringers solution and incubated for 30 minutes. After treatments the cells were washed twice with PBS. Then neutral red viability tests (as described in section 2.12.11) were carried out.

### **2.12.9 Antimicrobial Photodynamic treatment of T-lymphocytes**

Aliquots of T-lymphocytes culture suspension ( $8 \times 10^5$  cells/ml) were centrifuged at 1,200 rpm for 5 minutes to pellet cells. The media was discarded and the pellet gently resuspended in 10 ml warm medium, and the cell concentration adjusted to  $1 \times 10^5$  cells/ml. This suspension was dispensed into 96 well plate (100  $\mu$ l in each well). For APDT, MB final concentration 10  $\mu$ g/mL was added into the cell suspension in media and exposed to light for 20 minutes (total light dose 11 J/cm<sup>2</sup>), for dark control MB final concentration 10  $\mu$ g/mL was added into the cell

suspension in media and kept in the dark for 20 minutes. For light control the cell suspension was exposed to light only for 20 minutes (total light dose 11 J/cm<sup>2</sup>) and the control untreated cells. After the experiment cells were centrifuged at 1,200 for 5 minutes and resuspended in fresh media and then viability tests (section 2.12.11 MTS) were carried out immediately to determine the immediate cytotoxic effects and at 24h to test for recovery of cells after treatment. For each condition (n=6) the experiment was repeated 3 times.

#### **2.12.10 ECAS treatment of T-lymphocytes**

Aliquots of T-lymphocytes culture suspension ( $8 \times 10^5$  cells/ml) were centrifuged at 1,200 rpm for 5 minutes to pellet cells. The media was discarded and resuspend pellet gently in 10 ml warm medium cell and concentration adjusted to  $1 \times 10^5$  cells/ml. This suspension was dispensed into 96 well plate (100  $\mu$ l in each well) and into each well, ECAS (5,10,25 v/v) or positive control, bleach (0.5% v/v) was added to the required concentration and incubated for 30 minutes at 37°C in 95% air, 5% CO<sub>2</sub>. After 30 minutes incubation the cells were centrifuged and resuspended in fresh media. In one group of the treated cells viability tests (section 2.12.11 MTS) were carried out immediately after treatment and in the second group the cells were resuspended in fresh media and incubated for 24 hours at 37°C in 95% air, 5% CO<sub>2</sub> to measure 24h recovery

#### **2.12.11 Cell viability tests**

##### **Trypan blue test**

The percentage of viable cells was determined using trypan blue dye exclusion. The cell suspension (200 $\mu$ l) was mixed with an equal volume of filter sterilised 0.4% (w/v) trypan blue (Sigma-Aldrich), in PBS and cells observed under the microscope. As a non-vital dye, trypan blue is excluded from living cells but stains dead cells.

##### **Neutral red assay**

Neutral red method was employed to test viability of keratinocytes cells after exposure to different treatment conditions.

Neutral red (3-amino 7-dimethylamino-2-methylphenazine-hydrochloride) is a water-soluble dye that passes through intact plasma membranes of viable cells and is accumulated in the lysosomes (Repetto *et al.*, 2008). After experiments (APDT and ECAS) the supernatant in the 96 well plates was removed and replaced with PBS containing 50 µg mL neutral red (Sigma-Aldrich). The cells were incubated for 2 h at 37 °C to allow for the uptake of neutral red. After removal of the dye solution, the cells were washed gently with PBS, and the residual dye was extracted from the cells by the addition of 100 µL of extractant solution (51% H<sub>2</sub>O, 48% ethanol and 1% acetic acid). Optical densities were then read at 550 nm using a spectrophotometer (Cecil Instruments Ltd, Cambridge, U.K.). The mean optical density of extract from untreated control cells was set to represent 100% viability.

### **MTS assay**

The MTS was performed using the commercially available kit The CellTiter 96® Aqueous Non-Radioactive Cell Proliferation Assay (Promega). The instruction was followed CellTiter 96® Non-Radioactive Cell Proliferation Assay Technical Bulletin #TB112, Promega Corporation.

The reagent (20 µL of CellTiter 96® Aqueous One Solution) was added into each well of the 96 well assay plate containing the samples in 100 µL of culture medium to detect the viability of lymphocytes (treated and untreated cells). The 96 well assay plate were then incubated for 4 hours at 37°C in a humidified, 5% CO<sub>2</sub> atmosphere. During a 4-hour incubation, living cells convert the tetrazolium component of the dye solution into a formazan product. After the incubation period the absorbance of the formazan product at 490nm was measured directly from 96-well assay plate. The quantity of formazan product measured by the amount of 490nm absorbance is directly proportional to the number of living cells in culture.

The CellTiter 96® Aqueous Assay is composed of solutions of tetrazolium compound [3-(4,5-dimethylthiazol-2-yl)-5-(3-carboxymethoxyphenyl)-2-(4-sulfophenyl)-2H-tetrazolium, inner salt; MTS] and an electron coupling reagent,

phenazine methosulfate (PMS). MTS is bio-reduced by cells into a formazan product that is soluble in tissue culture medium. The conversion of MTS into the aqueous soluble formazan product is accomplished by dehydrogenase enzymes found in metabolically active cells (CellTiter 96® Non-Radioactive Cell Proliferation Assay Technical Bulletin #TB112, Promega Corporation).

### **2.13 Methods for genotoxic effects of APDT and ECAS on T lymphocytes (Jurkat cells) (Comet assay)**

#### **Comet (alkaline condition) assay**

Before comet assay was carried out the cells were exposed to treatments (APDT and ECAS) as follows and each experiment repeated 3 times. The comet assay was carried out using the commercially available kit from Trevigen (4250-050-K-CometAssay® Kit (25 X 2 well slides))

Materials Supplied: Lysis Solution, Comet LMAgarose (LMA), Trevigen CometSlide™, 200 mM EDTA, pH 10

#### **APDT**

Aliquots of T-lymphocytes culture suspension ( $1 \times 10^5$  cells/ml) were prepared for treatment. This suspension was dispensed into 96 well plate (100 µl in each well). For APDT MB final concentration 10 µg/mL was added into the cell suspension in media and exposed to light for 20 minutes (total light dose 11 J/cm<sup>2</sup>), for dark control MB final concentration 10 µg/mL added into the cell suspension in media and kept in the dark for 20 minutes. For light control the cell suspension was exposed to light only for 20 minutes (total light dose 11 J/cm<sup>2</sup>) and the control untreated cells. After the experiment cells were centrifuged at 1,200 for 5 minutes and resuspended in fresh media. Samples were prepared immediately for the comet assay and another prepared following a 6h and 24h incubation period at 37°C in a humidified, 5% CO<sub>2</sub> atmosphere.

#### **ECAS**

The T-lymphocytes cell suspension (concentration to  $1 \times 10^5$  cells/ml) was dispensed into 96 well plate (100 µl in each well) into each well ECAS (5 % v/v)

was added to the required concentration and incubated for 30 minutes at 37°C in 95% air, 5% CO<sub>2</sub>. After 30 minutes incubation the cells were centrifuged and resuspended in fresh media. Samples were prepared immediately for the comet assay and another prepared following a 6h and 24h incubation period at 37°C in a humidified, 5% CO<sub>2</sub> atmosphere.

After treatment (APDT and ECAS) for each sample cells were resuspended in cell culture medium (immediately, 6h and 24h), cell suspensions were harvested by centrifugation (200x g for 5 min). The cells were suspended at 1 x 10<sup>5</sup> cells/ml in ice cold 1X PBS (Ca<sup>2+</sup> and Mg<sup>2+</sup> free). Extra care was taken to remove any residual media used for cell culture as it can reduce adhesion of LM Agarose to the CometSlide™. A series of steps were followed as instructed in the protocol ([http://www.trevigen.com/docs/protocol\\_4250-050-K.pdf](http://www.trevigen.com/docs/protocol_4250-050-K.pdf))

1. The lysis solution provided in the kit was cooled at 4°C for 20 minutes before use.
2. The low melting (LM) Agarose melted in a beaker of boiling water for 5 minutes, with the cap of the bottle loosened. Before use the agarose was cooled in a 37°C water bath for at least 20 minutes. Care was taken with agarose to make sure it is cooled before mixing with the cells as the correct temperature is critical or the cells may undergo heat shock.
3. The cells (1 x 10<sup>5</sup>/ml) were carefully mixed with molten LM Agarose (at 37°C) at a ratio of 1:10 (v/v) and immediately pipetted 50 µl onto CometSlide™. Using the pipette tip to spread agarose cells mixture over sample area to ensure complete coverage of the sample area.
4. The slides were placed flat at 4°C in the dark for 30 minutes.
5. The slide was immersed in 4°C Lysis Solution for 60 minutes.
6. After draining the excess buffer from slides and the slides were then immersed in freshly prepared Alkaline Unwinding Solution, pH>13 (Alkaline Unwinding Solution, pH>13 (200 mM NaOH, 1 mM EDTA) for 1 hour at 4°C, in the dark.

Alkaline Unwinding Solution preparation: 50 ml of Alkaline Solution combined: 0.4 g NaOH Pellets, 250  $\mu$ l 200 mM EDTA, 49.75 ml distilled H<sub>2</sub>O. The solution was stirred until dissolved and cooled as the solution became warm during preparation.

8. For electrophoresis 850 ml 4°C Alkaline Electrophoresis Solution filled into the slide tray and slides were placed in electrophoresis slide tray (slide label adjacent to black cathode) slides aligned equidistant from electrodes and covered with Slide Tray Overlay. Electrophoresis carried at 4°C, in the dark. The voltage set to about 1 Volt/cm and the current was set is approximately 300 mA, and electrophoresis performed for 25 minutes.

9. The excess electrophoresis solution was gently drained, then gently immersed twice in dH<sub>2</sub>O for 5 minutes each, then in 70% ethanol for 5 minutes.

10. The samples were dried at 37°C for 10-15 minutes.

11. 100  $\mu$ l of diluted SYBR® Gold was placed onto each circle of dried agarose and stained 30 minutes (room temperature) in the dark. The excess SYBR removed by gently tapping the slide and rinsing briefly in water. The slides were then allowed to dry completely at 37 °C.

12. The slides were viewed by using epifluorescence microscopy (Nikon TE300 inverted epifluorescence microscope).

Samples stained with SYBR gold (SYBR® Gold's maximum excitation/emission is 496 nm/522 nm) when excited emits green light. The images were captured using a high resolution video camera attached to a microscope (epifluorescence microscope) and the software Comet Assay IV single cell electrophoresis assay quantification software was used to score the samples.

## 2.14 Flat-bed biofilm perfusion model

### **Flat-bed biofilm perfusion (Biofilm growth chambers and removable biofilm growth matrix)**

The apparatus and system for growing biofilm in continuous culture was conceived and devised by Thorn (Thesis, 2009) and Thorn and Greenman (2009).

A schematic (figure 2a) and images of sterile biofilm chambers (figure 2b) and the *in vitro* flat-bed perfusion biofilm model experimental set up (figure 2c) as shown. Microbial biofilms ( $n = 3$ ) were grown inside individual sterile chambers (Fig. 2b) as described by Thorn (Thesis, 2009) that consisted of a glass microscope slide cut to 50 mm and tapered to a point using a diamond glass cutter. Rubber supports and a surface methylpentene Delnet apertured film (Delstar, Bristol, UK) were glued to the microscope slide using extreme temperature-resistant glue (Bostik, Strafford, UK), and a 1-cm<sup>2</sup> hole cut into the surface film. The microbial biofilms were grown within 1-cm<sup>2</sup> cellulose support matrices (Sirane, Telford, UK), which comprise of loosely packed interconnecting strands, and these are placed within the confines of the rubber and film supports inside an airtight autoclavable growth chamber (Fig. 2b). The airtight autoclavable biofilm growth chambers were constructed from a modified 470-ml freezer storage box (Lock & Lock, Amazon, UK). The lid of these chambers were fitted with a sterile 0.2  $\mu\text{m}$  air filter (Fisher Scientific) facilitating gaseous exchange with the surrounding environment. Sterile perfusate growth media to the biofilm support matrix was supplied through a hyperdermic needle which was mounted into the corner of each chamber and connected to a media reservoir via silicone tubing. A peristaltic pump (model 205U; Matson & Marlow Bredel Pumps, Cornwall, UK) was used to perfuse growth media through the biofilm support matrix and a hole was cut into the bottom of each biofilm growth chamber to allow through-flow of fluids (eluate) into a 10 or 500 ml volume collection bottle for sample or waste via a thick silicone tube (internal diameter 2cm<sup>2</sup>). All components of the biofilm model were heat stable and were sterilized by autoclaving prior to use. Multiple models ( $n = 3$ ) were set up in parallel, drawing medium from a single reservoir as required. The media consisted of 1/5th strength nutrient broth (Oxoid Ltd., Basingstoke,

UK) supplemented with 10 mg/L kanamycin (the selective agent required to maintain the recombinant plasmids).

### **Inoculating the biofilm model**

Microbial target cell inocula were prepared transferring a single colony of *E. coli* Nissle 1917/pGLITE from a nutrient agar plate into TYE broth (1% tryptone-0.5% yeast extract) supplemented with kanamycin (10 mg/l) in a 250ml flask to give an initial standard OD<sub>600</sub> of 0.02. Flasks were then incubated at 37°C with orbital shaking 250rpm (model S 150, Stuart shakers, UK) until cultures reached mid to late exponential phase corresponding to 10<sup>8</sup> cfu/ml; 0.6 OD<sub>600</sub> measured using a spectrophotometer (Helios, Thermo Electron Corporation, UK). Aliquots of 300µl of this culture containing approximately concentration 10<sup>8</sup> cfu/ml were deposited onto a 1-cm<sup>2</sup> cellulose matrix layered onto a nutrient agar plate. The inoculated matrices were then incubated for 4 hours in an anaerobic cabinet before being transferred aseptically into the support matrix of each sterile biofilm chamber. The media was perfused immediately after placing the biofilm matrix in the chamber. Biofilm experiments were performed within a large incubator (model eurotherm 91e, Carbolite Ltd., London, UK) or, for bioluminescence measurements a smaller incubator (Sanyo MCO-15 AC CO<sub>2</sub>) set at 37 °C.

### **Growth of biofilm within the in vitro flat-bed perfusion biofilm model**

The model was inoculated with target organism bioluminescent *E. coli* Nissle 1917 pGLITE and the perfusate output (eluate) sequentially sampled for 48 hours to determine the initial growth, development and the establishment of the biofilm steady state. Eluate and the total biofilm matrix (TMP) was also sampled from three biofilms (n=3) every 4 hours until 24 hours and then at 36 hours and 48 hours, and these samples were analysed by determining the viable count and bioluminescence. It was expected that the biofilm would reach a steady state in 20 to 24 hours of growth (Thorn and Greenman, 2009). A separate experiment was carried out where the photon counts of the developing bioluminescent biofilms were continually measured by low light photometry (0-16 hours).

### **Control of biofilm specific growth rate ( $\mu$ ) in the flat bed perfusion biofilm model**

The flat-bed perfusion biofilm system was previously shown to be suitable for producing biofilm populations with different growth rate by altering the nutrient media perfusion rates (Thorn and Greenman, 2009). Therefore in this study the model was used to set biofilm growing at 3 different growth rates described as; slow, intermediate and fast growth rates. The biofilm matrix was perfused with 1/5<sup>th</sup> strength TYE. The flow rate of perfused biofilm systems (n=3) was set up at range of flow rates; 1ml h<sup>-1</sup> (low), 15ml h<sup>-1</sup> (intermediate), or 50ml h<sup>-1</sup> (high). The TMP and eluate count were determined by sequential sampling by viable count and bioluminescence for low flow rate and photon count of developing bioluminescent biofilms were continually measured by low light photometry (0-16 hours) for low, intermediate and high flow rate. Under quasi steady state conditions, the biofilm growth rate ( $\mu$ ) is equal to the production rate which is equal to the elution rate of detached daughter cells (cfu/ml<sup>-1</sup> h<sup>-1</sup>) divided by the total attached population in the cellulose matrix (TMP) (Thorn and Greenman, 2009; Saad *et al.*, 2013). Using this formula the growth rate for each flow condition was determined and or derived.

### **Visualization of the bioluminescence and measurement of photon count by low light photometry after APDT or ECAS treatment**

*Escherichia coli* Nissle 1917/pGLITE was used to inoculate the cellulose matrix (n=3) at time zero and the perfusate pump (Watson Marlow, Cornwall, UK) switched on at a slow (1 ml h<sup>-1</sup>) intermediate (15 ml h<sup>-1</sup>) and fast (50 ml h<sup>-1</sup>) flow rates. The media consisted of 1/5<sup>th</sup> strength TYE supplemented with kanamycin (10  $\mu$ g/ml) as selective agent to maintain pGLITE and lux expression. When the biofilm had reached quasi-steady state (after 16 to 24 hours of perfusion), APDT treatment was applied (MB 100  $\mu$ g/ml and total light dose 25.2 J/cm<sup>2</sup> (30 minutes continuous light irradiation (light intensity 14.5mW/cm<sup>2</sup>) for each biofilm (at 3 different growth rates), and 3 repeat treatments as described below were applied on the same biofilm. The first treatment was carried when the biofilm reached steady state (light output constant) (MB 100  $\mu$ g/ml and total light dose 25.2 J/cm<sup>2</sup>

(30 minutes continuous light irradiation (light intensity  $14.5 \text{ mW/cm}^2$ ) and then second treatment was applied when the biofilm reached steady state (biofilm recovery to constant light output levels) around 24 hours post first treatment. The third treatment was carried out after 1 hour following the second treatment. In all cases the APDT treatment was same (MB  $100 \text{ }\mu\text{g/ml}$  and total light dose  $25.2 \text{ J/cm}^2$  (30 minutes continuous light irradiation (light intensity  $14.5 \text{ mW/cm}^2$ ). The photon camera was stopped for the duration of the APDT treatment time and the flow of media to the biofilm was also stopped, just prior to duration of treatment, and was then switched back on, immediately after treatment. When photon measurements were re-started and continued for the duration of the experiment.

The mature quasi-steady state biofilm at a determined growth rate (perfused for 16-24 h) was treated with ECAS (pH 2.2 and ORP 1143) by taking  $300\mu\text{l}$  of (5% v/v) ECAS and depositing this on to the matrix by slow injection  $300\mu\text{l}$  over 5 minutes. Experiments were repeated 3 times for each treatment condition.

### **Sampling of the biofilm model**

The biofilm matrix was sequentially sampled to determine the total biofilm matrix population (TMP), at different time points to construct the biofilm growth curve, by removing the cellulose support matrix and dispersing the attached biofilm cells into a defined volume of PBS by vortex mixing. Cell suspensions were serially diluted ( $10^{-1}$ – $10^{-5}$ ) and spirally plated onto appropriate recovery medium to determine the number of CFU per biofilm. The corresponding biofilm matrix eluates were also periodically sampled by aseptically replacing growth chamber output waste bottles (500ml) with sterile small glass sample bottles, and the number of biofilm shed cells per ml were quantified by serial dilution, plating and counting of recovered cells after incubation.

### **Bioluminescence**

Integration of a bioluminescent target organism facilitated real time *in situ* measurements to be made by setting up the biofilm model within a blacked out incubator (Sanyo MCO-15AC  $\text{CO}_2$  incubator) at maintained at  $37^\circ \text{ C}$  in a dark room facility. The ICCD225 (model 225; Photek, UK) photon counting camera

controlled by a computer running IFS32 data acquisition and image processing software was set up on the top of the blacked out incubator. The photon production rate of a given biofilm was continually monitored at sequential time points by using photon integration time of 60 s every 5 min. The IFS32 software permitted image capture, data acquisition from an isolated area (biofilm matrix 1-cm<sup>2</sup> area) of the image.

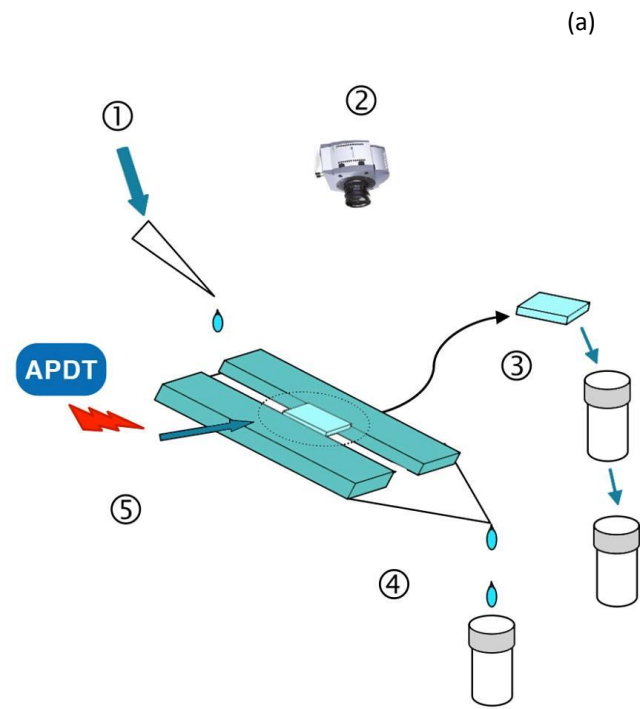
### **Analysis of Results**

Biofilm growth and antimicrobial kill kinetic profiles graphs were produced in Microsoft excel program (Microsoft excel 2010). The specific growth rate ( $\mu$ ) of the biofilms was calculated using the following formula

$$\text{Growth rate } (\mu) = \frac{\text{Rate of elution of cells (h}^{-1}\text{)}}{\text{Total biofilm population}}$$

The specific growth rate ( $\mu$ ) equals the biofilm production rate of new cells in the perfusate output (cfu per ml x flow rate in mlh<sup>-1</sup>) divided by the total attached matrix population (total matrix cfu).

**Figure 2-1 (a) Schematic of the flat-bed perfusion biofilm model. 1. Growth medium is perfused onto the biofilm via needle. 2. Low-light photometry is used to monitor growth and kill kinetics of bioluminescent biofilms. 3. Biofilms can be removed and disrupted to determine the total biofilm population density. 4. Biofilm eluate is collected (at any time point) and analysed by viable count to ascertain the biofilm growth rate. 5. treatment applied APDT 1 ml of MB and light was delivered from fiber optic light source (MB 100 µg/ml and total light dose 25.2 J/cm<sup>2</sup> (light intensity 14.5mW/cm<sup>2</sup> or ECAS was applied on to the surface of cellulose membrane (b) Photograph of the biofilm growth chamber. (c) Photograph of three flat-bed units running in parallel**



(b)



(c)



**Chapter 3: Development of bioluminescent target based  
assay to study kill kinetics of APDT and ECAS**

### 3.1 Introduction

The use of APDT as a non-antibiotic approach to inactivate pathogenic microorganisms seems to be very promising (Huang *et al.*, 2012). As discussed in chapter 1 APDT has various applications as alternative therapies for localized infections. Similarly ECAS, a fast acting biocide, may have many important applications in health care settings. These therapies are therefore considered to be potential alternatives to antibiotics treatments in the future. Therefore in order to study and understand their effectiveness, a rapid method of detecting viability is important. To monitor the bacterial APDT efficacy, including the APDT mechanism, rapid methods are required to replace of the laborious and time-consuming conventional methods of serial dilutions, plating, overnight incubation and counting of colony-forming units (CFU). New approaches are essential to accelerate the development of APDT and ECAS. The bacterial bioluminescence method, when applied to APDT studies, to monitor the bacterial viability in real-time, is considered to be a rapid, sensitive and a cost-effective option (Alves *et al.*, 2008; Tavares *et al.*, 2011; Hamblin *et al.*, 2002). In experimental systems, a strong correlation between bioluminescence and viable counts can be demonstrated (Rocchetta *et al.*, 2001). The light output is noncumulative, reflecting the actual metabolic rate, and can be measured directly, continuously and non-destructively in high-throughput screening or continuous-culture models (Beard *et al.*, 2002).

Bioluminescence has been previously employed to study *in vitro* APDT using porphyrins as PS (Alves *et al.*, 2008; Tavares *et al.*, 2011) and to monitor the antimicrobial activity of ECAS (Robinson *et al.*, 2011). However a bioluminescent assay has not been applied to compare the two biocides using kill kinetics. Moreover APDT using MB kill kinetics has not been studied before using bioluminescence. Therefore in this study a bioluminescence assay was developed to measure the kill kinetics of the two agents under same standardized conditions and the kill rates were compared.

A simple rapid and robust accurate assay development will help better understand the effectiveness of these treatments.

### **3.1.2 Applications of bioluminescence to study antimicrobial activity of fast acting biocides- ECAS**

ECAS is known to be a fast acting biocide. Traditional microbiological techniques are used to provide reliable data on the rate and extent of kill for a range of biocides. However, such techniques provide very limited data regarding the initial rate of kill of fast-acting biocides over very short time domains.

### **3.2 Aims of the chapter**

To develop reliable kill curve assays (based on bioluminescence) from which can be measured the target microbial kill rate and final populations at the end of the treatment period. The traditional methods of measuring kill rates by recovering cell survivors by viable count following antimicrobial treatments is impossible to apply when the kill kinetics are either rapid, or complex in nature (e.g. biphasic or multiphasic survival curves with “shoulders” (discussed in chapter 1).

To study the effectiveness of APDT and ECAS it is required to be tested *in vitro* before testing on animal and humans. Therefore to better understand effectiveness and killing mechanisms, faster methods of evaluating the PS effectiveness under different conditions using methods such as bioluminescence is very important. The main aim of this chapter is to study APDT using the rapid methods of bioluminescence and comparing the effectiveness of APDT and ECAS.

### **3.3 Results**

#### **3.3.1 Correlation between bioluminescence and viable count**

*P. aeruginosa* MCS5-lite growth was followed for 24 hours by bioluminescence output and viable counts. The growth curve (figure 3.1) shows difference in shape with either bioluminescence output or viable counts. During the first 2 hours (lag phase), viable counts show a slightly lower rate of increase in viable number compared to bioluminescence where it shows a rapid increase in bioluminescence. In the exponential phase both parameters appear to increase exponentially from 2 to 5 hours. It is during this exponential phase of growth that there is good correlation between the two variables ( $r^2 = 0.8433$ ) (Figure 3.2). The

bioluminescence starts to plateau earlier than the viable numbers. When the cells enter the deceleration phase at the end of exponential growth, the light output of the cells plateaus between 3 and 4 hours earlier than observed using viable counts and, at late stationary phase the cells give out low but stable light output up to 24 hours (Figure 3.1).

The growth pattern of *E. coli* Nissle 1917 pGLITE followed a similar pattern to *P. aeruginosa* MCS5-lite. The growth of *E. coli* Nissle 1917 pGLITE (figure 3.4) shows the lag phase followed by exponential phase and then stationary phase. This is a general growth pattern shared by all species of bacteria in closed batch culture system. Lag phase is where the bacteria adjust to the new environment by synthesizing enzymes. Exponential phase is where bacteria use the available nutrient to increase their number by dividing. Bacteria enter the stationary phase when the nutrients run out and/or is due to the accumulation of metabolic waste in the system leading to unfavourable conditions. The bioluminescence output increases up to 2 hours during the exponential phase and by 3 hours the bioluminescence start to decline reaching a steady level at 24 hours. This was not the case for viable count which continues to increase up to 5 hours before reaching steady levels from 8 hours to 24 hours. It is during this exponential phase of growth that there is good correlation between the two variables ( $r^2 = 0.8868$ ) (figure 3.5). Figure 3.5 shows that a standard culture of *E. coli* Nissle 1917 pGLITE in exponential phase gives viable counts that closely correlate with bioluminescence in dilutions of the culture.

The graph of bioluminescence output against viable numbers of series of log fold dilution of a suspension of exponential phase culture is shown in figure 3.6 for bioluminescent *E. coli* Nissle 1917 pGLITE and figure 3.3 for bioluminescent *P. aeruginosa* MCS5-lite. The bioluminescence results closely reflect viable bacterial number for exponential culture of these target organisms used in later experiments to monitor the antimicrobial activity of APDT and ECAS.

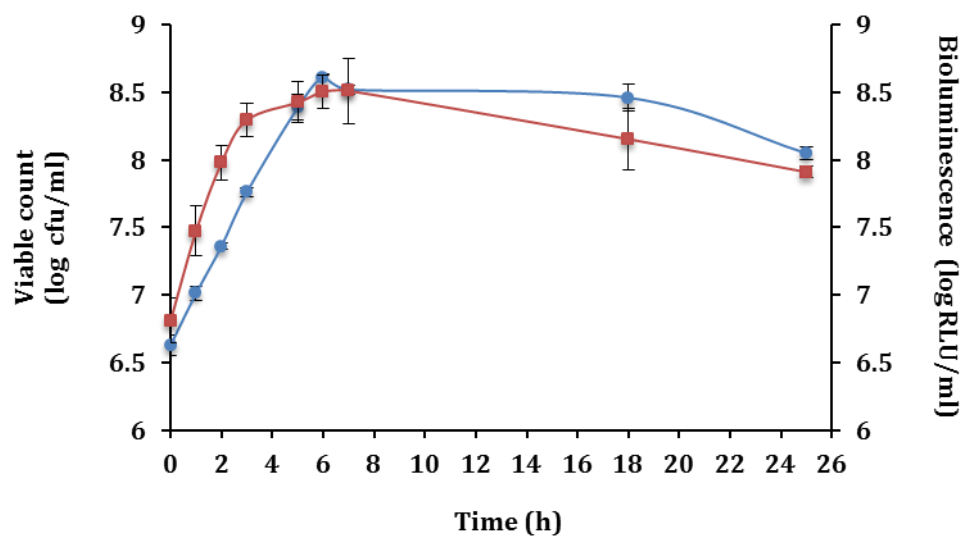


**Figure 3-1 Growth curves of *P. aeruginosa* MCS5-lite followed by bioluminescence and viable count. Symbols represent mean of 3 experiments, and error bars  $\pm$  standard deviation (SD),  $\bullet$ —viable count,  $\blacksquare$ —bioluminescence.**

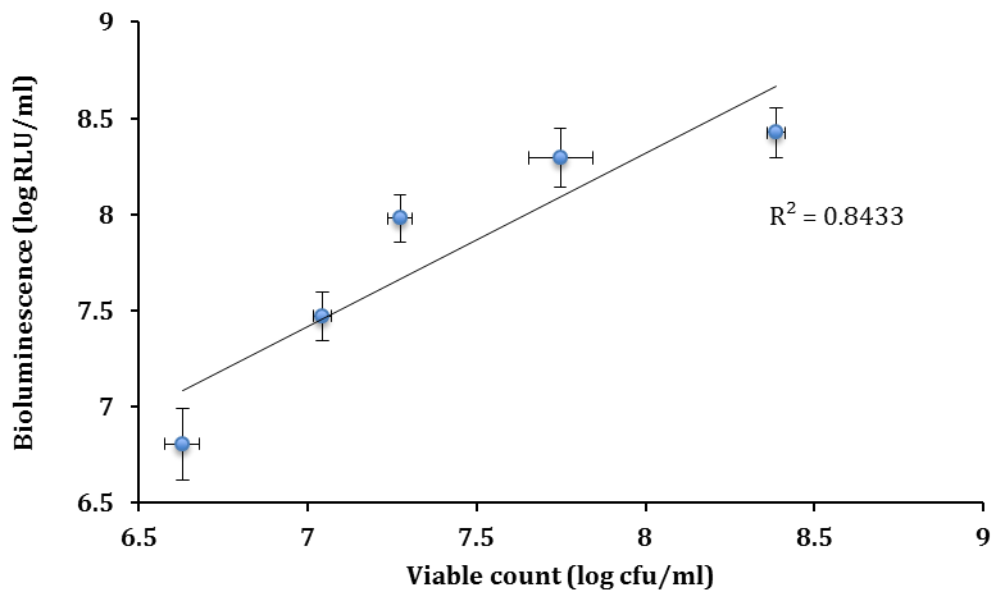


**Figure 3-2 Correlation between bioluminescence of *P. aeruginosa* MCS5-lite (relative light units) and viable count of bacteria in exponential phase of growth (2-6 hours). Symbols represent mean of 3 experiments, and error bars  $\pm$  SD.**

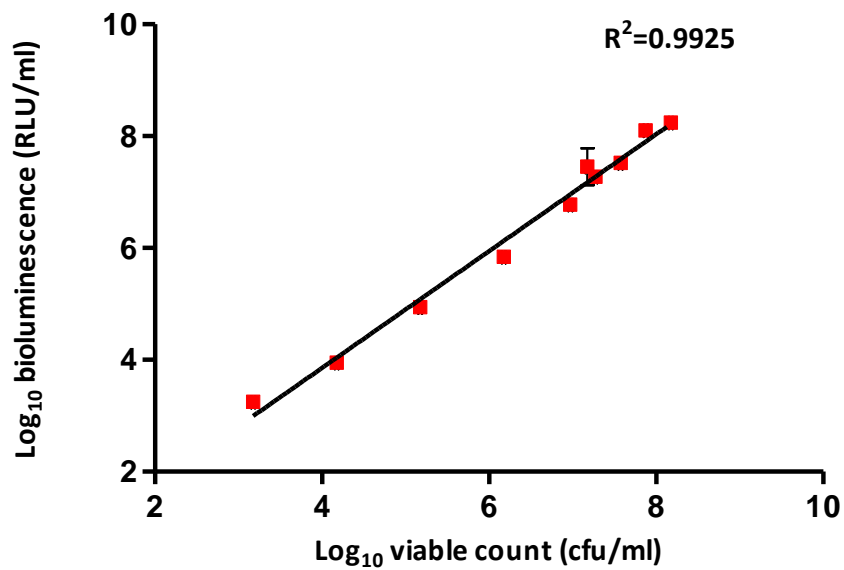


**Figure 3-3 Correlation between bioluminescence (relative light units) and viable counting in bacteria in exponential phase of growth of a suspension of series of log fold dilutions of *P. aeruginosa* MCS5-lite. Symbols represent mean of 3 experiments, and error bars  $\pm$  SD.**

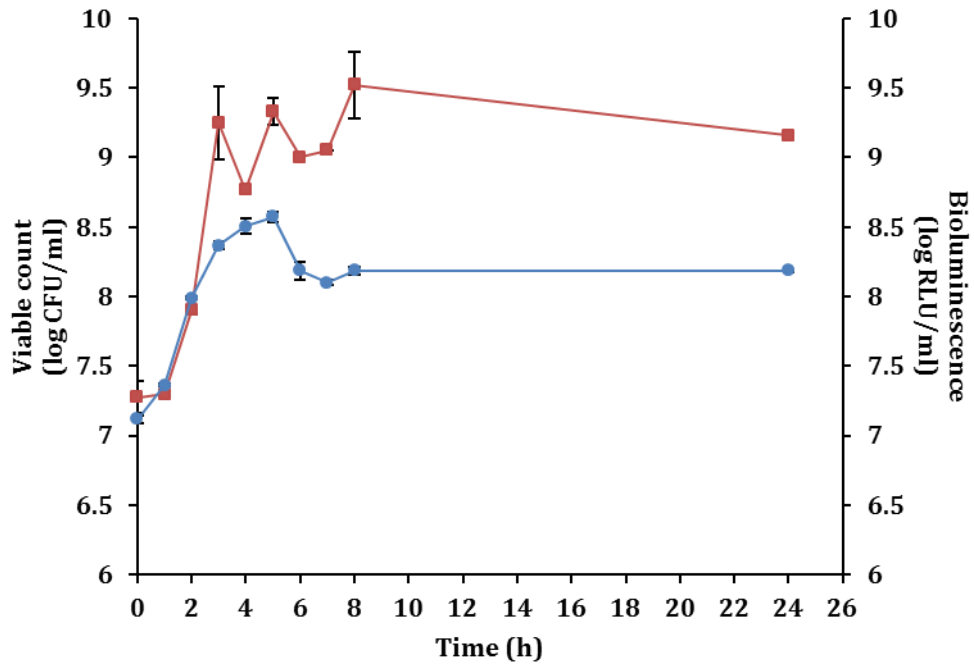


**Figure 3-4 Growth curves of *E. coli* Nissle 1917 pGLITE followed by bioluminescence (relative light units) and viable count. Symbols represent mean of 3 experiments, and error bars  $\pm$  SD,  $\bullet$  -bioluminescence,  $\blacksquare$  - viable count.**

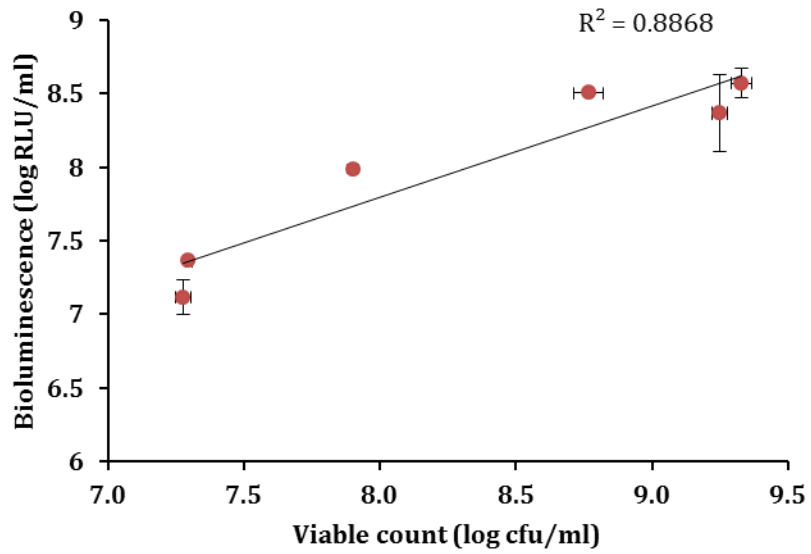


**Figure 3-5 Correlation between bioluminescence of *E. coli* Nissle 1917 pGLITE (relative light units) and viable count of bacteria in exponential phase of growth (1-6 hours). Symbols represent mean of 3 experiments, and error bars  $\pm$  SD.**

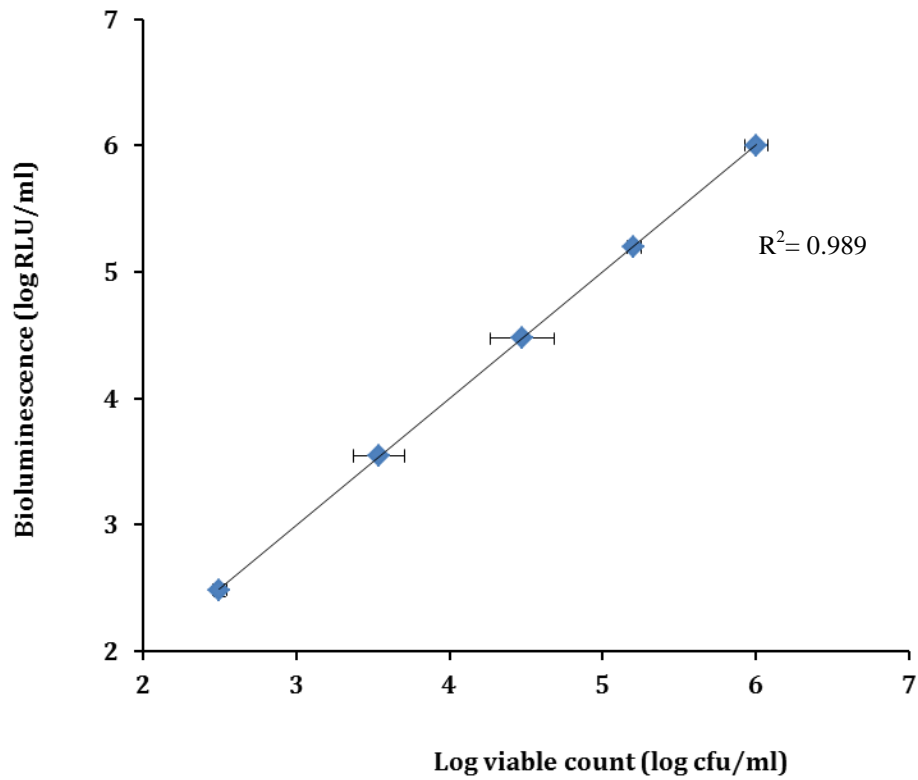


**Figure 3-6 Correlation between bioluminescence (relative light units) and viable counting in bacteria in exponential phase of growth of a suspension of series of log fold dilutions of *E. coli* Nissle 1917 pGLITE. Symbols represent mean of 3 experiments, and error bars the  $\pm$  SD.**

### 3.3.2 APDT kill kinetic assay

Figure 3.7 shows the kill rates of *E. coli* Nissle 1917 pGLITE exposed to APDT with different concentration of MB and the same dose of light (total light 11 J/cm<sup>2</sup> at light intensity of 9.4mW/cm<sup>2</sup>). It shows that as the concentration of MB increased while keeping the light dose constant, the kill rate *E. coli* Nissle 1917 pGLITE increases up to 10 µg/ml and thereafter the kill rate decreases as the concentration of MB increases. The highest kill rate was at 10 µg/ml of MB and lowest kill rate was observed at 100 µg/ml of MB.

Figure 3.8 shows the reduction in bioluminescence of *E. coli* Nissle 1917 pGLITE exposed to APDT for 20 minutes. MB was used at 10µg/ml after optimization (data not shown). The graph shows increase in the reduction of bioluminescence as the cumulative light irradiation increase over 20 minutes. At the end of the treatment there was nearly a 4 log reduction in bioluminescence. A viable count measure at the start of the experiment and at the end of the experiment showed a similar reduction of nearly a 4-log drop in viable count. This showed that bioluminescence closely correlated with viable bacterial number during killing phase. The assays revealed that for “cells only” control showed no change in the light output by the bacteria, showing that the bioluminescence output was constant for the duration of the experiment. To measure the toxicity level of MB alone *E. coli* was incubated with MB in the dark and bioluminescence was measured every 2 minutes for 20 minutes. This showed no reduction in bioluminescence, and the viable count did not change significantly over the 20 minutes, showing that MB is not toxic to bacteria in the dark. Both light and sensitizer are required for cell killing.

The results show that APDT is effective in killing *E. coli* Nissle 1917 pGLITE and that this treatment is effective and bioluminescence could be incorporated into the assay to enable rapid assessment antimicrobial activity of APDT. The slope of the graph gave the reduction in the rate of bioluminescence (table 3.1) which was -0.1709 RLU/min and rate of reduction viable numbers -0.2096 log cfu/min; this gave the corresponding D values (time required to reduce bioluminescence by 1 log) 5.85 minutes and 4.98 minutes respectively.

The same assay was repeated with other bioluminescent species *P. aeruginosa* MCS5-lite (figure 3.9). When treated with MB 10µg/ml and light there was a light dose related increase in reduction in bioluminescence. There was no change in bioluminescence in the controls (dark control). APDT treatment (30 minutes) gave nearly a 4-log reduction in both bioluminescence and viable count. The kill rate was calculated from the slope -0.121 RLU/min and -0.126 cfu/ml and the D values were 7.94 minutes and 7.93 minutes respectively.

As the bioluminescent strain of *S. aureus* could not be used in the assay (because of its low light output and thus an inability to capture a 3-log reduction) it was only possible to use viable count to assess the activity of APDT towards Gram positive organisms. Therefore two Gram positive *S. aureus* species were tested *S. aureus* ATCC 6538 and MRSA strain for their sensitivity towards APDT

As can be seen from the graph (figure 3.10) MRSA exposed to APDT showed a 3-log reduction in viable counts over 30 minutes. The kill rate (table 3.1) obtained was -0.11 log cfu/min and D value was 9.1 minutes. *S. aureus* ATCC 6538 strain (figure 3.10) was very sensitive and gave 3-log reduction in viable counts in 10 minutes (K= -0.3244 log cfu/min) and the D value was 3.1 minutes. Both MRSA (figure 3.9) and *S. aureus* ATCC 6538 strain (figure 3.10) shows no change in viability when cells were incubated with MB in the dark (dark controls).

Table 3.1 shows the comparisons of kill rate for each test organism exposed to APDT. *S. aureus* was the most sensitive and the least sensitive organism was *P. aeruginosa*. MRSA gave a similar kill rate to *P. aeruginosa*.

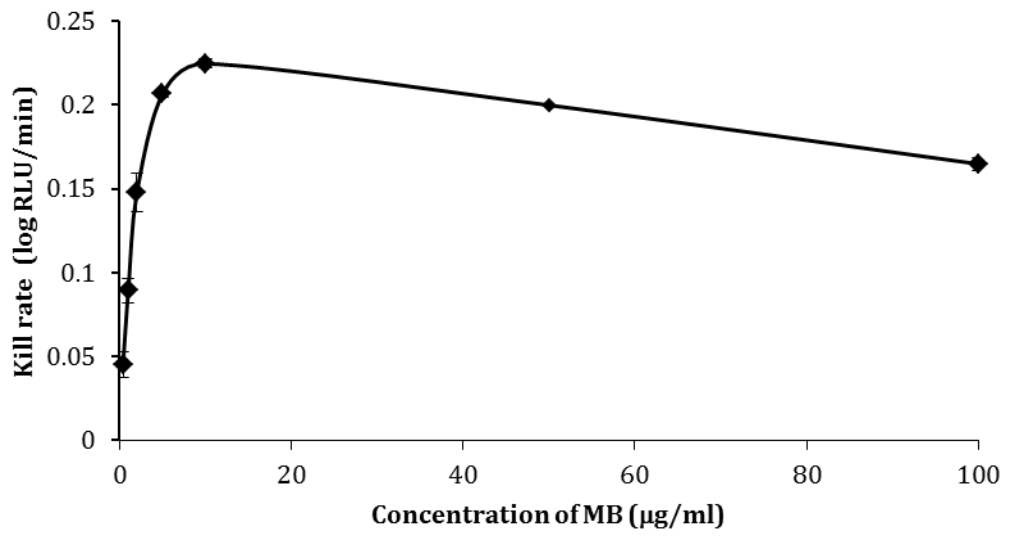


**Figure 3- 7 Kill rates of *E. coli* Nissle 1917 pGLITE exposed to APDT with different concentrations of MB. Error bars show means  $\pm$  SD (n=3)**

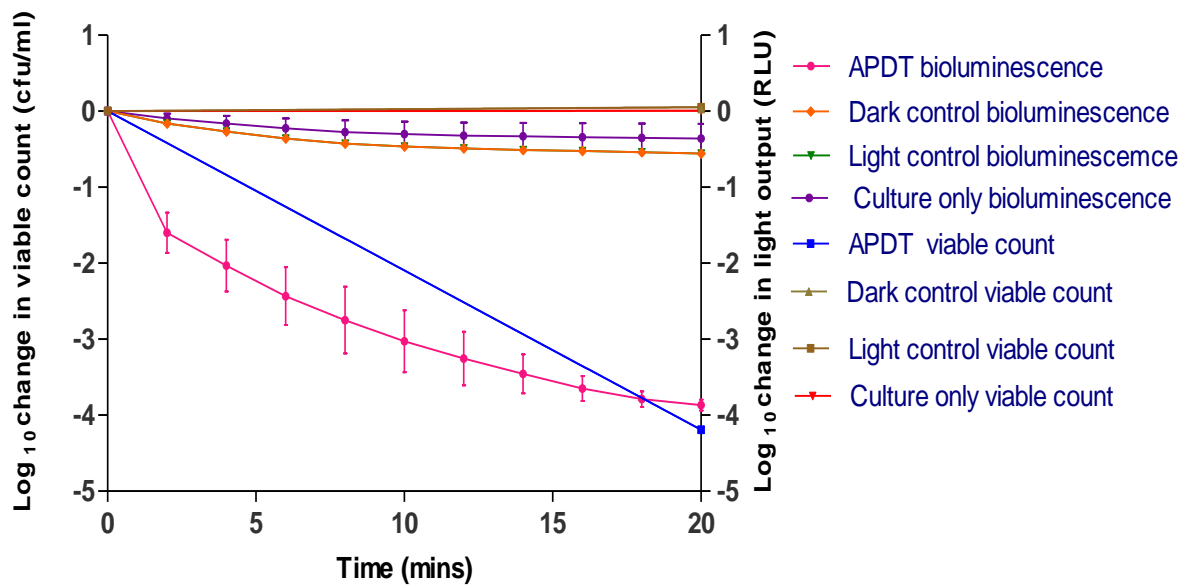


**Figure 3- 8 Reduction of bioluminescence and viable count of *E. coli* Nissle 1917 pGLITE exposed to APDT (MB concentration 10 $\mu$ g/ml and total light 11J/cm<sup>2</sup> at light intensity of 9.4mW/cm<sup>2</sup>) compared to controls. Error bars show means  $\pm$  SD (n=3).**

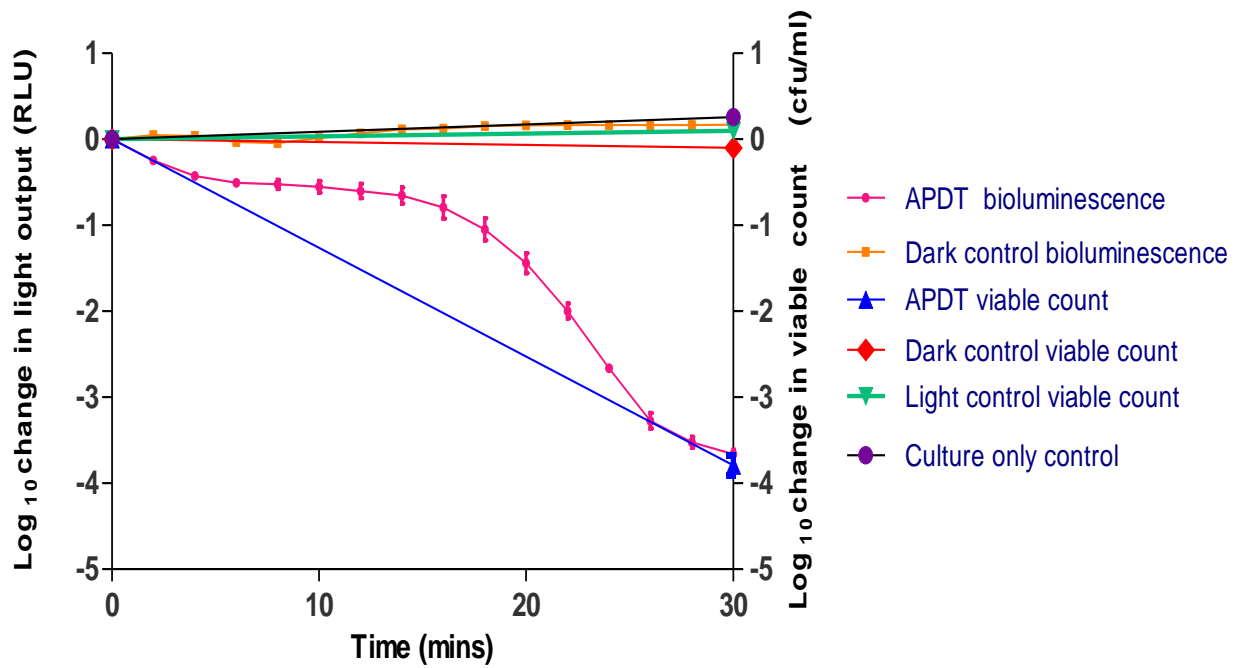


**Figure 3- 9 Reduction bioluminescence and viable count of *P. aeruginosa* MCS5-lite exposed to APDT (MB concentration  $10\mu\text{g/ml}$  and total light  $17\text{ J/cm}^2$  at light intensity of  $9.4\text{ mW/cm}^2$ ) compared to controls. Error bars show mean  $\pm$  SD (n=3).**

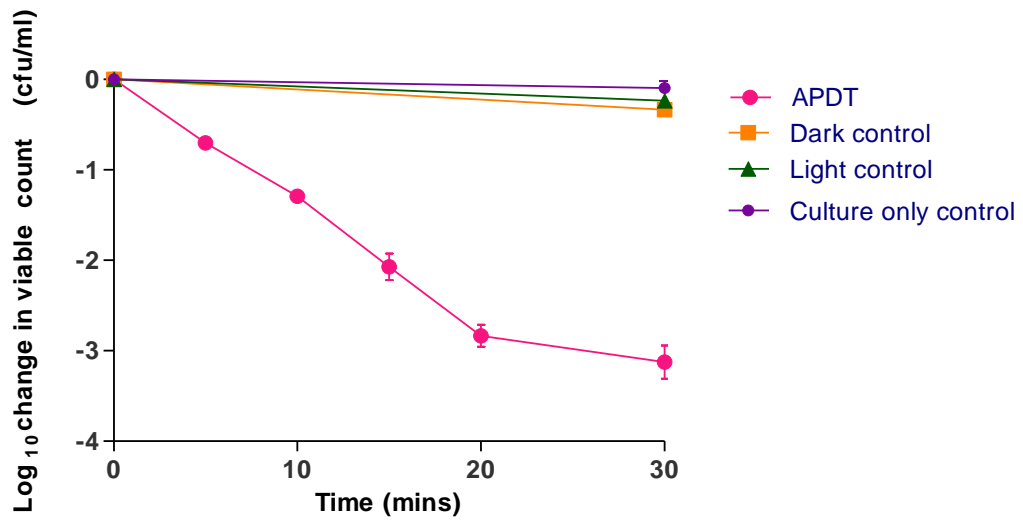


**Figure 3- 10 Reduction in viable count of MRSA exposed to APDT (MB concentration 10 $\mu$ g/ml and total light 17 J/cm<sup>2</sup> at light intensity of 9.4mW/cm<sup>2</sup>) compared to controls. Error bars show mean  $\pm$  SD (n=3).**

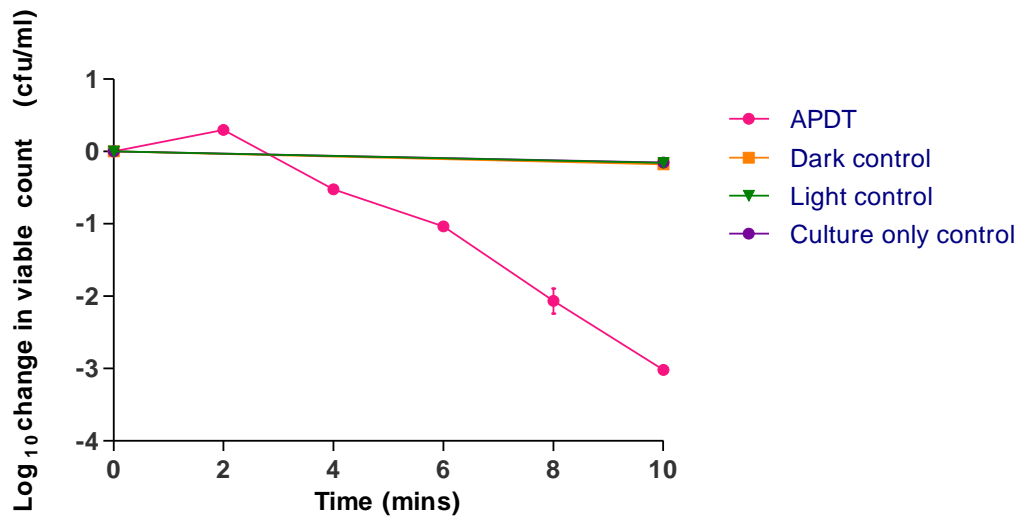


**Figure 3- 11 Reduction in viable count of *S. aureus* exposed to APDT (MB concentration 10 $\mu$ g/ml and total light dose 5.6 J/cm<sup>2</sup> at light intensity of 9.4mW/cm<sup>2</sup>) compared to controls. Error bars show mean  $\pm$  SD (n=3).**

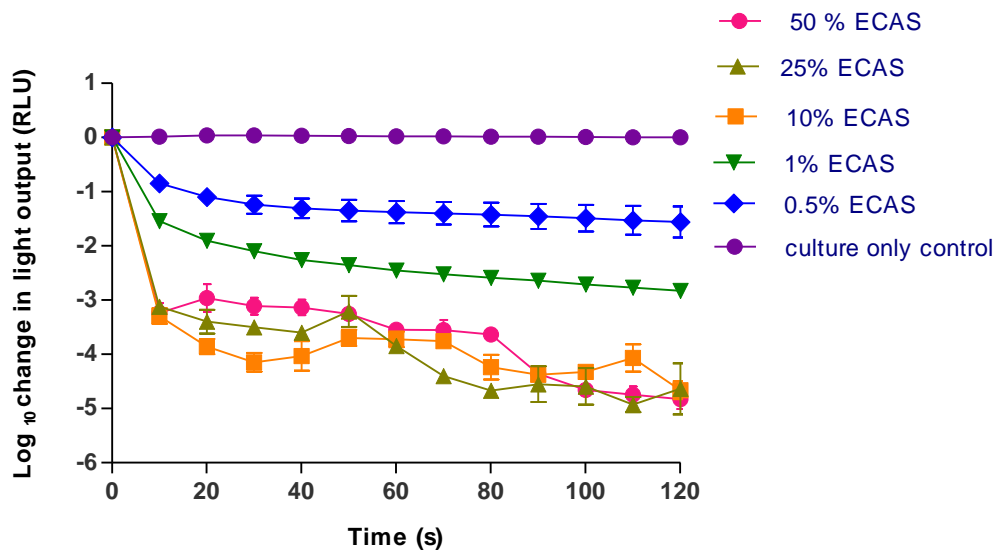
**Table 3-1 Rate of change in bioluminescence or viable count of target organisms when exposed to APDT**

Target organism	Bioluminescence	Viable count	r <sup>2</sup> & P value	r <sup>2</sup> & P value
	Kill rate (log RLU/min)	Kill rate (log (cfu/ml/min))	Bioluminescence	Viable count
<i>E. coli</i> Nissle 1917 pGLITE	-0.171 ± 0.011	-0.210 ± 0.008	0.926 < 0.0001	0.993 < 0.0001
<i>P. aeruginosa</i> MCS5-lite	-0.121 ± 0.009	-0.126 ± 0.008	0.861 < 0.0001	0.993 0.0037
MRSA	-	-0.110 ± 0.008	-	0.925 < 0.0001
<i>S. aureus</i>	-	-0.324 ± 0.027	-	0.900 < 0.0001

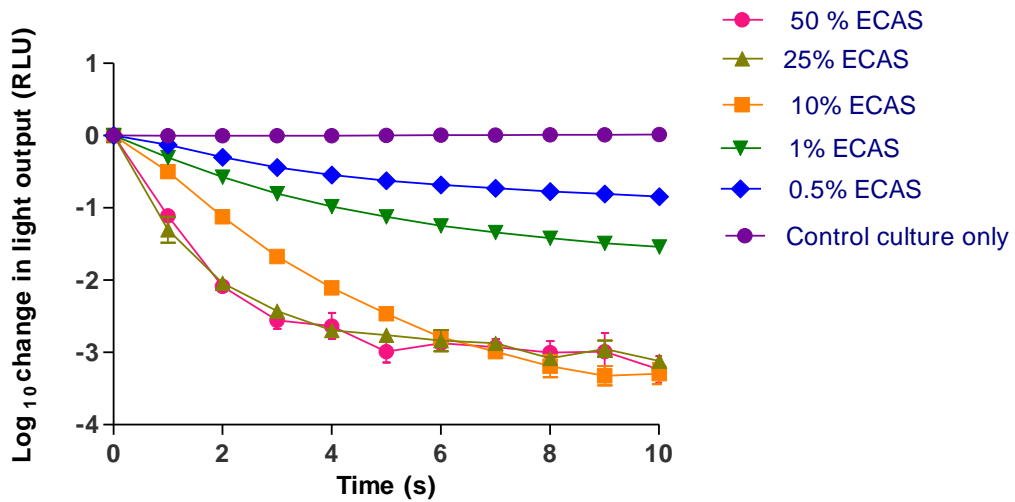
### 3.6.2 ECAS kill curve

Figure 3.12 shows *E. coli* Nissle 1917 pGLITE exposed to different concentrations of ECAS for 2 minutes (total assay time) and figure 3.13 shows the initial kill kinetics (change in light output for the first 10 seconds). The main difference between APDT and ECAS is that ECAS reduces the bioluminescence output by the bacteria within seconds. It only takes 4s for the 25% and 50% ECAS to reduce the bioluminescence to the limit of detection. Even the low concentration of 0.5 and 1% ECAS gave nearly a 1-log reduction in bioluminescence. The kil

l rate shown in table 3.2, was proportional to the concentration of ECAS up to 10%, however at higher concentrations the reduction rate in bioluminescence is not proportionately any faster. This may be due to inaccuracy in capturing the kill rate because ECAS act in milliseconds at high concentration.



**Figure 3- 12 Reduction in bioluminescence of *E. coli* Nissle 1917 pGLITE when exposed to ECAS at different concentrations for 2 minutes. Error bars show mean  $\pm$  SD (n=3).**



**Figure 3- 13 Initial reduction (first 10 seconds) in bioluminescence of *E. coli* Nissle 1917 pGLITE when exposed to ECAS at different concentrations. Error bars show mean  $\pm$  SD (n=3).**

**Table 3- 2 Rate of change in bioluminescence of *E. coli* Nissle 1917 pGLITE when exposed to ECAS at different concentrations**

<b>Target organism</b> <i>E. coli</i> Nissle 1917 pGLITE	<b>50%</b> <b>ECAS</b>	<b>25%</b> <b>ECAS</b>	<b>10%</b> <b>ECAS</b>	<b>1%</b> <b>ECAS</b>	<b>0.5%</b> <b>ECAS</b>
Bioluminescence Kill rate (log RLU/min) ±SD	-26.28 ±1.38	-24.72 ± 1.32	-28.8 ±0.48	-12.38 ± 0.24	-7.26 ±0.18
r <sup>2</sup>	0.795	0.791	0.978	0.971	0.946
P value	<0.0001	<0.0001	<0.0001	< 0.0001	< 0.0001

### 3.5 Discussion

The purpose of this part of the study was to develop a rapid kill assay by integrating a bioluminescent reporter target species to determine the kill kinetics of two ROS generating systems namely APDT and ECAS. First aim of the study was to validate the correlation between viable count and bioluminescence during cell growth conditions. The growth of both *E. coli* Nissle 1917 pGLITE and *P. aeruginosa* MCS5-lite was followed by bioluminescence and viable count. The growth curves showed three characteristic phases: lag phase, exponential phase and the stationary phase. In the lag phase immediately after inoculation of the cells into fresh medium, the population remains temporarily constant before any cell division occurs. The cell can only divide after the intracellular components have been synthesized (e.g ribosomes, cell polymer building blocks and precursors, essential coenzymes). Hence viable count remains constant in this phase while the metabolic activity starts to increase. Therefore slight correlation between bioluminescence and viable found was found in this phase.

It was that found for both *E. coli* Nissle 1917 pGLITE and *P. aeruginosa* MCS5-lite there was a strong correlation in the exponential phase of growth giving  $r^2 = 0.8868$  (figure 3.5) and 0.8433 (figure 3.2) respectively. Good correlation between viable count and bioluminescence in the exponential phase can be explained by considering the different properties that the two methods measure. Bioluminescence is based on the metabolic activity of the cells and increase according to the increase in metabolic activity of the cell population (Nelson *et al.*, 2003; Thorn *et al.*, 2007). In the exponential phase the cells are dividing regularly by binary fission at a constant rate depending on the growth medium and incubation conditions hence the correlation between viable counts and bioluminescence. During stationary phase bioluminescence does not correlate with viable count. As the cells stopped dividing the metabolic activity of the cell starts to decrease.

In a study carried out to use a bioluminescent *P. aeruginosa* strain to test antimicrobial efficacy of wound dressing (Thorn *et al.*, 2007), it was concluded that bioluminescence correlated with viable count in the exponential growth in

planktonic cultures ( $r^2 = 0.969$ ) and hence in this study exponential cultures were incorporated in to the *in vitro* wound infection model (Thorn *et al.*, 2007). In previous studies also workers have shown this growth phase dependent conditions in *in vitro* experiments using bioluminescent bacterial strains (Nelson *et al.*, 2003; Marques *et al.*, 2005). Discrepancies between bioluminescence and viable count were found when there was a different response by the cell of its metabolic activity compared to viability (Marques *et al.*, 2005). The different cell density of exponential phase culture of the two bioluminescent organisms (*E. coli* Nissle 1917 pGLITE (figure 3.6) and *P. aeruginosa* MCS5-lite (figure 3.3), showed good correlation between viable counts and bioluminescence. Therefore an exponential phase planktonic culture of the bioluminescent target organism was used throughout the current study to develop and use in the assay.

Most of the APDT studies carried out to date by other workers do not attempt to measure the kill rate as discussed in chapter 1, merely the numbers of survivors at the end of the experiment. Measuring the kill rate of an antimicrobial agent is the most important parameter for comparing different targets, different treatments and different physicochemical conditions of the assay. How long a biocide takes to reduce the number of bacteria by >3-log is an important indicator for it to have clinical application. The assay used in this thesis used a kinetic approach and bioluminescence enabled this kill kinetic of the test agent to be monitored rapidly and accurately. This was one advantage of using this method over traditional viable count methods. The reduction in bioluminescence was measured in real time especially in the case of ECAS where most of the antimicrobial activity occurs at the initial stages.

In this study 10 µg/ml was chosen to use in the assay after optimisation studies (figure 3.7). It was important to determine the concentration of MB that will give a significant kill rate over a 3 log reduction in viable count. As the concentration of MB increased, the photodynamic kill rate of bacteria decreased (figure 3.7). This is different to what would normally be expected when the concentration of a biocide is increased where the expected outcome is to observe a greater killing effect rather than less. The explanation for this difference is due to the property of

MB to dimerize as the concentration increases. As the concentration of MB increases there are more molecular collisions and a higher proportion of dimer to monomer. Monomer and dimers may be involved in different kinds of photochemical reactions, which may affect the mechanism and efficiency of cell kill (Tardivoa *et al.*, 2005). In addition the increase in PS molecules gives an optical shielding effect that prevents the absorption of light by the PS. Hence it is important to optimise the concentration of PS.

It was shown that MB alone and light alone is not active against either of the Gram-positive or Gram-negative species; both species require both light and photosensitizer to inactivate the micro-organism. The results showed that for both bioluminescent species there was significant correlation between viable count and bioluminescence in the killing phase (figure 3.8 and 3.9). A very similar kill rate for APDT was obtained with both bioluminescence and viable methods (table 3.1). Therefore loss of bioluminescence under these conditions may clearly indicate the loss in viability of bacterial cells. This proved that monitoring viability and/or bioluminescence appears to be feasible.

The assay system generated data showing conclusively that *E. coli*, *P. aeruginosa*, MRSA and *S. aureus* were susceptible to APDT. A study carried out to test APDT with MB and visible light, and a range of microbial species by Zeina *et al.* (2001) showed APDT to be effective in eliminating these microbial species. MB at 100µg/ml and standard light intensity conditions (42 mW/cm<sup>2</sup>) were used. The kill rates and subsequent D-values were determined against *Staphylococcus aureus*, *S. epidermidis*, *Streptococcus pyogenes*, *Corynebacterium minutissimum*, *Propionibacterium acnes* and *Candida albicans*. D-values for these species were 1.2, 1.1, 0.8, 2, 0.5 and 11 minutes, respectively. The D value obtained in the current study for *S. aureus* (3.1 mins) is 2.5 times higher than the study by Zeina *et al.* (2001). This is not surprising since the parameters used were different (the MB dye (10µg/ml) and light intensity (9.4mW/cm<sup>2</sup>) compared to the above study. Of all the target organisms *S. aureus* was the most sensitive organism. This is also expected as it is known that Gram-positive organism are more sensitive than Gram negative species to MB (Tegos and Hamblin, 2006).

The kill rate for MRSA when compared with *S. aureus* kill rate was much lower. It has been reported that phenothiaziniums were less effective against the MRSA strains than against the standard *S. aureus* (Wainwright *et al.*, 1998). However the decreases in activity were not as great as those for fucloxacillin and vancomycin (Wainwright *et al.*, 1998). This may be an important advantage of APDT as MRSA is a major organism associated with nosocomial infection (Chambers and Deleo, 2009). There is growing concern due to widespread occurrence of infections and limited alternative drug regimens. Moreover the reports on vancomycin-resistant *S. aureus* make this issue more urgent (Wainwright *et al.*, 1998). In addition staphylococcal related infections or colonisation sites are accessible to topical treatments (e.g. in epidermal wounds or burns) (Wainwright *et al.*, 1998) therefore APDT can be applied to these infections in practice. The result of the current study shows that kill rate is high for both these organisms and effective killing (3 log reduction) can be seen in less than 30 minutes of treatment. This indicates APDT application need require only short treatments and may be a feasible treatment option for localised infections.

The kill rates for *E. coli* Nissle 1917 pGLITE and *P. aeruginosa* MCS5-lite were 0.172 RLU/min (D value of 5.85 mins) and 0.121 RLU/min (D value 7.94 mins) respectively. Within this assay system the *E. coli* kill rate was slightly higher than that measured for *P. aeruginosa*. The kill rates for both the gram negative organisms were lower compared to the Gram positive *S. aureus*

In a study carried out with MB 10  $\mu\text{mol L}^{-1}$  and light dose of 12 J  $\text{cm}^{-2}$  10 minutes exposure at 630 nm showed a decrease of 5 log for *P. aeruginosa* and 4 log for *E. coli* (Melo *et al.*, 2011) showing that APDT is effective against these organisms as was found in the present study. Differences in log reduction in number of cells may be due to the differences in the protocol (e.g concentration of PS, light dose, pre-incubation time, cell inoculum density). Several other studies have also reported by viable count methods that APDT is effective against a variety of organisms using MB and light (Wainwright *et al.*, 2007). It is difficult to make direct comparisons to these studies as different test parameters were used.

However, in general this study is in agreement with previous studies that APDT is effective in killing the target organism after short treatments.

In an APDT study a bioluminescent indicator strain was used to assess the activity of three cationic *meso*-substituted porphyrin derivatives. It was shown that in the presence of the PSs under artificial ( $40 \text{ W m}^{-2}$ ) or solar irradiation ( $620 \text{ W m}^{-2}$ ) that both were effective against bioluminescent *E. coli* ( $>4$  log bioluminescence decrease) (Alves *et al.*, 2008). The results of this study showed that bioluminescence analysis is an efficient, sensitive and faster approach to study APDT activity.

Bioluminescence allows only living or viable cells to be detected (Rocchetta *et al.*, 2001). The reduction in bioluminescence in a killing environment may not directly show the loss in viability. However it is reasonable to assume that, when the changes in treated samples are compared with those of untreated samples, the relative difference is reflective of changes in cell viability. Therefore bioluminescence output by the cells may produce characteristic kill curve relating to the inactivation kinetics of APDT under defined conditions.

Several other studies carried out using bioluminescent organisms have also proved the effectiveness of this method of using bioluminescent organisms in APDT (Hamblin *et al.*, 2002; Hamblin *et al.*, 2003; Demidova *et al.*, 2005). Furthermore, use of bioluminescence as a measure of cell viability has been shown to correlate well with standard recovery techniques such as viable counts under defined conditions (Beard *et al.*, 2002; Kadurugamuwa *et al.*, 2003). From these results it can be concluded that in a killing environment the loss of bioluminescence can be a good indicator of loss of viability of bacterial cells.

The ECAS kill kinetic assay showed that ECAS gave the highest kill rate compared to APDT and reduces the bioluminescence level to the limit of detection within 10 seconds. The kill rates for 50% v/v, 25% v/v, 10% v/v, 1% v/v and 0.5% v/v were -26.28, -24.72, -28.8, -12.38, -7.26 logRLU/min respectively. The kill rates for ECAS were considerably faster than APDT even at the lowest dose of 0.5% ECAS.

Because it is a very fast acting agent the initial kill by ECAS would not be possible to measure easily by traditional viable count method. The bioluminescence method enabled full capture of the kill rates of ECAS. Hence ECAS kill kinetic assay is a very useful development. Fast action is highly desirable if ECAS was to be used as a hand disinfection biocide where short contact time is required. Therefore it is very important to develop studies to test the efficacy of ECAS, especially by comparing to other known antimicrobial agents. Most importantly this method is more accurate for measuring rates because greater number of data points can be achieved compared with viable count in a specific time. This is because viable count requires taking a sample, diluting and plating out whereas with bioluminescence a measurement gives 600 data points in a 10 minutes test. However, with viable counts the maximum number of data point likely to be obtained would be 10 points. With higher number of data points greater knowledge of variation can be seen and more accurate results will be achieved. Since bioluminescence can be measured within seconds it is also possible to obtain kill curves for microbial agents that kill in a short duration in contrast with viable count. This is evident with ECAS used in this research, which can reduce the number of bacteria by 2 or 3 logs in a few seconds and reading were recorded every 0.2 seconds.

Bioluminescence technique has been previously used to compare ECAS activity with a range of biocides (Robinson *et al.*, 2011). This study reported that bioluminescence method was very effective to measure initial kill rates over very short time domains and compared ECAS with the range of biocides. It was found that 80% v/v ECAS produced the highest kill rate compared to bleach, Virkon, and ethanol at matched concentrations. Also it was reported that in the presence of fetal bovine serum (FBS) the activity of ECAS was reduced considerably (reported kill rates 80% v/v ECAS kill rate  $-2.336 \log_{10} \text{ RLU s}^{-1}$ , in the presence 5% FBS  $1.579 \text{ RLU s}^{-1}$  and 10% FBS  $0.165 \text{ RLU s}^{-1}$ ). Even though the presence of organic soiling reduced the kill rate to  $0.165 \text{ RLU s}^{-1}$  it still produced 9.9 log reductions in 1 minute, which is more than the effective range of 3 log.

The results of this study confirmed that the developed bioluminescence assay is rapid and accurate, and can be used to monitor bacterial inactivation by both APDT and ECAS. Therefore this assay may enable further elucidation of their mechanism of action of both the agents.

**Chapter 4: Comparative mechanistic study of APDT and ECAS using bioluminescent rapid assay and ROS specific fluorescent probes**

#### 4.1. Introduction

In chapter 3 a bioluminescent-based assay was developed and using this assay the kill rates of APDT and ECAS treatments were accurately determined. The assay was rapid and gave real time data on the kill kinetics of the reaction occurring. It was shown that the kill rates by both APDT and ECAS were reduced or increased in line with the dose of treatment (APDT and ECAS) used. Therefore bioluminescence enabled kill kinetics of the reaction to be monitored. The main aim of this chapter is to understand the likely killing mechanisms by using the bioluminescent assay with or without specific ROS scavengers and other compounds that inhibit or enhance killing activity, and also to determine if ROS specific fluorescent probes could detect real-time ROS generation in the system.

A broad definition of free radicals is any chemical species that has one or more unpaired electrons. These species are highly unstable, short-lived intermediates that stabilize by abstracting hydrogen from another chemical species (Laguerre *et al.*, 2007). The term reactive oxygen species (ROS) is a collective term used for oxygen free radicals that includes not only oxygen-centred radicals such as  $\text{OH}^\bullet$  and  $\text{O}_2^-$  but also some non-radical derivatives of oxygen, such as hydrogen peroxide ( $\text{H}_2\text{O}_2$ ), singlet oxygen  $^1\text{O}_2$  and hypochlorous acid (HOCl)

Free radical and ROS can be generated in wide variety of biological and chemical systems. These ROS display different kinetics and activity in biological systems. The effects of superoxide and hydrogen peroxide are less acute than those of hydroxyl and singlet oxygen, because superoxide and hydrogen peroxide can be detoxified by endogenous antioxidants including enzymes that may be induced by oxidative stress. In contrast, no enzyme can detoxify hydroxyl and singlet oxygen possibly due to their high capacity to immediately react upon production making them extremely toxic and lethal (Vatansever *et al.*, 2013).

The cytotoxicity effects of APDT are due to the cytotoxic ROS produced by the excited triplet state PS upon absorption of light (Wainwright, 1998; Hamblin and Hassan, 2004). The ROS produced in type I mechanisms include free radicals such as hydroxyl radicals and in type II mechanisms singlet oxygen is produced.

Oxygen is required for type II mechanism. Type I and Type II reactions can occur simultaneously.

Although the photophysics behind the photodynamic reaction and the types of ROS produced is well understood, the mechanistic details of how the ROS generated during APDT lead to microbial killing are not fully understood. Singlet oxygen is the main species thought to be involved in APDT (Ergaieg *et al.*, 2008) and is a highly reactive molecule that can result in extreme detrimental effects to biological systems (Halliwell, 2006). Hydroxyl radical is thought to be the main active species produced in ECAS (Thorn *et al.*, 2012) and also produced in type I pathway in APDT (Hamblin and Hassan, 2004). It is the strongest oxidising agent known, being characterised to react non-selectively with extremely high rate constants with almost every type of organic molecule found in living cells. The hydroxyl radical is so active that, if formed in living systems, will react with whatever biological molecule is in their close vicinity, and can damage virtually all types of organic biomolecules, including carbohydrates, nucleic acids, lipids, proteins, DNA, and amino acids (Halliwell, 2006).

ECAS has been reported to have strong antibacterial effects against a range of pathogenic micro-organisms (Liao *et al.*, 2007). In the literature this high antimicrobial activity has been attributed to various inherent characteristics of ECAS. It has been proposed that high Oxidation Reduction Potential (ORP) creates an unbalanced osmolarity which damages the cell membrane. This may cause oxidizing moieties present in ECAS to penetrate into the cell cytoplasm leading to further damage to intracellular proteins, lipids and nucleic acid, ultimately killing the cells (Thorn *et al.*, 2012). In addition to this, chlorine concentration and pH has also been shown to play an important role (Park *et al.*, 2004). Many researchers have concluded the presence of free chlorine species such as HOCl as the main primary species responsible for disrupting the microbial structure (Thorn *et al.*, 2012).

In research carried out to study the fungicidal efficacy of ECAS, hydroxyl radicals were detected in ECAS, and significantly contributed to fungicide efficiencies (Xiong *et al.*, 2010). Therefore it has been concluded that for ECAS a

combination of both reactive free radical and ROS may contribute to its antimicrobial efficacy (Thorn *et al.*, 2012). However, very few studies have attempted to identify the ROS species in ECAS. This may be due to difficulties of directly detecting these species due to their low levels and their high reactivity and instability. In one study the presence of hydroxyl radical in ECAS was shown using the direct method of electron spin resonance spectroscopy (ESR) (Suzuki *et al.*, 2002). However no studies have attempted to determine the rate of generation of ROS in real-time and how this relates to the kill kinetics of the target organism.

Many studies conclude that  $^1\text{O}_2$  is in fact the major ROS of importance in APDT (Ergaieg *et al.*, 2008; Maisch *et al.*, 2007), while others attribute the killing to radicals including  $\text{OH}^\bullet$  (Martin and Logsdon, 1987). Moreover these studies are carried out under different conditions with different light sources with different PS therefore making it difficult to compare the results. The various factors affecting the production of ROS and kill kinetics is dependent on microenvironment conditions (Yamakoshi *et al.*, 2003). Therefore it is essential to carry out studies using the same experimental conditions to distinguish and quantify each type of ROS produced.

To the author's knowledge no study has previously been carried out to monitor the ROS production kinetics at the same time as monitoring the kill kinetics using bioluminescence. In this study the effects of specific scavenger addition was monitored in real time using the bioluminescent target organism. In addition, fluorescence probes were used to monitor the ROS production kinetics by the two agents (APDT and ECAS). The combination of these two methods, addition of scavenger and use of fluorescent probes, will enable a better understanding of the mechanism of APDT. Moreover comparative study of APDT to another ROS generating system (ECAS) using the same standardised method will enable better understanding of the mechanisms behind both antimicrobial agents.

Previous studies of microbial killing employed viable count recovery and workers only monitored the relative survival of the microorganisms in the presence or absence of scavenger by comparing the final survival population numbers at the end; not by comparing the killing rates (Sabbahi *et al.*, 2008; Wong *et al.*, 2005;

Bhatti *et al.*, 1998). Using viable count methods to determine kill would be very laborious and probably inaccurate since minimum of five different time points in the presence of scavenger with all the relevant controls would be required to obtain a rate. For this reason most researchers do a single viable count after fixed time interval to show inhibition of the killing in the presence of specific ROS. Using the bioluminescence method to measure kill rates rather than mere survival numbers at the end of the reaction time is more accurate since a killing may deviate from first order kinetics. Bioluminescence method is especially important in the case of fast acting biocides since it is the only method to enable the capture of the rapid kill kinetics of ECAS (Robinson *et al.*, 2011). Therefore using bioluminescence will enable the accurate capture of kill rate changes in the presence or absence of scavengers enabling the detection of ROS involvement in ECAS or APDT.

#### **4.2 Indirect method of detecting singlet oxygen and free radicals**

Indirect methods of evaluating the presence of singlet oxygen or other ROS have been used to verify the hypothesis of involvement of singlet oxygen and ROS in PDT and APDT (Gorman and Rodgers 1992; Nitzan *et al.*, 1989; Bhatti *et al.*, 1998). Using this method various studies have confirmed ROS production in APDT (Nitzan *et al.*, 1989; Ergaieg *et al.*, 2008; Abe *et al.*, 1997; Wong *et al.*, 2005).

Numerous compounds exist that can react competitively with ROS, providing protection against its cytotoxic effects. A variety of scavengers and quenchers of specific ROS has been employed to assess their relative contributions to cytotoxic events in APDT. Table 4.1 shows the type of scavenger molecule and the respective ROS inhibited in different systems.

Tryptophan is a scavenger with reported activity against singlet oxygen (Henderson and Miller, 1986) however it is thought to be less specific since it has also been reported to inhibit hydroxyl radical (Maskos *et al.*, 1992).

**Table 4-1 Indirect method of detecting ROS using specific scavengers**

Reference	Microbial target species	Singlet oxygen quenchers	Free radical quenchers	ROS generation	Effect of scavenger
Ergaieg <i>et al.</i> , 2008	<i>E. hirae</i> <i>E. coli</i>	Sodium azide Histidine $\beta$ -carotene	Superoxide dismutase Catalase Dimethyl sulfoxide (DMSO)	meso-substituted cationic porphyrin (TMPyP) (114 $\mu$ M) plus 0.285W polychromatic light for 3 min	Reduction of EPR signal Both type I and type II mechanisms
Sabbahi <i>et al.</i> , 2008	<i>S. aureus</i>	Sodium azide Tryptophan	Mannitol	APDT MB(20 $\mu$ M) and 10 minutes light exposure	Inhibition of killing  APDT MB occurred in part, via a Type I mechanism in which OH <sup>*</sup> was produced.
Tavares <i>et al.</i> , 2011	bioluminescent <i>E. coli</i>	Sodium azide (10 mM)	Mannitol (100 mM)	0.5 mM Tri-Py <sup>+</sup> -Me-PF, 5.0 mM Tetra-Py <sup>+</sup> -Me or 5.0 mM Tri-SPy <sup>+</sup> -Me-PF  270 min with artificial white light	Inhibition in reduction in bioluminescence activity  Type I and type II mechanisms (type II mechanism more important compared to type I mechanism)

Huang <i>et al</i> 2012	<i>S. aureus</i> , <i>E. faecalis</i> ,  <i>E. coli</i> , <i>P. mirabilis</i> , <i>P. aeruginosa</i>	Sodium azide (10 mM)	DMT (200 mM)	conjugate between polyethylenim ine and chlorin(e6) (PEI-ce6) 400 nM and 660 nm light 5 Jcm <sup>-2</sup>  (PEI-ce6) 2 μM and light 660 nm 100 mWcm <sup>-2</sup>	Inhibition killing (viable count cfu/ml)  Inhibition of fluorescence by HPF(10 μM)  Gram-negative bacteria are more susceptible to HO· (type I mechanism) while Gram- positive bacteria are more susceptible to <sup>1</sup> O <sub>2</sub> (type II mechanism)
Nitzan <i>et al.</i> , 1989	<i>S. aureus</i>	Methionine Tryptophan DABCO	Propylgallate	Deutero- porphyrin	Both type I and type II mechanisms
Omar <i>et al.</i> , 2008)	<i>S. aureus</i>	Tryptophan Deuterium oxide (enhancer of singlet oxygen	-	Indocyanine green	Type II mechanisms

#### 4.2.2 Fluorescence Probes to determine APDT and ECAS mechanisms

Sensitive and selective detection of ROS is vital for understanding its involvement and antimicrobial mechanism in ROS generating systems such as in APDT and ECAS. Use of fluorescence and chemiluminescence probes is a rapid and simple method exhibiting high sensitivity and desirable selectivity for detecting particular ROS species; therefore having great potential for ROS determination (Price *et al.*, 2009).

ROS activity and production can be determined using different analytical techniques such as high performance liquid chromatography, gas chromatography and mass spectrometry by detecting specific biomarker or products from the oxidation of protein, DNA, lipid or other biomolecules (Vivekanandan-Giri *et al.*, 2011). These analytical procedures also provide specific detection, for example for, hypochlorous acid species (Winterbourn and Kettle, 2000). However, the main disadvantage of these methods is it does not provide for rapid real time monitoring (Winterbourn, 2014). It is preferable to detect ROS in real time within live cells or in cell free systems as they are generated. Specific fluorescent probes with fluorescent imaging techniques allows for real time monitoring and hence will give better insight into the mechanisms and role of ROS in systems investigated.

The literature contains numerous reports of the use of fluorescent probes for the detection of ROS (Gomes *et al.*, 2005). However, most commonly used traditional probes (e.g. dihydro-compounds such as dihydrorhodamine 123 (DHR123) and 2',7'-dichlorodihydrofluorescein (DCFH) reacts with a wide range of ROS (Soh, 2006). These probes are also highly photosensitive and as a result are autoxidized to produce large background fluorescence in the absence of ROS in fluorescent measurements that involve irradiation of excitation light (Soh, 2006).

A new generation of fluorescent probes have been developed to overcome these limitations (Setsukinai *et al.*, 2003). These include APF, and HPF, which were shown to be stable against autoxidation and specific (or relatively specific) to detect OH<sup>•</sup> and peroxynitrite (Setsukinai *et al.*, 2003). APF also showed

fluorescence in the presence of hypochlorite ( $\text{OCl}^-$ ) while HPF showed no activity.

SOSG is also a recently developed probe to detect  $^1\text{O}_2$  (Ragas *et al.*, 2010). Previous work has shown the specificity of SOSG using a range of conditions known to involve the production of singlet oxygen. For example it was demonstrated that SOSG can be used effectively to detect singlet oxygen in diatoms and leaves (Flors *et al.*, 2006). SOSG exhibits weak blue fluorescence with excitation peaks at 372 nm and 393 nm and emission peaks at 395 nm and 416 nm (Molecular Probes, 2005). In the presence of  $^1\text{O}_2$  SOSG emits a green fluorescence with excitation and emission peaks at 504 nm and 525 nm, respectively, which can be readily detected for singlet oxygen (Flors *et al.*, 2006). Even in the presence of mixed oxidants (superoxide and hydroxyl radicals) SOSG appears to give specific dose dependent fluorescence in proportion to the concentration or production rate of singlet oxygen (Molecular Probes, 2005).

These fluorescent molecules physically change shape (and brightness) when they come into contact with specific reactive molecules. These conformational changes enhance or reduce the fluorescence of the indicators at certain given frequencies of light. This change in fluorescence is then measured using a fluorospectrometer that measures the intensity of the spectrum of light emitted from the indicators. The change in fluorescence of these indicators before and after exposure to these reactive molecules therefore indicates existence of such reactive molecules and their generation in the system. Each of these three indicators (APF, HPF and SOSG) is sensitive to specific types of reactive molecules and considered to be resistant to false positives and have been well studied and routinely used to detect ROS.

Price *et al.* (2009) assessed ROS production in PDT using APF, HPF and SOSG. It was shown that both APF and HPF could be used to monitor the formation of  $\text{OH}^\bullet$  as well  $^1\text{O}_2$  in PDT. The portion of the fluorescence quenched by sodium azide ( $\text{NaN}_3$ ) (scavenger of singlet oxygen) represents the contribution of singlet oxygen and the portion quenched by DMSO (quencher of  $\text{OH}^\bullet$ ) represents the

contribution of hydroxyl radical. Using SOSG probe these workers confirmed production of singlet oxygen in PDT. SOSG is mainly specific to singlet oxygen as the fluorescence was quenched to large extent in the presence  $\text{NaN}_3$  and only minor quenching with DMSO. The authors concluded that this procedure could represent a useful means for evaluating formation of both ROS in the context of PDT (Price *et al.*, 2009). In another recent study HPF and SOSG was employed to examine the relative contributions  $^1\text{O}_2$  and  $\text{OH}^\bullet$  in APDT mediated killing of Gram-positive and Gram-negative bacteria (Huang *et al.*, 2012).

#### **4.4 Aims and objectives of this chapter**

To apply the bioluminescent target based rapid assay in order to determine the mechanisms of two oxidative biocides (APDT and ECAS) in the presence or absence of ROS specific inhibitors. To develop a fluorescence-based assay using ROS specific fluorescent probes in order to detect the real-time production of ROS by APDT and ECAS. Both APDT and ECAS have elements of highly reactive oxidizing species but with some similarities and differences in their ROS profile. To compare the two systems side by side using standardized assays in order to understand the relative contribution of  $^1\text{O}_2$  and  $\text{OH}^\bullet$  to the mechanisms of killing of target organism in each system.

## 4.5 Results

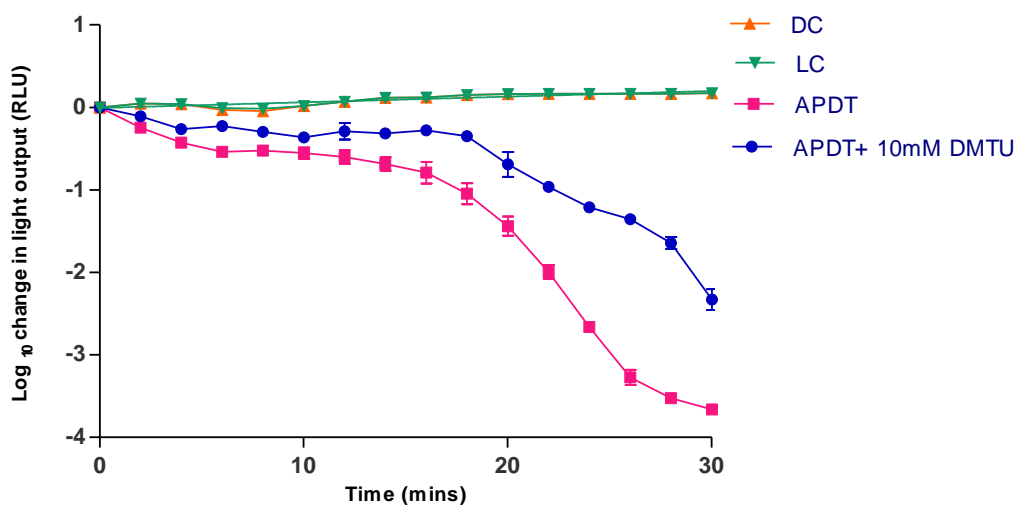
### 4.5.1 APDT kill kinetics of *P. aeruginosa* MCS5-lite in the presence of hydroxyl radical scavengers, singlet oxygen scavenger and D<sub>2</sub>O

All assays were run using appropriate controls. Exposure to scavengers invariably caused inhibition of killing actions that would have been expected in the light and MB treatment. All other controls without light or MB gave flat profile with little change in viable numbers or bioluminescence throughout the assay.

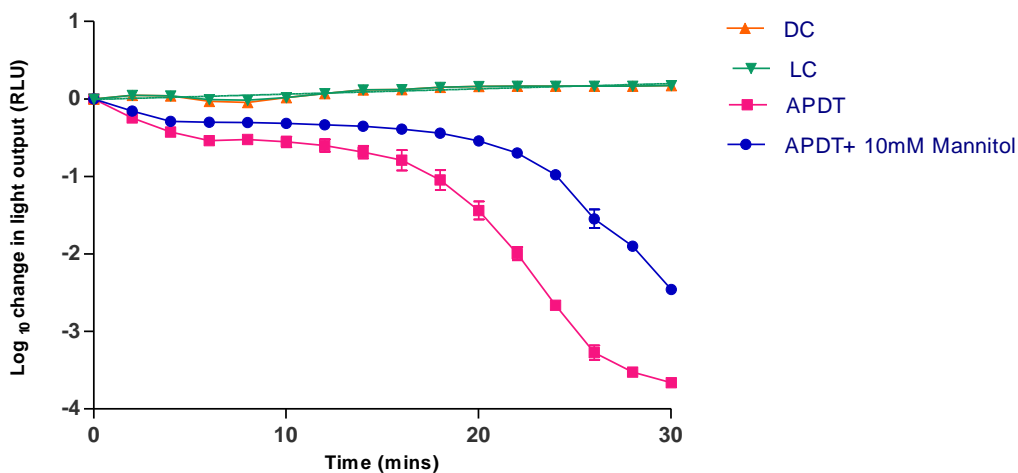
Data presented in figures 4.1 to 4.2 show the effects of hydroxyl radical scavengers N,N'-dimethylthiourea (DMTU) and mannitol on *Pseudomonas aeruginosa* MCS5-lite. Both gave significant reductions compared with the control kill rate and this may suggest some role for hydroxyl radical in the killing mechanism for this microbial species. It was of interest to note that there was a difference in the kill rate when D<sub>2</sub>O was included in the assay (figure 4.3) showing statistically significant enhancement, and thus suggesting a role for singlet oxygen in the normal control killing process. However it was interesting to note that the initial kill rate (first 8 minutes of exposure) showed a slight increase.

Figure 4.4 shows the greater inhibition of killing in the presence 10mM tryptophan, again suggesting singlet oxygen mediated involvement in the killing of the target species. Table 4.2 summarises the kill rates and the percentage of protection that is afforded to the target species by the different compounds. It is interesting to note that tryptophan at 10mM gave strong protection of killing effect (89% reduction in the kill rate), whilst the hydroxyl scavengers gave around 50% protection suggesting a role for type-1 hydroxyl radical killing mechanisms as well as a role for singlet oxygen (type II mechanisms).

As a significant difference was found between the initial (first 8 min) and later kill rate therefore the initial rate was also calculated. Table 4.3 summarise the kill rates and relative protection.



**Figure 4-1** Changes in bioluminescence of *P. aeruginosa* MCS5-lite treated with APDT (MB 10  $\mu\text{g/ml}$  and total light dose 17  $\text{Jcm}^{-2}$  (light intensity 9.47  $\text{mWcm}^{-2}$ ) compared to APDT in the presence of 10 mM DMTU (hydroxyl radical scavenger). DC, dark control; LC, light control, error bars show mean  $\pm$  SD (n=3).



**Figure 4-2** Changes in bioluminescence of *P. aeruginosa* MCS5-lite, treated with APDT (MB 10  $\mu\text{g/ml}$  and total light dose 17  $\text{Jcm}^{-2}$  (light intensity 9.47  $\text{mW/cm}^2$ ) compared to APDT in the presence of 10 mM mannitol (hydroxyl radical scavenger). DC, dark control; LC, light control, error bars show mean  $\pm$  SD (n=3).

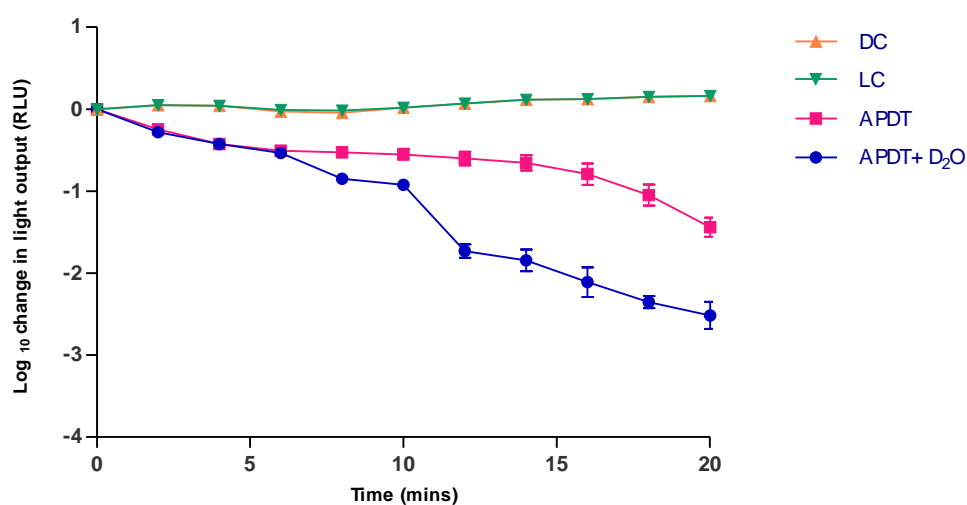


**Figure 4-3** Changes in bioluminescence of *P. aeruginosa* MCS5-lite treated with APDT (MB 10  $\mu\text{g/ml}$  and total light dose 11  $\text{Jcm}^{-2}$  (light intensity 9.47  $\text{mW/cm}^2$ ) compared to APDT in the presence of  $\text{D}_2\text{O}$  (singlet oxygen enhancer). DC, dark control; LC, light control, error bars show mean  $\pm$  SD (n=3).

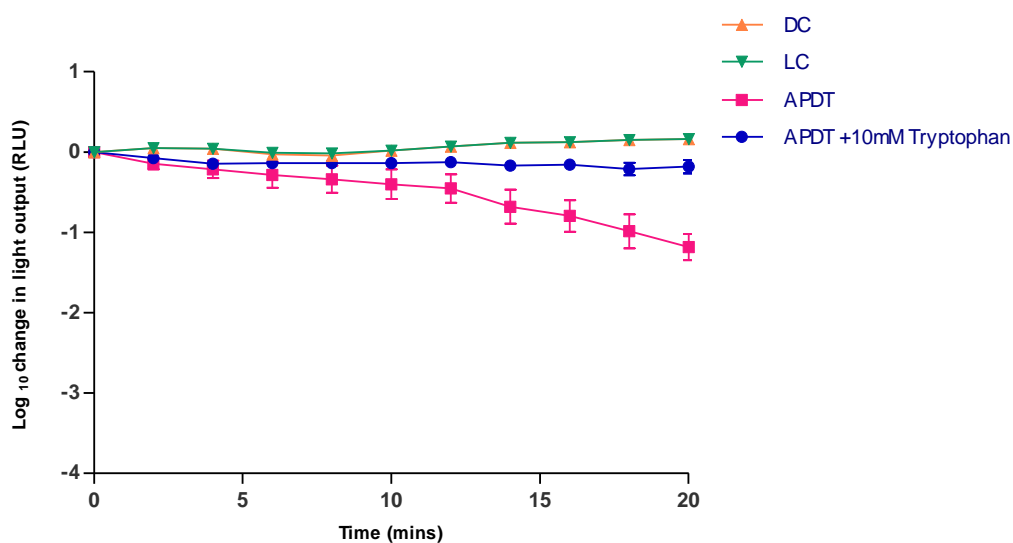


**Figure 4-4** Changes in bioluminescence of *P. aeruginosa* MCS5-lite treated with APDT (MB 10  $\mu\text{g/ml}$  and total light dose 11  $\text{Jcm}^{-2}$  (light intensity 9.47  $\text{mW/cm}^2$ ) compared to APDT in the presence of 10 mM tryptophan (scavenger of singlet oxygen). DC, dark control; LC, light control, error bars show mean  $\pm$  SD (n=3).

**Table 4-2 Showing the APDT kill rate over 20-30 minutes assay of *P.aeruginosa* MCS5-lite in the presence or absence of singlet oxygen scavengers or hydroxyl radical scavengers**

Treatment	Kill rate (log RLU/min)	r <sup>2</sup>	P value	Deviation from zero?	Percentage relative kill	Percentage relative protection
APDT	-0.121 ± 0.007	0.852	< 0.0001	Significant	100	0
APDT +10 mM Tryptophan	-0.005 ± 0.001	0.423	0.001	Significant	10.579	89.421
APDT+ D <sub>2</sub> O	-0.134 ± 0.005	0.963	< 0.0001	Significant	247.730	-147.730
APDT +10 mM DMTU	-0.059 ± 0.007	0.817	< 0.0001	Significant	48.519	51.481
APDT +10 mM Mannitol	-0.060 ± 0.010	0.712	< 0.0001	Significant	49.785	50.215

**Table 4-3 Showing the APDT kill rate of *P. aeruginosa* MCS5-lite over the first 8 minutes in the presence or absence of singlet oxygen scavengers or hydroxyl radical scavengers**

Treatment	Kill rate (log RLU/min)	r <sup>2</sup>	P value	Deviation from zero?	Percentage relative kill	Percentage relative protection
APDT	-0.065 ± 0.07	0.873	< 0.0001	Significant	100	0
APDT +10 mM Tryptophan	-0.016 ± 0.005	0.546	0.015	Significant	54.549	45.451
APDT+ D <sub>2</sub> O	-0.097 ± 0.006	0.953	< 0.0001	Significant	148.923	-48.923
APDT +10 mM DMTU	-0.039 ± 0.008	0.880	0.018	Significant	59.771	40.229
APDT +10 mM Mannitol	-0.038 ± 0.010	0.809	0.038	Significant	57.632	42.368

#### 4.5.2 APDT kill kinetics *S. aureus* in the presence of hydroxyl radical scavengers and singlet oxygen scavenger

Figure 4.5. shows the effects of tryptophan at 10mM (potentially a singlet oxygen scavenger at this concentration), and the hydroxyl radical inhibitors DMTU and mannitol; all gave significant reductions in the rate of killing. The kill rate data and percentage protection is summarised in Table 4.4 and shows a 97% reduction of kill for tryptophan, and 90% and 80% for DMTU and mannitol respectively. However, it should be noted that the bioluminescence-based assay could not be applied to *Staphylococcus* (since no suitable lux variant could be sourced) so all rate data presented are from viable counts of starting and surviving populations through the time of the assay. Accurate kill rates could not be obtained due to the lack of sample points for all conditions at all times; a feat that is difficult using viable count.

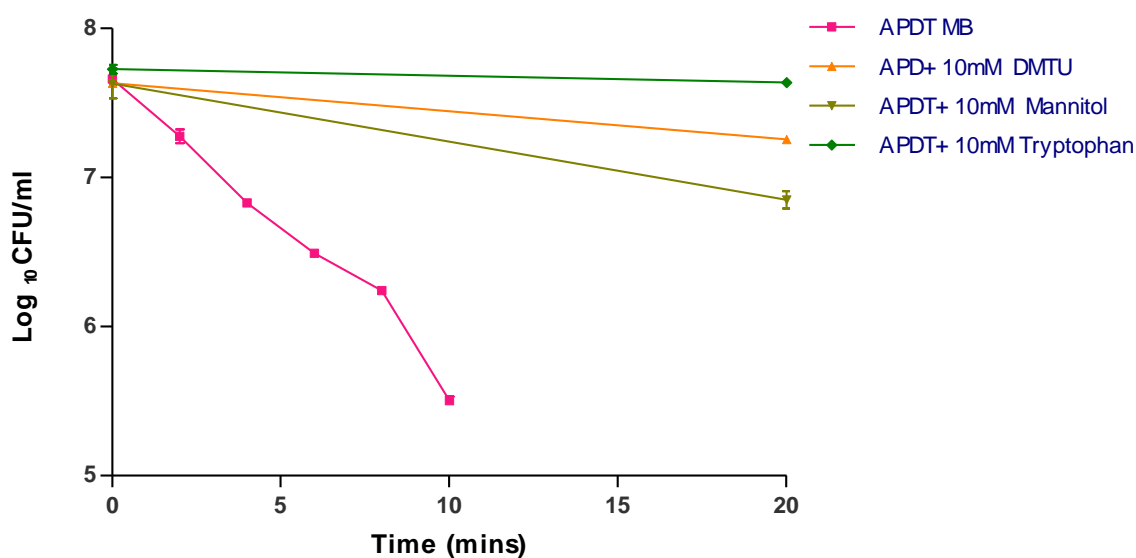


**Figure 4-5 Changes in bioluminescence of *S. aureus* treated with APDT (MB 10  $\mu$ g/ml and total light dose 11  $\text{Jcm}^{-2}$  (light intensity 9.47  $\text{mW/cm}^2$ ) compared to APDT in the presence of 10 mM tryptophan, mannitol and DMTU. Error bars show mean  $\pm$  SD (n=3).**

**Table 4- 4 Showing the APDT kill rate of *S. aureus* in the presence or absence of singlet oxygen scavengers or hydroxyl radical scavengers**

<b>Treatment</b>	<b>kill rate (slope log cfu/ml/min)</b>	<b>Percentage Relative protection</b>	<b>Percentage Relative kill</b>
APDT MB	-0.203 ± 0.009	0.00	100
APDT MB10mM DMTU (scavenger of hydroxyl radical)	-0.019 ± 0.003	90.69	9.31
APDT MB10mM Mannitol (scavenger of hydroxyl radical)	-0.039 ± 0.006	80.77	19.23
APDT MB 10mM tryptophan (scavenger of singlet oxygen)	-0.004 ± 0.002	97.81	2.19

### **4.5.3 APDT kill kinetics *E. coli* Nissle 1917/pGLITE in the presence of hydroxyl radical, singlet oxygen scavenger and D<sub>2</sub>O**

Figure 4.6 shows the APDT activity compared to dark control and light only control. Figures 4.7, 4.8 and 4.9 show the effects of tryptophan (at 10mM and 1 mM), mannitol (10mM) and DMTU (10mM) respectively. All showed significant reductions in the expected kill rate seen in the treatment control. The kill rate data and percentage protection given by the treatments is summarised in table 4.5. Figure 4.10 shows the effects of the use of D<sub>2</sub>O replacement of H<sub>2</sub>O. The rate of kill was markedly increased, strongly supporting the role of singlet oxygen in APDT killing. However, the dark control also showed reduction in bioluminescence over the first 5 to 7.5 minutes before completion of the treatment response at 20 minutes with an overall 1-log drop of light output compared to control. It shows later recovery from 7.5 minutes. In comparison, the APDT with D<sub>2</sub>O continued to reduce bioluminescence another two log-fold, showing a clear-cut difference in effect.

As with previous findings, tryptophan (10mM) was shown to be the most effective overall inhibitor of total APDT killing. Mannitol and DMTU also gave protection, supporting the role of hydroxyl radical involvement (type-I mechanisms) in cell killing. However the protection effect of mannitol was less compared to DMTU.

Table 4.6 summarises the initial kill rate calculations based on the first 8 minutes (5 data points)

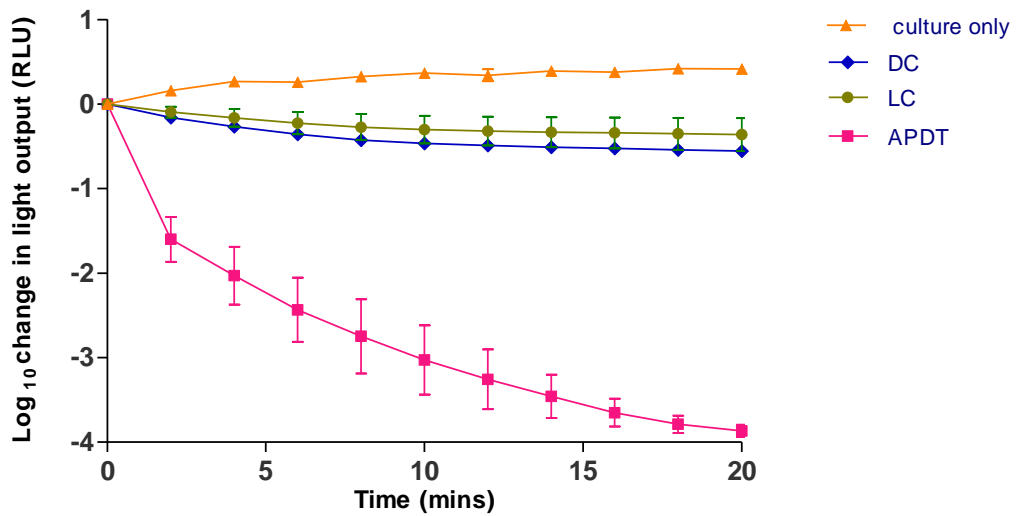


Figure 4-6 Changes in bioluminescence of *E. coli* Nissle 1917 pGLITE treated with APDT (MB 10  $\mu\text{g/ml}$  and total light dose 11  $\text{J/cm}^2$  (light intensity 9.47  $\text{mW/cm}^2$ ) compared to controls. DC, dark control; LC, light control, error bars show mean  $\pm$  SD (n=3).

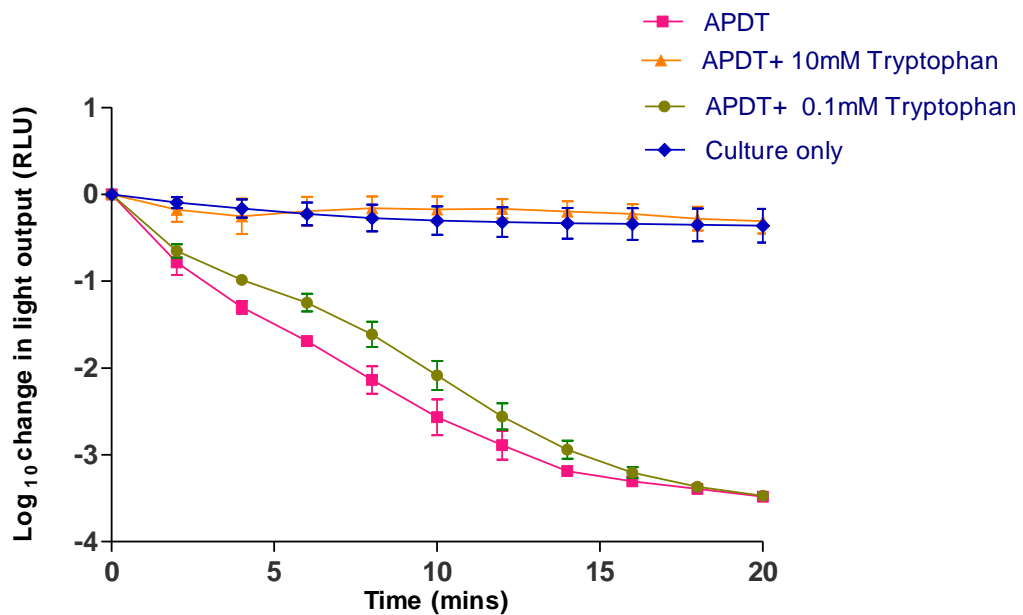
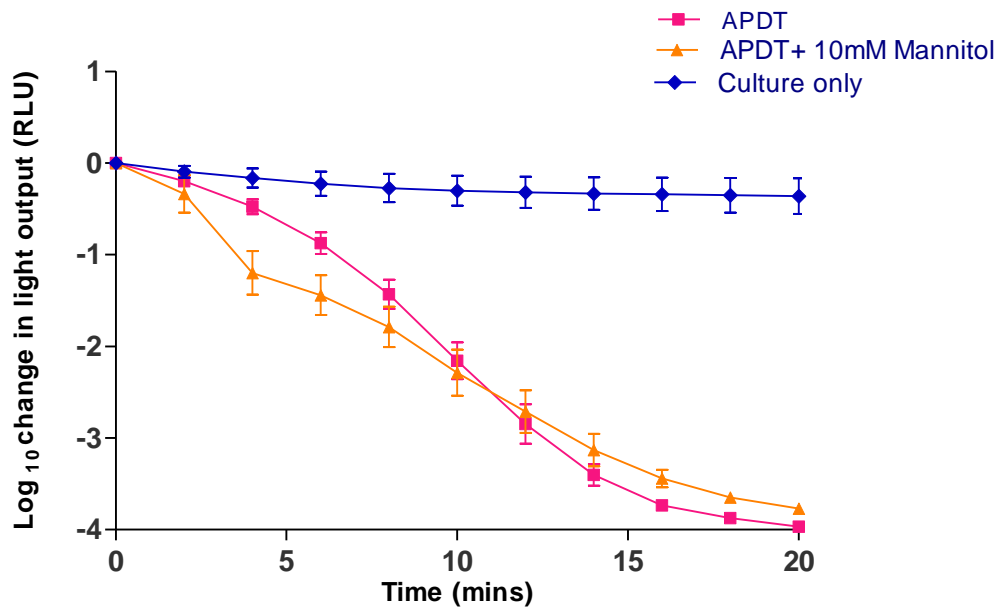
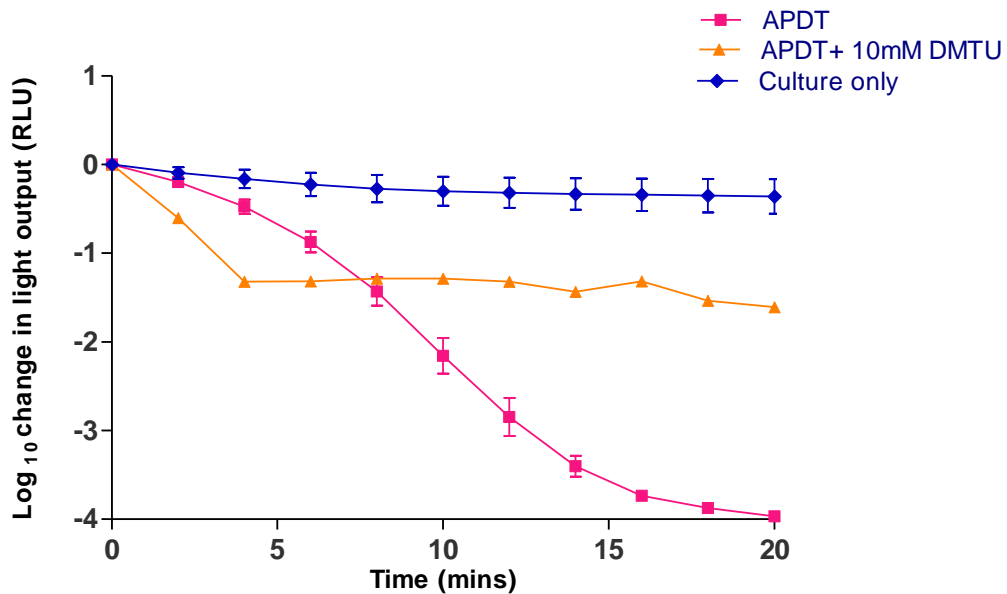


Figure 4-7 Changes in bioluminescence of *E. coli* Nissle 1917 pGLITE treated with APDT (MB 10  $\mu\text{g/ml}$  and total light dose 11  $\text{J/cm}^2$  (light intensity 9.47  $\text{mW/cm}^2$ ) compared to in the presence of 0.1 mM or 10 mM tryptophan. Error bars show mean  $\pm$  SD (n=3).



**Figure 4-8** Changes in bioluminescence of *E. coli* Nissle 1917 pGLITE treated with APDT (MB 10  $\mu\text{g}/\text{ml}$  and total light dose 11  $\text{J}/\text{cm}^2$  (light intensity 9.47  $\text{mW}/\text{cm}^2$ ) compared to assay in the presence of 10 mM mannitol. Error bars show mean  $\pm$  SD (n=3).



**Figure 4-9** Changes in bioluminescence of *E. coli* Nissle 1917 pGLITE treated with APDT (MB 10  $\mu\text{g}/\text{ml}$  and total light dose 11  $\text{J}/\text{cm}^2$  (light intensity 9.47  $\text{mW}/\text{cm}^2$ ) compared to in the presence of 10 mM DMTU. Error bars show mean  $\pm$  SD (n=3).

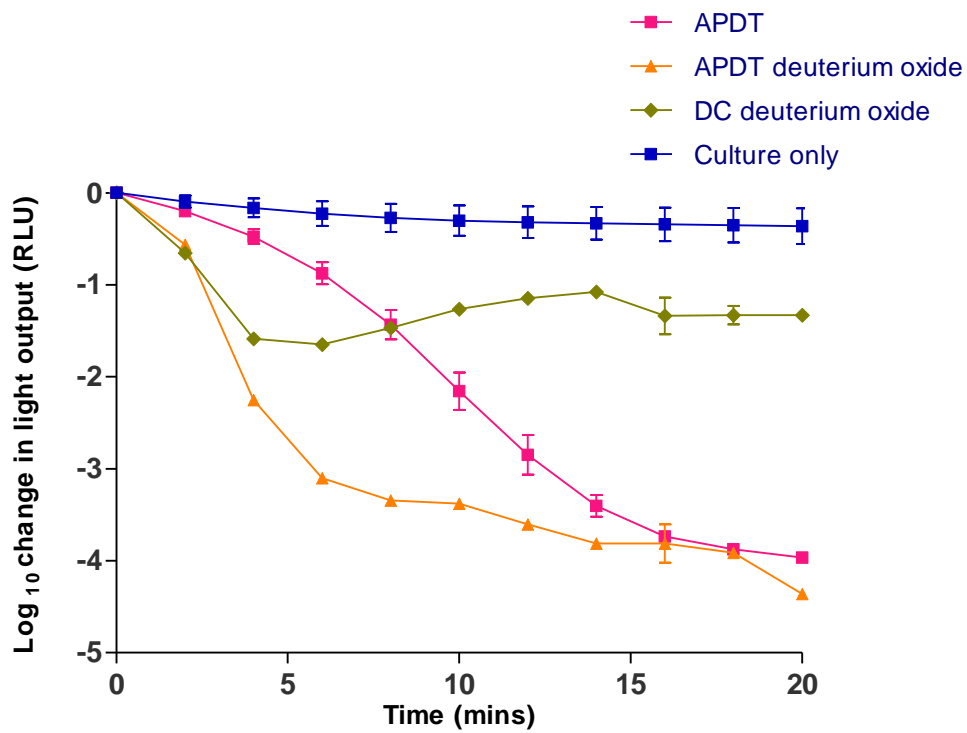


**Figure 4-10 Changes in bioluminescence of *E. coli* Nissle 1917 pGLITE treated with APDT (MB 10  $\mu\text{g}/\text{ml}$  and total light dose 11  $\text{J}/\text{cm}^2$  (light intensity 9.47  $\text{mW}/\text{cm}^2$ ) compared to assay in the presence of  $\text{D}_2\text{O}$ . Error bars show mean  $\pm$  SD (n=3).**

**Table 4- 5 Showing the APDT kill rate of *E. coli* Nissle 1917 pGLITE in the presence or absence of singlet oxygen scavengers and/or hydroxyl radical scavengers (summary of rate data from figures 4.6 to 4.10)**

Treatment	Kill rate (log RLU/min)	r <sup>2</sup>	P value	Deviation from zero?	Percentage relative kill	Percentage relative protection
APDT	-0.171 ± 0.011	0.926	< 0.0001	Significant	100	0
APDT+ 10 mM Tryptophan	-0.009 ± 0.006	0.069	0.141	Not Significant	5.049	94.951
APDT+ 0.1 mM Tryptophan	-0.178 ± 0.006	0.966	< 0.0001	Significant	104.272	-4.272
APDT+ 10 mM Mannitol	-0.196 ± 0.009	0.959	< 0.0001	Significant	114.687	-14.687
APDT+ 10 mM DMTU	-0.055 ± 0.015	0.599	0.005	Significant	32.048	67.952
APDT+ D <sub>2</sub> O	-0.190 ± 0.033	0.785	0.000	Significant	111.176	-11.176

**Table 4- 6 Showing the APDT kill rate of *E. coli* Nissle 1917 pGLITE over the first 8 minutes in the presence or absence of singlet oxygen scavengers and/or hydroxyl radical scavengers (summary of rate data from figures 4.6 to 4.10)**

Treatment	Kill rate (log RLU/min)	r <sup>2</sup>	P value	Deviation from zero?	Percentage relative kill	Percentage relative protection
APDT	-0.259 ± 0.018	0.962	< 0.0001	Significant	100	0
APDT+ 10 mM Tryptophan	-0.017 ± 0.021	0.045	0.445	Not Significant	6.514	93.486
APDT+ 0.1 mM Tryptophan	-0.191 ± 0.015	0.919	< 0.0001	Significant	73.745	26.255
APDT+ 10 mM Mannitol	-0.234 ± 0.029	0.884	< 0.0001	Significant	90.386	9.614
APDT+ 10 mM DMTU	-0.164 ± 0.051	0.773	0.050	Significant	63.436	36.564
APDT+ D <sub>2</sub> O	-0.461 ± 0.066	0.942	0.006	Significant	178.147	-78.147

#### **4.5.4 ECAS kill kinetics of *E. coli* Nissle 1917/pGLITE in the presence of hydroxyl radical scavengers dimethyl thiourea (DMTU), mannitol and singlet oxygen scavenger, tryptophan and enhancer of singlet oxygen, D<sub>2</sub>O**

Figures 4.11 to 4.16 show the effects of ECAS on bioluminescence output by *E. coli* Nissle 1917 pGLITE in control conditions and with the addition of tryptophan (fig. 4.12), azide (fig 4.13), D<sub>2</sub>O (figure 4.14), mannitol (figure 4.15) and DMSO (figure 4.16). Figure 4.11 shows changes in bioluminescence of *E. coli* Nissle 1917 pGLITE treated with ECAS at 50, 25, 10, 5 and 1% (v/v of neat). This shows a dose concentration dependency between ECAS and kill rate for this species.

Table 4.7 summarises the effects of free radicals and singlet oxygen scavengers on the kill rate of bioluminescent *E. coli* Nissle 1917 pGLITE by ECAS. It shows that in the presence of tryptophan a strong protective effect is exhibited although the azide which is more specific to singlet oxygen does not afford the same protection level as tryptophan, suggesting less involvement of singlet oxygen in killing mechanism, whilst the majority of putative hydroxyl radical inhibitors (mannitol, DMSO) give between 40 to 60% protection, suggesting a role for hydroxyl radical.

Significant differences were found between the initial killing (first 1min) and later killing therefore initial kill rates were calculated and shown in table 4.7 and 4.8

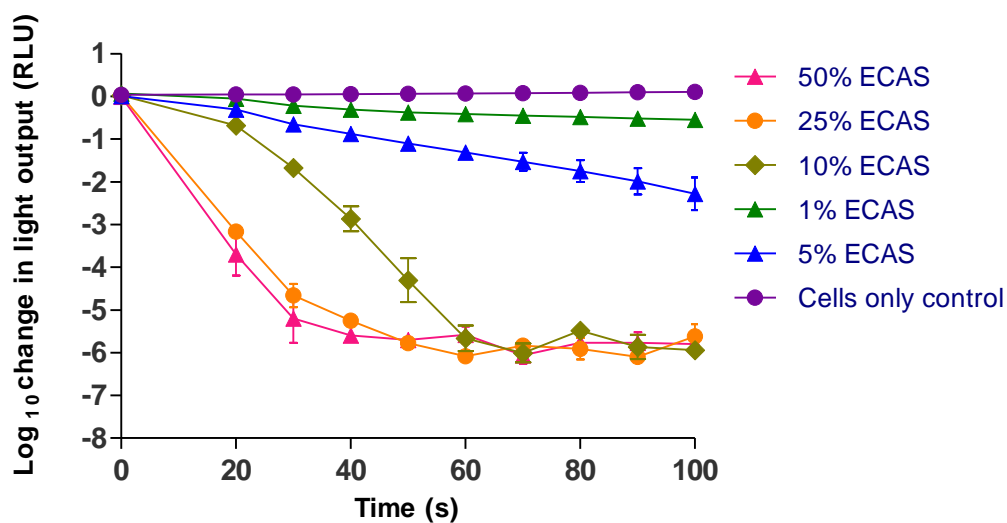


Figure 4-11 Changes in bioluminescence of *E. coli* Nissle 1917 pGLITE treated with ECAS at 50, 25, 10, 5 and 1% (v/v of neat). Error bars show mean  $\pm$  SD (n=3).

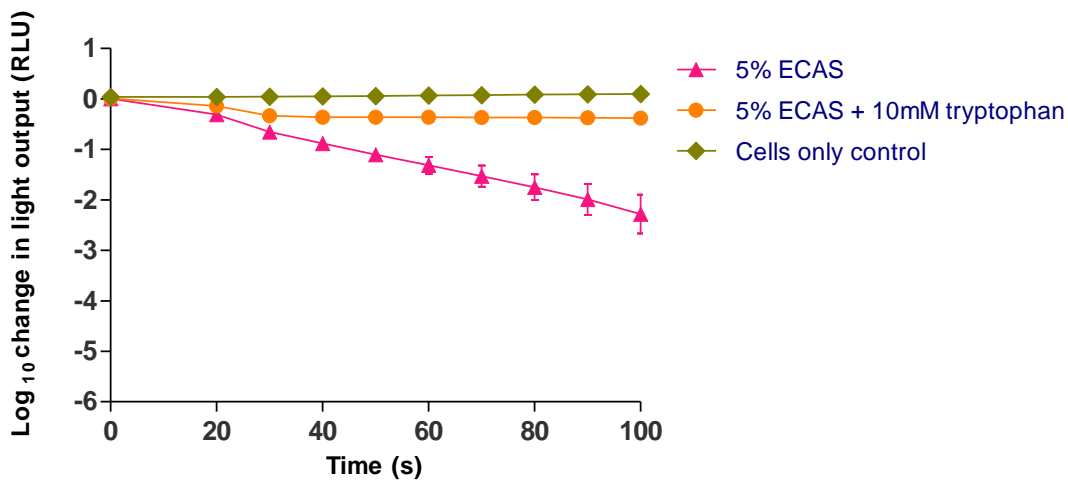


Figure 4-12 Changes in bioluminescence of *E. coli* Nissle 1917 pGLITE treated with ECAS: effects of tryptophan (10 mM). Error bars show mean  $\pm$  SD (n=3).

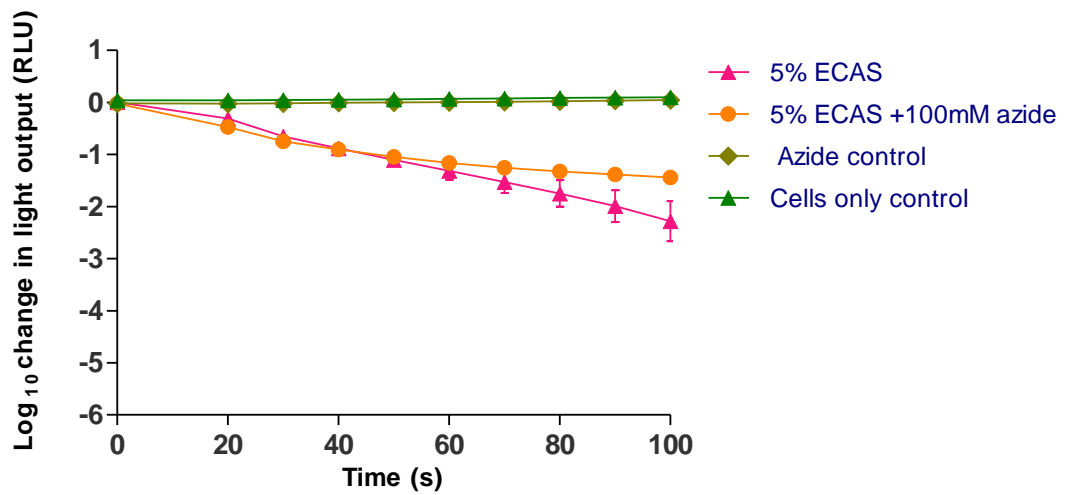


Figure 4-13 Changes in bioluminescence of *E. coli* Nissle 1917 pGLITE treated with ECAS: effects of sodium azide (100 mM). Error bars show mean  $\pm$  SD (n=3).

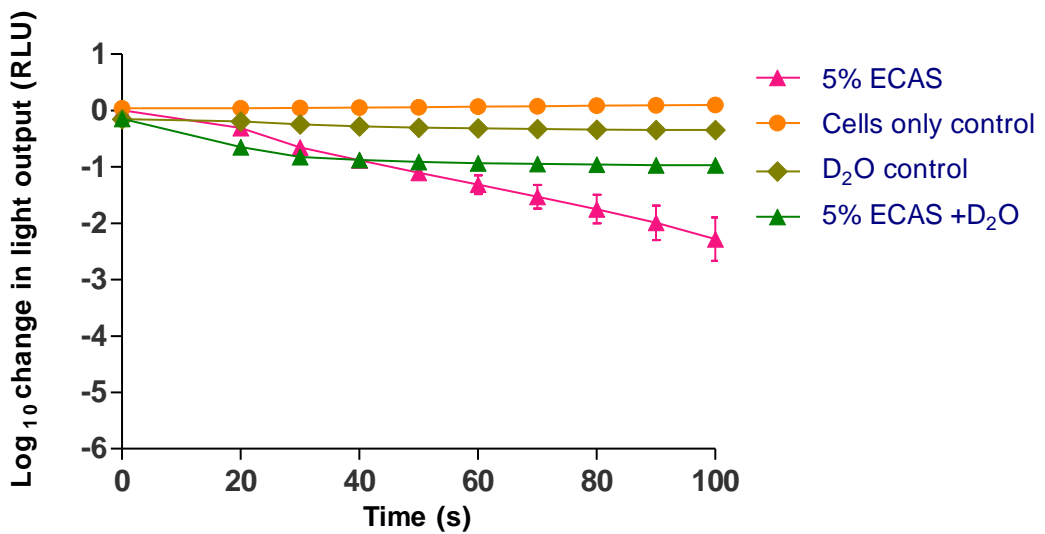


Figure 4-14 Changes in bioluminescence of *E. coli* Nissle 1917 pGLITE treated with ECAS: effects of D<sub>2</sub>O. Error bars show mean  $\pm$  SD (n=3).

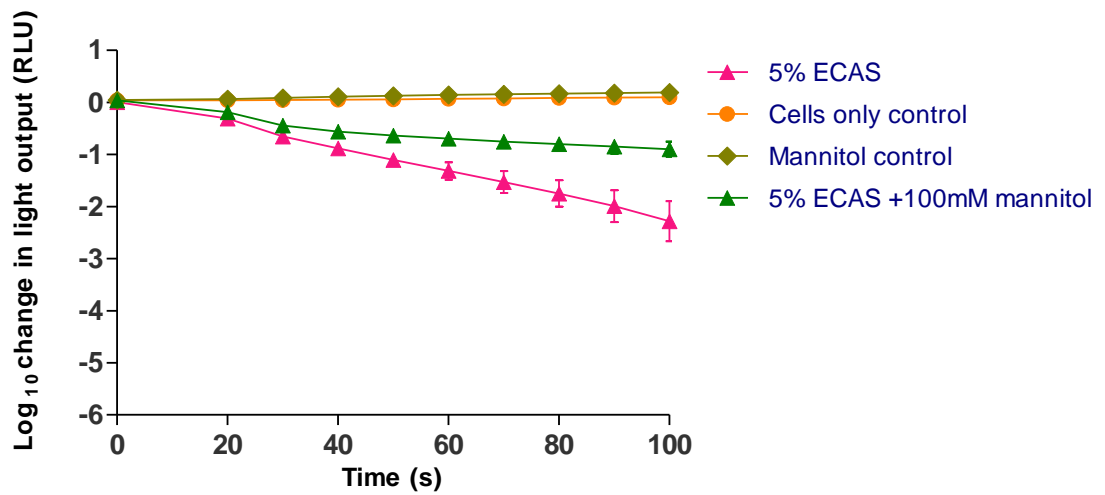


Figure 4-15 Changes in bioluminescence of *E. coli* Nissle 1917 pGLITE treated with ECAS: effects of mannitol (100 mM). Error bars show mean ± SD (n=3).

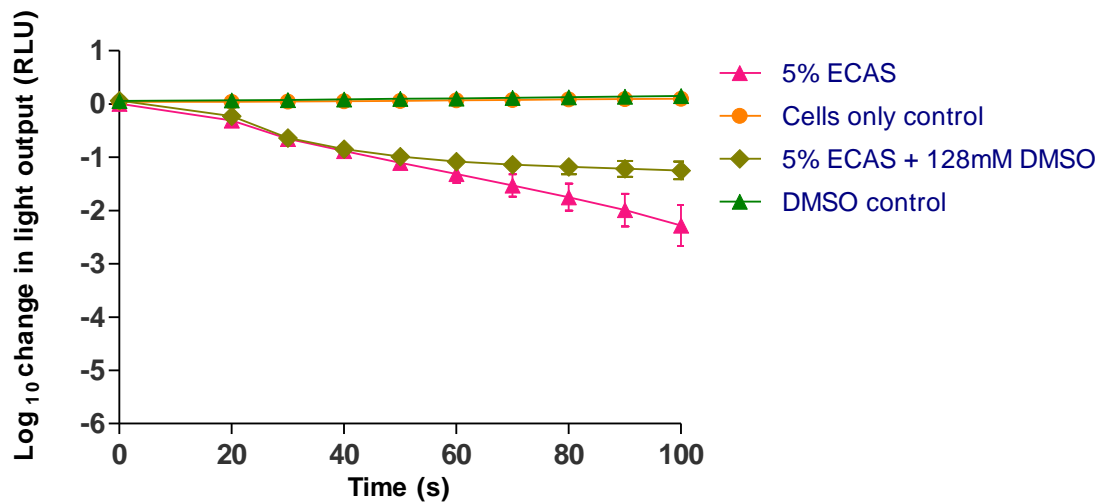


Figure 4-16 Changes in bioluminescence of *E. coli* Nissle 1917 pGLITE treated with ECAS: effects of DMSO (128 mM). Error bars show means ± SD (n=3).

**Table 4- 7 The effects free radicals and singlet oxygen scavengers on the kill rate of bioluminescent *E. coli* Nissle 1917 by ECAS (calculations based on the total assay times 2 minutes)**

Reagents	Kill rate(log RLU/min)	R <sup>2</sup>	Percentage relative protection	Percentage relative kill
5% ECAS	-1.5± 0.12	0.847	0	100
5% ECAS + 10 mM tryptophan	-0.192 ± 0.036	0.4844	86.92	13.07
5% ECAS +100 mM azide	-0.852 ± 0.084	0.7834	42.61	57.38
5% ECAS +100 mM mannitol	-0.57 ± 0.072	0.6781	61.69	38.30
5% ECAS + 128 mM DMSO	-0.822 ± 0.096	0.7279	44.55	55.44

**Table 4- 8 The effects free radicals and singlet oxygen scavengers on the kill rate of bioluminescent *E. coli* Nissle 1917 by ECAS (calculations based on the first 1 minute- Initial kill rate)**

Treatment	Kill rate (log RLU/min)	R <sup>2</sup>	P value	Deviation from zero?	Percentage relative kill	Percentage relative protection
5% ECAS	-1.674 ± 0.148	0.889	< 0.0001	Significant	100.000	0.000
5% ECAS + 10 mM tryptophan	-0.450± 0.081	0.659	< 0.0001	Significant	26.885	73.115
5% ECAS +100 mM azide	-1.352± 0.144	0.845	< 0.0001	Significant	80.681	19.319
5% ECAS +100 mM mannitol	-0.923± 0.137	0.741	< 0.0001	Significant	55.125	44.875
5% ECAS + 128 mM DMSO	-1.486± 0.137	0.880	< 0.0001	Significant	88.746	11.254

#### **4.5.5 ROS detection using SOSG, APF and HPF in APDT and ECAS**

Fluorogenic interactions involving  $^1\text{O}_2$  and  $\text{OH}^\bullet$  and fluorescent probes were assessed against APDT or ECAS in the absence *vs* presence of inhibitors (tryptophan, histidine,  $\text{NaN}_3$  mannitol, DMSO), enhancer ( $\text{D}_2\text{O}$ ) using SOSG, APF or HPF. The cuvette containing the solutions of MB and the probe was exposed to visible light. The fluorescence was monitored by acquisition of the fluorescence signal by the fluorimeter. For ECAS studies, the reaction mixture consisted of ECAS of appropriate concentration and the probe (APF and HPF at 5  $\mu\text{M}$ ). Fluorescent probe assays were repeated in the presence of inhibitors or scavengers of ROS or  $\text{D}_2\text{O}$  to show inhibition or enhancement of fluorescence.

##### **4.5.5.1 Detection of singlet oxygen, using Singlet Oxygen Sensor Green (SOSG) in APDT and ECAS**

Figure 4.17 shows the increasing fluorescence observed when SOSG probe is exposed to APDT. The fluorescence intensity of 5  $\mu\text{M}$  SOSG probe containing 10  $\mu\text{g/mL}$  MB solutions increased linearly as the irradiation time increased. These results suggest that the greater the light energy absorbed by the MB dye, the greater the extent of  $^1\text{O}_2$ . It should be noted the fluorescence also increased slightly in the light only control, indicating that SOSG probe is itself photodynamic and autocatalytic in light. There was no significant increase in fluorescence in the dark control. Figure 4.18 shows the effects of  $\text{D}_2\text{O}$ , which increased markedly the production of fluorescence from the probe, indicating increased generation of singlet oxygen. Figures 4.19 and 4.20, show the effects of the addition of tryptophan and mannitol respectively. Both these compounds inhibited fluorescence from the SOSG probe with a large reduction for tryptophan, but only a slight reduction with mannitol.

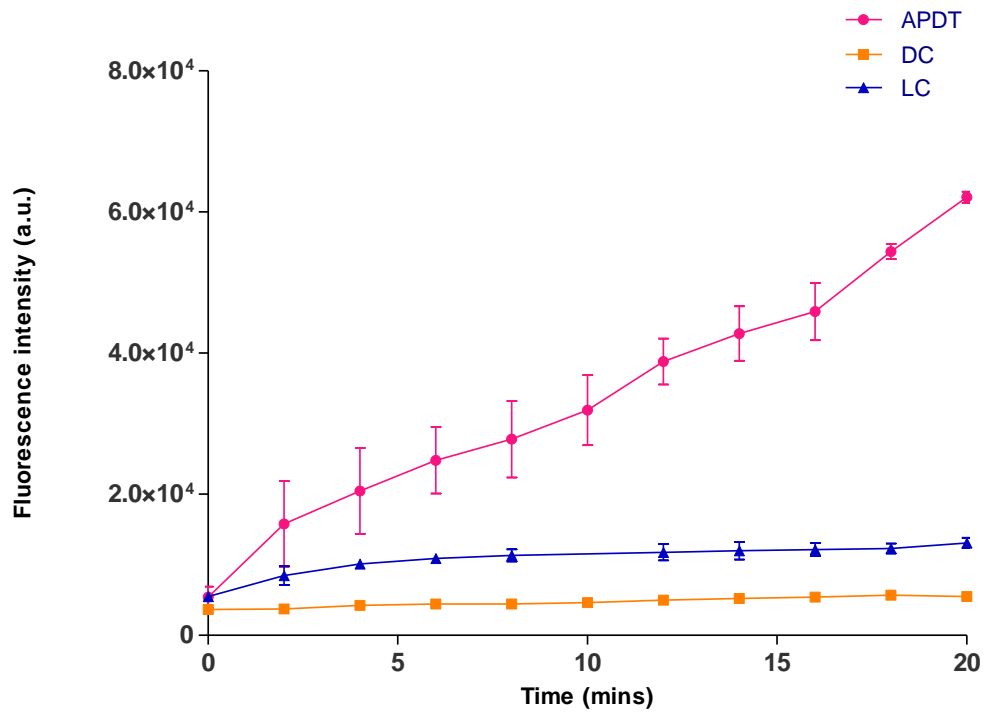


**Figure 4-17** Fluorescence response by SOSG probe ( $5\mu\text{M}$ ) exposed to APDT ( $10\mu\text{g/ml}$  MB and total light dose  $11\text{ Jcm}^{-2}$  (light intensity  $9.47\text{mW/cm}^2$ ) compared to controls. DC, dark control; LC, light control, error bars show mean  $\pm$  SD (n=3).

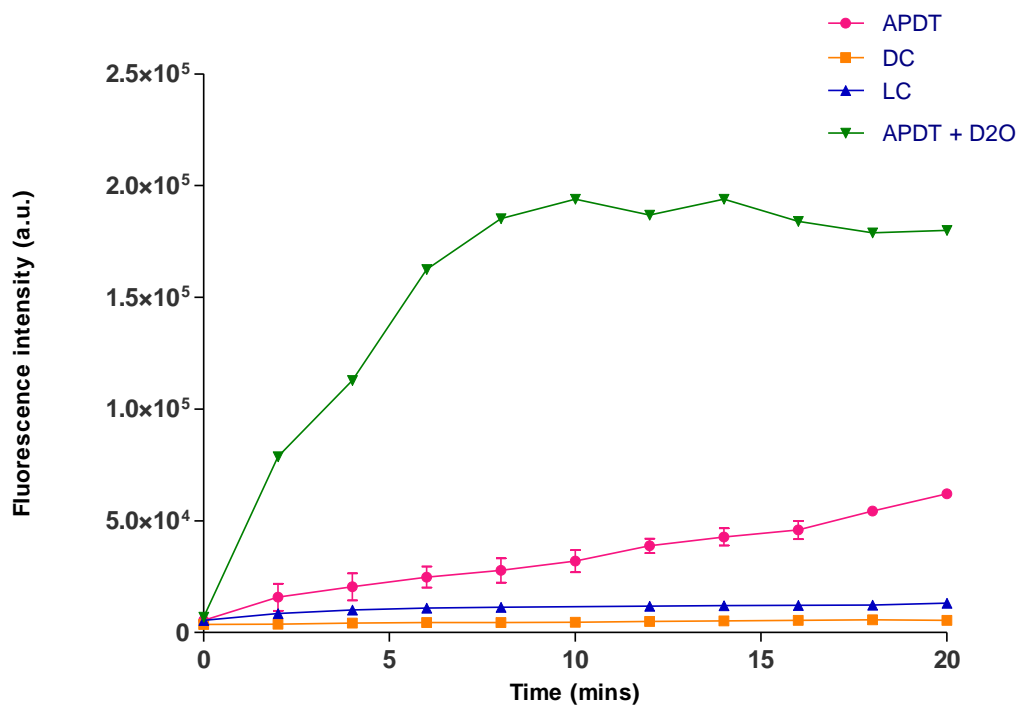


**Figure 4-18** Fluorescence response by SOSG probe (5  $\mu\text{M}$ ) exposed to APDT (10  $\mu\text{g/ml}$  MB and total light dose 11  $\text{Jcm}^{-2}$  (light intensity 9.47  $\text{mW/cm}^2$ ) compared APDT in presence of  $\text{D}_2\text{O}$ . DC, dark control; LC, light control, error bars show mean  $\pm$  SD (n=3).

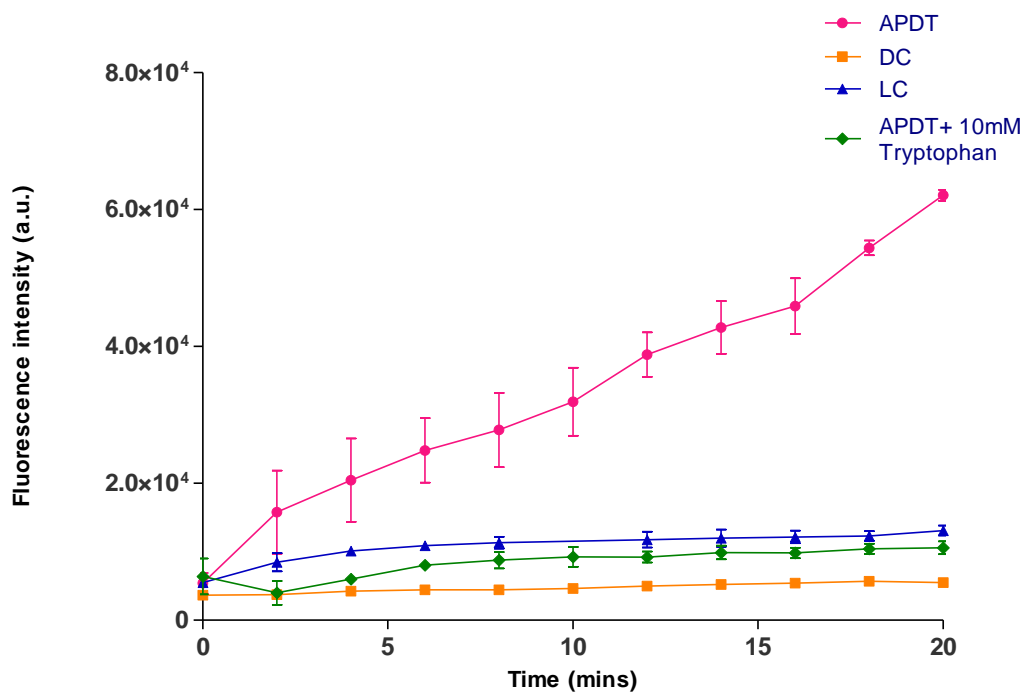


**Figure 4-19** Fluorescence response by SOSG probe ( $5 \mu\text{M}$ ) exposed to APDT ( $10 \mu\text{g/ml}$  MB and total light dose  $11 \text{ Jcm}^{-2}$  (light intensity  $9.47 \text{ mW/cm}^2$ ) compared APDT in the presence of tryptophan ( $10 \text{ mM}$ ). DC, dark control; LC, light control, error bars show mean  $\pm$  SD ( $n=3$ ).

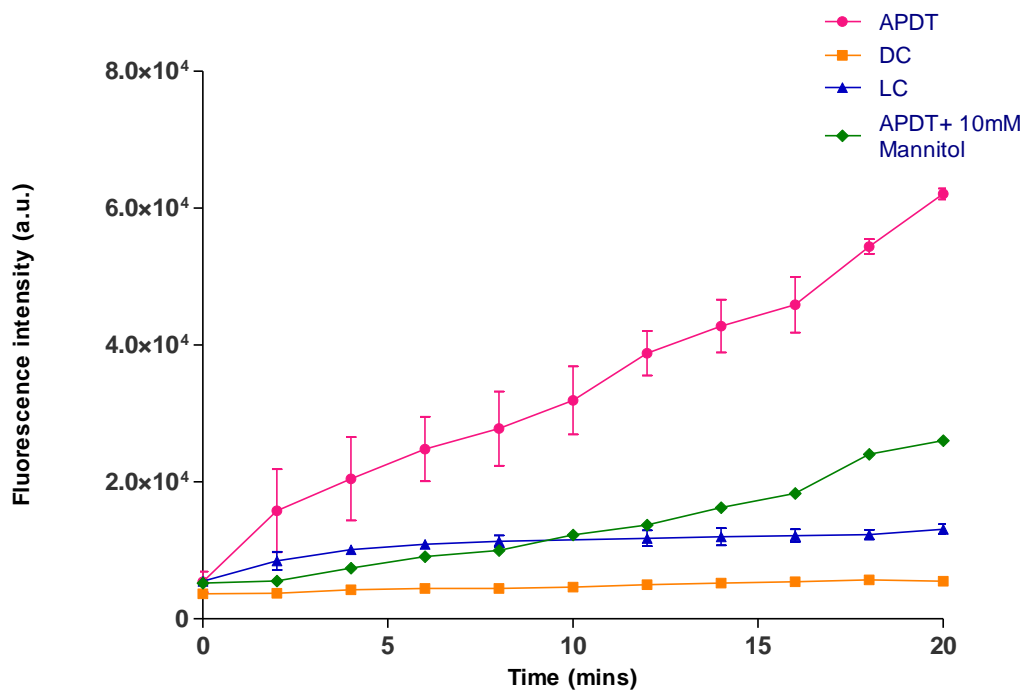


**Figure 4-20** Fluorescence response by SOSG probe (5  $\mu\text{M}$ ) exposed to APDT (10  $\mu\text{g/ml}$  MB and total light dose 11  $\text{Jcm}^{-2}$  (light intensity 9.47  $\text{mW/cm}^2$ ) compared APDT in the presence of mannitol (10 mM). DC, dark control; LC, light control, error bars show mean  $\pm$  SD (n=3).

Figure 4.21 shows the effects on SOSG fluorescence in the presence of 1% and 5% (v/v) of ECAS. To determine if the ROS produced in ECAS can be detected by the fluorescent probes the cell free solutions were mixed with the probe and fluorescence measured. It was found that when SOSG probe was added into different concentration of ECAS there was a very slight increase in fluorescence compared to SOSG alone. At higher concentrations the fluorescence was lower than the background (SOSG alone).

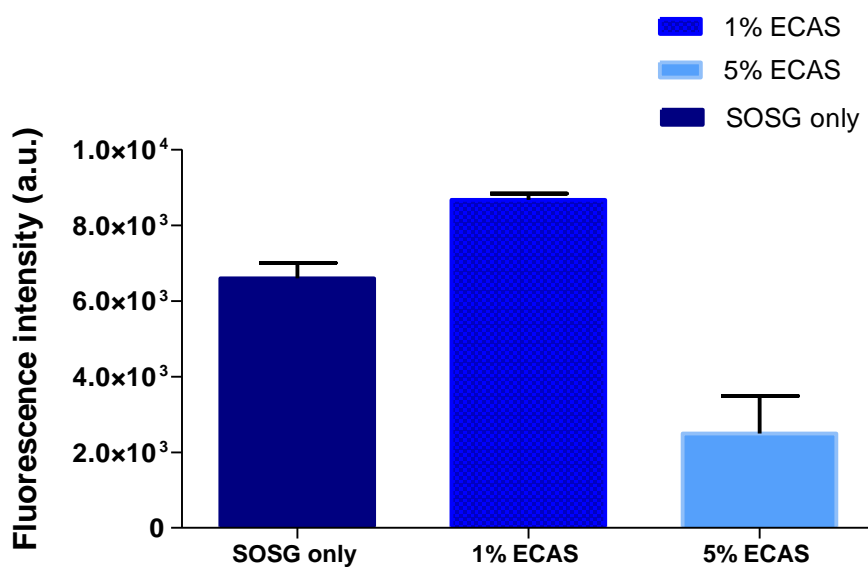


**Figure 4-21** Fluorescence by SOSG probe ( $5 \mu\text{M}$ ) with ECAS at 1 % and 5% (v/v of neat) following 5 minutes incubation. Error bars show mean  $\pm$  SD (n=3).

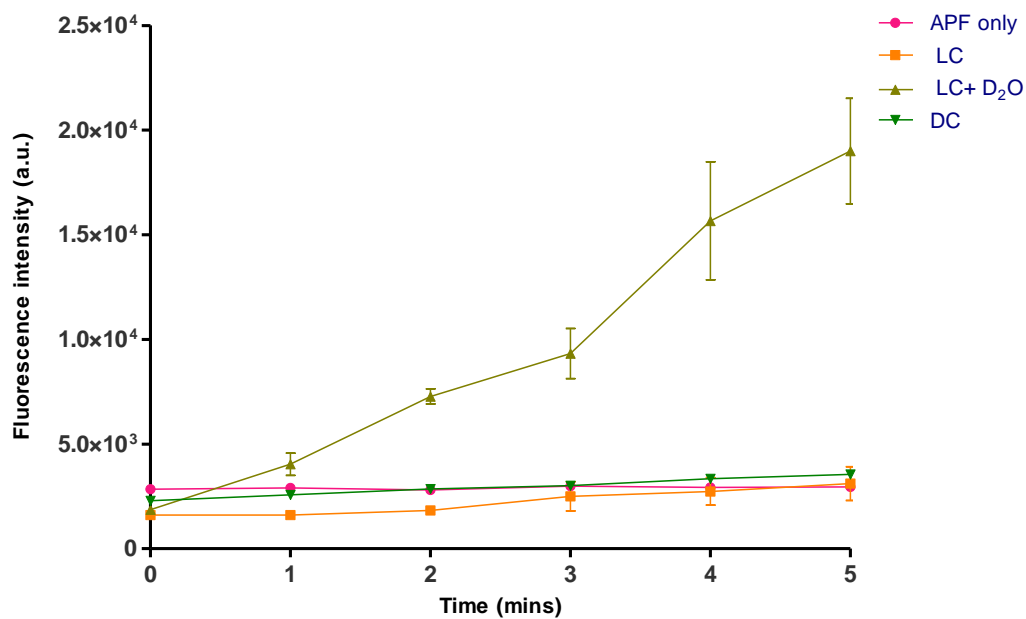
#### 4.5.5.2 Detection of ROS using APF in APDT and ECAS

Figure 4.22 shows the fluorescence response by the APF probe at 5 $\mu$ M under control conditions: APF probe was exposed to increasing amount of irradiation in PBS without MB and the effects of D<sub>2</sub>O was observed. There was a light dose dependent increase in fluorescence intensity compared to APF alone in phosphate buffer medium (figure 4.24). This highlights that the APF probe itself act as a photosensitizer when exposed to light and the increased fluorescence in D<sub>2</sub>O indicates that the probe may be generating singlet oxygen itself when exposed to light. APF on its own without light is not active and did not show any change in the fluorescence. APF probe in the dark mixed with MB 10 $\mu$ g/ml also showed no fluorescence, indicating that in the dark conditions neither MB nor APF produce ROS without light. APF probe was used to detect the production ROS in APDT. Figure 4.23 shows the fluorescence response of APF exposed to APDT (MB 10  $\mu$ g/ml and total light dose 11 J/cm<sup>2</sup> (light intensity 9.47mW/cm<sup>2</sup>) compared to controls (light control, dark control, APF probe only). For APDT the graph shows fluorescence intensity increased linearly as the irradiation time increased.

To determine the specificity of the APF probe to singlet oxygen APDT was carried out with singlet oxygen specific scavengers and enhancers. Figure 4.24 shows fluorescence response of APF exposed to APDT in the presence of singlet oxygen enhancer (D<sub>2</sub>O) and figure 4.25, 4.26, 4.27 shows effects of APDT compared with APDT in the presence of singlet oxygen specific scavengers. Figure 4.24 showed that when APDT was carried out in D<sub>2</sub>O medium compared to phosphate buffer the fluorescence intensity by APF was almost doubled and reached a steady level at 2 minutes of light exposure. This indicated that the APF probe could detect singlet oxygen in APDT. The large drop in fluorescence intensity in the presence of 10mM tryptophan (figure 4.26) showed a fluorescence drop may be due to competitive reaction of singlet oxygen produced in APDT with scavenger. Figure 4.25 and figure 4.27 showed similar reduction in fluorescence in the presence of singlet oxygen specific scavengers histidine and sodium azide. In the case of tryptophan and sodium azide increasing the concentration in solution from 1mM to 10mM (for tryptophan) and 10mM to 100mM (for azide) further decreased the fluorescence. To determine the extent of

fluorescence by APF due to hydroxyl radical the hydroxyl radical specific scavenger mannitol was mixed in the solution with APDT. Figure 4.28 showed that there was no a reduction in the florescence in the presence of mannitol and an increase in concentration of mannitol from (10mM to 100mM) showed no change in fluorecence intensity. Table 4.9 summarises the change in the rate of fluorescence by APF compared to the absence and presence of scavengers and D<sub>2</sub>O.

When APF probe was tested with ECAS it showed that there was no deactivation of the probe as in the case of SOSG and HPF. Therefore the only probe that could be employed to detect ROS in ECAS was with the APF probe. Figure 4.29 shows that fluorescence response of APF with 1% ECAS with and without ROS specific scavengers. It shows that the APF probe or 1% ECAS on its own does not produce any fluorescence. Increase APF fluorescence response is seen when APF probe is mixed with 1% ECAS. Therefore APF can be used to monitor the production of ROS in ECAS. Singlet oxygen and hydroxyl radical specific scavengers were used to determine the fluorescence response by APF attributed to singlet oxygen or hydroxyl radical. ECAS and APF probe in heavy water medium produced an increase in the fluorescence. Tryptophan reduced the fluorescence to nearly background level. Sodium azide (100mM) contributed to 53% reduction in fluorescence. These results indicate there may be role of singlet oxygen in ECAS and that APF can detect singlet oxygen. The fluorescence response to 1% ECAS by APF was reduced in the presence of hydroxyl radical scavengers (DMSO and mannitol). DMSO (128mM) showed a greater reduction (97%) compared to mannitol (100mM) (42% reduction). The table 4.10 summarises the relative change in fluorescence response by APF exposed to 1% ECAS compared to different conditions specific to singlet oxygen or hydroxyl radical. The data are consistent with the view that D<sub>2</sub>O enhances the fluorescence intensity, whilst tryptophan, DMSO, and to a lesser extent azide and mannitol cause the fluorescent intensity to be inhibited, suggesting mixed ROS reactions. Overall the results show that APF probe can detect both the singlet oxygen and hydroxyl radical in ECAS.



**Figure 4-22** Fluorescence response of 5  $\mu\text{M}$  APF probe to control conditions; (LC; Light control (light dose 3  $\text{J}/\text{cm}^2$  (light intensity 9.47  $\text{mW}/\text{cm}^2$ ), DC; dark control (MB (10  $\mu\text{g}/\text{ml}$ ) only), APF probe only and APF probe in the presence of  $\text{D}_2\text{O}$  exposed to light (light dose 3  $\text{J}/\text{cm}^2$  (light intensity 9.47  $\text{mW}/\text{cm}^2$ ). Error bars show mean  $\pm$  SD ( $n=3$ ).

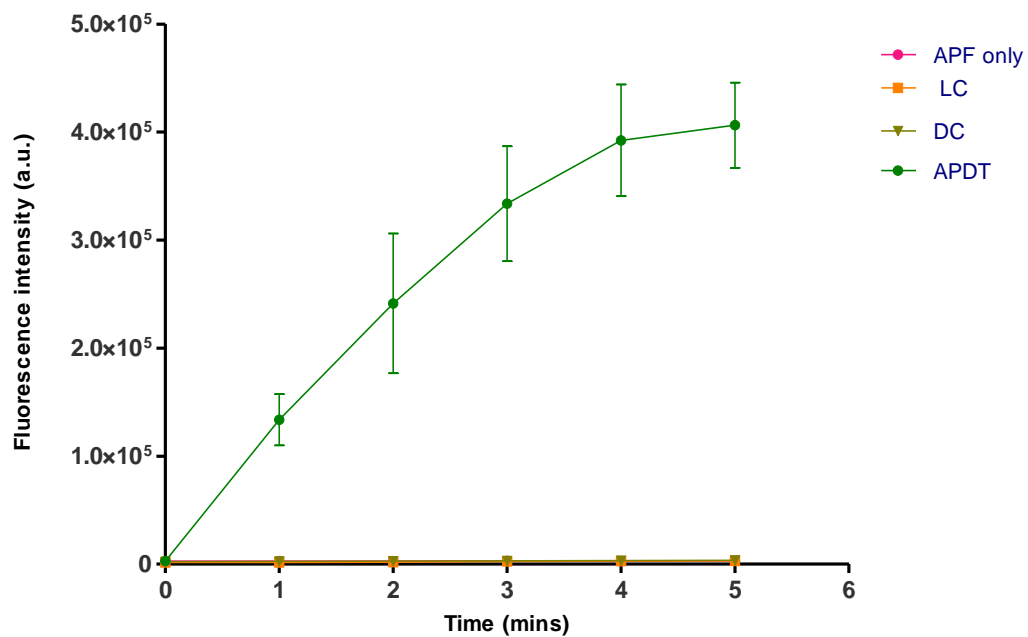


**Figure 4-23** Fluorescence response of 5  $\mu\text{M}$  APF probe to APDT (MB 10  $\mu\text{g/ml}$  and total light dose 3  $\text{J/cm}^2$  (light intensity 9.47  $\text{mW/cm}^2$ ) compared to control conditions; (LC; Light control (light dose 3  $\text{J/cm}^2$  (light intensity 9.47  $\text{mW/cm}^2$ ), DC; dark control (MB (10  $\mu\text{g/ml}$ ) only), APF probe only. Error bars show mean  $\pm$  SD (n=3).

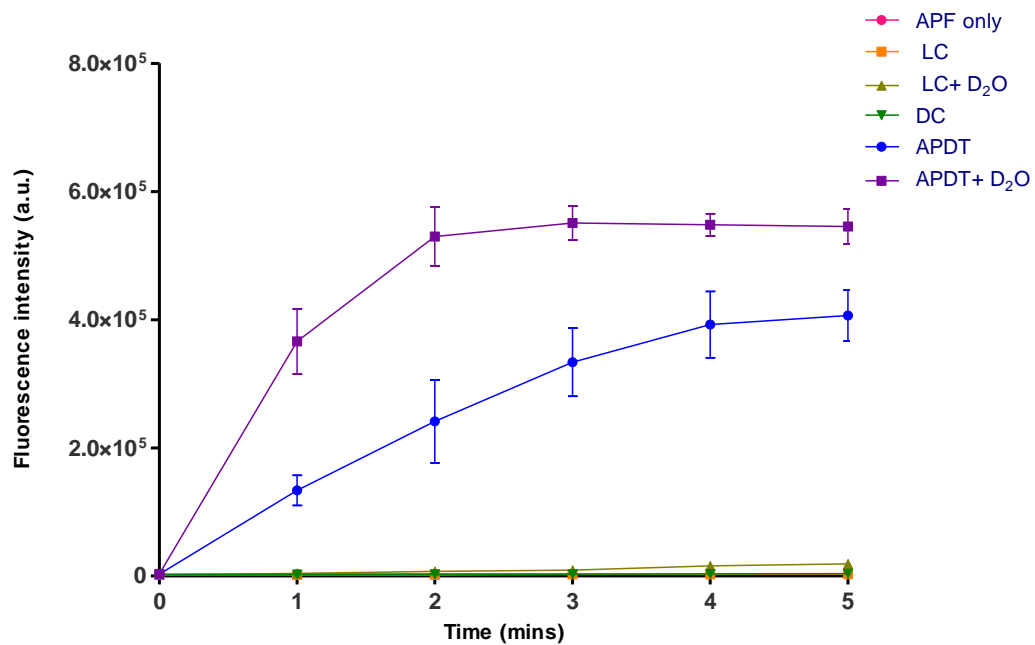


**Figure 4-24** Fluorescence response of 5  $\mu\text{M}$  APF probe to APDT (MB 10  $\mu\text{g}/\text{ml}$  and total light dose 3  $\text{J}/\text{cm}^2$  (light intensity 9.47  $\text{mW}/\text{cm}^2$ ) compared to APDT same conditions in the presence of D<sub>2</sub>O. DC, dark control; LC, light control. Error bars show mean  $\pm$  SD (n=3).

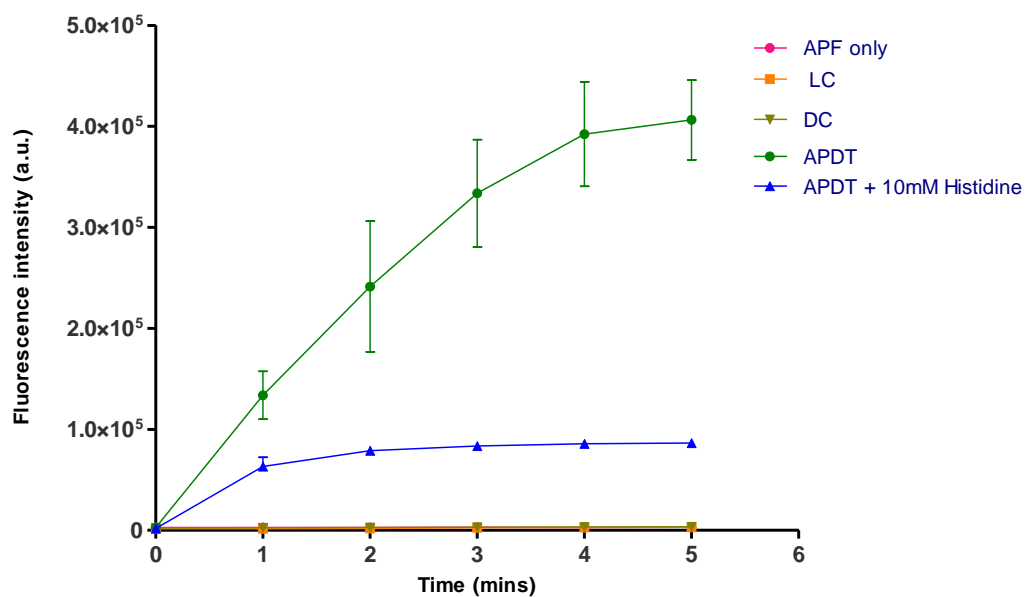


**Figure 4-25** Fluorescence response of 5  $\mu\text{M}$  APF probe to APDT (MB 10  $\mu\text{g/ml}$  and total light dose 3  $\text{J/cm}^2$  (light intensity 9.47  $\text{mW/cm}^2$ ) compared to APDT same conditions in the presence histidine (10 mM). DC, dark control; LC, light control. Error bars show mean  $\pm$  SD (n=3).

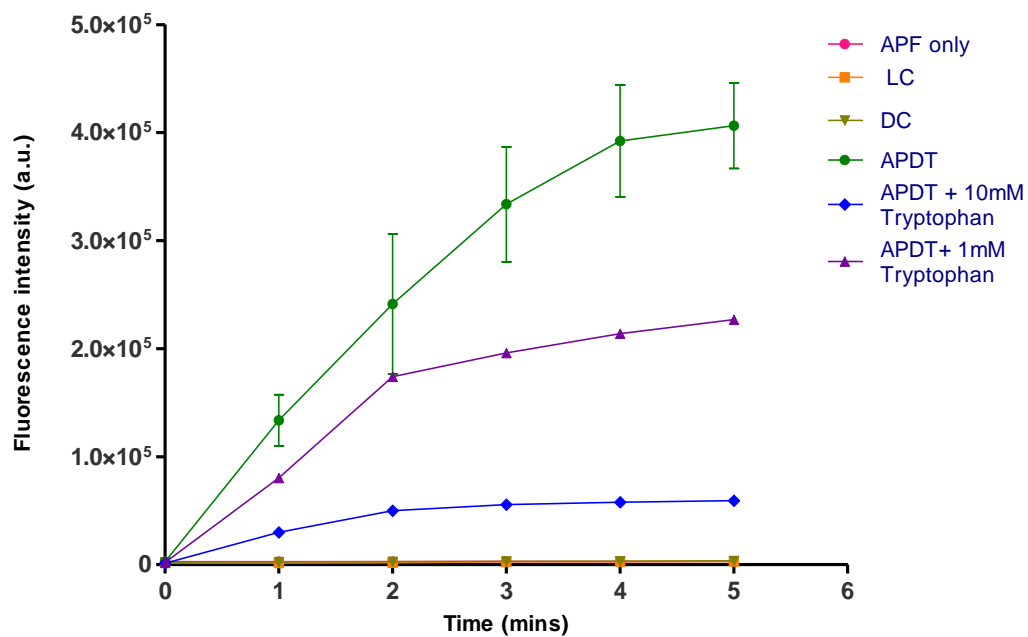


**Figure 4-26** Fluorescence response of 5  $\mu\text{M}$  APF probe to APDT (MB 10  $\mu\text{g}/\text{ml}$  and total light dose 3  $\text{J}/\text{cm}^2$  (light intensity 9.47  $\text{mW}/\text{cm}^2$ ) compared to APDT same conditions in the presence tryptophan (1 mM and 10 mM). DC, dark control; LC, light control. Error bars show mean  $\pm$  SD (n=3).

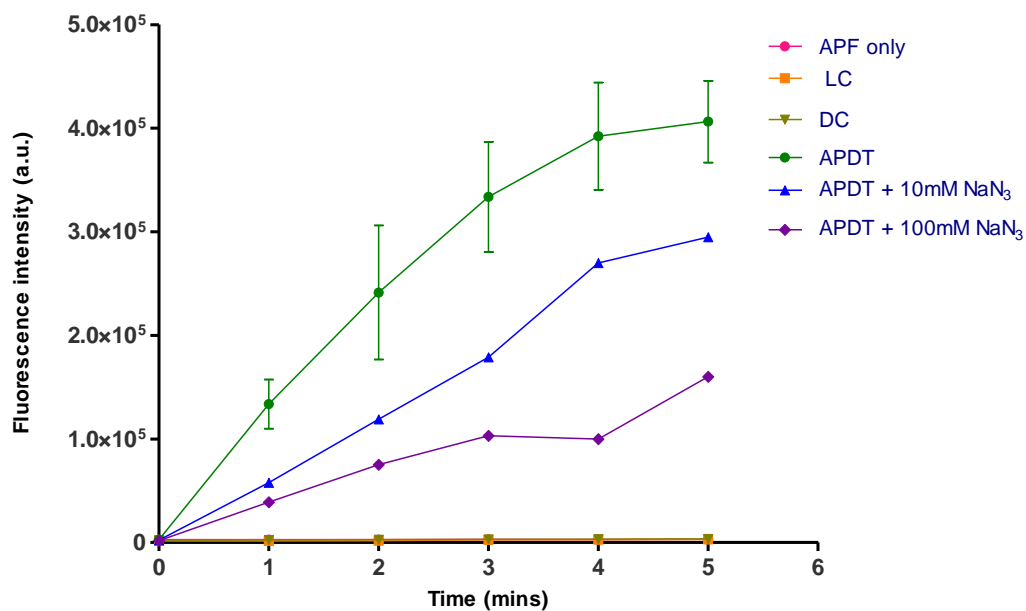


**Figure 4-27 Fluorescence response of 5  $\mu\text{M}$  APF probe to APDT (MB 10  $\mu\text{g}/\text{ml}$  and total light dose 3  $\text{J}/\text{cm}^2$  (light intensity 9.47  $\text{mW}/\text{cm}^2$ ) compared to APDT same conditions in the presence sodium azide (10 mM and 100 mM). DC, dark control; LC, light control. Error bars show mean  $\pm$  SD (n=3).**

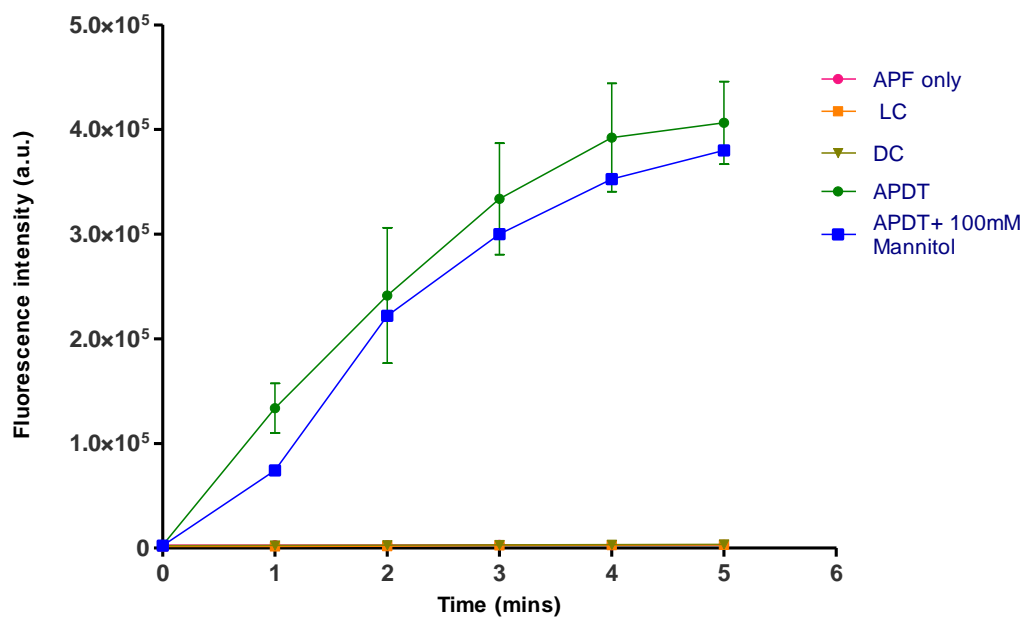


**Figure 4-28** Fluorescence response of 5  $\mu\text{M}$  APF probe to APDT (MB 10  $\mu\text{g}/\text{ml}$  and total light dose 3  $\text{J}/\text{cm}^2$  (light intensity 9.47  $\text{mW}/\text{cm}^2$ ) compared to APDT same conditions in the presence mannitol (100 mM). DC, dark control; LC, light control. Error bars show mean  $\pm$  SD (n=3).

**Table 4- 9 Summary of rate change in fluorescence following APDT in the presence or absence of ROS inhibitors or enhancers (D<sub>2</sub>O) using APF (5 μM )**

<b>APDT and reagent</b>	<b>Rate of change in fluorescence (fluorescence intensity/mins) in the presence of 5μM APF</b>	<b>R<sup>2</sup></b>	<b>Percentage change in fluorescence in the presence of enhancer or inhibitors of singlet oxygen and ROS</b>
MB alone	85610 ± 5790	0.9086	0
Deuterium oxide	263200 ± 2637	0.9343	207.44
10 mM L-Histidine	38530 ± 5388	0.8796	-54.99
10 mM Tryptophan	24390 ± 1066	0.9868	-71.51
10 mM Sodium azide	61720 ± 3373	0.9882	-27.90
100 mM Sodium azide	28610 ± 3408	0.9463	-66.58
10 mM Mannitol	78280 ± 8083	0.9591	-8.56
100 mM Mannitol	81760 ± 1070	0.9359	-4.50

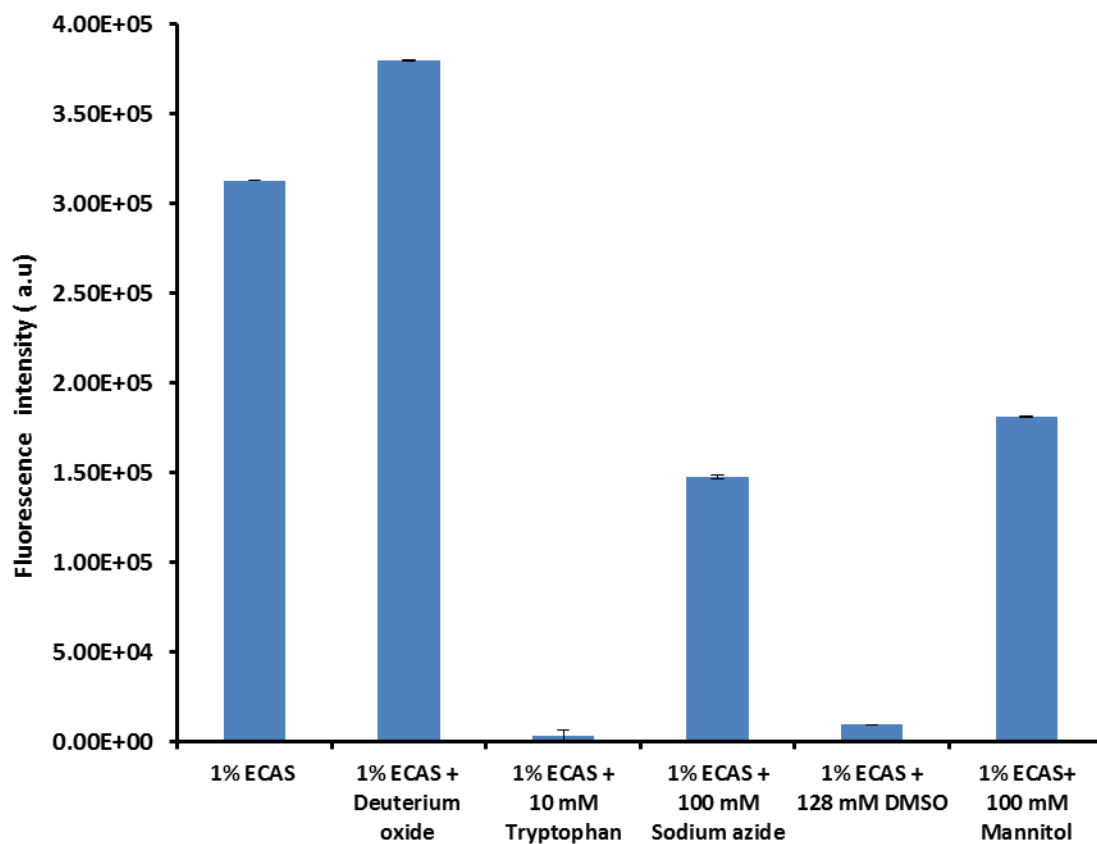


**Figure 4-29** Fluorescence response of 5  $\mu$ M APF with ECAS ( 1% v/v neat) and ECAS ( 1% v/v neat) in the presence of ROS scavengers (tryptophan, sodium azide, DMSO and mannitol) or enhancer ( $D_2O$ ) incubated for 5 minutes. Error bars show mean  $\pm$  SD (n=3).

**Table 4-10 Summary of the data obtained from APF fluorescence study with ECAS**

<b>Condition</b>	<b>Florescence intensity signal by 5 <math>\mu</math>M APF probe</b>	<b>Percentagechange in fluorescence in presence or absence of enhancers or inhibitors of singlet oxygen and ROS (compared to probe and 1% ECAS)</b>
1% ECAS	312776	0
1% ECAS + D <sub>2</sub> O	379553	21.35 (increase)
1% ECAS + 10 mM Tryptophan	3096	-99.01
1% ECAS + 100 mM Azide	147418	-52.87
1% ECAS + 128 mM DMSO	9617	-96.93
1% ECAS+ 100 mM Mannitol	181169	-42.08

#### 4.5.5.3 Detection of ROS production using HPF in APDT

HPF probe was used to measure the production of ROS produced in APDT. Figure 4.30 and 4.31 shows the fluorescence response to APDT at 5 $\mu$ M and 10 $\mu$ M HPF respectively. At higher concentration of HPF probe greater fluorescence was observed compared to the lower concentration. In both cases the fluorescence response by HPF increased linearly with increase in light dose in APDT. In the light control and dark control there was no significant increase in the fluorescence by HPF probe, showing that only if ROS are generated is there detection by the HPF probe.

To determine the fluorescence response by the HPF due to singlet oxygen or hydroxyl radical APDT was carried out with specific scavengers of singlet oxygen (tryptophan) and specific scavengers of hydroxyl radical, (mannitol). Figure 4.32 shows that with APDT, tryptophan reduced the fluorescence to nearly background levels. Figure 4.33 shows that with mannitol there was no such reduction; indeed a slight increase was observed compared to APDT in the absence of mannitol.

From the graphs the change in fluorescence was linearly correlated with the irradiation time and the calculated  $r^2$  values were significant. Hence the rate of change in fluorescence was calculated and showed in table 4.11. The rate of change was compared relative to APDT with 5 $\mu$ M HPF probe. It showed that that at 10 $\mu$ M HPF there was 37% increase in fluorescence. The increase may be due to more molecules of HPF probe are available to react with ROS produced in APDT and produce the fluorescence end product. When APDT was carried out in the presence of 10mM tryptophan there was 89% reduction in fluorescence. This may be due to the ROS quenched by the tryptophan instead of reacting with the HPF thereby preventing formation of fluorescence product. Tryptophan is a known singlet oxygen quencher. When APDT was carried out with the hydroxyl radical scavenger mannitol (10mM) there was 4% increase in fluorescence. This indicates the ROS produced in APDT is not hydroxyl radical and that under APDT, HPF can detect singlet oxygen and not hydroxyl radical.

When HPF probe was mixed with different concentrations of ECAS (figure 4.34) the fluorescence decreased with increase in concentration of ECAS. It is interesting to note that HPF showed a reduction in fluorescent signal with increasing concentrations of ECAS, from zero (probe only) up to 1% ECAS. This is contrary to the expected results of the fluorescence increase with increase in concentration of ECAS. As the concentration of ECAS increases the ROS concentration should increase in proportion and therefore it was expected the fluorescence response should increase. This indicates the breakdown of the probe molecule by ECAS.

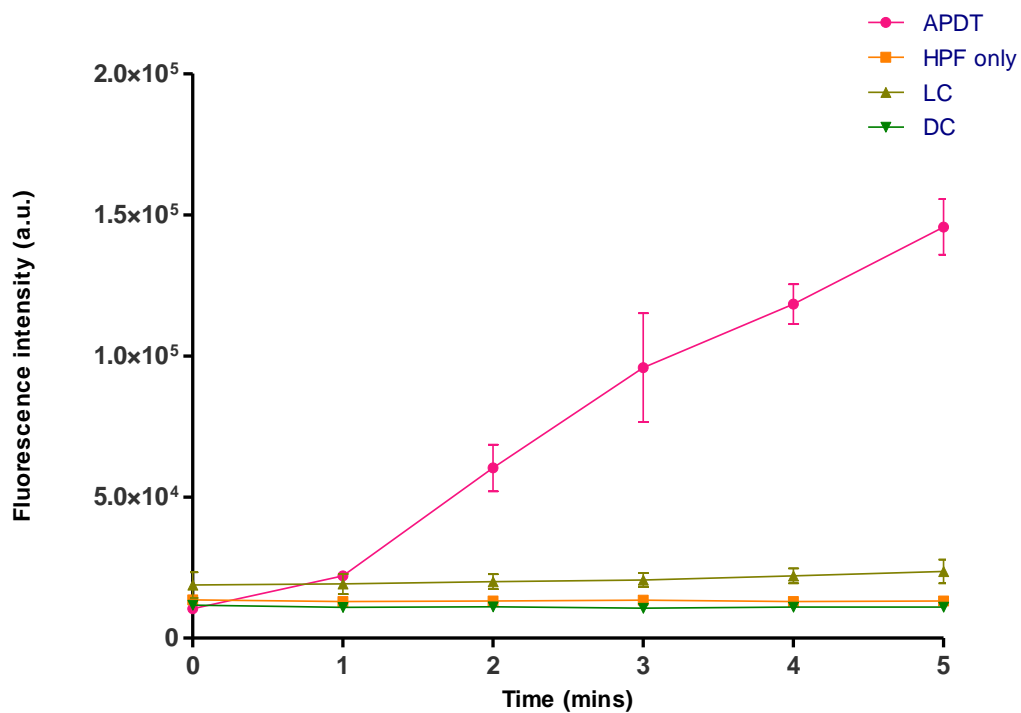


**Figure 4-30** Fluorescence response of 5  $\mu\text{M}$  HPF probe to APDT (MB 10  $\mu\text{g}/\text{ml}$  and total light dose 3  $\text{J}/\text{cm}^2$  (light intensity 9.47  $\text{mW}/\text{cm}^2$ ) compared to control conditions; (LC; Light control (light dose 3  $\text{J}/\text{cm}^2$  (light intensity 9.47  $\text{mW}/\text{cm}^2$ ), DC; dark control (MB (10  $\mu\text{g}/\text{ml}$ ) only), HPF probe only. Error bars show mean  $\pm$  SD (n=3).

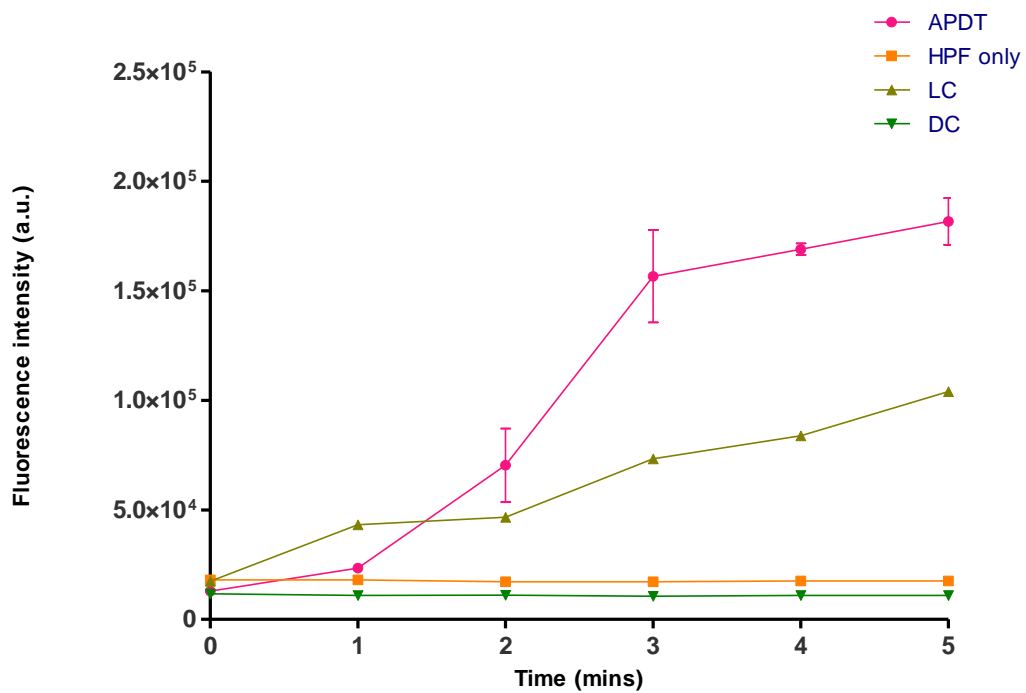


**Figure 4-31** Fluorescence response of 10  $\mu\text{M}$  HPF probe to APDT (MB 10  $\mu\text{g}/\text{ml}$  and total light dose 3  $\text{J}/\text{cm}^2$  (light intensity 9.47  $\text{mW}/\text{cm}^2$ ) compared to control conditions; LC; Light control (light dose 3  $\text{J}/\text{cm}^2$  (light intensity 9.47  $\text{mW}/\text{cm}^2$ ), DC; dark control (MB (10  $\mu\text{g}/\text{ml}$ ), 10  $\mu\text{M}$  HPF probe only. Error bars show mean  $\pm$  SD (n=3).

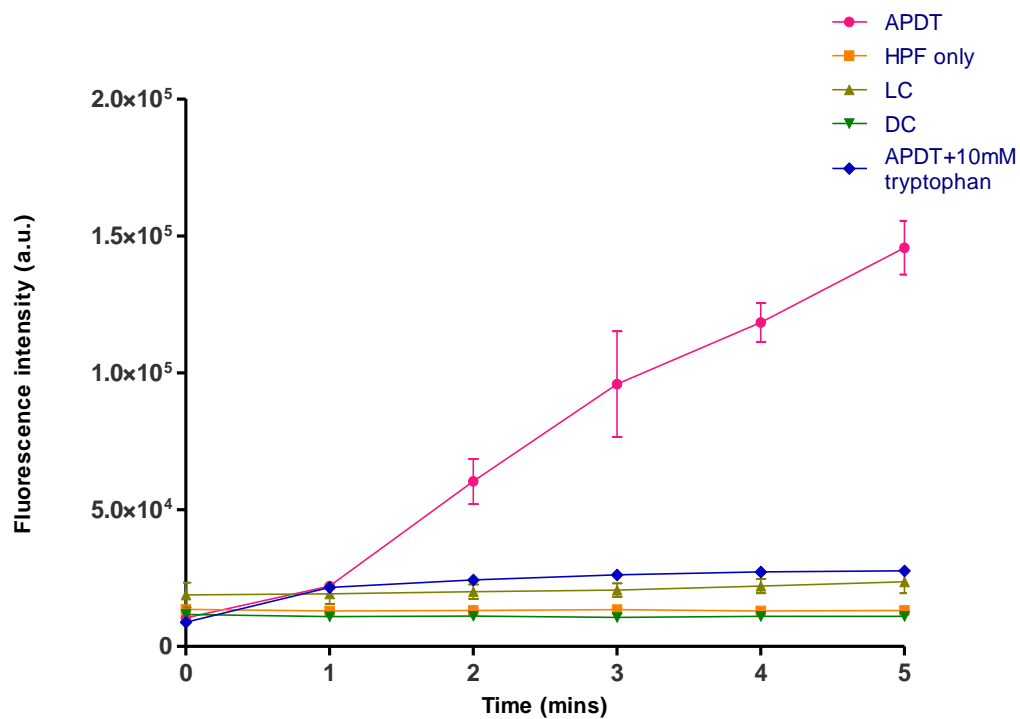


**Figure 4-32** Fluorescence response of 10  $\mu\text{M}$  HPF probe to APDT (MB 10  $\mu\text{g}/\text{ml}$  and total light dose  $3 \text{ J}/\text{cm}^2$  (light intensity  $9.47 \text{ mW}/\text{cm}^2$ ) compared to in the presence of tryptophan (10 mM). DC, dark control; LC, light control. Error bars show mean  $\pm$  SD (n=3).

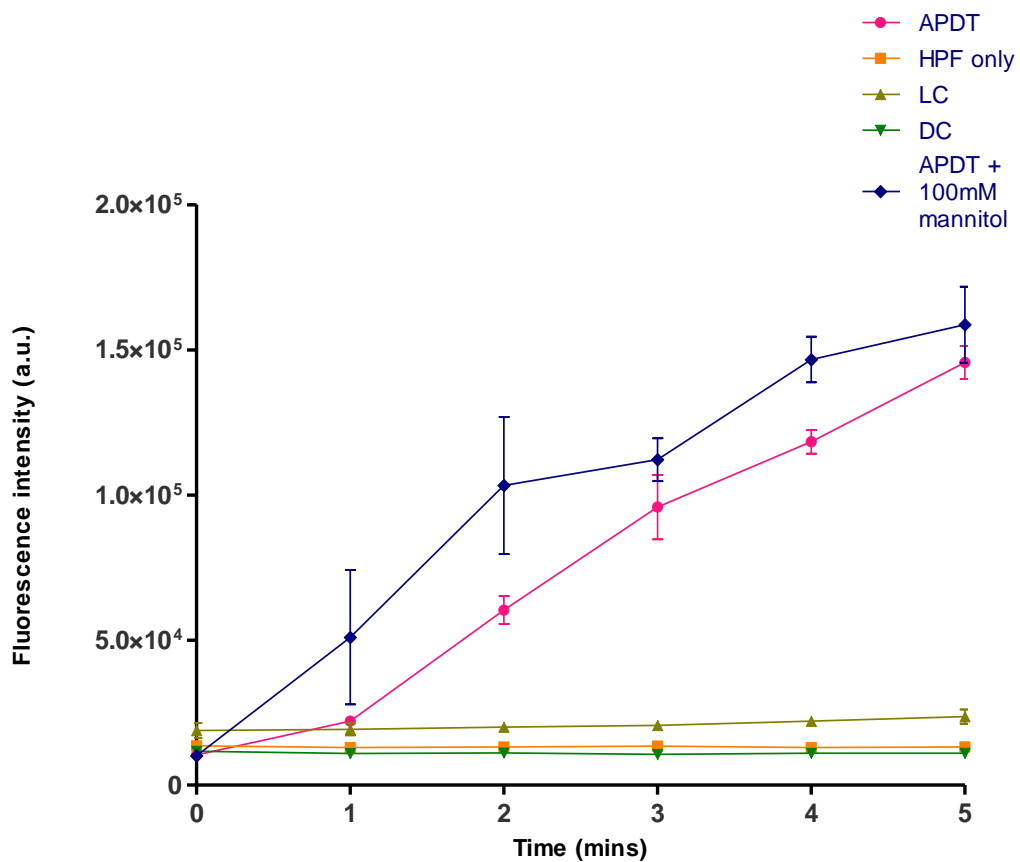


**Figure 4-33** Fluorescence response of 10  $\mu\text{M}$  HPF probe to APDT (MB 10  $\mu\text{g}/\text{ml}$  and total light dose 3  $\text{J}/\text{cm}^2$  (light intensity 9.47  $\text{mW}/\text{cm}^2$ ) compared to in the presence of mannitol (10  $\text{mM}$ ). DC, dark control; LC, light control. Error bars show mean  $\pm$  SD (n=3).

**Table 4- 11 Summary of rate change in fluorescence following APDT in the presence or absence of ROS inhibitors using HPF probe**

<b>APDT and reagent</b>	<b>Fluorescence intensity</b>	<b>r<sup>2</sup></b>	<b>Percentage change in fluorescence intensity</b>
APDT- 5μM HPF	28590 ± 1444	0.9608	0
APDT- 10μM HPF	39060 ± 3754	0.8712	36.62
APDT- 5μM HPF 10mM tryptophan	3231 ± 505.5	0.7187	-88.70
APDT- 5μM HPF 10mM mannitol	29680 ± 3566	0.8124	3.81

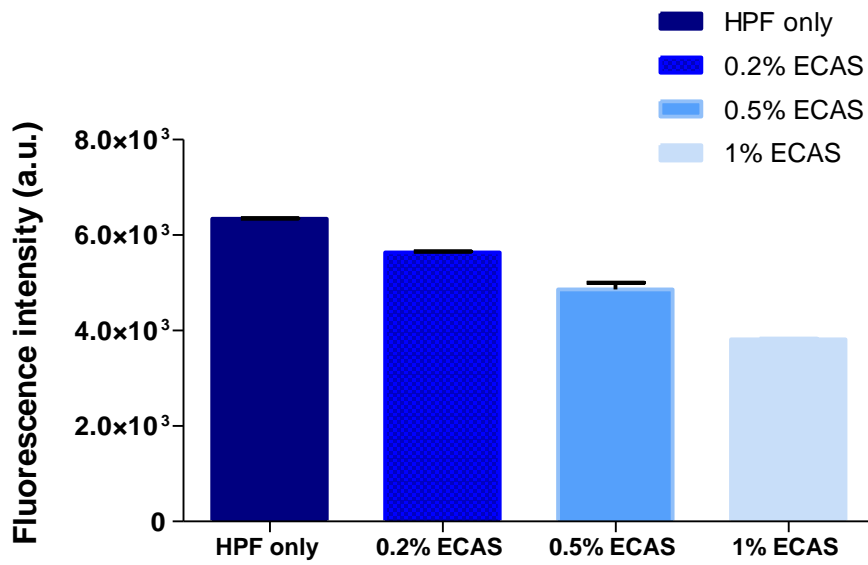


**Figure 4-34** Fluorescence by HPF probe ( $5 \mu\text{M}$ ) with ECAS at 0.2, 0.5 and 1 % (v/v of neat) compared to HPF ( $5 \mu\text{M}$ ) probe alone incubated for 5 minutes. Error bars show mean  $\pm$  SD (n=3).

#### 4.6 Discussion

In order to determine the active species involved and the mechanisms in APDT and ECAS mediated killing of target organisms, a range of different compounds were incorporated into the standard bioluminescent-based rapid assay. The rapid assay mixture contained 1. Bioluminescent Gram-negative species of target organism or non-bioluminescent Gram-positive strain 2. Killing agent (APDT or ECAS) 3. ROS inhibitors or enhancer. Similarly in the fluorescent probe assay to detect ROS production, the killing agent (APDT or ECAS) was combined with the fluorescent probe in the presence or absence of ROS specific scavengers.

In all cases for both APDT and ECAS the treatments showed significant kill in the absence of any scavengers. It showed a linear correlation between treatment exposure time and killing. The kill curve showed first order kill kinetics without a significant shoulder. In terms of photodynamic killing effect appear to be a single hit process in bacteria where all the putative targets in the cell are equally susceptible and if damaged can lead to cell death (Zeina *et al.*, 2001). Photodynamic treatment against micro-organisms is considered as mainly involving singlet oxygen that reacts against a wide range of cell target molecules such as cytoplasmic enzymes, membrane lipids and nucleic acids (Zeina *et al.*, 2001). In the case of ECAS as it has very high antimicrobial activity it reduces the bioluminescence output giving a flat line as it reaches the limit of detection. This was observed with higher concentrations of ECAS (25% and 50% v/v) where in 30s the bioluminescence output flattens as it reached the limit of detection giving a multiphasic kill curve. However, even if it is multiphasic but without a significant shoulder, the initial reaction rate is proportional to the concentration or magnitude of flux of killing molecules. Therefore initial kill rate is important in ECAS. The kill rates for ECAS increase with the increase in dose of the agent (5%-50% v/v ECAS).

To evaluate the ROS generation kinetics of the specific ROS in the systems the assay included: 1. D<sub>2</sub>O, which is considered to be specific enhancer of singlet oxygen. 2. Compounds that are regarded as singlet oxygen or free radical scavengers. The generation of specific ROS was inferred by the real time

inhibition of bioluminescence (killing) or increase in the viable count in the presence of the ROS specific scavengers for either APDT or ECAS. Change in bioluminescence of *E. coli* Nissle 1917 pGLITE and *P. aeruginosa* MCS5-lite and change in viable count for *S. aureus* (non lux strain) in the presence or absence of scavenger was monitored after APDT. Whilst with ECAS only bioluminescent *E. coli* 1917 pGLITE strain was used. Very interesting results were obtained from this line of study especially by comparing the kill kinetic activity of the two systems. First in APDT the MB dark control (no light but MB), light control (light but no MB) or untreated cells (no light and no MB) showed no change in killing or in bioluminescence. Similarly for ECAS the controls (untreated cells suspended in PBS, or cells with scavenger only) again showed no change in bioluminescence showing a flat line response. This confirms that under control conditions no ROS are generated and hence no killing of the target organisms. The only exception to this was D<sub>2</sub>O control, where D<sub>2</sub>O had a slight inhibitory effect in the first few minutes on the bioluminescence but after that the bioluminescence quickly stabilises. This difference shows that D<sub>2</sub>O environment may have slight effects on the cells metabolism.

APDT carried out in the presence of singlet oxygen specific scavenger 10 mM tryptophan showed a very high degree of protection for all the three bacterial strains. Gram-positive *S. aureus* was afforded the highest protection of (97%) with *E. coli* (95%) protection and *P. aeruginosa* (89%) protection. In the presence of the hydroxyl radical scavengers it showed different levels of protection depending on the bacterial strains and the scavenger. In the presence of 10 mM DMTU *S. aureus* was afforded the highest protection (91%) with *E. coli* (68%) protection and *P. aeruginosa* (51%). In the presence of 10 mM Mannitol again *S. aureus* was afforded the highest protection (81%), with *P. aeruginosa* (50%) protection and with *E. coli* no protection. By comparing the protection afforded by singlet oxygen scavengers and hydroxyl radical scavengers demonstrates that in the case Gram-positive *S. aureus* strain both the type I and type II may be equally important in the killing mechanism however with the Gram-negative strains *E. coli* and *P. aeruginosa* the type II mechanism appears to be more significant compared to type I mechanisms of killing.

The effect of D<sub>2</sub>O replacing the H<sub>2</sub>O in the PBS buffer used in the assay increased the kill rate (*E. coli* and *P. aeruginosa* strains) several fold in the D<sub>2</sub>O medium when the ROS generation system was APDT. Singlet oxygen has a lifetime of 3 μs in water and is increased to 65 μs in D<sub>2</sub>O (Gorman and Rodgers, 1992). The increase in singlet oxygen lifetime in D<sub>2</sub>O presumably increases the biological interaction effect of singlet oxygen increasing the damage to the cells. This explains the higher kill rate when D<sub>2</sub>O was present, suggesting the involvement singlet oxygen (type II mechanism) in MB mediated APDT killing of *E. coli* and *P. aeruginosa*.

These results suggest the involvement of ROS in cell killing and were in agreement with previous findings that showed involvement of both types I and type II mechanisms in APDT (Bhatti *et al.*, 1998; Ergaieg *et al.*, 2008; Huang *et al.*, 2012; Wong *et al.*, 2005). However, in one study it was shown that tryptophan failed to protect *S. aureus* MB mediated killing (Sabbahi *et al.*, 2008). The authors concluded that the bactericidal activity of APDT was mediated in part, via a type I reaction in which hydroxyl radical is the dominant species.

To reveal the underlying mechanism of ECAS (5% v/v) and to compare with APDT mechanism, kill kinetics reaction in the presence of singlet oxygen or hydroxyl radical scavenger were carried out. The scavengers are considered to be specific to singlet oxygen: Tryptophan (10 mM) (less specific to singlet oxygen) strongly inhibited the bioluminescence (87%) whilst the sodium azide (100 mM) provided 43% protection. The enhancer of singlet oxygen life span (D<sub>2</sub>O) showed no increase in the kill rate. The scavengers considered as specific to hydroxyl radical, mannitol (100 mM) gave 62% protection and DMSO (128 mM) showed a 45% protection. When this data was compared to the initial killing (first 60s) it showed that the singlet oxygen scavengers sodium azide and tryptophan gave reduced protection whilst mannitol showed only slight reduction in protection. This indicates that kill mechanism of ECAS is mainly dependent on hydroxyl radical particularly in the initial stages of killing although the contribution of singlet oxygen cannot be rejected. Comparing these results to APDT, the clearest difference between APDT and ECAS was seen in the kill effect when water was

replaced in the PBS with D<sub>2</sub>O, while APDT showed a several fold increase in kill rate ECAS showed no such increase suggesting that singlet oxygen may not be important in the ECAS kill mechanisms. In addition to this sodium azide (100 mM) a specific scavenger of singlet oxygen showed low level protection while tryptophan (10 mM) used as a singlet oxygen scavenger in APDT studies (Wong *et al.*, 2005) provided higher protection compared to azide. It has been suggested that tryptophan is less specific to singlet oxygen and is known to quench hydroxyl radical as well (Sabbahi *et al.*, 2008). In APDT (10 mM) mannitol provided no protection for *E. coli* while presented 62% protection ECAS. The overall conclusion drawn from this approach of comparative evaluation of protection provided by the ROS specific scavengers in these two systems (APDT and ECAS) is that the mechanism of APDT is dependent on both singlet oxygen (type II mechanisms) and hydroxyl radical (type I) mechanism whilst the mechanism of ECAS is mainly hydroxyl radical with only a small contribution by other ROS such as singlet oxygen.

It was found that the effect of scavenger changed as the reactions proceeded with the killing agent. For this reason the initial kill rates were also calculated. A very interesting finding was made with APDT of *P. aeruginosa* and *E. coli*. When the initial kill rate for the two organisms were compared it was found that *P. aeruginosa* killing was largely dependent on hydroxyl radical and *E. coli* was largely dependent on singlet oxygen but at the latter half for *P. aeruginosa* singlet oxygen was important. *P. aeruginosa* killing was overall more dependent on type I mechanism compared to *E. coli*.

The scavengers work via different mechanisms and are effective at different concentrations. The concentrations of scavengers used in this thesis were based on those previously used by others reported in the literature. These concentrations may not be optimised concentrations for their use. The bioluminescent assay developed in this thesis can be rapidly used to optimise the concentrations of the scavenger. This will be much easier and accurate to carry out using bioluminescence compared to viable count methods. Hence this may be an interesting area to carry out further research.

Fluorescent probes showed ROS production in both APDT and ECAS. When 5  $\mu\text{M}$  SOSG was mixed with 10  $\mu\text{g/ml}$  MB, the fluorescence intensity increased linearly as the light dose increased while the aqueous solution of SOSG alone or SOSG probe and MB in dark showed no increase in the fluorescence. The greater the light energy absorbed by MB molecules, the greater the extent of  $^1\text{O}_2$  formation. However when SOSG alone was irradiated with increasing light doses there was slight increase in fluorescence indicating the probe alone could produce  $^1\text{O}_2$ . The quenching of fluorescence in the presence of tryptophan and increase in fluorescence when PBS was replaced by  $\text{D}_2\text{O}$  confirms that the increase in fluorescence is due to production of  $^1\text{O}_2$  by MB upon exposure to light. The low level of quenching of fluorescence intensity by mannitol (10 mM) compared to 10 mM tryptophan indicates that the probe is specific to  $^1\text{O}_2$  with little if any activity towards hydroxyl radical. These results are in good agreement with a previous study that showed SOSG is specific to singlet oxygen in APDT and comparatively less reactive to hydroxyl radical (Price *et al.*, 2009; Flors *et al.*, 2006). When SOSG probe was mixed with ECAS to detect singlet oxygen production there was only slight increase in fluorescence at the lower concentration and at higher concentration of ECAS fluorescence was lower than the background (SOSG probe only). This may be because the SOSG probe is deactivated by the ECAS and its low pH may be a contributing factor. Therefore without further study and pH control (by introduction of non-interfering buffer systems and pH neutralisation) SOSG probe cannot be used to study ROS production by ECAS.

Both APF and HPF showed increase in fluorescence following irradiation of MB. When  $\text{H}_2\text{O}$  was replaced by  $\text{D}_2\text{O}$  the fluorescence response by APF increased 207% while the singlet oxygen scavengers histidine (10 mM) provided 55% reduction, tryptophan (1 mM) showed only 0.4% reduction however at 10 mM tryptophan suppressed fluorescence by 72% similarly sodium azide 10 mM suppressed fluorescence 28% and 100 mM sodium azide 67%. In contrast to singlet oxygen scavengers hydroxyl radical mannitol (10 mM) showed only 9% reduction in fluorescence and mannitol (100 mM) showed 5% reduction. Similarly MB irradiated with HPF (5 $\mu\text{M}$ ) probe showed 87% suppression in the presence of tryptophan (10 mM) while only 4% suppression of fluorescence in the

presence of mannitol (10 mM). In conclusion these data show that both the probes can detect  $^1\text{O}_2$  generated by irradiation of MB which is in agreement with a previous study (Price *et al.*, 2009).

Overall the results confirmed the previously known mechanisms for APDT with MB. Further studies may be carried out with Fenton reagent a hydroxyl radical generating system or PS that produce exclusively produce singlet oxygen (type II) and free radical (type I) to increases the effectiveness of the test with ROS scavengers.

In a study where both the APF and HPF probes were used to detect singlet oxygen production it showed that fluorescence by the probes increased with porphine tetra (p-phenylsulfonate) (TPPS) irradiation and fluorescence was only quenched in the presence of singlet oxygen scavengers (1 mM sodium azide) and no quenching was observed in the presence of hydroxyl radical scavengers (1% v/v DMSO). The singlet oxygen enhancer ( $\text{D}_2\text{O}$ ) increased fluorescence response >25-fold in  $\text{D}_2\text{O}$  when (TPPS) was irradiated. However, the probes showed increase in fluorescence with Fenton reagent (a system that reported to generate only hydroxyl radical) and 0.02% (v/v) DMSO quenched ~50% fluorescence. A concentration of 0.1% DMSO, was found to decrease the fluorogenic response of APF to  $\bullet\text{OH}$  by >90%. It was concluded that the probes APF and HPF represent a useful means for evaluating formation of both  $^1\text{O}_2$  and  $\bullet\text{OH}$  in the presence of specific ROS scavengers (Price *et al.*, 2009).

Unlike SOSG and HPF, APF was not inactivated by ECAS and showed an increase in fluorescence response compared to probe only. To confirm the fluorescence increase in the presence of ECAS was specific to singlet oxygen or hydroxyl, ROS specific scavengers were added into the system and relative contribution was compared. These showed that the fluorescence was inhibited by tryptophan (10 mM) (99%) and azide (53%) whilst the singlet oxygen enhancer ( $\text{D}_2\text{O}$ ) showed only a small increase in fluorescence (21%). Fluorescence was reduced in the presence of DMSO (128 mM) (97%) and mannitol (100 mM) (42%). These results indicate that ECAS fluorescence response is due to both singlet oxygen and hydroxyl radical generation, but mainly due to latter. These

results were consistent with the results of bioluminescence kill kinetic assay confirming that ECAS involves mixed ROS mechanism.

## **Chapter 5: Cytotoxicity of APDT and ECAS on mammalian cells**

## 5.1 Introduction

The inappropriate use of antibiotics in both clinical and non-clinical settings has resulted in the increased threat of infections resulting from micro-organism resistant to all the currently available antibiotics (Alanis, 2005). The problem of antibiotic resistance is made worse due to decreases in the number of developments of new antibacterial agents in the last 10 to 15 years (Alanis, 2005). Consequently there is an urgent need to develop potential alternative therapies that can be useful in clinical application in the future (Alanis, 2005; Moellering, 2011).

Previous studies and work in this thesis have shown that both APDT and ECAS are effective antimicrobial agents against a wide range of microbial species. Both APDT (Embleton *et al.*, 2002; Kashef *et al.*, 2012) and ECAS (Tanaka *et al.*, 1996; Tsuji *et al.*, 1999) can effectively kill multi drug resistant bacteria including MRSA. Owing to these and many other favourable features both APDT (Kharkwal *et al.*, 2011) and ECAS (Thorn *et al.*, 2012) are now widely accepted as potential alternative therapies to localised antibiotics or other biocides.

One of the important characteristics of an ideal antimicrobial agent is that the target pathogenic microbes are selectively inactivated while host cells and tissues are preserved. In evaluating the usefulness of new antimicrobial agents it is important to determine its cytotoxic effects towards mammalian cells. By carrying out *in vitro* cytotoxicity tests the ability of the test agent to cause damage to mammalian cells can be assessed.

The two agents were compared in both the kill effect and mechanisms because of their ability to generate ROS (chapter 3 and 4). In chapter 4 it was shown that APDT damages microbial cells mainly by singlet oxygen whereas ECAS involves mixed ROS species with mainly hydroxyl radical being the predominant active species. To determine the clinical application of these treatments studies have been carried out to assess the potential cytotoxicity of APDT and ECAS to mammalian cells.

Due to the high reactivity of ROS and the potential to damage mammalian cells as

well as microbial cells it is important to study the cytotoxicity effects of ROS producing antimicrobial agents on mammalian cells. One of the reasons for restricted application of oxidizing agents is due to the lack of specificity toward microbial cells when compared with host mammalian cells causing unacceptable damage to normal cells. However, the development of new ROS based antimicrobial systems (such as APDT, ECAS and cold atmospheric plasma) may be less damaging to mammalian cells and so are leading areas of research from which therapies can be considered for localized infections (Vatansever *et al.*, 2013).

APDT can be designed to exhibit minimal damage to host cells and high selectivity towards the target pathogen (Sharma *et al.*, 2011). APDT studies carried out with PS belonging to different classes combined with light source where mammalian cells were exposed to the same condition showed that mammalian cells were killed at much lower rates compared to the target bacterial cells (Vatansever *et al.*, 2013). Phenothiazinum dyes MB and TBO are the lead PS compounds most widely investigated in PDT against infectious agents (Phoenix *et al.*, 2009). *In vitro* studies carried out using TBO as PS showed low cytotoxicity towards keratinocytes and fibroblast cells compared to microbial cells (Soukos *et al.*, 1996). PS such as TBO has been used successfully at 2,000 fold higher concentration than required for antibacterial effect in the diagnosis of premalignant disease without adverse effects (Mashberg, 1983). MB has been proposed to be safe for endodontic treatments based on its low toxicity towards gingival fibroblasts and osteoblasts under conditions similar to what may be applied in a clinical setting for endodontic disinfection (Xu *et al.*, 2009). MB has been shown in a recent study to have optimal properties for killing bacteria while preserving the viability of neutrophils (Tanaka *et al.*, 2012). This is beneficial because neutrophils are the primary mediators of host defense to invading bacteria and will improve the therapeutic efficiency of APDT, whilst surviving bacteria may re-grow if APDT kills neutrophils as well (Tanaka *et al.*, 2012).

Cytotoxic effects of APDT and ECAS on different mammalian cells may be different. Soukos *et al.* (1996) showed different cytotoxicity levels of

photodynamic treatment with TBO on fibroblast cells and keratinocytes. It was shown that fibroblasts were susceptible ( $>5.0 \mu\text{g/ml}$  TBO) whilst keratinocytes were more susceptible ( $>2.0 \mu\text{g/ml}$  TBO). Therefore it is important to compare the relative *in vitro* cytotoxicity of APDT and ECAS to different mammalian cell types. Since both APDT and ECAS may be applied in periodontal and wound irrigation, it is important to include cell types which may be exposed in these environments including leukocytes. Leukocytes are critical cells involved in the inflammatory processes of repair of burns or wounds (Eming *et al.*, 2007). However, very few studies have been carried out on leukocytes. Therefore in the current study cytotoxicity of APDT and ECAS were tested on both keratinocytes and lymphocytes (as an example of one type of leukocyte).

Current studies show ECAS to be safe and non-toxic (Prilutsky and Bakhir, 1997). ECAS have also been used without any adverse effects on mammalian cells (Robinson *et al.*, 2012). Mice given free access to ECAS as drinking water for 8 weeks showed no changes in body weight and no abnormalities on visual inspections of the oral cavity. Moreover, histopathological tests and measurements of surface enamel roughness and observations of enamel morphology showed no abnormal findings (Morita *et al.*, 2011). Therefore it was concluded ECAS has no systemic toxicity (Morita *et al.*, 2011). ECAS has been shown to have high biocompatibility at relatively high exposure levels compared to the anticipated low levels that would be necessary in the real clinical situation (Marais, 2002). However in the literature *in vitro* studies where ECAS was incubated with mammalian cell lines showed mixed results with some studies showing no toxic effect while others have shown significant cytotoxicity (Thorn *et al.*, 2012). Therefore further studies are required to determine the levels of cytotoxicity to mammalian cells before a therapeutic system suitable for clinical evaluation can be developed. To determine the toxicity level of ECAS it is needed to carry out *in vitro* studies on human cell lines specifically on the skin cells if it is intended to apply ECAS to a localised infection site. Therefore in this study the cytotoxicity of ECAS was also tested against keratinocytes and lymphocytes allowing comparison with APDT. It is difficult to compare animal studies, as the *in vivo* response may be different for different animals or even different strains of

the same species, whereas cell cultures have advantages over animal studies since the culture and treatment conditions can be more tightly defined. The same cells grown under standard conditions can be easily subjected to different treatments and results can be compared.

*In vitro* cytotoxicity studies have been used as suitable method in detecting the cytotoxicity potential of different agents and assessing the toxicity and occupational health risk of different compounds (Bakand *et al.*, 2006). Both the MTS and neutral red uptake assays have been used as a convenient method for assessing cell viability (Bakand *et al.*, 2006). MTS (3-[4,5-dimethylthiazol-2-yl]-5-[3-carboxymethoxyphenyl] 2-[4-sulfophenyl]-2H tetrazolium) assay is based on the ability of viable cells to convert a soluble tetrazolium salt to a formazan product. This method has been proven to be a highly sensitive, rapid and convenient system (Bakand *et al.*, 2006). The Neutral red (3-amino-7-dimethylamino-2-methylphenazine hydrochloride) uptake assay is a cell survival/viability technique based on the ability of viable cells to incorporate and bind supravital neutral red dye (Borenfreund and Puerner 1985). In the current study both MTS and NR assay were used to study *in vitro* cytotoxicity of APDT and ECAS.

Most of the cytotoxicity studies reported in the literature involve determining the effective dose of the biocide to kill target microbial cells and then (in separate assays) re-test at the same dose to see if it is cytotoxic to mammalian cells (Soukos *et al.*, 1996; Soukos *et al.*, 1998; Zeina *et al.*, 2002). However, none of the previous investigators have compared APDT and ECAS for relative cytotoxicity. Moreover, with one exception (George and Kishen, 2007) none of the previous workers have attempted to measure cytotoxicity of killing treatments against microbes and mammalian cells simultaneously using mixed cell assays. George and Kishen, (2007) used cell mixtures to study the cytotoxic effects of APDT on both fibroblast cells and *Enterococcus faecalis*. The results from viable counts showed that *E. faecalis* were killed at a faster rate than fibroblasts.

APDT and ECAS cytotoxicity effects on the mammalian cells were carried out in the presence of different concentration of fetal calf serum (FCS) since serum presence may more closely mimic occurrence *in vivo* (Lambrechts *et al.*, 2005).

It is important to show the same dose that are effective for microbes do not have any detrimental effect on mammalian cells by studying the *in vitro* levels of cytotoxicity on mammalian cells. By carrying out *in vitro* cytotoxicity of APDT and ECAS the likely cytotoxicity to mammalian cells *in vivo* could be predicted. If it were found that mammalian cells were equally susceptible to APDT and ECAS at the doses that are effective for microbial species, it would suggest that the treatment would not be safe for use in practice.

For APDT treatments two different photosensitizer doses were used. MB concentration of 10 µg/ml and 100 µg/ml, both combined with the light dose of 11 Jcm<sup>-2</sup>. A higher concentration of PS was required to be tested for several reasons. In chapter 3 it was shown that Gram negative *P. aeruginosa* required longer irradiation time for 3 log reductions with lower concentration of PS. It is generally known that Gram-negative bacteria are more resistant to milder treatments and may require higher concentration of PS and longer treatment time to produce an antimicrobial effect (Nitzan *et al.*, 1992). Similarly fungal cells also required longer time to produce effective kill (Zeina *et al.*, 2001). Several studies have also shown that when APDT is applied to biofilm it is more resistant and requires higher dose of treatment (Lin *et al.*, 2004). By increasing the concentration of PS while keeping the light dose the same the antimicrobial outcome may be improved, because more PS molecules are available to produce cytotoxic ROS when activated by light. Also the effectiveness of the treatment could be modified by keeping the PS concentration constant while changing the light intensity or irradiation time (Wainwright, 1998). However higher light intensities and longer irradiance times are not preferred because high light intensity may cause damage to tissue due to heat and a longer treatment time is not convenient to the patient. Therefore higher concentrations of the PS are required to be tested to confirm that it does not damage mammalian cells significantly. Therefore, both low and higher concentration of MB was used in combination with same light dose was tested on keratinocytes.

## **5.2 Aims of this chapter**

This study was carried out to compare the cytotoxicity of the two agents, APDT and ECAS, against keratinocytes and leukocytes. In addition the effects of post-treatment incubation and recovery were studied by comparing the cytotoxicity levels immediately after treatment and after a 24 hour recovery period. The effects of serum addition at a range of concentrations in preventing cytotoxicity to human cells for both APDT and ECAS treatments were also determined. Most importantly, co-mix assays of bacteria and keratinocytes together were conducted, in order to study comparable kill rates in the same assay following simultaneous treatments for APDT.

### 5.3 Results

In this study two types of mammalian cells were used to test the cytotoxicity levels after APDT and ECAS treatment. The cells used were keratinocytes (H103) and human lymphocytes (Jurkat).

The cytotoxicity levels of APDT towards keratinocytes were tested using the neutral red assay. Neutral red (NR) assay optical density readings were used to calculate the relative viability compared to the control without treatments. In addition, appropriate light controls where cells were exposed to light irradiation only and dark controls where cells were incubated with the PS only, were carried out.

ECAS cytotoxicity was measured using neutral red assay after incubating the keratinocytes with different concentrations of ECAS for 30 minutes. Neutral red assay optical density readings were used to calculate the relative viability for each ECAS treatment compared to the control untreated cells.

MTS assay was used to measure the cytotoxicity levels of both APDT and ECAS to lymphocyte (Jurkat) cells. The recorded optical density values obtained were used to calculate the percentage of viability of cells compared to control without treatment.

The formula given below was used to calculate the percentage viability for both *in vitro* assays.

$$\% \text{ cell viability} = \left( \frac{\text{mean absorbance of exposed cells}}{\text{mean absorbance of unexposed control cells}} \right) \times 100$$

#### 5.3.1 APDT cytotoxicity to keratinocytes (H103) cells

Figure 5.1 shows the percentage viability of keratinocytes exposed to APDT (MB concentration 10  $\mu\text{g/ml}$  and total light dose of  $11\text{Jcm}^{-2}$  [intensity  $9.4\text{mWcm}^{-2}$ ] and irradiation time of 20 minutes) compared to cells exposed to higher concentration of MB (100 $\mu\text{g/ml}$ ) and the same light dose  $11\text{Jcm}^{-2}$ . The recoveries of keratinocytes were tested by comparing at which point the NR assay was

performed. The NR assay was performed immediately after APDT exposure and after after 24 hours incubation of cells with fresh media. Figure 5.1 shows that performing the NR assay immediately after exposure to APDT resulted in significantly ( $p$  value  $< 0.001$ ) lower percentage viability than when the NR assay was performed after 24 hour incubation.

For keratinocytes treated with APDT (at high and low PS dose) the percentage viability was reduced for both immediate and after 24 hour recovery and this was significantly different ( $p$  value  $< 0.001$ ) when compared to the light only controls (cells exposed to light dose of  $11\text{Jcm}^{-2}$  only) and untreated controls.

Keratinocytes exposed to APDT with high and low concentration of PS was compared to the respective dark controls (cells incubated with MB at  $100\mu\text{g/ml}$  or  $10\mu\text{g/ml}$  for 20 minutes in the dark) and was significantly different ( $p$  value  $< 0.001$ ), after the immediate viability test but not after 24 hour recovery. The graph (figure 5.1) shows that there was no significant difference between exposures to high and low concentration of PS following light treatment. Likewise there were no significant differences between high and low concentration of PS for dark control. However after 24 hour recovery a difference was now revealed for both light treatment and dark controls with regard to high or low PS. Comparison of viability of keratinocytes immediately, and after 24 hours recovery with both the high and low concentration of PS there a was significant increase in viability ( $p$  value  $< 0.001$ ).

In the case of the dark control for high concentration PS after 24 hour recovery there was significant reduction in viability of keratinocytes ( $p$  value  $< 0.001$ ) but for lower concentration PS dark control, there was no significant difference after the recovery period.

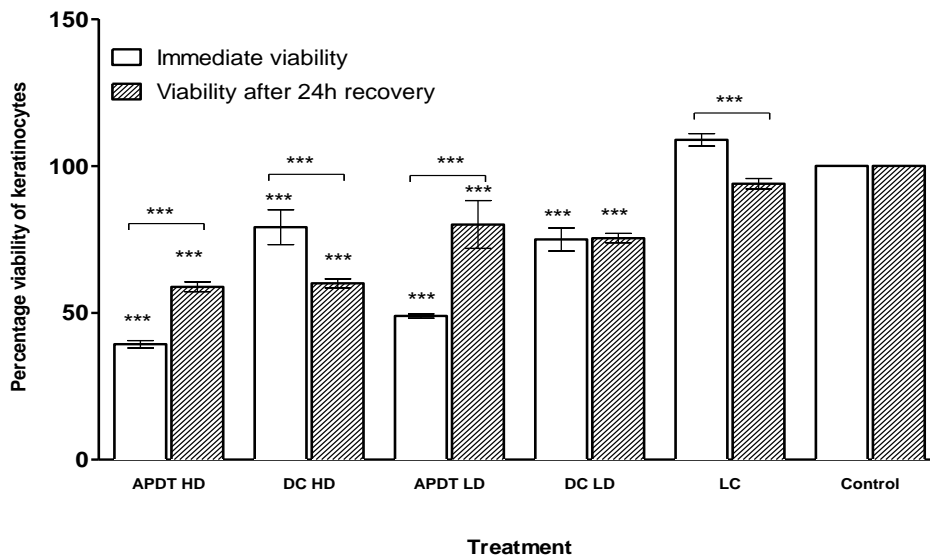


**Figure 5-1 Influence of the time point at which the viability test was performed, after APDT of keratinocytes on the outcome of the assay. NR assay performed immediately after APDT (immediate viability) and after 24 hours (viability after 24h recovery). HD, high dose (MB 100  $\mu\text{g/ml}$  and 11  $\text{Jcm}^{-2}$  light irradiation); LD, low dose (MB 10  $\mu\text{g/ml}$  and 11  $\text{Jcm}^{-2}$  light irradiation); DC, dark control; LC, light control; Control (cells not treated). Error bars represent mean  $\pm$  SD (n=3). Asterisks indicate the values that differ significantly from the control. Lines with asterisks on top compare the groups that significantly differ from each other. \*\*\* P value < 0.001.**

Figure 5.2 shows the effects APDT on the viability of keratinocytes in the presence of different concentrations of foetal bovine serum (FBS) compared to absence of FBS. Table 5.1 shows the comparison of significance values between different treatment conditions. In the absence of FBS, APDT with higher and lower concentration of PS was more cytotoxic to keratinocytes and was significantly different compared to dark control, light control and untreated control. When 10% FBS was present in media, for the higher concentration of PS there was no significance difference between treatment and dark control, but there was significant difference between treatment and, light control and untreated control. However, in the presence of 10% FBS, APDT low dose showed significant difference compared to dark control, light control and untreated. When the FBS concentration was further increased to 25% and 50% for all conditions including the treatments there was a clear protective effect and an increase in viability of keratinocytes.

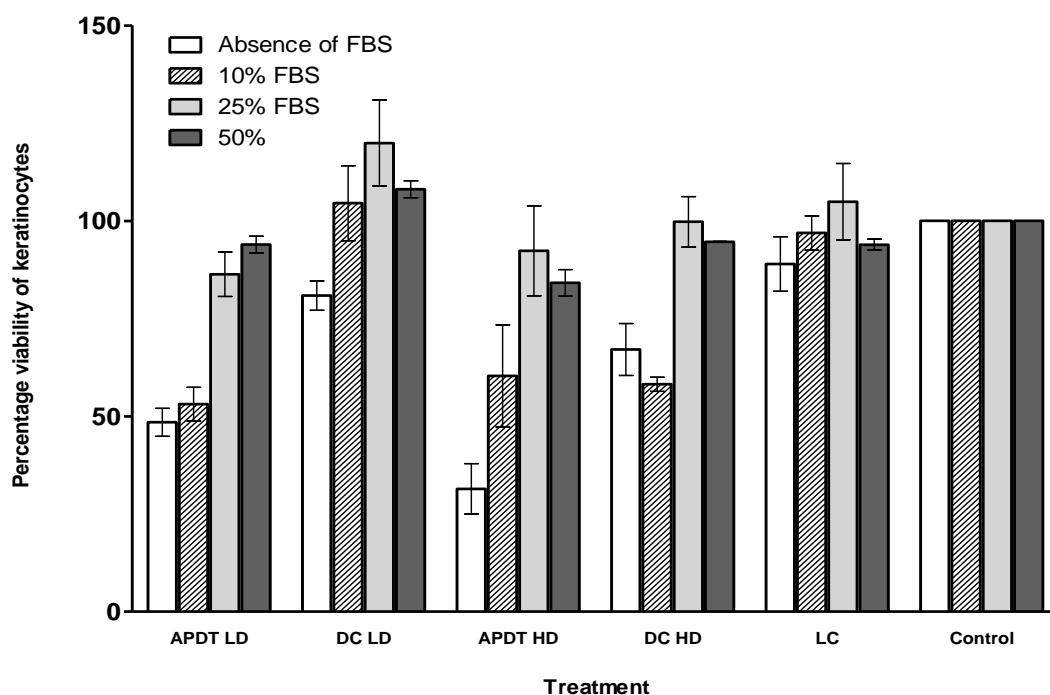


**Figure 5-2 Influence of FBS on APDT inactivation of keratinocytes in 10% FBS, 25% FBS and 50% FBS. For comparison APDT of keratinocytes in PBS (absence of FBS) is shown. HD, high dose (MB 100  $\mu\text{g/ml}$  and 11  $\text{Jcm}^{-2}$  light irradiation); LD, low dose (MB 10  $\mu\text{g/ml}$  and 11  $\text{Jcm}^{-2}$  light irradiation); DC, dark control; LC, Light control; Control (cells not treated). Error bars represent mean  $\pm$  SD (n=3).**

**Table 5-1 Significance level comparison of keratinocytes exposed to APDT or control conditions in the presence or absence of FBS**

conditions	Significant? P < 0.05 No FBS	Significant? P < 0.05 10% FBS	Significant? P < 0.05 25% FBS	Significant? P < 0.05 50% FBS
APDT LD vs DC LD	Yes ***	Yes ***	Yes **	Yes ***
APDT LD vs LC	Yes ***	Yes ***	No	No
APDT LD vs Control	Yes ***	Yes ***	No	Yes *
APDT HD vs DC HD	Yes ***	No	No	Yes ***
APDT HD vs LC	Yes ***	Yes ***	No	Yes **
APDT HD vs Control	Yes ***	Yes ***	No	Yes ***
DC LD vs Control	Yes ***	Yes ***	No	Yes ***
DC LD vs LC	No ns	No	No	Yes ***
DC HD vs Control	Yes ***	Yes ***	No	No
DC HD vs LC	Yes **	Yes ***	No	No
LC vs Control	No	No	No	No

HD, high dose (MB 100 µg/ml and 11 Jcm<sup>-2</sup> light irradiation); LD, low dose (MB 10 µg/ml and 11 Jcm<sup>-2</sup> light irradiation); DC, dark control; Light control, LC; Control (cells not treated), FBS, foetal bovine serum. Asterisks indicate significance difference, \*\*\* P < 0.001, \*\* P < 0.01. \* P < 0.05.

Figure 5.3 shows comparative killing of mammalian cells versus bacterial cells in co-mix assays. The graph shows that mammalian cells only reduced by 0.1 log in Figure 5.3 shows killing of mammalian cells versus bacterial cells in a co-mix assay. The graph shows that keratinocytes are only reduced by 0.1 log in 20 minutes of APDT whereas a 3 log reduction in *E. coli* Nissle 1917 pGLITE numbers is seen during this time. The log reductions in *E. coli* Nissle 1917 pGLITE numbers were calculated by measuring relative change in bioluminescence output at every 5 minute interval during the treatment. The log reductions in mammalian cells were calculated by measuring the viability of cells using the NR assay and were calculated as relative change before and after 20 minutes treatment. Previous experiment with mammalian cells showed that the change in viability was very small therefore viability was measure before and after treatment. Previous results showed no significant dark and light toxicity for both mammalian and bacterial cells.

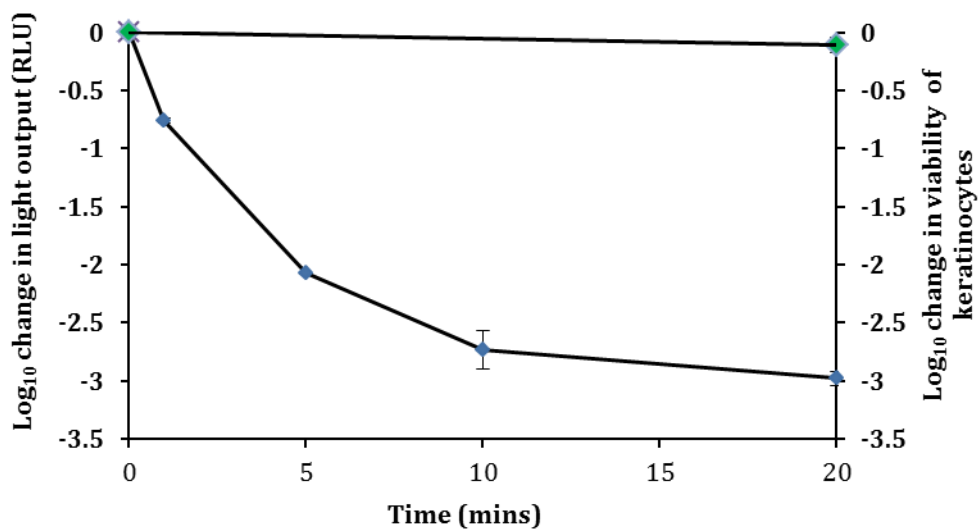


**Figure 5-3 Measurement of cell cytotoxicity of a co-mixture of mammalian (Keratinocytes (♦)) and bacterial cells (*E. coli* Nissle 1917 pGLITE (◆)) within the same reaction mixture exposed to APDT (MB 10 µg/ml and light dose 11 J/cm<sup>2</sup> (9.4 W/cm<sup>2</sup>)). Viability measured by neutral red assay for keratinocytes and for bacteria change in bioluminescence (RLU). Error bars represent mean ± SD (n=3).**

Table 5.2 shows the kill rate of mammalian cells compared to bacterial cells exposed to APDT. Table 5.3 shows the kill rate of mammalian cells compared to bacterial cells exposed to ECAS. The kill rates for mammalian cells are significantly lower compared to bacterial cells for both APDT and ECAS (table 5.2 and 5.3).

**Table 5-2 Kill rates of mammalian cells compared to bacterial cells after APDT**

Species	Kill rate (slope- log cell number/min)
Keratinocytes	0.012
Lymphocytes	0.022
<i>E. coli</i> Nissle 1917 pGLITE	0.150
<i>S. aureus</i>	0.300

**Table 5-3 Kill rates of mammalian cells compared to bacterial cells after ECAS**

Species	Kill rate (slope- log cell number/min)
Keratinocytes	No kill
Lymphocytes	5% ECAS 0.002
<i>E. coli</i> Nissle 1917 pGLITE	5% ECAS 1.5

### 5.3.2 ECAS cytotoxicity to keratinocytes (H103) cells

Figure 5.4 shows keratinocytes incubated with ECAS for 30 minutes at 25% v/v, 10% v/v and 5% v/v. As positive control keratinocytes were also incubated for 30 minutes with 5% v/v bleach. The treatments compared to controls showed that all the treated cells are significantly different from the control for immediate viability. Treatment with 5% v/v bleach was most toxic to the keratinocytes, followed by 25% v/v, 10% v/v and 5% v/v ECAS.

After 24 hour recovery, cells treated with 5% v/v ECAS showed a viability increase nearly to the control levels. Cells treated with 10% ECAS showed no recovery and nearly 50% reduction in viability. This was significant compared to immediate viability. Both 25% v/v ECAS and 5% v/v bleach showed no significant recovery after 24 hours.

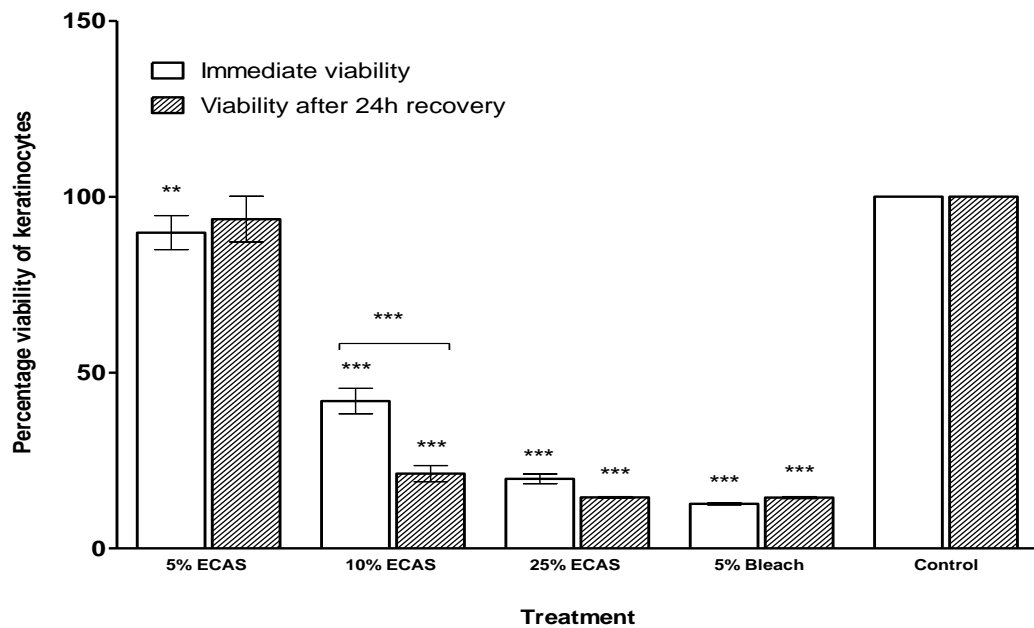


**Figure 5-4 Influence of the time point at which the NR assay was performed, after ECAS treatment of keratinocytes on the outcome of the assay. NR assay performed immediately after ECAS treatment (immediate viability) and after 24 hours (viability after 24h recovery). Error bars represent mean  $\pm$  SD (n=3). Asterisks indicate the values that differ significantly from the control (cells not treated). Lines with asterisks on top compare the groups that significantly differ from each other. \*\*\* P < 0.001, \*\* P < 0.01.**

Figure 5.5 shows percentage viability of cells incubated with different concentration of ECAS (v/v %) in the presence or absence of FBS. The table 5.4 shows the significance level for each different condition. Both 5 and 10% FBS gave protection to cells against 5% and 10% v/v ECAS however no protective effect was seen with 25% v/v ECAS treatment. There was no significant difference when 1% FBS is present compared to absence of FBS. The 5% v/v ECAS was least cytotoxic and 25% v/v ECAS was the most cytotoxic to the cells.

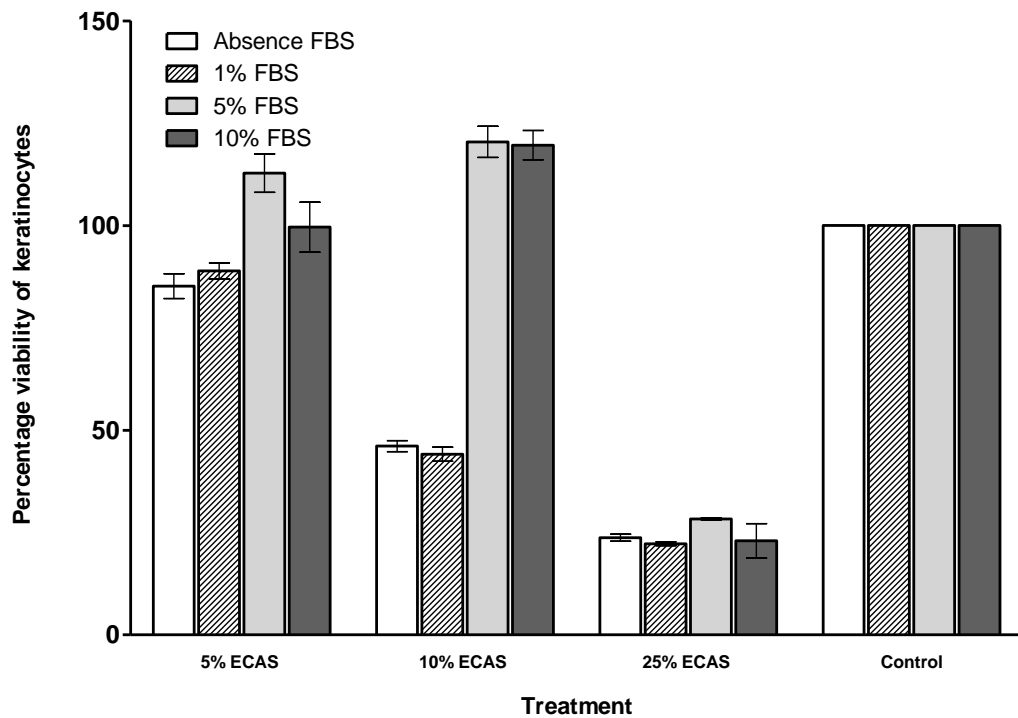


**Figure 5-5 Influence of FBS on ECAS inactivation of keratinocytes in 10% FBS, 25% FBS and 50% FBS. For comparison ECAS treatment of keratinocytes in PBS (absence of FBS) is shown. Error bars represent mean  $\pm$  SD (n=3).**

**Table 5-4 Significance level comparison of keratinocytes exposed to ECAS and/ or control conditions in the presence and absence of FBS**

	0 FBS	1% FBS	5% FBS	10% FBS
Tukey's Multiple Comparison Test	Significant? P < 0.05?	Significant? P < 0.05?	Significant? P < 0.05?	Significant? P < 0.05?
5% ECAS vs 10% ECAS	Yes***	Yes***	No	Yes*
5% ECAS vs 25% ECAS	Yes***	Yes***	Yes***	Yes***
5% ECAS vs Control	Yes**	Yes**	No	No
10% ECAS vs 25% ECAS	Yes***	Yes***	Yes***	Yes***
10% ECAS vs Control	Yes***	Yes***	Yes**	Yes*
25% ECAS vs Control	Yes***	Yes***	Yes***	Yes***

Asterisks indicate significance difference, \*\*\* P < 0.001, \*\* P < 0.01, \* P < 0.05.

### 5.3.2 APDT cytotoxicity to Jurkat (lymphocyte) cell

Figure 5.6 shows the viability of Jurkat cells exposed to APDT immediately and after 24-hour incubation. APDT treated cells immediate viability shows 35.2% and after 24 hour incubation gave 43.5% viability. In the controls there was no significant change in the percentage viability of cells. The positive control showed that 1% bleach is more toxic compared to APDT treatment and after 24 hour incubation there was no recovery as seen with APDT. Also it can be seen that on incubation for 24 hours the cells are able to recover.

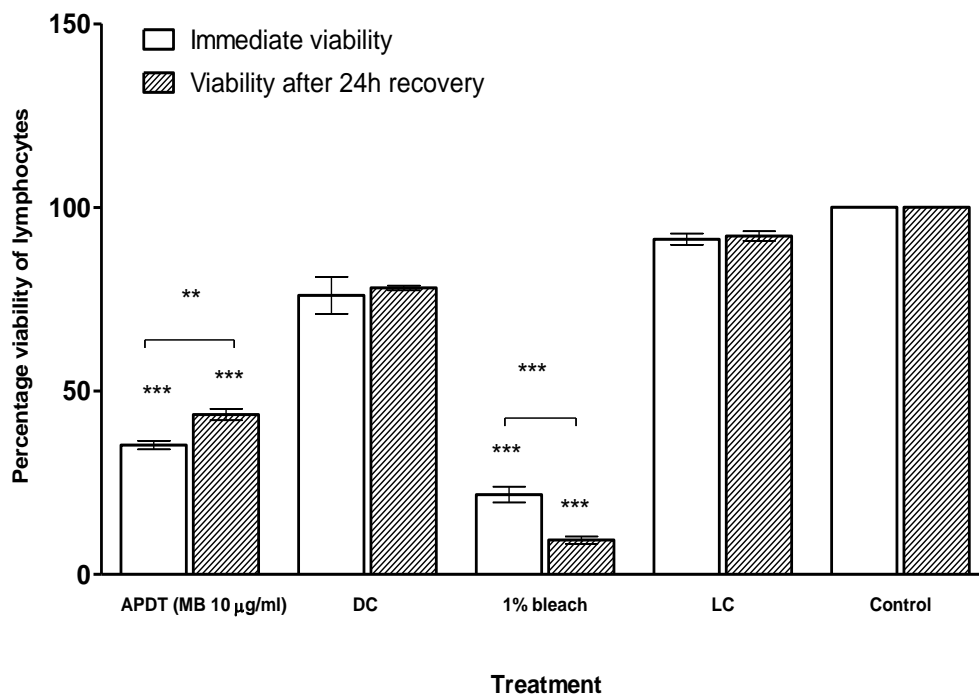


**Figure 5-6 Influence of the time point at which the MTS assay was performed, after APDT of lymphocytes on the outcome of the assay. MTS assay performed immediately after APDT (immediate viability) and after 24 hours (viability after 24h recovery). Error bars represent mean  $\pm$  SD (n=3). Asterisks indicate the values that differ significantly from the control (cells not treated). Lines with asterisks on top compare the groups that significantly differ from each other. \*\*\* P < 0.001, \*\* P < 0.01.**

### 5.3.4 Jurkat cell cytotoxicity and ECAS

Figure 5.7 shows lymphocytes incubated with different concentration of ECAS and cytotoxicity levels tested immediately or after 24-hour incubation. It shows that at 5% ECAS there is no change in viability almost identical to control conditions. On incubation for 24 hours after 5% ECAS treatment there was slight increase in viability. A dose dependent decrease in viability of cells with increase in ECAS concentration was then observed. The positive control (0.5% bleach) was the most toxic. With each ECAS treatment after 24 hours recovery incubation an increase in viability was observed and 5% bleach also showed a slight recovery.

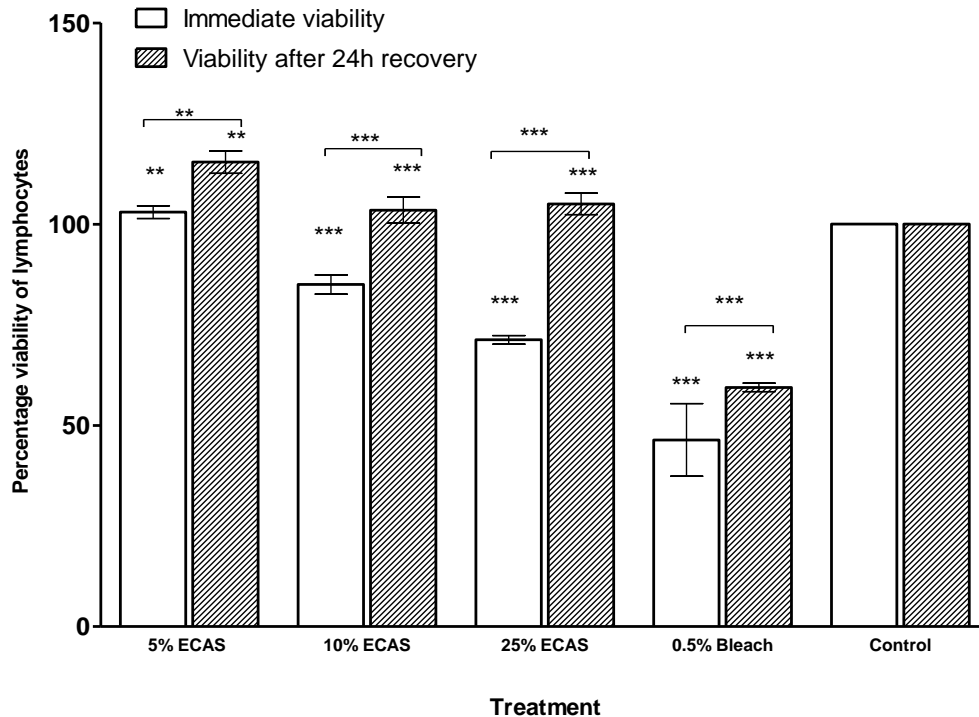


**Figure 5-7 Influence of the time point at which the MTS assay was performed, after ECAS treatment of lymphocytes on the outcome of the assay. MTS assay performed immediately after ECAS treatment (immediate viability) and after 24 hours (viability after 24h recovery). Error bars represent mean  $\pm$  SD (n=3). Asterisks indicate the values that differ significantly from the control (cells not treated). Lines with asterisks on top compare the groups that significantly differ from each other. \*\*\* P < 0.001, \*\* P < 0.01.**

Table 5.5 shows comparison of the effects APDT and ECAS on the viability of keratinocytes. It shows that keratinocytes are more sensitive to APDT compared to lower concentration of ECAS. The time point at which the NR assay was performed has a significant influence on the reduction in viability of keratinocytes. It shows that when NR assay was performed 24 hours after APDT or ECAS treatment there is an increase in viability compared to when it is carried out immediately after treatments. Table 5.6 shows comparison of the effects APDT and ECAS on the viability of lymphocytes. It shows that after exposure of lymphocytes to APDT there was significantly higher reduction in viability of lymphocytes which is in contrast to 5% ECAS that showed very low level in reduction in viability. However, increase in the concentration of ECAS increases the reduction in viability of lymphocytes. 1% and 0.5 % bleach are cytotoxic to lymphocytes. The time point at which the MTS assay was performed shows a significant influence on the reduction in viability of keratinocytes. It shows that when MTS assay was performed 24 hours after APDT or ECAS the survival value increases compared to when the MTS was performed immediately after APDT or ECAS treatment. Table 5.7 shows the influence of FBS on the viability of keratinocytes after APDT and after ECAS treatment (table 5.8). FBS has a significant influence on the viability of keratinocytes for the both APDT and ECAS treatments. In the case of APDT (high and low dose) the photoinactivation of keratinocytes in FBS compared to in PBS (absence of FBS) is significantly lower. Table 5.7 shows that for all treatment conditions of APDT of keratinocytes, with the increase in concentration of FBS the percentage viability of keratinocytes increases. FBS (50%) gives the highest protection against APDT. Similarly the viability of keratinocytes after ECAS treatment in FBS compared to in PBS (absence of FBS) shows increase in viability (table 5.8). Increase in the concentration of FBS protects the keratinocytes against ECAS. Table 5.9 shows the cytotoxicity levels of APDT and ECAS against keratinocytes and lymphocytes. ECAS is less cytotoxic to both keratinocytes and lymphocytes compared to APDT. Both APDT and ECAS treatment show higher cytotoxicity levels to lymphocytes compared to keratinocytes.

**Table 5-5 Reduction in percentage viability of keratinocytes after exposure to APDT and ECAS (data from figure 5-1 and figure 5-4)**

**HD, high dose (MB 100 µg/ml and 11 Jcm<sup>-2</sup> light irradiation); LD, low dose (MB 10 µg/ml and 11 Jcm<sup>-2</sup> light irradiation); DC, dark control; Light control, LC; Control (cells not treated).**

Type of cell	Type of assay	Treatment	Immediate reduction viability	SD	Reduction in viability after 24h recovery (significant difference- 24h recovery compared to immediate reduction. s, significant; ns, not significant.)	SD	% Recovery
Keratinocytes (H103) cells	NR	APDT HD	60.7	1.04	41.13 (s)	1.36	19.57
		DC HD	20.86	4.85	39.95 (s)	1.25	-19.09
		APDT LD	51.09	0.60	19.94 (s)	6.66	31.15
		DC LD	25.03	3.19	24.57 (ns)	1.30	0.46
		LC	No reduction (increase in viability 8.89)	1.72	6.01 (s)	1.45	
		5% ECAS	10.2	4.20	6.38 (ns)	5.62	3.83
		10% ECAS	58.09	3.13	78.71 (s)	1.98	-20.62
		25% ECAS	80.21	1.21	85.51 (ns)	0.22	-5.3
		5% Bleach	87.34	0.24	85.55 (ns)	0.25	1.79
		Control	0	0.00	0	0.00	

**Table 5-6 Reduction in percentage viability of lymphocytes after exposure to APDT and ECAS**

Type of cell	Type of assay	treatment	Immediate reduction (viability)	SD	Reduction in viability after 24h recovery (significant difference- 24h recovery compared to immediate reduction. s, significant; ns, not significant.)	SD	% Recovery
Lymphocytes	MTS	APDT LD	64.77	0.96	56.47 (s)	1.29	8.3
		DC LD	23.97	4.13	21.95 (s)	0.51	2.02
		1% bleach	78.25	1.74	90.64 (s)	0.82	-12.39
		Light control	8.67	1.25	7.82 (ns)	1.05	0.85
		5% ECAS	+3.00	1.28	+15.41 (s)	2.28	12.41
		10% ECAS	28.73	0.86	+3.49 (s)	2.16	18.49
		25% ECAS	15	1.96	+5.03 (s)	2.64	33.76
		0.5% Bleach	53.62	7.37	40.56 (s)	0.88	13.06
		Control	0		0		

**Table 5-7 Influence of FBS on the viability of keratinocytes after exposure to APDT**

Cell type	Assay	Treatment	No FBS Percentage viability	10% FBS Percentage viability	25% FBS Percentage viability	50% FBS Percentage viability
Keratinocytes	NR	APDT LD	48.48 SD 2.92	53.65 SD 2.96	62.31 SD 16.30	86.36 SD 4.66
		DC LD	80.88 SD 3.08	97.16 SD 14.40	108.30 SD 5.38	119.92 SD 9.96
		APDT HD	31.42 SD 5.26	53.90 SD 17.12	63.43 SD 15.02	92.36 SD 9.40
		DC HD	67.10 SD 5.43	62.27 SD 6.87	69.44 SD 16.32	99.78 SD 5.25
		LC	88.96 SD 5.70	93.89 SD 4.23	100.72 SD 1.82	104.92 SD 7.96
		Control	100	100	100	100

**Table 5-8 Influence of FBS on the viability of keratinocytes after exposure to ECAS treatment**

Cell type	Assay	Treatment	No FBS Percentage viability	1% FBS Percentage viability	5% FBS Percentage viability	10% FBS Percentage viability
Keratinocytes	NR	5% ECAS	85.20 SD 4.31	86.61 SD 1.38	99.61 SD 15.19	112.81 SD 6.66
		10% ECAS	46.12 SD 1.88	44.68 SD 2.80	71.15 SD 35.78	120.44 SD 5.39
		25% ECAS	23.75 SD 1.23	22.57 SD 0.33	24.46 SD 3.20	28.34 SD 0.39
		Control	100	100	100	100

**Table 5-9 Comparison keratinocytes and lymphocytes cytotoxicity levels of APDT and ECAS**

Treatment	Lymphocytes (MTS assay)	SD	Keratinocytes (NR assay)	SD
	Percentage reduction in viability relative to the control (media supplemented with 10% FBS)		Percentage reduction in viability relative to the control (media supplemented with 10% FBS)	
APDT (low concentration PS)	64.77	0.96	46.35	2.96
Dark control (low concentration PS)	23.97	4.13	2.84	14.40
Light control	8.67	1.25	6.11	4.23
Control	0	0.00	0	0.00
5% ECAS	+3.00	1.28	+12.81	6.66
10% ECAS	28.73	1.96	+20.44	5.39
25% ECAS	15	0.86	71.66	0.39
0.5% Bleach	53.62	7.37	-	
1% bleach	78.25	1.74	-	
5% Bleach	No live cells (trypan blue test)		14.45	0.25

## 5.4 Discussion

This study was carried out to find the cytotoxicity levels of APDT and ECAS since both ROS generating systems have been proved to be effective against a wide range of microbes (Dai *et al.*, 2009; Loshon *et al.*, 2001). The two systems were compared in their ability to damage mammalian cells at a dose that that led to  $>3\log_{10}$  bacterial killing (dose determined in chapter 3). To use these treatments *in vivo* would require a therapeutic window where bacteria could be killed without damage to adjacent normal tissue.

In this study it was demonstrated that lymphocytes were more susceptible to APDT compared to keratinocytes. For this reason keratinocytes were exposed to high and low PS dose while lymphocytes cells were only exposed low dose PS. There was no significant reduction in viability for both cell types after exposure to light only. When cells were exposed to MB in the dark (dark control) for lymphocytes there was no significant reduction in viability. However, keratinocyte showed reduction in viability for both the low and high PS concentration although this was significantly lower compared to keratinocytes exposed to APDT. It was found for the higher concentration PS there was a significant recovery of keratinocytes after 24 h incubation. This indicates that the MB in the dark is not cytotoxic to the cells since the cells can reverse any damage caused by PS alone.

When lymphocytes were exposed to APDT there was reduction in viability by 65%; and however upon 24 h incubation there was 8% recovery. Similarly when keratinocytes were exposed to APDT there was reduction in viability by 61% and 51% for the high and low PS concentration respectively. When the cells were incubated for 24 h after treatment for both the high and low PS there was 20% and 31% recovery respectively. Keratinocytes exposed to 5% bleach reduced viability to 87% and showed only 0.25% recovery after 24 h incubation while lymphocytes exposed to 5% bleach were completely destroyed (no viable cells). When lymphocytes were exposed to 1% bleach viability was reduced to 78% and upon incubation for 24 h there was delayed cytotoxicity with a further 12% reduction in viability. Even 0.5% bleach was cytotoxic to lymphocytes, which reduced viability to 54% with only 13% recovery after 24 h incubation. APDT for both cell types were several fold less cytotoxic compared to the

bleach positive control (5%). These results indicate that to mammalian cells APDT is much safer than bleach, which is an agent commonly used in clinical practice (Xu *et al.*, 2009). These results are in agreement with a previous study where APDT carried out with MB (50µg/ml) showed only modest reduction in viability of mammalian fibroblast cells and osteoblast cells while 3% bleach completely eliminated these cells (Xu *et al.*, 2009).

In another APDT study with test parameters MB PS at 100 µg/ml with a light dose 151 Jcm<sup>-2</sup> (light intensity 42 mWcm<sup>-2</sup>) cytotoxic levels to keratinocytes were apparent with viability reduced to 58% after 60 minutes and 62% after 90 minutes treatments (Zeina *et al.*, 2002). The present study showed similar reduction in viability on average but with a lower light dose (11 Jcm<sup>-2</sup> (light intensity 9.4 mWcm<sup>-2</sup> and 20 minutes treatment was used)). The difference in these results from the present study may be explained by variation in test parameters and due sensitivity of mammalian cells to variations in experimental test conditions. However, overall the data presented in this thesis was found to be in agreement with previous work carried out on APDT-MB showing that it is not strongly cytotoxic to keratinocytes. Moreover, when the cytotoxicity levels of keratinocytes exposed to APDT were measured after 24 hours, recovery of cells was evident under all treatment conditions and in the dark controls. This indicated that the cells were able to recover after APDT. This is also in agreement with the findings of Zeina *et al.* (2002) who showed recovery after treatments following 6 hours incubation in the dark.

ECAS (5% v/v) was not cytotoxic to lymphocytes and keratinocytes cells. However 10% v/v ECAS showed reduced viability of keratinocytes and lymphocytes. Similarly 25% v/v ECAS reduced viability of keratinocytes to 80% while bleach 5% v/v reduced viability to 87% in both cases with no recovery and further reduction in viability upon 24 h incubation. It was found lymphocytes were less cytotoxic to 10 and 25% v/v ECAS compared to keratinocytes. These results indicate that 5% v/v ECAS is the safest concentration for mammalian cells. Also ECAS was several fold safer to mammalian cells compared to APDT.

Bleach (5% v/v) compared to same concentration of ECAS was 5 times more cytotoxic to keratinocytes and completely eliminated lymphocytes cells. This is an interesting

observation since in the literature ECAS has been compared to bleach. ECAS has been shown to produce the same active hypochlorite as in bleach but despite this, ECAS is far less cytotoxic (Robinson *et al.*, 2011); highlighting that other factors may be present contributing to its high antimicrobial activity yet not contributing to any cytotoxicity to mammalian cells and specifically targeting the bacterial cells.

Experiments were carried out to find out whether the presence of serum in the treatment media gave protection to the cells from the cytotoxic effects of APDT. It was found that the protective role is dependent on the concentration of FBS. For both low and high PS concentration, 10% FBS was slightly protective but increasing the concentration to 25% and 50% FBS had significant protective effect. The presence of 50% FBS completely inhibited any cytotoxic effects of the treatment on the keratinocytes. Similarly FBS was protective against ECAS (5% and 10% v/v). However, 25%v/v ECAS FBS provided no further protection. ECAS cytotoxicity effects tested in the presence of FBS may more closely represent an *in vivo* environment.

Similar results were shown by a study carried out by Lambrechts *et al.* (2005) the PS used in their study was cationic porphyrin. It was shown that fibroblast survival increased with increasing fetal calf serum (FCS) concentration. Protective role of serum may be due to quenching and scavenging of ROS and PS may have higher affinity to serum and bind to it (Lambrechts *et al.*, 2005).

Recovery suggests that some aspects of both APDT-MB and ECAS treatment may be non-lethal and reversible. Moreover the data comparing the addition of higher concentrations of serum indicate that it may also protect the mammalian cells throughout treatment and aid in cell recovery.

The longer duration of application of APDT (20 minutes) is not a feature of ECAS which kills microbial cells quite rapidly hence reducing cytotoxicity to the surrounding mammalian cells. Therefore because the doses that are effective at killing the microbial cells are not cytotoxic to mammalian cells it confirms the applicability of this treatment to infected environments where mammalian cells may also be present.

When cytotoxicity effects of both APDT and ECAS treatment on keratinocytes and lymphocytes were compared it showed that lymphocytes cells are more sensitive to both

treatments compared to keratinocytes. It is important to note that the methods used to assess the cytotoxicity of the two types of cells were different although for each test the percentage viability was calculated relative to the control. For lymphocytes the viability test carried out used MTS which measures the metabolic activity of the cell whereas the NR assay used to measure cytotoxicity of keratinocytes is viability based assay. Of the 2 treatments ECAS had the least cytotoxic effect on both type of cells. However APDT was shown to be more cytotoxic to the lymphocytes compared to keratinocytes. Cytotoxicity level of ECAS at low concentration of 5% was not toxic to lymphocytes or keratinocytes but both cell types were more affected when the concentration was increased.

For APDT, Boehncke *et al.* (1996) showed that the difference in susceptibilities is proportional to the uptake of MB and that this is dependent on the type of the cells. Lymphocyte (Jurkat) cells may take up a greater amount of PS compared to keratinocytes and when irradiated produce more cytotoxic ROS in close vicinity of cells and therefore account for the difference in cytotoxicity levels in this study. However it is difficult to compare this precisely because the viability tests employed were different for the two types of cells.

When the co-mix assay containing keratinocytes and bacterial cells was exposed to 10  $\mu\text{g/ml}$  MB and  $11\text{Jcm}^{-2}$  light it was shown that bacterial cells were killed at a higher rate compared to keratinocytes. The treatment has lower cytotoxicity effect on the mammalian cell compared to bacterial cells when treatment was carried out simultaneously. APDT killing of keratinocytes was 12.5 fold lower than *E. coli* Nissle 1917 pGLITE and keratinocytes killing was 25 fold lower than Gram positive species *S. aureus* (based on kill rates calculated in separate assays).

This shows that when the APDT was carried out simultaneously in the same mixture it specifically targets to the bacterial cells over mammalian cells. It is known that bacterial cells take up cationic PS at faster rate compared to mammalian cells. It is known that the process of dye uptake by mammalian cells is by endocytosis whereas bacterial cells take up the dye by passive process (Dai *et al.*, 2009). Therefore the short duration of treatments means that bacterial cells may take up more dye compared to mammalian cells. If illumination is performed with short intervals after PS application (minutes) the

APDT mediated damage to mammalian cells will be minimized. It has been shown that the kill rates for keratinocytes after APDT treatment was 18 to 200-fold lower than that microbial species under the parameters employed in the study (Zeina *et al.*, 2002).

In this study it was found lymphocytes are more sensitive to APDT compared to keratinocytes and it was found that under conditions of this study APDT was only 7 fold lower at killing lymphocytes compared to Gram-negative *E. coli* Nissle 1917 pGLITE strain. In contrast to APDT, ECAS (5% v/v) was found to be even less cytotoxic to keratinocytes and lymphocytes. When *E. coli* Nissle 1917 pGLITE were exposed ECAS (5% v/v) a 1.5 log/min kill rate was obtained and only 0.002 log/min kill rate for lymphocytes. This indicated that after ECAS (5% v/v) lymphocytes were killed 750 fold lower than bacterial cells (Gram-negative strain). No significant kill was observed when keratinocytes were exposed to ECAS (5% v/v).

PDT of cancer requires longer pre-incubation of PS for the cancerous cells to take up the dye to effectively kill the cells; however this is not required of APDT because the bacterial cells are killed at a faster rate, eliminating the need for long pre-incubation of the PS with the cells. This will minimize the cytotoxicity to mammalian cells. In fact this is the main difference between APDT and PDT for cancer. For cancer therapy the PS is allowed to accumulate in the hyperproliferative cells. Treatments where the kill rates for bacterial cells are faster compared to mammalian cells highly desired. This will mean that the treatment periods will be shorter and easier for patients to comply and duration of the treatment exposure to mammalian cells are also reduced decreasing the chances of side effects of the treatment.

In conclusion it can be said that for ECAS there is wider safe therapeutic window where treatments can effectively target microbial cells over mammalian cells. In the case of APDT even though bacterial cells are more susceptible compared to mammalian cells the treatment may need to be used more carefully. APDT may need further study and optimisation to increase the ratio of bacterial cells killed to that of mammalian cells. The use of MB is well established in medicine and it is used for the routine staining of vital organs and the treatment of septic shock (Wainwright, 2000).

It has been shown that APDT with MB showed lower level of cytotoxicity to murine

peripheral-blood neutrophils compared to the PSs erythrosine B, rose bengal, crystal violet and photofrin. In the study it was shown that under conditions for each PS that exerted the maximum bactericidal effect on methicillin-resistant *Staphylococcus aureus* most neutrophils were viable (>80%) after APDT using toluidine blue-O (TB) or MB while neutrophils viabilities were decreased (<70%) after APDT using other PSs (erythrosine B, rose bengal, crystal violet, Photofrin, new MB and Laserphyrin). These results indicate that APDT using TB or MB can preserve host neutrophils while exerting bactericidal effect (Tanaka *et al.*, 2012).

One reason that eukaryotic mammalian cells may be protected from the cytotoxic effect while prokaryotic cells are damaged is due to the presence of nuclear membrane protecting the nucleus and acting as a barrier either to the penetration of PSs or cytotoxic reactive oxygen species formed during the treatment (Zeina *et al.*, 2002). It is possible that the same reason can account for the resistance to APDT killing of the eukaryotic fungal pathogen *C. albicans* compared to bacterial cells. *C. albicans* are reported to be hardest to kill by APDT when compared with Gram-positive or Gram negative strains (Zeina *et al.*, 2001; Demidova and Hamblin, 2005). Moreover it was proposed that the large size of *C. albicans* compared to bacterial cells, presents more targets to be damaged per cell, consequently the amount of ROS necessary to kill yeasts is much greater than amount necessary to kill bacteria (Zeina *et al.*, 2001; Demidova and Hamblin, 2005).

The wide applicability of these two ROS generating systems to a wide range of micro-organisms and the low toxicity against two important mammalian cell lines may indicate that these techniques could be applied *in vivo* as a method to reduce the pathogenic organisms in localised infections. The positive safety and efficacy results of these treatments warrant further studies. As it is shown that the serum plays a protective role from cytotoxic damages to cells also require further study to understand how exactly it protects the cells and how it may effect on the efficacy of the treatment *in vivo*.

In this study it was shown that when the bacterial and mammalian cells are in co-mix assay and simultaneously treated considerably higher kill rates were observed for the bacterial cells only and only a slight change for mammalian cells. This faster kill rate of

bacterial cells means mammalian cells are not damaged for the duration of the treatment and short treatments can be carried without damage of the mammalian cells. If the microbial kill rate is slow that means that the mammalian cells will be exposed to longer treatments making it more likely to damage the mammalian cells.

The co-mix assay was a very useful model as it may be more relevant to an *in vivo* assay. As both types of cells are in close proximity. One reason for low toxicity may be that PS is taken up at faster rate and it accumulates only in the microbial cells and not in the keratinocytes and hence with irradiation the PS molecules are in close proximity to microbial cells are damaged sparing the mammalian cells from damage. The co-mix assay shows that the PS is more specific to bacterial cells (greater reduction in bacterial cells compared to mammalian cells). This assay indicates a therapeutic index and can predict treatment protocols where only microbes are damaged and mammalian cells are left undamaged. This assay could be repeated in future work to compare the cytotoxicity of PS used in APDT or new PS that are being developed. The use of bioluminescent *E. coli* in the co-culture mixture helped to carry out the test swiftly and effectively.

It would be very interesting to carry out this co-mix assay with other antimicrobial agents. The assay could not be carried out with ECAS as there was technical difficulty measuring the bioluminescence change because ECAS is a very fast acting agent and the kill rate was not easily determined for bacteria cells and mammalian cells together. However this assay can be modified in the future studies.

The results of this study are significant and indicate that the MB mediated photodynamic therapy and ECAS may be two distinct alternatives to conventional antibiotic therapy. Both the APDT and ECAS approaches may be of use for creating aseptic skin surfaces before surgery. This is more attractive as it shows no toxicity to keratinocytes *in vitro*. Use in treatments could also be of significant potential benefit for the future.

**Chapter 6: Genotoxicity effects of APDT and ECAS on lymphocytes (Analysis of DNA damage in lymphocytes using the Comet assay)**

## 6.1. Introduction

Several studies have shown both APDT and ECAS are effective biocides against a wide range of microbial species including antimicrobial resistant bacteria and bacterial spores and is non-toxic to mammalian cells. Low level of cytotoxicity and genotoxicity on mammalian cells would indicate that these alternative treatments could be used as a safe alternative to conventional antimicrobial treatments. Therefore it is important to show that the treatments do not cause genotoxicity to mammalian cells.

In chapter 5 it was shown that treatment doses of ECAS and APDT sufficient to effectively kill bacteria are not cytotoxic to keratinocytes and lymphocytes. Both were found to be several fold less cytotoxic towards mammalian cells compared to bacterial cells. Therefore this suggests that both treatments can be used effectively to treat microbial infections without damage to host cells. However, prior to testing of these agents *in vivo*, it is important to determine possible genotoxic effects on mammalian cells *in vitro*. A previous study showed that APDT using MB as PS does not cause DNA damage to keratinocytes (Zeina *et al.*, 2003). To the best of author's knowledge no previous studies have been carried out to test the potential genotoxic effects of both APDT and ECAS on lymphocytic cells at concentrations relevant to microbial killing.

A previous report showed that MB mediated PDT is genotoxic to human myeloid leukaemia cell line (K562) (McNair *et al.*, 1997). The comet assay showed damage to DNA immediately after treatment; however no residual DNA damage was present after 4 hour post treatment "recovery" incubation at 37°C. The method used in their study was different to the current study. The treatment protocol involved first, incubating the cells with MB for 1 or 16 hours, and then removing any unbound MB before the cells were irradiated with 20W argon ion pumped dye laser with light dose of 20 Jcm<sup>-2</sup>. This method is more relevant in cancer PDT as it usually involves a long preincubation time for PS to be taken up by the cancer cells. This is not necessary in the case of APDT.

A search of the published literature found no reports on testing for the *in vitro* genotoxicity of ECAS. ECAS is reported to be safe since ECAS failed to induce genotoxicity, when tests were carried out to for DNA damage, using either the Ames test (Tsuji *et al.*, 2008) or the genotoxicity micronucleus test (Gutierrez, 2006; Thorn *et al.*, 2012). Moreover, a recent study showed that ECAS did not degrade nucleic acids or

induce oxidative damage in dermal fibroblasts *in vitro* (Martínez-De Jesús *et al.*, 2007). These studies support the view that ECAS does not cause DNA damage and is not genotoxic to mammalian cells. However the number of studies carried out is limited. No studies have focused on the DNA damage to lymphocytes. Therefore in this study genotoxicity of ECAS and APDT were measured at concentration/dose conditions known to be highly biocidal to test microbes (determined in chapter 3).

### **6.1.1 Comet assay**

Comet is a well-known simple assay used to assess DNA damage caused by chemicals or other possible mutagenic treatments. The comet assay is also known as a single-cell gel (SCG) electrophoresis because it detects DNA damage caused within individual cells. The comet assay is a method of detecting DNA strands breakage (double, single, alkali-labile sites expressed as single strand breaks) in virtually any nucleated cell.

Ostling and Johanson (1984) were the first to quantify DNA damage using the comet assay (Fairbairn *et al.*, 1995). They used neutral conditions, which allowed the detection of only DNA double strands breaks. Later the assay was adapted under alkaline conditions by Singh (Anderson *et al.*, 1998; Singh *et al.*, 1988), which lead to a sensitive version of the assay that could assess both double and single strand DNA breaks as well as the alkali labile sites.

The comet assay allows for the direct visualisation of DNA damage in individual cells. A small number of treated cells, suspended in a thin agarose gel on a microscope stage were lysed, electrophoresed and stained *in situ* with a fluorescent DNA binding dye (Fairbairn *et al.*, 1995). The results of the test were based on the migration of relaxed and broken DNA fragments further than intact pieces of DNA when electric current is applied. The resulting images, (named for their appearance as comets) were measured to determine migration and “spread” and therefore the extent of the DNA damage (Fairbairn *et al.*, 1995). The comet assay provides a direct determination of the extent of DNA damage in individual cells. The single cell gel assay has also been used to examine DNA damage and repair under a variety of experimental conditions (Collins *et al.*, 1995; Fairbairn *et al.*; 1995, McNair *et al.*, 1997). This technique has proved to be valuable in discriminating the different mechanism involved in genotoxicity and DNA repair (Collins *et al.*, 1995).

The comet assay possesses a number of advantages as compared to other genotoxicity tests. Significant advantages include its sensitivity for detecting low levels of DNA damage (Olive *et al.*, 1990), the requirement for only small numbers of cells per sample, its ease of application and low cost, and the short time needed to perform the assay providing rapid production of data (Liao *et al.*, 2009; Fairbairn *et al.*, 1995). In addition this assay is flexible as it can be used to evaluate various types of DNA damage, and is readily modifiable for adaptation to a variety of experimental requirements (Liao *et al.*, 2009; Tice *et al.*, 2000). Therefore comet assay has been used in many studies to investigate DNA damage and repair by a variety of DNA-damaging agents.

The comet has been previously used for successful screening of human lymphocytes obtained from large numbers human subjects to determine the extent of DNA damage occurrence with time and lifestyle (cigarettes smoked/day). (Betti *et al.*, 1995). The alkaline comet assay has been previously applied as an effective screening assay for DNA damage induced by PDT on K562 cell line (McNair *et al.*, 1997).

The principle of the assay is based upon the ability of denatured, cleaved DNA fragments to migrate out of the nucleoid under the influence of an electric field, whereas undamaged DNA migrates slower and remains within the confines of the nucleoid when current is applied. Evaluation of the DNA “comet” tail shape and migration pattern allows for assessment of DNA damage. Olive *et al.* (1990) introduced the concept of tail moment measure; tail length and amounts of DNA in the tail as a measure of DNA migration. (Olive *et al.*, 1990).

Two main principles that determine the pattern of comet formation are the size of the DNA and the number of broken ends which may be attached to large pieces of DNA but which can still migrate a short distance from the comet head. The tail length initially increases with damage but reaches a maximum that is largely defined by the electrophoresis conditions, not the size of the fragments. At the low damage levels, stretching of the attached strands of DNA, rather than migration of individual pieces is likely to occur. With the increase in number of breaks, DNA pieces migrate freely into the tail of the comet, at the extreme (e.g. in apoptotic cells), the head and tail will be separated. The intensity of the fluorescence of the tail relative to the head provides information about the numbers of strand breaks. These concepts, stretching and

migration of separated strands are generally accepted to explain the DNA migration patterns observed in the comet assay (Collins *et al.*, 1995, Fairbairn *et al.*, 1995). Modifications of the comet assay can allow detection of DNA double-strand breaks, crosslinks, base damage and apoptotic nuclei enabling more information about the nature of the damage (Olive and Banáth, 2006). The limit of sensitivity of the assay is approximately 50 strand breaks per diploid mammalian cell (Olive and Banáth, 2006).

The series of steps in the comet assay procedure are:

1. cells mixed with low melting agarose at 37° C (Low melting (LM) agarose)
2. immobilise cells on comet slide
3. treats cells with lysis solution
4. samples treated with alkali (unwinds and denatured DNA)
5. samples stained with intercalated dye and visualised with epifluorescence microscopy following alkaline electrophoresis, which reveals DNA breaks

### **6.1.2 DNA damage**

DNA damage could be defined as any modification of DNA that changes its sequence or coding properties such that it loses the normal information transfer fidelity (Swain and Rao, 2011). DNA damage can occur by two mechanisms by spontaneous damage caused by sources within a cell or damage caused by external sources such as chemicals and radiation (ultraviolet or ionizing radiation (X-rays,  $\gamma$ -rays,  $\alpha$  particles and cosmic rays). These substances may induce inter-strand and intra-strand cross-links, DNA–protein cross-links, bulky DNA adducts, single strand breaks (SSBs) and double strand breaks (DSBs) (Swain and Rao, 2011).

### **6.2 Aims of this chapter**

The purpose of the present study was to assess the *in vitro* genotoxicity of APDT and ECAS on lymphocytes using the comet assay and to determine repair of DNA damage following incubation after treatment.

### 6.3 Results

In figure 6.1 the untreated lymphocytes shows undamaged DNA as it appears as round spots as the intact DNA does not migrate out of the cells and is confined to the nucleoid area. In contrast, figure 6.2 the positive control (100  $\mu\text{M}$  of hydrogen peroxide) shows cells with DNA damage that appear as fluorescent comets (migrating fragments of DNA the comet tail moving away from the nucleoid the comet head) with tails of DNA fragmentation

Figure 6.3 shows the light control (cells exposed to light for 20 minutes total light dose 11  $\text{Jcm}^{-2}$  at light intensity of 9.4  $\text{mWcm}^{-2}$ ). The image shows round spots because the DNA is intact showing that exposure of cells to only light does not damage the DNA.

Similarly in figure 6.4, 6.5 and 6.6 shows the dark control (cells incubated with only MB (10  $\mu\text{g/ml}$ ) in the dark for 20 minutes) without recovery period, after 6 hours recovery period and 24 hours recovery period respectively. All the three images show no DNA damage as cells appears as round fluorescent spots.

Figure 6.7 shows cells treated with APDT without incubation. It shows cells with damaged DNA that appear as fluorescent comets. In contrast the control (figure 6.4) where cells were incubated with only MB (10  $\mu\text{g/ml}$ ) in the dark without incubation shows cells with undamaged DNA that appears as round spots.

The respective dark control (figure 6.5) shows no damaged DNA while cells incubated for 6 hours following APDT (figure 6.8) shows cells with damaged DNA that appear as fluorescent comets indicating DNA damage.

Figure 6.9 shows cells incubated for 24 hours following APDT. It shows cells with damaged DNA that appear as fluorescent comets while the dark control (figure 6.6) cells that were incubated with only MB (10  $\mu\text{g/ml}$ ) in the dark for 20 minutes and incubated for 24 hours shows cells with undamaged DNA that appears as round spots.

Figure 6.10 shows DNA damage measured immediately after ECAS treatment; figure 6.11 and 6.12 shows a recovery period 6 hours and 24 hours respectively. These show no detectible damage which is similar to the negative controls (untreated).

Using the comet Assay IV single cell electrophoresis assay quantification software the tail moment was determined for each sample. The graph shows tail moment against type of treatment at different incubation time. Box plot graph shows the distribution of tail moment obtained for 50 cells for each treatment. Tail moment is a parameter which increases in proportion to the number of DNA strand breaks (Sparrow *et al.*, 2003).

Figure 6.13 shows the tail moment of cells exposed to APDT (MB concentration 10  $\mu\text{g/ml}$  and total light 11  $\text{Jcm}^{-2}$  at light intensity of 9.4  $\text{mWcm}^{-2}$ ) plotted against the incubation time following treatment. The positive control ( $\text{H}_2\text{O}_2$ ) showed the highest mean value of tail moment. The untreated cells, light only and dark only showed very low mean tail moment. The magnitude of tail moment after APDT treatment was increased compared to the control. The magnitude of the tail moment was dependent on the incubation time. 24 hours shows the highest mean value of tail moment.

The Exposure of cells to 5% v/v ECAS for 30 minutes (figure 6.14) immediately or following 6 hours or 24 hours incubation shows tail moment values similar to the control negative (the untreated cells) while the positive control ( $\text{H}_2\text{O}_2$ ) was significantly greater compared to both the control and ECAS treated cells for all incubation times. The magnitude of tail moment was not dependent on the incubation time.

### 6.3.1 Comet images of APDT treated cells compared with untreated cells

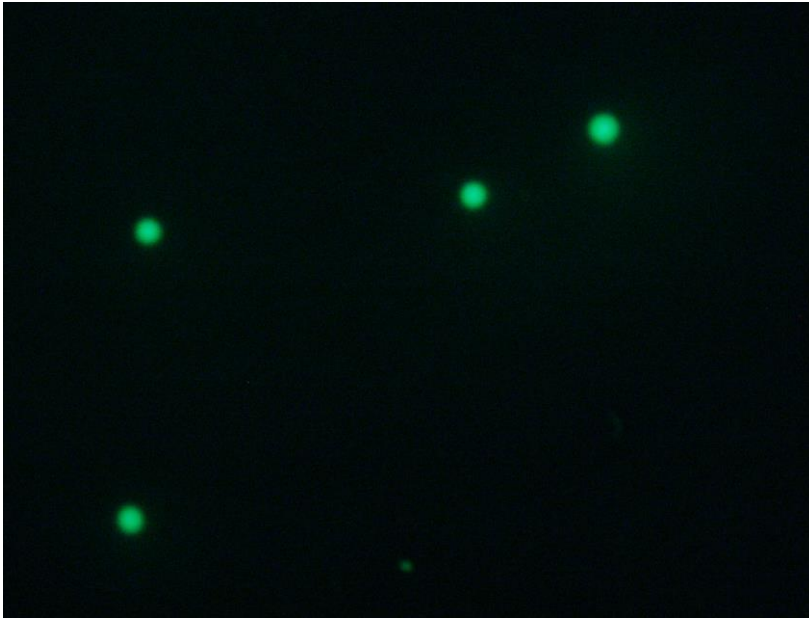


**Figure 6-1** Comet image of lymphocytes not exposed to treatment (negative control).

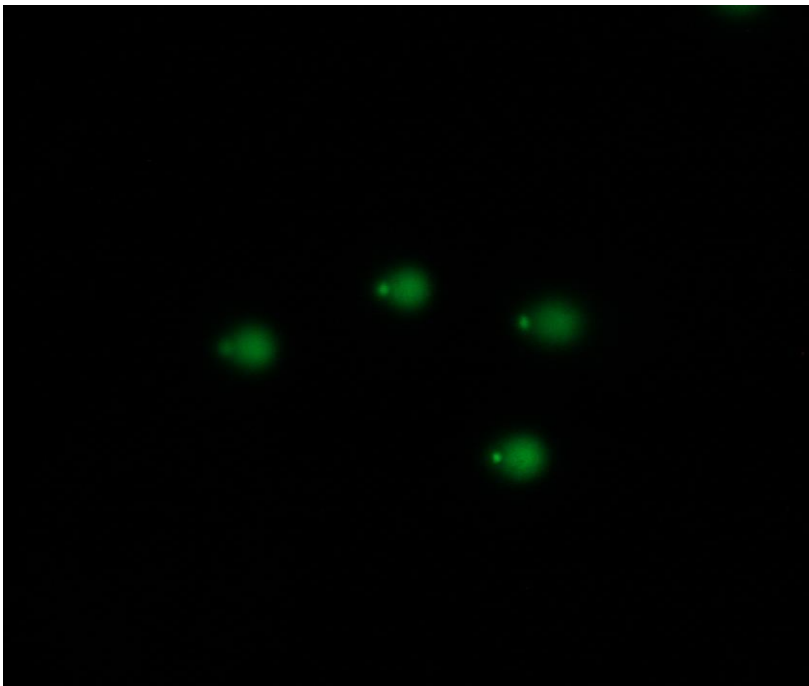


**Figure 6-2** Comet image of lymphocytes treated with 100  $\mu\text{M}$  of hydrogen peroxide (positive control).

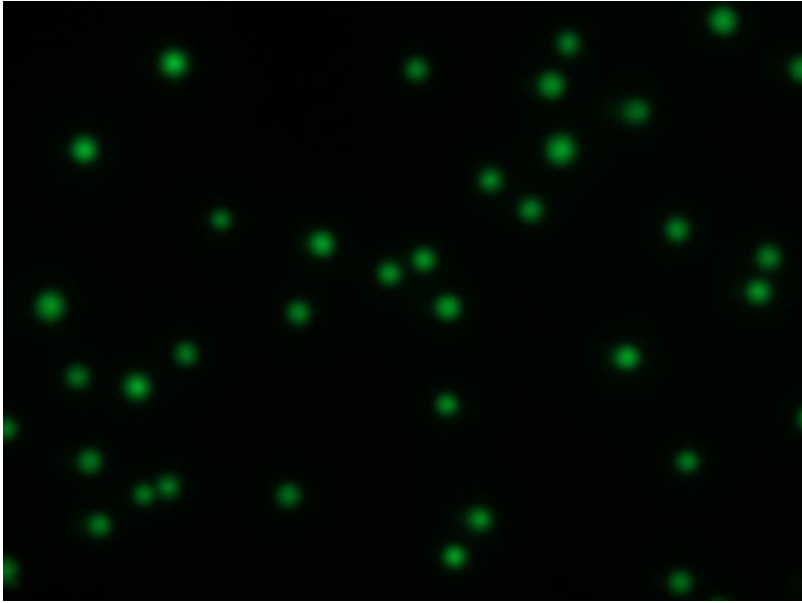


**Figure 6-3 Comet image of lymphocytes exposed to light only (total light  $11 \text{ J/cm}^2$  at light intensity of  $9.4 \text{ mW/cm}^2$ ) and no incubation after treatment.**

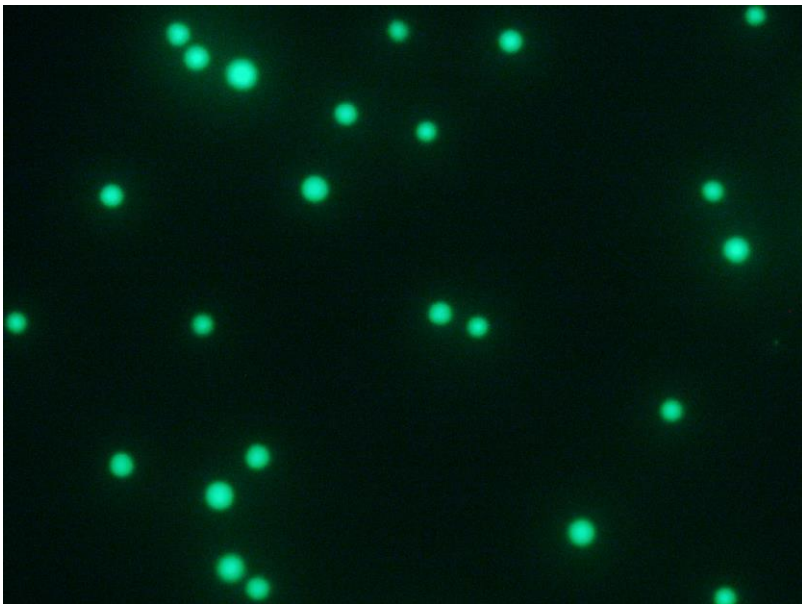


**Figure 6-4 Comet image of lymphocytes exposed to MB in the dark (cells incubated with MB concentration  $10 \text{ }\mu\text{g/ml}$  for 20 minutes) and no incubation after treatment.**

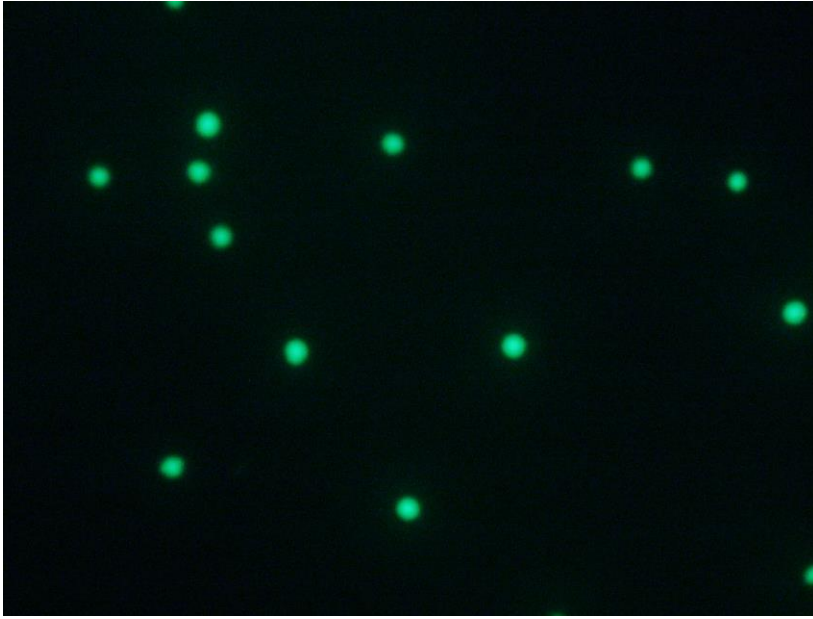


**Figure 6-5** Comet image of lymphocytes exposed to MB in the dark (incubated with MB concentration 10  $\mu\text{g/ml}$  for 20 minutes) and after treatment incubated for 6 hours.

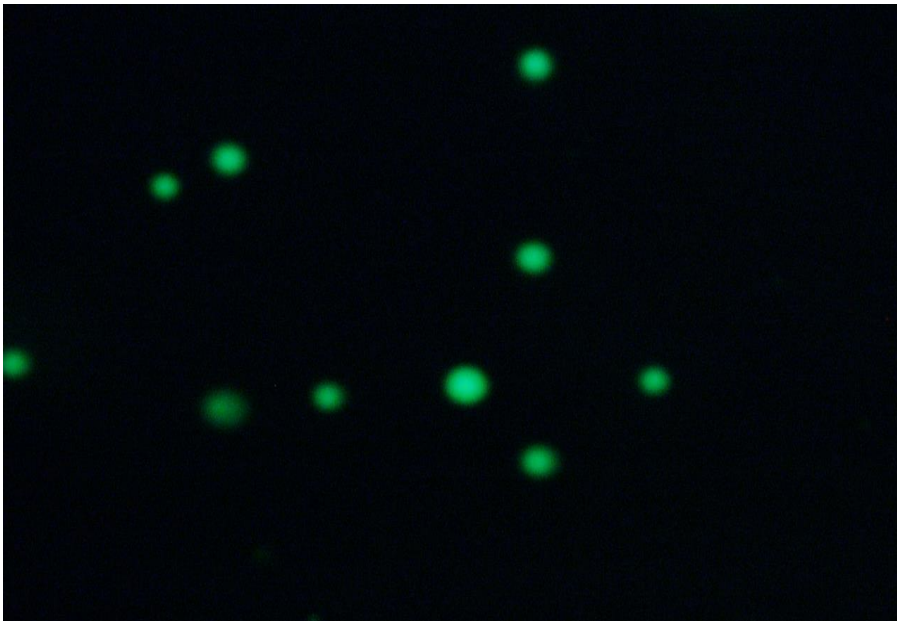


**Figure 6-6** Comet image of lymphocytes exposed to MB in dark (incubated with MB concentration 10  $\mu\text{g/ml}$  for 20 minutes) and after treatment incubated for 24 hours.

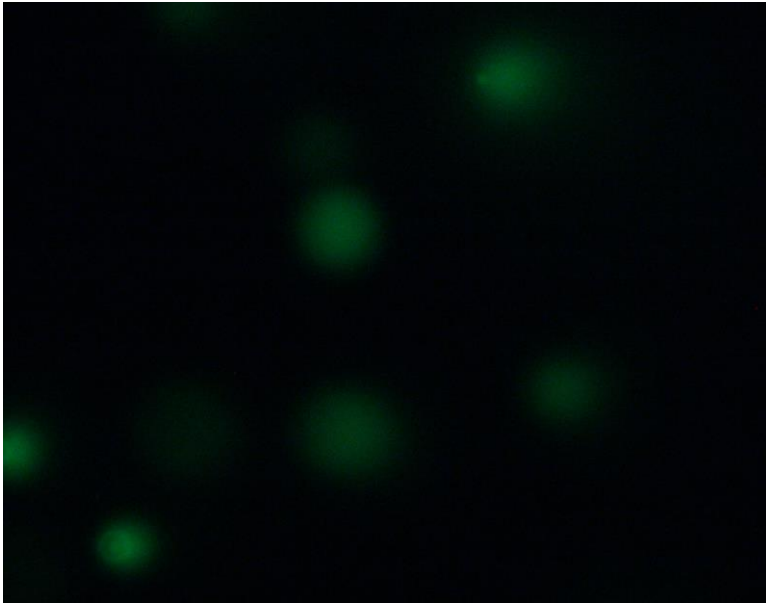


**Figure 6-7 Comet image of lymphocytes after APDT (MB concentration 10  $\mu\text{g}/\text{ml}$  and total light 11  $\text{J}/\text{cm}^2$  at light intensity of 9.4  $\text{mW}/\text{cm}^2$ ) and not incubated after treatment.**



**Figure 6-8 Comet image of lymphocytes after APDT (MB concentration 10  $\mu\text{g}/\text{ml}$  and total light 11  $\text{J}/\text{cm}^2$  at light intensity of 9.4  $\text{mW}/\text{cm}^2$ ) and incubated for 6 hours after treatment.**



**Figure 6-9 Comet image of lymphocytes after APDT (MB concentration 10  $\mu\text{g/ml}$  and total light 11  $\text{J/cm}^2$  at light intensity of 9.4  $\text{mW/cm}^2$ ) and incubated for 24 hours after treatment.**

### 6.3.2 Comet images of ECAS treated cells

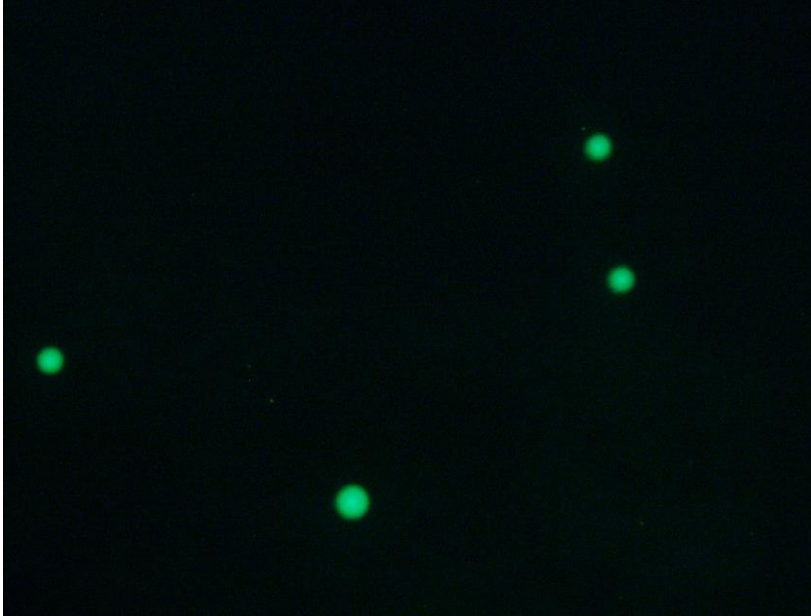


**Figure 6-10** Comet image of lymphocytes treated with 5% ECAS for 30 minutes and without incubation after treatment.

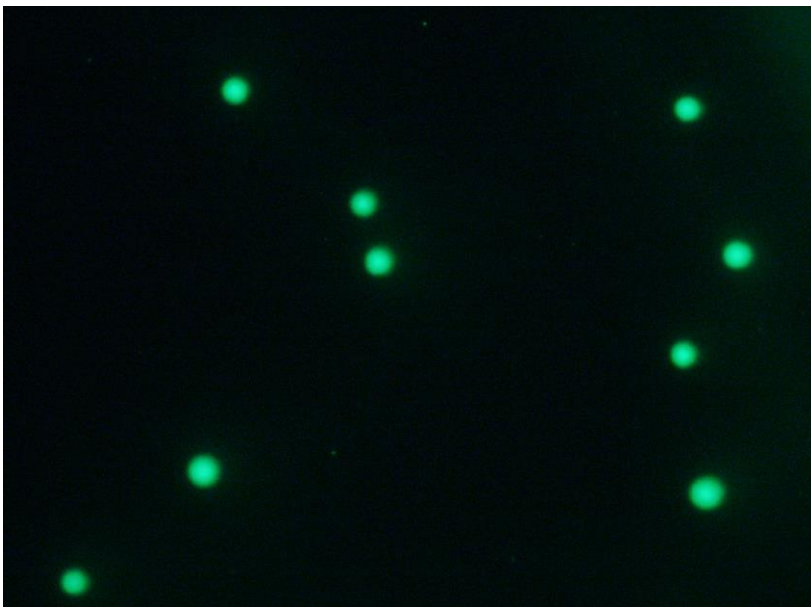


**Figure 6-11** Comet image of lymphocytes treated with 5% ECAS for 30 minutes and incubated for 6 hours after treatment.



**Figure 6-12 Comet image of cells treated with 5% ECAS for 30 minutes and incubated for 24 hours after treatment.**

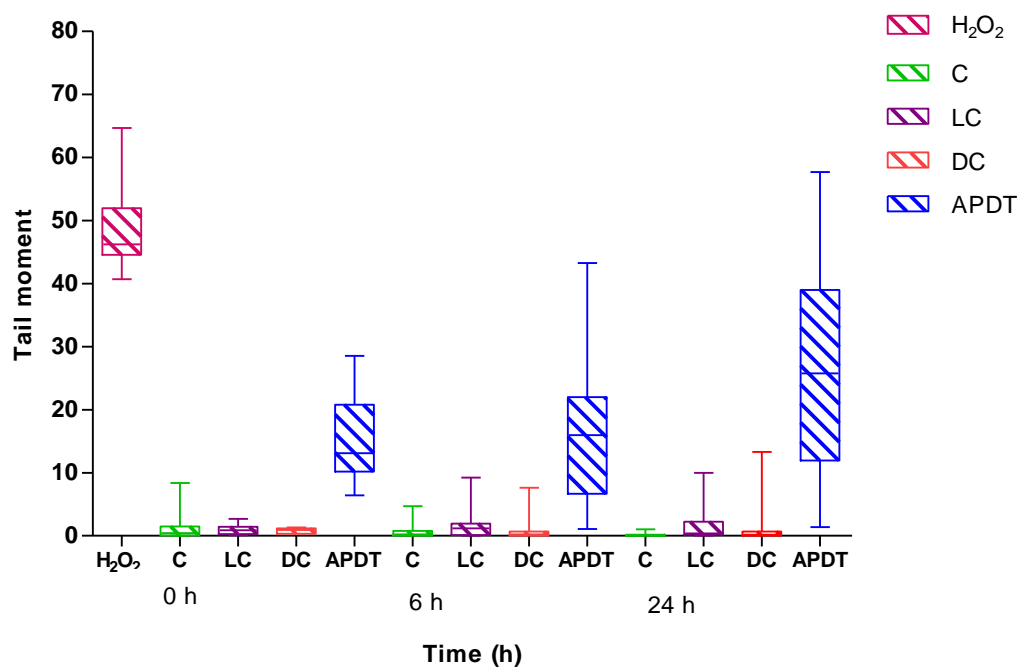


**Figure 6-13** Box-Whiskers plot of data collected for each comet assay for lymphocytes (Jurkat cells) treated with APDT (MB concentration 10  $\mu\text{g/ml}$  and total light 11  $\text{Jcm}^{-2}$  at light intensity 9.4  $\text{mWcm}^{-2}$ ). The comet assay was performed, immediately after treatment (time, 0 h), 6 hours incubation after treatment (time 6 h) and 24 hours incubation after treatment (time 24 h). Control population for each treatment is shown side by side for comparison. (n=75).

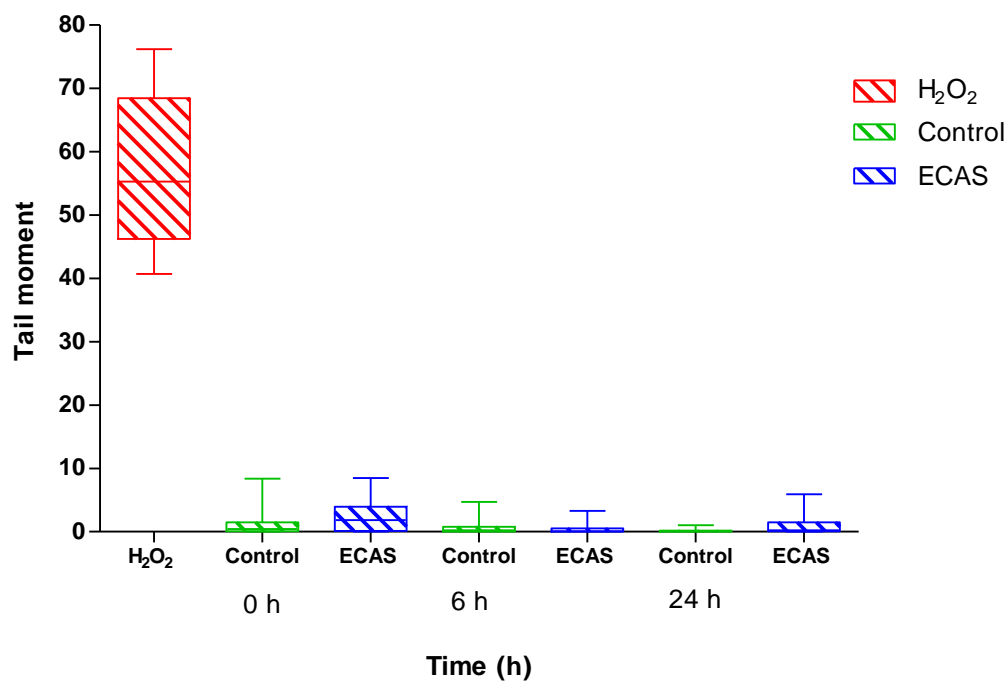


**Figure 6-14** Box-Whiskers plot of data collected for each comet assay for lymphocytes (Jurkat cells) treated with 5% v/v ECAS for 30 minutes. The negative control population for each treatment is shown side by side for comparison. The comet assay was performed, immediately after treatment (time, 0 h), 6 hours incubation after treatment (time 6 h) and 24 hours incubation after treatment (time 24 h). (n=75).

## 6.4 Discussion

This study was carried out to detect genotoxic effects of APDT and ECAS on lymphocytes (Jurkat cells) at doses previously shown (chapter 3) to effectively kill bacterial cells and doses that were shown to be non-cytotoxic to mammalian cells (chapter 5). The comet assay was employed to detect damage to DNA resulting after exposure of Jurkat cells to treatment (APDT or ECAS). The comet assay detects very small amount of damage to DNA (Olive and Banáth, 2006).

Lymphocyte cells exposed to hydrogen peroxide showed very high level of DNA damage. The images captured after exposure to hydrogen peroxide (figure 6.9) showed a typical comet appearance confirming that the technique is capable of detecting DNA damage and this corresponds to very high tail moment measurement. This confirms that hydrogen peroxide damages the DNA and is genotoxic to lymphocytes.  $H_2O_2$  is frequently used as a positive control in genotoxicity studies (Zeina *et al.*, 2003; Shimabukuro *et al.*, 2011). Hydrogen peroxide is known to cause oxidative stress in mammalian cells which leads to DNA damage (Benhusein *et al.*, 2010). The extent of this damage is dependent on the concentration of  $H_2O_2$  (Benhusein *et al.*, 2010). Untreated (figure 6.8) cells and Light alone (figure 6.7) showed no visually detectable damage to DNA and also gave low tail moment. Dark control cells exposed to 10  $\mu\text{g/ml}$  MB alone showed no visual comet formation after immediate exposure or following 6 or 24 hours incubation after treatment. This confirmed that MB alone in the dark does not damage the DNA and there are no delayed genotoxicity effects.

Lymphocytes exposed to APDT (10  $\mu\text{g/ml}$  MB total light  $11\text{Jcm}^{-2}$  at light intensity of  $9.4\text{mWcm}^{-2}$ ) and comet assay carried out immediately showed increased tail moment compared to respective dark control. Although APDT showed significantly higher tail moment compared to the respective controls it was not as high as the hydrogen peroxide at the concentration used, indicating that APDT of stated exposure time (20 min) causes less DNA damage compared to hydrogen peroxide. Comet assay has been used detect delayed DNA damage (e.g. apoptosis) or DNA repair following a recovery period (Olive *et al.*, 1993). To determine the DNA damage recovery or delayed DNA damage to lymphocytes after APDT, the comet assay was carried out immediately after APDT or 6 h or 24 h incubation of cells. The mean tail moment was significantly different ( $p <$

0.005) when comet assay was carried out immediately after treatment, 6 h or 24 h incubation after treatment. Comet assay carried out after APDT and following 24 h incubation showed the highest mean tail moment. The ability of the cells to repair the damage is dependent on the extent of DNA damage (Sparrow *et al.*, 2003). The failure of the cells to repair following incubation therefore may indicate that the severity of damage to lymphocyte DNA.

The Exposure of cells to 5% v/v ECAS for 30 minutes immediately or following 6 hours or 24 hours incubation after treatment showed no visual damage to DNA hence very low tail moment. The DNA damage after ECAS was very small therefore incubation after treatment did not show any significance. This shows that ECAS is not genotoxic to the cells and there was no delayed genotoxicity. Compared to APDT, ECAS resulted in considerably less damage to DNA.

This significantly higher genotoxicity level of APDT compared to ECAS is very interesting. This difference may be due the difference in the predominant ROS involved in the mechanisms of these two treatments. APDT mechanism involves predominantly singlet oxygen while ECAS may be mainly hydroxyl radicals as discussed in chapter 4.

Reactive oxygen species are known to induce chromosomal aberrations with high efficiency. It has been reported that MB photodynamic therapy (MB-PDT) might be expected to cause DNA damage, as MB is known to bind to DNA (Norden and Tjerneld 1982). MB was shown to intercalate rapidly into DNA, predominantly binding to purine nucleotides resulting in significant oxidative DNA damage (Tuite and Kelly, 1995). It has been identified that singlet oxygen is able to react with DNA molecule resulting in the formation of 8-oxo-7,8-dihydro-2'-deoxyguanosine (8-oxodG) with toxic and mutagenic effects (Agnez-Lima *et al.*, 2012). Singlet oxygen mediated damage may explain high DNA damage to the lymphocytes and inability of cells to repair the DNA damage. However, despite this evidence of *in vitro* DNA damage effects of MB plus light, this has not been reproduced *in vivo* (Wagner *et al.*, 1995). MB mediated PDT caused DNA damage to human myeloid leukaemia cell line (K562). However, upon incubation for 4 hour post treatment at 37°C the DNA damage was repaired. (McNair *et al.*, 1997). Singlet oxygen has a very limited diffusion distance 50µm (Moan, 1990; Fu

*et al.*, 2013). Therefore it is to be expected that the target for damage is likely to be restricted to sites close to the site of localisation of PS.

One of the major concerns of using ECAS is the potential to cause DNA oxidation and genotoxicity. This study confirmed that ECAS at concentrations tested (5% v/v) is not genotoxic to lymphocytes. Previous studies also failed to show any genotoxicity of ECAS using *in vitro* mutagenicity tests, Ames test (Tusji *et al.*, 1999) or the genotoxicity micronucleus test (Gutierrez, 2006; Thorn *et al.*, 2012). Moreover, it was shown that when dermal fibroblast cells were exposed to neutralised ECAS it did not degrade nucleic acids or induce oxidative damage in dermal fibroblasts *in vitro* (Martínez-De Jesús *et al.*, 2007). Therefore it can be concluded that together with the results of this study that ECAS does not target cell nuclei and does not induce damage to DNA (Martínez-De Jesús *et al.*, 2007). These are very encouraging results and indicate that ECAS can be safely used to develop treatment protocols for various localised infections including more invasive systemic infections.

This study (chapter 6) confirmed that lymphocytes incubated with 5% v/v ECAS for 30 minutes do not incur significant damage to their DNA. In optimal treatment, it may not be necessary for such long exposure of mammalian cells, higher than that required for efficacious antibacterial effect for ECAS. This indicates 2 minutes required for 4 log reduction in bacterial number will not cause any safety issues to mammalian cells. This indicates that ECAS may be safer to use in deep-seated tissue infections.

This study showed that APDT is genotoxic to lymphocyte cells and the damage was not repaired following incubation up to 24 hours. APDT damage compared with ionizing radiation is likely to be relatively low, as the damage reported consists predominantly of oxidative damage to guanine leading to single-strand breaks or an alkali-labile site, which are likely to be relatively easily repaired and also are likely to be highly dependent on the treatment agents (Evans *et al.*, 1997). Sparrow *et al.* (2003) reported that the repair of the DNA damage is dependent on the extent of DNA damage and may vary depending on the type of the cells. Therefore the lymphocytes may require more than 24 h incubation time to repair the damage.

A study carried out Zeina *et al.* (2003) to assess the DNA damage caused to keratinocytes by APDT mediated by MB showed no genotoxicity on keratinocytes. This indicates that lymphocytes are more sensitive to DNA damage and also, it was found (chapter 5) that APDT is more cytotoxic to lymphocytes compared to keratinocytes. The fact that keratinocytes are more resistant to genotoxicity levels than lymphocytes means that APDT may be more applicable for outer layers of skin infection rather than deep seated wound infections. Further studies may need to be carried out to optimise the APDT treatment.

Although it is known that DNA damage is an important factor in cancer development, direct evidence linking DNA damage and cancer have not been established (Poulsen *et al.*, 1998). There is no straightforward link between DNA modification and cancer initiation, most cells are repaired or killed and only small proportion of cells become cancerous (Noodt *et al.*, 1993) Also long term exposure to the mutagen might be an important contributing factor in cancer development. US, FDA Guidelines for carcinogenicity testing of pharmaceuticals (CDER, 1996) indicate that all drugs expected for continuous clinical use for at least 6 months or more are required to undergo long-term carcinogenicity studies should be performed in rodents. APDT and ECAS may need short treatment times and may not be needed for long-term use therefore minimizing any potential risk.

**Chapter 7: Application of APDT and ECAS against biofilm**  
**Real time monitoring of metabolic activity in biofilms exposed**  
**to APDT and ECAS within an *in vitro* flat-bed perfusion**  
**biofilm model**

## 7.1 Introduction

In the first part of this thesis it was established that APDT and ECAS are both effective against the planktonic bacterial cultures. In recent years bacterial biofilms have been implicated in various non-healing wounds and chronic infections (Schierle *et al.*, 2009). Furthermore biofilm has been frequently reported to dominate in infections associated with foreign-body (implants), cystic fibrosis (chronic bronchopneumonia), endocarditis, persistent otitis media, chronic osteomyelitis, infected prosthetic joints and intravenous catheters and stents (Høiby *et al.*, 2011). According to National Institutes of Health (NIH) biofilms are responsible for more than 80% of infectious diseases in the body (Davies, 2003). Moreover biofilm infections are characterized by persistent inflammation and tissue damage (Høiby *et al.*, 2011). These infections persist in spite of the innate and adaptive immune system and the inflammatory response of the host. Evidence supports the view that the biofilm mode of growth of bacteria lead to increased resistance to antimicrobial products compared to their “planktonic counterpart” making it difficult to eliminate biofilms (Costerton *et al.*, 1999). The emergence of highly resistant bacteria to conventional antimicrobials and high tolerance of biofilms to disinfectant and antibiotic therapy clearly shows that new biofilm control strategies are required (Simões *et al.*, 2010).

In the literature there are reports on the effectiveness of various disinfectants and antimicrobial agents including ECAS (Liao *et al.*, 2007) and APDT (Hamblin and Hassan, 2004), all based upon the results of tests carried out on planktonic bacteria. Such tests using planktonic cultures of micro-organisms have demonstrated the effectiveness of these agents; however these results will be unlikely to predict their potential effects *in vivo*. Biofilm growing bacteria differ from planktonic bacteria with respect to their genetic and biochemical properties and biofilm bacteria show enhanced tolerance to antimicrobial agents (Donlan and Costerton, 2002). It has been shown that the minimal inhibitory concentration (MIC) and minimal bactericidal concentration (MBC) of antibiotics required with biofilm-growing bacteria may be up to 100 to 1000-fold higher than those needed for equivalent populations of free-floating counterpart planktonic bacteria (Davies 2003). Biofilm represents a far more realistic representation of bacterial behavior in the clinical settings (Costerton *et al.*, 1999). Therefore biofilm

models may be more appropriate to evaluate the efficacy of a given antimicrobial agent than the currently used assays on planktonic bacteria. It is therefore essential to assess the *in vitro* efficacy of APDT and ECAS against bacteria growing in a biofilm mode using the most appropriate *in vitro* biofilm model in order to obtain clinically relevant information.

It is known biofilms form in wound and it is detrimental for the recovery of the wound by delaying the recovery processes (Bjarnsholt *et al.*, 2008). In excisional wounds of pigs the presence of *S. aureus* biofilms have been demonstrated and further showed that the planktonic bacteria recovered from the wounds were more susceptible to topical antimicrobial agents than the biofilm bacteria recovered from the same wounds (Davies 2003). Microbial biofilms cause various oral conditions, including caries, periodontal and endodontic diseases, dental implant failures and oral malodor (Soukos and Goodson, 2000). APDT and ECAS proposed as topical methods with broad-spectrum disinfection may therefore have applications in these localized infections.

As described in previous chapters the antimicrobial activity of both APDT and ECAS are dependent on highly reactive non-specific ROS (singlet oxygen and hydroxyl radical). Due to the high reactivity and non-specific activity of ROS, both APDT and ECAS may be active against the biofilm structure, causing general oxidative breakdown alongside cell killing (Wainwright and Crossley, 2004; Thorn *et al.*, 2012). It has been demonstrated that APDT mediated by NMB caused both cell killing and the breakdown of EPS, while the antibiotic ampicillin showed little damage to the EPS (Wainwright *et al.*, 2002). In *Escherichia coli* biofilms, extracellular matrix exposed to ECAS was removed (Thorn *et al.*, 2012). It was also proposed that hydroxyl radicals present in ECAS may cause the collapse of the highly structured hydrated biofilm matrix by removing hydrogen ions (through oxidation), and exposing deeper biofilm cells to antimicrobial agents (Thorn *et al.*, 2012; Marais and Brözel, 1999). Such dual activity is not seen in conventional antibiotics (Wainwright *et al.*, 2002). The mechanism of killing in APDT is non-specific and cytotoxic species damaged a variety of bacterial components and the development of resistance from repeated use is unlikely

(Wainwright and Crossley, 2004). Therefore non-specific ROS generating agents such as APDT and ECAS may be promising alternatives to treat biofilm infections.

As discussed in the introduction (chapter 1) APDT has been shown to be effective against biofilms using various biofilm models (Lee *et al.*, 2004; Beil *et al.*, 2011). The numbers of studies carried out are still limited and mainly focus on oral biofilm bacteria using different *in vitro* (batch culture or fluid-feed replacement within the same biofilm vessel) biofilm models (Zanin *et al.*, 2005).

When *S. aureus* biofilms treated with APDT using TBO PS a significant reduction in viability and disruption of the structure of biofilm was observed (Sharma *et al.*, 2008). Another study showed the APDT using PS merocyanine 540 on *S. aureus* biofilms required higher light dose to inactivate compared to planktonic cultures (Lin *et al.*, 2004). These studies concluded that the number of bacterial cells killed within a biofilm was considerably lower than what can be achieved when treating their planktonic counterparts and EPS may be one contributing factor for biofilm resistance. More evidence concerning the application APDT against biofilm is needed to understand the higher protection afforded by the biofilm mode of growth in order to improve APDT before it can be widely implemented in clinical settings. Also reliable *in vitro* biofilm models that closely represent the biofilm growth *in vivo* need to be tested to study effectiveness of APDT against the target biofilm organism.

Several studies have confirmed that ECAS is effective in removing biofilms formed by different bacteria associated with different surfaces (Thorn *et al.*, 2012). Similar to APDT it has been reported that ECAS exposure removed micro-organisms from tooth surfaces (Hata *et al.*, 1996) indicating application of ECAS to target biofilms involved in oral cavity diseases. ECAS was found to effectively reduce *Listeria monocytogenes* biofilms by 9 log<sub>10</sub> after 5 min of treatment (Venkitanarayanan *et al.*, 1999). ECAS activity has also been confirmed against clinically relevant species such as *Staphylococcus aureus* including, methicillin resistant *S. aureus* (MRSA), *Enterococcus faecalis*, *E. coli*, *Acinetobacter baumannii* (Thorn *et al.*, 2012). These studies further support potential applications of ECAS against biofilm infections in healthcare settings.

However, the number of studies of ECAS against biofilms are limited and the studies carried out so far are mainly focused on bacteria growing on different surfaces such as cutting boards (Venkitanarayanan *et al.*, 1999; Park *et al.*, 2002) relevant to applications in food industry or in disinfection of medical equipment (endoscope) (Masuda *et al.*, 1995; Sakurai *et al.*, 2002) Therefore further research is required to elucidate the kill kinetics and to develop optimised treatment protocols (Thorn *et al.*, 2012).

For studying biofilm a number of different *in vitro* biofilm models have been used (e.g. flow cells, continuous perfusion systems, microtitre plates). Most of the studies were carried out using models based on batch culture biofilm models. These finding from the studies were highly significant and showed that APDT may be effective against biofilms. However, these batch biofilm models do not account for the dynamic growth environment in which biofilms grow *in vivo* (Thorn and Greenman, 2009). Batch culture models are simple and easy to set up and in some cases may be adequate for gaining understanding of microbial activities upon exposure to antimicrobial agents (Thorn and Greenman, 2009). The major limitations of batch culture biofilm model is that limited control of the whole physicochemical environment (number of cells, concentrations of substrates, nutrients, products, pH and oxygen tension) (Greenman *et al.*, 2013).

In contrast to batch culture biofilm, open continuous flow biofilm models (biofilm model used in the current study) are not isolated from their surrounding environment and can therefore be more representative of biofilms growth *in vivo* (Thorn and Greenman, 2009). In these models nutrients can be continually supplied/ refreshed with additional nutrients, substrates and buffer of controlled composition and flow rate, so as to stabilize parameters such as microbial density (Thorn and Greenman, 2009). A novel continuous culture dynamic biofilm model for testing active surfaces was developed by Thorn *et al.* (2009) described as an *in vitro* flat-bed perfusion biofilm matrix model and used developed in order to test the efficacy of topical wound dressing. Mature steady-state target species biofilms was reproducibly grown within the model and used to assess the antimicrobial efficacy of topical treatments, producing kill kinetic profiles that differentiate bactericidal from bacteriostatic effects (Thorn and Greenman, 2009). Moreover it is known that the low growth rate of its constituent cells may be one of the

resistance mechanisms of biofilm (Lewis, 2001). In this biofilm model the growth rate can be controlled by changing the flow rate of nutrients into the system which changes the growth rate and therefore the number of cells in the eluted perfusate. Therefore the growth rate effect contributing to the resistance mechanisms may be studied using this model.

This model with slight modifications has also been used to test the efficacy of biologically active anti-odour compounds (Saad *et al.*, 2013; Greenman *et al.*, 2013). Therefore in this thesis the most appropriate model was considered to be the *in vitro* flat-bed perfusion systems and this was chosen to test APDT and ECAS activity against target bacterial biofilms.

Even though many studies have been carried out to test APDT and ECAS in eliminating biofilms these studies focus on the end point bacterial reduction in the biofilm after treatment. Some of the studies only provided a qualitative description of APDT effects on the structure of natural oral plaque biofilms using techniques such as confocal laser scanning microscopy (CLSM) (Wood *et al.*, 2006). So far no kill kinetics data is available on biofilms exposed to APDT or ECAS treatments. In all the studies the biofilm was destroyed after treatment to enable colony count of the survivors. Therefore in the current study the bioluminescent organism was incorporated into the *in vitro* flat-bed perfusion model to allow continuous monitoring of the biofilm after treatment exposure without disrupting the biofilm, enabling metabolic activity of the biofilm to be monitored in real time.

To model the closest conditions possible to that found in clinical conditions *in vivo* testing in animal models are performed. Bioluminescence imaging was used in these animal models to monitor the efficacy of APDT in real time (Hamblin *et al.*, 2002; Hamblin *et al.*, 2003). Due to the non-invasive nature of this technique, animals can be repeatedly imaged, considerably reducing the number of animals needed to carry out *in vivo* studies. This was a significant development towards reducing the number of live animals for scientific studies. However it is still preferable to find alternatives to the use of live animals in research. It was considered that the use *in vitro* flat-bed perfusion biofilm model will be very useful to test the efficacy of APDT without the need for testing in animal models to replace or more selectively use live animals.

## 7.2 Aims of the investigation

The first aim of this chapter was to monitor the change in metabolic activity of bioluminescent bacteria growing in biofilms after APDT and ECAS exposure. The second aim was to assess whether the growth rate of biofilm contributes to susceptibility of biofilm to the treatments.

## 7.3 Results

### Growth of bioluminescent *E. coli* Nissle 1917 pGLITE within the biofilm model

Figure 7.1 shows the growth and development of bioluminescent *E. coli* Nissle 1917 pGLITE within the flat-bed perfusion biofilm model over 48 hours for low growth rate (nutrient perfused at a flow rate of  $1 \text{ ml h}^{-1}$ ). During the growth of *E. coli* Nissle 1917 pGLITE the total matrix population (TMP) and eluate reduced during the first 8 hours, and after this both TMP and eluate measurements were more or less remained unchanged for up to 48 h, indicating that the biofilm growth reaches quasi steady state from 24 h and remains in steady state for 48 h.

The growth of bioluminescent *E. coli* Nissle 1917 pGLITE biofilm was monitored by both viable count methods (figure 7.1 a) and bioluminescence (figure 7.1 b). The viable count results largely correlated with that of bioluminescence. The bioluminescence also showed a decrease for the first 8 hours for the TMP, from 12 hours it showed an increase and reaches a steady state from 24 to 48 hours. The bioluminescence for the eluate showed increase at 8 hours and then a drop in bioluminescence at 12 hours. From 12 to 24 hours the eluate bioluminescence increased and started reaching a steady state. By 24 hours the eluate levels of bioluminescence was steady and remain at steady levels up to 48 hours.

Figure 7.2 shows the data from figure 7.1 of *E. coli* Nissle 1917 pGLITE biofilm (low growth rate biofilm: flow rate of  $1 \text{ ml h}^{-1}$ ) in steady state of growth from 24 hours to 48 hours. Both the viable count and bioluminescence method showed that by 24 hours the biofilm is in steady state and remained in steady state from 24 hours to 48 hours. This result shows both viable count and bioluminescence to give the same pattern of growth and shows correlation between bioluminescence and viable count.

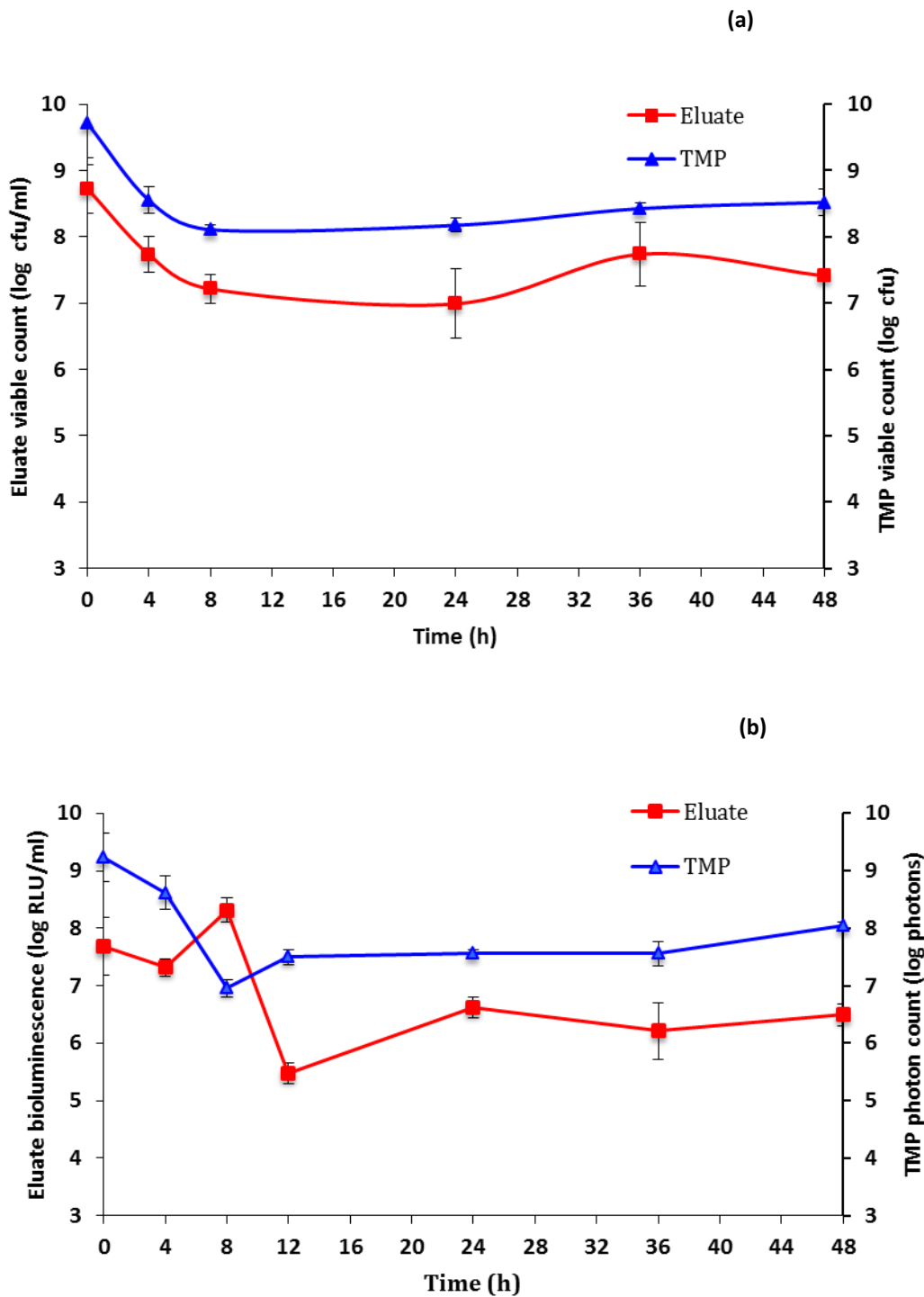


**Figure 7-1 Development of *E. coli* Nissle 1917 pGLITE biofilm from inoculation /colonization (t=0) to steady state growth (at nutrient flow rate of 1 ml/h) within an *in vitro* flat-bed perfusion biofilm model measured by (a) viable count of total matrix population (TMP) and eluate, and (b) bioluminescence of TMP and eluate, the biofilm sampled at every 4 hours up to 12 hours and then sampled at 24h, 36h and at 48h. Error bars show mean  $\pm$  SD (n=3).**

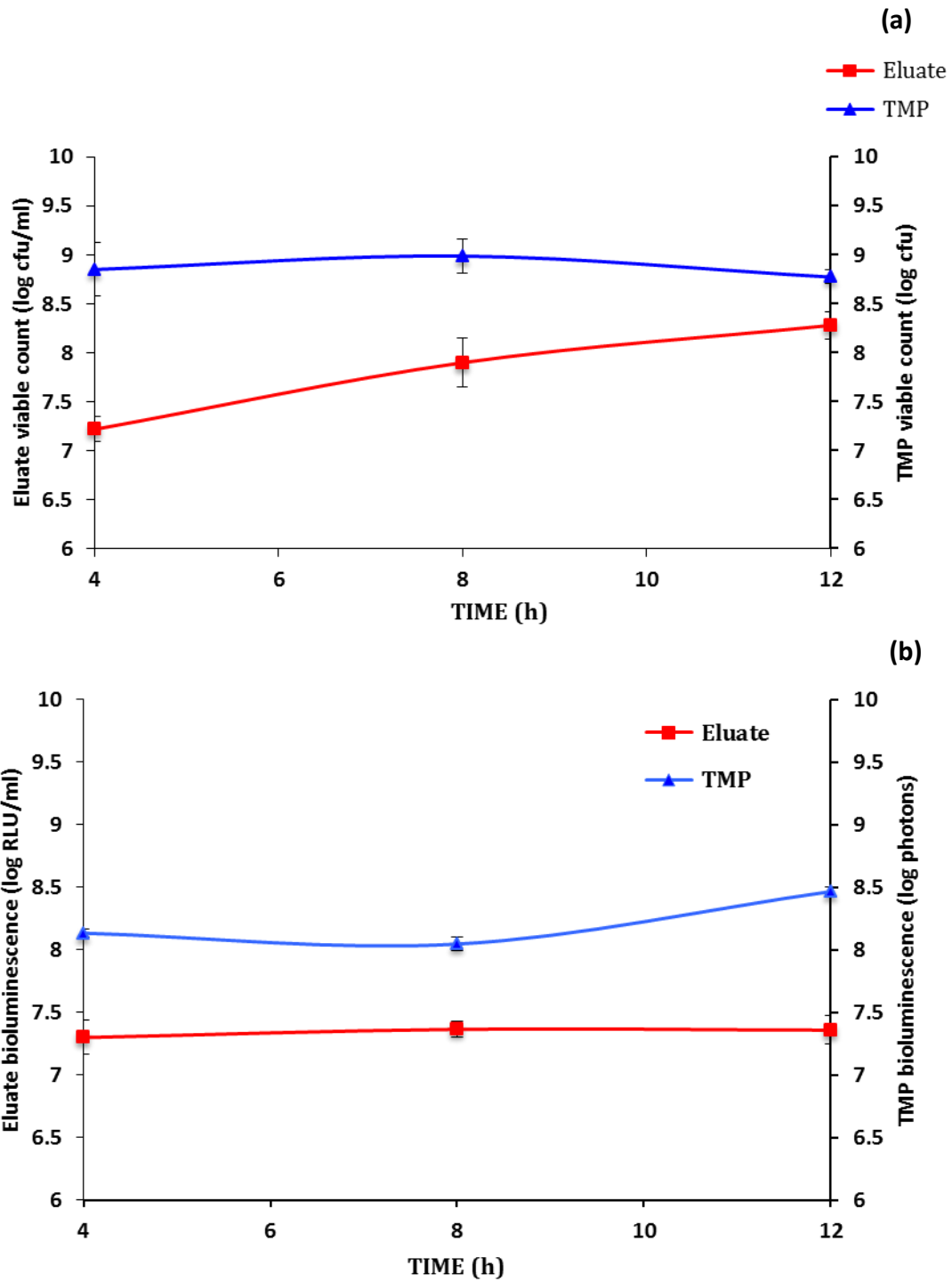


**Figure 7-2** Steady state of *E. coli* Nissle 1917 pGLITE biofilm monitored by (a) viable count (b) bioluminescence, of both total matrix population (TMP) and corresponding eluate (upper and lower values respectively shown for each graph). Error bars show means  $\pm$  SD (n=3).

Figure 7.3 shows measurement of photon output by the *E. coli* Nissle 1917/pGLITE biofilm cells growing at 3 different growth rates. The growth rate was controlled by the flow of nutrient into the system. The fastest growth rate (nutrient flow rate set up as 50ml/h) shows the fastest growth rate. It takes shorter time to reach the steady state of growth. The intermediate growth (nutrient flow rate set up as 15ml/h) rate shows that the growth rate is at an intermediate level in between low and faster rate. The low growth rate (nutrient flow rate set up as 1ml/h) shows that it takes the longest time to reach the steady state. This shows that bioluminescence allow differential growth rate to be monitored. From the graph it can be clearly seen that when the nutrient flow rate is set at three different rates the biofilm bacteria shows distinct bioluminescence output indicating different growth rates. The growth rate was calculated for each flow rate as shown in table 7.1 which shows that at the calculated growth rate was different for each flow rate. The fastest flow rate gave the highest growth rate per hour and with lowest flow rate lowest growth rate and intermediate flow rate gave growth rate in between the fastest and lowest flow rate.

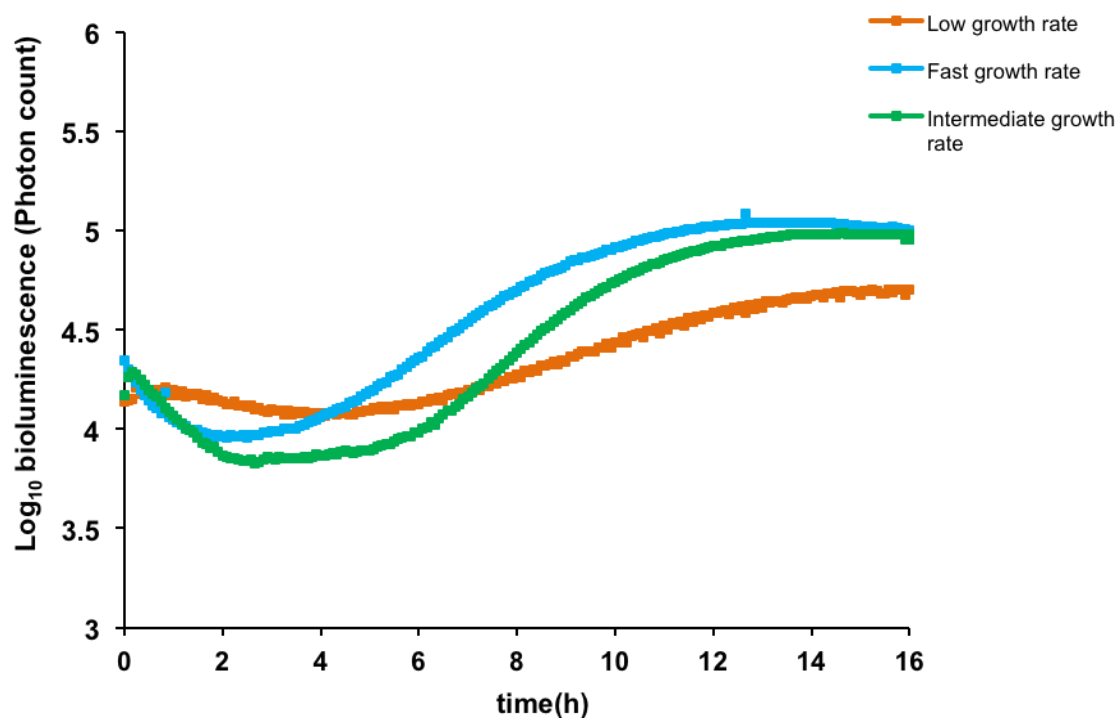
Growth rate calculation:

The growth rates were calculated using the formula given below for biofilm grown up to 24 hours at low, intermediate and fast flow rate by measuring the total biofilm population TMP (biofilm on: 1cm<sup>2</sup> cellulose membrane) and eluate viable counts

$$\text{Growth rate } (\mu) = \frac{\text{Rate of elution of cells (h}^{-1}\text{)}}{\text{Total biofilm population}}$$

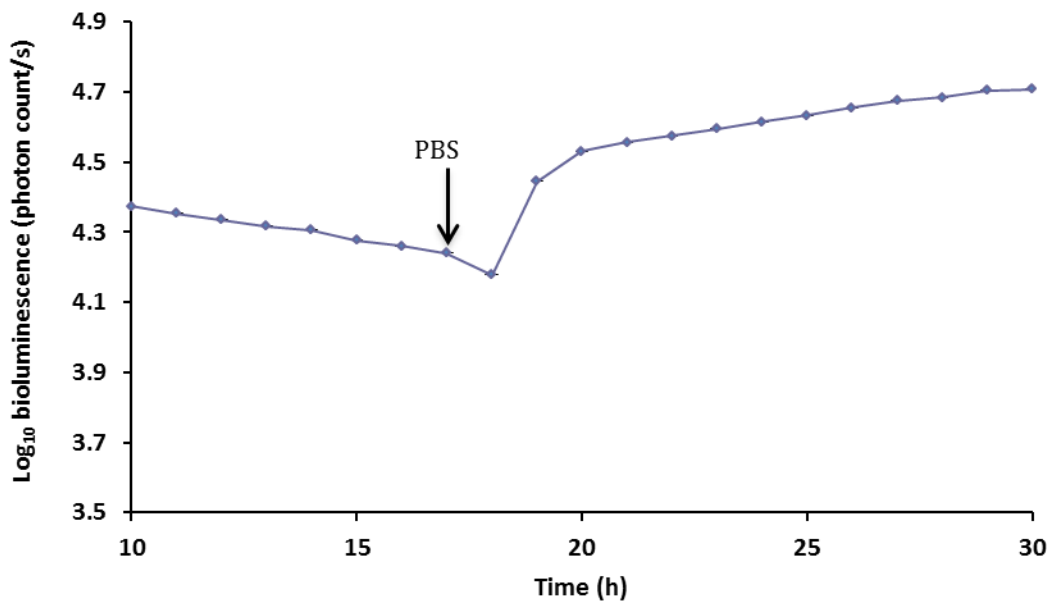
**Table 7.1** Calculated specific growth rate h<sup>-1</sup> at low, intermediate and fast rate of *E. coli* Nissle 1917 pGLITE biofilm

Flow rate	Growth rate (h <sup>-1</sup> )
Low (1 ml h <sup>-1</sup> )	0.34
Intermediate (15 ml h <sup>-1</sup> )	0.58
Fast (50 ml h <sup>-1</sup> )	0.98



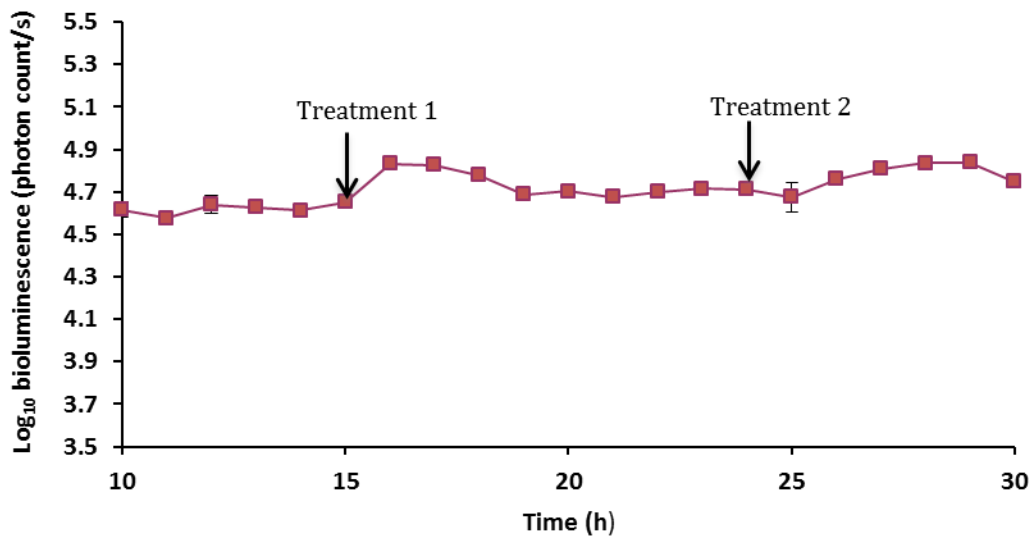
**Figure 7-3 Development of *E. coli* Nissle 1917 pGLITE biofilms (over first) 12 hours and the start of steady state phase, for fast (50ml/h), intermediate (15ml/h) and slow (1ml/h) flow rates, followed by bioluminescence output by the biofilm matrix (TMP photon count). (T=0 on the graph corresponds to inoculation of biofilm). Symbol represent mean  $\pm$  SD (n=3).**

Figure 7.4 shows a control biofilm of *E. coli* Nissle 1917/pGLITE where a mock treatment with phosphate buffer solution (PBS) was carried out. The graph shows (unlike treatment with APDT and ECAS) that there is no significant reduction in photon count following the PBS treatment. It also shows that immediately following the PBS injection there was a slight drop in photon count and then a quick recovery to the level before treatment and thereafter the bioluminescence remained constant level for 30 hours, showing that the bioluminescence remains stable for the duration of the experiment.

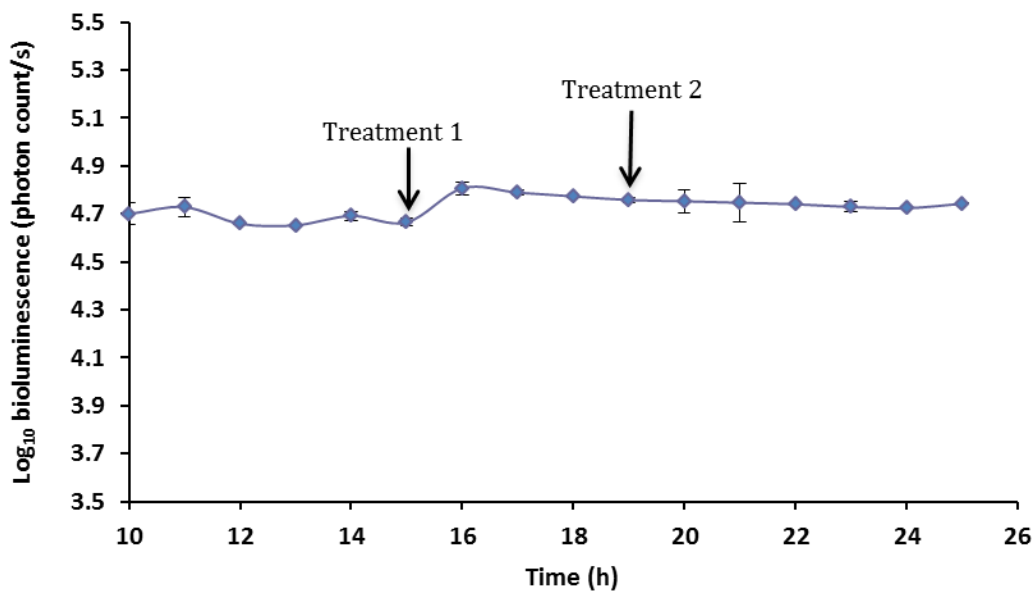


**Figure 7-4** Showing the application of PBS (1ml) as a control treatment (negative control) to the surface of the *E. coli* Nissle 1917 pGLITE biofilm (intermediate growth rate) and bioluminescence monitored for up to 30 hours. (T=10 on the graph corresponds to the start of experiment on steady state biofilm following maturity at 16 h). Error bars show mean  $\pm$  SD (n=3).

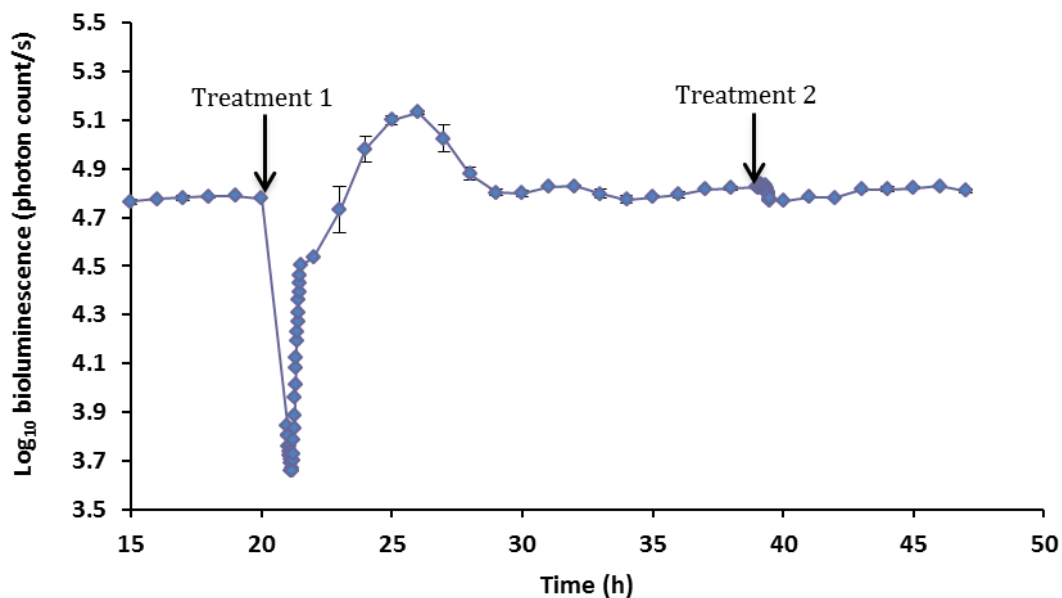
Figure 7.5, figure 7.6 and figure 7.7 shows *E. coli* Nissle 1917/pGLITE biofilm at low, intermediate and fast growth rate respectively treated with ECAS. Each biofilm was treated with two treatments of ECAS: treatment 1 biofilm treated with 300  $\mu$ L of 5% v/v of ECAS and treatment 2 treated with 300  $\mu$ L of undiluted ECAS (100% ECAS) (for both treatments 300  $\mu$ L of ECAS was transferred on to the biofilm matrix 1cm<sup>2</sup> cellulose membrane and nutrient supply stopped for 5 minutes). When ECAS treatment was applied on low growth rate biofilm (figure 7.5) and intermediate growth rate biofilm (figure 7.6) it shows only a slight increase in bioluminescence after each treatment and then light output remains steady. It was interesting to see an increase in light output after treatment instead of a drop in light output; these were in contrast to when the same treatment was carried out on a fast growth rate biofilm (figure 7.7). When the fast growth rate biofilm is exposed to ECAS there is nearly a one log drop in light output. However it shows a quick recovery and reaches slightly higher light output than the initial pretreatment level before light output returns to steady state.



**Figure 7-5** Change in photon count by bioluminescent *E. coli* Nissle (low growth rate biofilm) following ECAS treatment (300 $\mu$ L) (treatment 1-5% v/v ECAS), (treatment 2-100% ECAS). (T=10 on the graph corresponds to the start of experiment on steady state biofilm following maturity at 16 h). Symbol represent mean  $\pm$  SD (n=3).



**Figure 7-6** Change in photon count by bioluminescent *E. coli* Nissle (intermediate growth rate biofilm) following ECAS treatment (300 $\mu$ L) (treatment 1- 5% v/v ECAS), (treatment 2- 100% ECAS). (T=10 on the graph corresponds to the start of experiment on steady state biofilm following maturity at 16 h). Error bars show mean  $\pm$  SD (n=3).



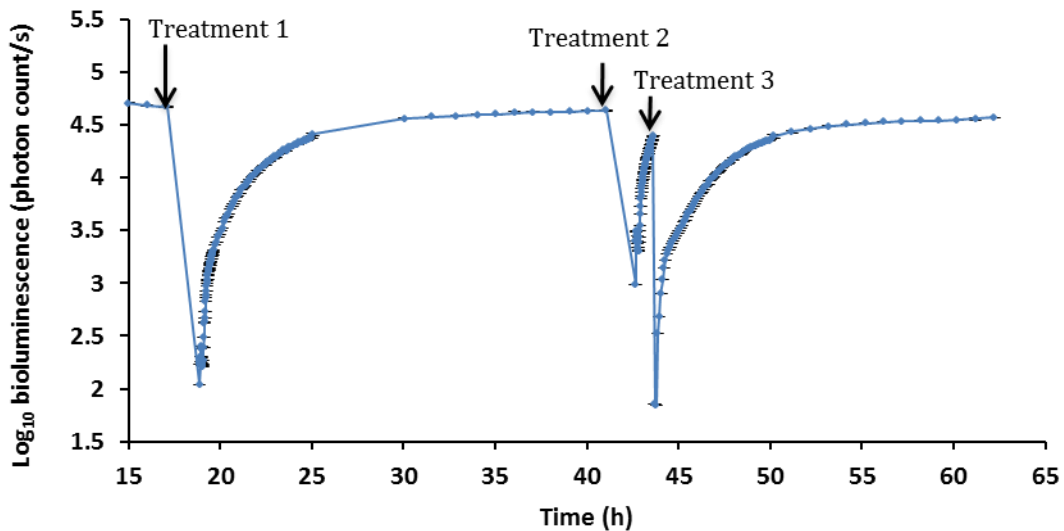
**Figure 7-7 Change in photon count by bioluminescent *E. coli* Nissle (fast growth rate biofilm) following ECAS treatment (300 $\mu$ L) (treatment 1-5% v/v ECAS), (treatment 2-100% ECAS). (T=10 on the graph corresponds to the start of experiment on steady state biofilm following maturity at 16 h). Error bars show mean  $\pm$  SD (n=3).**

Figure 7.8, 7.9 and 7.10 shows *E. coli* Nissle 1917/pGLITE biofilm at low, intermediate and fast growth rate respectively, treated with the APDT (treatment duration 30 minutes) 100  $\mu$ g/ml MB and total light dose of 25.2 J/cm<sup>2</sup> (light intensity 14.5mW/cm<sup>2</sup>). The treatment was repeated three times. The first treatment for low growth rate (figure 7.8) shows that after the first APDT treatment it shows nearly 2.5 log drop in light output. However, light output starts to increase immediately after treatment and reaches the pre-treatment levels in 8 hours. After the recovery period the second treatment was applied. This shows a 1 log drop in light output and there was quick recovery. The third treatment was applied after 1-hour recovery period following the second treatment.

Following the third treatment there was a drop in light output by 2-log and immediate recovery to steady state in 5 hours.

The treatment procedure was repeated for the intermediate (figure 7.9) and fast growth rate (figure 7.10). The graph shows the same general pattern in reduction in light output after treatments. However unlike the slow and intermediate growth rate biofilms, the faster growth rate biofilm recovers quickly (figure 7.10).

Figure 7.11 shows comparisons of growth rate effects on the light output after exposure to APDT treatments. It shows that the fastest growth rate biofilm is more resistant to treatment and shows quick recovery compared to low and intermediate. Low growth rate biofilm is the most sensitive to treatments since it takes longer for the biofilm to return to pretreatment light output levels.



**Figure 7-8 Change in photon count by bioluminescent *E. coli* Nissle biofilm (low growth rate) following APDT treatment with 100  $\mu\text{g/ml}$  MB (1 ml) and total light dose of  $25.2 \text{ J/cm}^2$  (light intensity  $14.5 \text{ mW/cm}^2$ ) APDT treatment was repeated 3 times shown by the arrow. Error bars show mean  $\pm$  SD (n=3).**

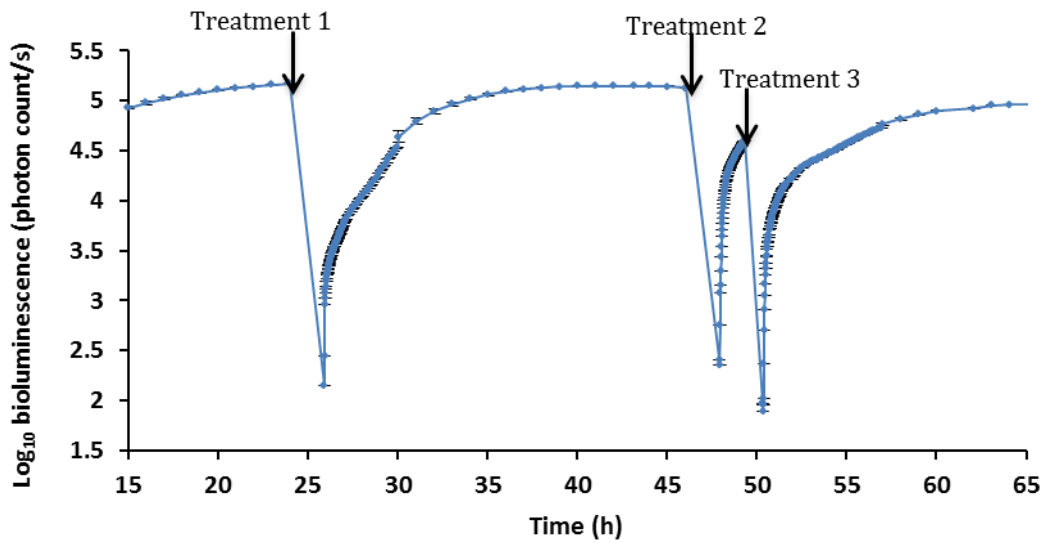


Figure 7-9 Change in photon count by bioluminescent *E. coli* Nissle biofilm (intermediate growth rate) following APDT treatment with 100  $\mu\text{g/ml}$  MB (1 ml) and total light dose dose of 25.2  $\text{J/cm}^2$  (light intensity 14.5 $\text{mW/cm}^2$ ) was repeated 3 times shown by the arrow. Error bars show mean  $\pm$  SD (n=3).

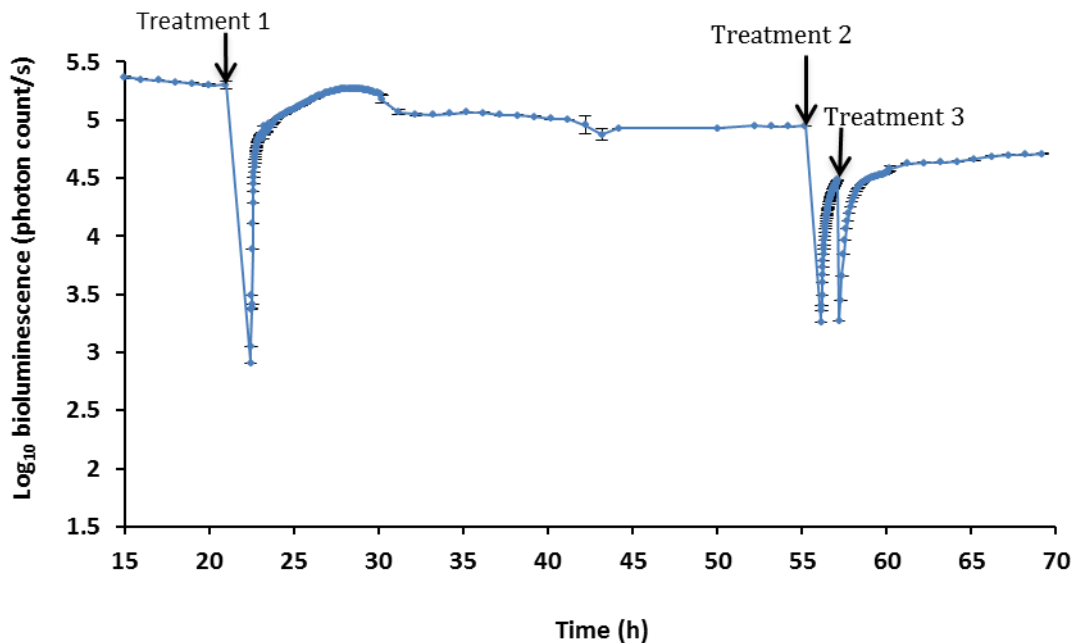
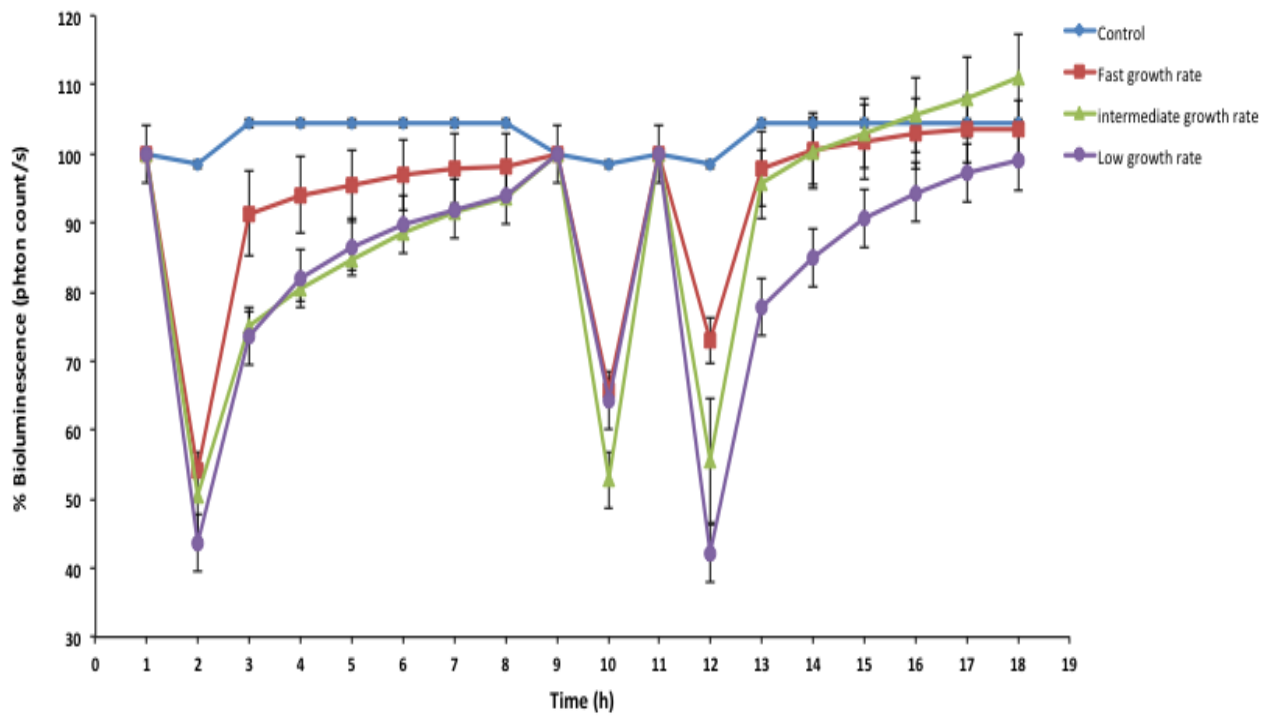


Figure 7-10 Change in photon count by bioluminescent *E. coli* Nissle biofilm (fast growth rate) following APDT treatment with 100  $\mu\text{g/ml}$  MB (1 ml) and total light dose dose of 25.2  $\text{J/cm}^2$  (light intensity 14.5 $\text{mW/cm}^2$ ). APDT treatment was repeated 3 times shown by the arrow. Error bars show mean  $\pm$  SD (n=3).



**Figure 7-11** Showing the bioluminescence of *E. coli* Nissle 1917 biofilm as a function of recovery time in hours following APDT MB treatment for each biofilm compared to control (treated with PBS). Error bars show means  $\pm$  SD (n=3).

#### 7.4 Discussion

In this study biofilms were grown within an *in vitro* flat-bed perfusion biofilm model to evaluate APDT and ECAS efficacy against biofilm. The flat-bed perfusion biofilm was inoculated with a bioluminescent *E. coli* Nissle 1917. The media perfused into the system at three different flow rates low ( $1 \text{ ml h}^{-1}$ ), intermediate ( $15 \text{ ml h}^{-1}$ ) and fast ( $50 \text{ ml h}^{-1}$ ). When media continuously perfuses the matrix to feed the cells, the cells divide and produce daughter cells that are eluted from the matrix. In the case of low growth rate biofilm both the viable counts and bioluminescence was measured. The total matrix population (TMP) and detached cells removed from the matrix in the fluid flow (eluate) was measured by viable methods and bioluminescence, and showed that the biofilm density initially decreases due to loosely bound cells detaching from the matrix and being removed through flow of fluid. After this period the cells colonised the matrix and the density steadily increases as the cells grow and replicate. Finally the biofilm reaches a quasi steady state around 16 hours as the maximum biofilm density is reached. The biofilm once in steady state will remain in steady state unless no change occurs in the biofilm growth environment. There was correlation between the viable count data and bioluminescence, confirming that bioluminescence can be used to follow the growth of biofilm and that bioluminescence gives similar information as viable counts. The steady state was maintained 24 to 48 hours.

When the growth of biofilm was continuously followed only by bioluminescence output from inoculation to steady state, it showed that for low growth rate there was an initial reduction in bioluminescence as was seen with viable counts. Similarly for the fast and intermediate growth rate there was initial decrease in light output by the biofilm. This decrease may be due to cells detaching from the matrix which results in reduction in the cell density. Once cells start to colonise by adapting to the new environment they multiply and metabolic activity increases and consequently, light output increases. The cells reach the maximum cell density and produce a maximum steady light output. It was shown that when the flow of media was low, cells take a longer time to reach steady state than intermediate and fast flow rates which take less time to reach steady state. This indicates that light production by the cell is dependent on the supply rate availability of nutrients. The flat-bed perfusion biofilm model

enabled the growth of steady state reproducible dynamic steady state biofilm growth. The growth of the biofilm was consistent with the studies carried out by Thorn and Greenman (2009), where the biofilm reached a mature steady state. However in the present study the biofilm reached steady state in a faster time (16 hours) of growth, this difference is due to different target organisms and growth conditions. It was found in general that the pattern of growth was similar and the biofilm reached a mature steady state of growth, confirming that the mature target species biofilm could be used to study the efficacy and kill kinetics of APDT and ECAS.

Biofilm grown in the *in vitro* flat-bed perfusion model was monitored continuously by bioluminescence and once a steady state of growth is achieved, the model was used to study the efficacy of ECAS and APDT. ECAS was applied to biofilms at three different growth rates. ECAS was applied twice on each biofilm. In the first treatment 300 $\mu$ l of 5% v/v ECAS applied on the matrix and in the second treatment on the same biofilm, 300 $\mu$ l of undiluted ECAS (100%) was applied to the biofilm matrix. Slow and intermediate growth rate biofilms showed a slight increase in bioluminescence immediately upon treatment after both the treatments. Increasing the concentration of ECAS showed no increase in reduction of bioluminescence for these biofilms. However, when the fast growth rate biofilm was treated with ECAS, after the first treatment (300 $\mu$ l of 5% v/v ECAS) there was a 1 log drop in bioluminescence but with the second treatment (undiluted ECAS (100%)) there was initial increases in bioluminescence and then a steady state light output which was slightly lower than the pretreatment steady state light output. These results indicate that the ECAS treatment employed is not a strongly effective against biofilm and its effects are dependent on the biofilm growth rate. The reduction in bioluminescence in the fast growth rate condition and the quick recovery means that ECAS has bacteriostatic rather than biocidal effects. Which means ECAS acts by reducing growth rate and inhibiting other cell functions (light output is closely dependent on the metabolic activity of the cells (Thorn *et al.*, 2007). Therefore removal of treatment immediately reversed the effects of ECAS and light output returns to normal. The slight increase upon treatment may be explained by ECAS killing cells on the top layer of the biofilm hence the nutrients per cell is increased thereby increases the growth rate of the biofilm (increasing light output) as

the biofilm get repopulated it returns to the original steady state of growth (John Greenman personal communication). The slightly low light output steady state after ECAS treatment means there was some effect on the metabolic activity of the biofilm cells. The high resistance of biofilm to ECAS may be explained by the ROS generated being competitively quenched by the organic material of the extracellular matrix. It has been reported in the literature that ECAS activity is significantly reduced for planktonic culture in the presence of organic material (Robinson *et al.*, 2011). Therefore the extracellular matrix of the biofilm may inhibit the interactions of ECAS with attached “mother layers” of biofilm cells. This means that the biofilm may need to be perfused with a larger volume of ECAS to compensate for the inhibitory action of the extracellular matrix. In this study only 300µl of ECAS was applied to the biofilm with 5 minutes of application time (nutrient supply to the biofilm was stopped). Therefore ECAS concentration and volume need to be optimised. To confirm that extracellular polymer material rather than specific genes (a biofilm phenotype) contribute resistance to ECAS, bacterial cells dispersed from the biofilm and resuspended in suspension can be compared to an intact biofilm and non biofilm derived planktonic cells in suspension. If there is a difference in resistance then it may confirm that the extracellular polymer matrix or a change phenotype that may contribute to resistance of biofilm cells. In a study carried out to evaluate the interaction of tobramycin with *P. aeruginosa* mucoid exopolysaccharide, it was shown that the dispersed biofilm cells were 15-times more susceptible to tobramycin than those in the intact biofilms (Hoyle and Costerton, 1991).

When the biofilm was treated with APDT it showed that APDT was more effective compared to ECAS. After APDT the bioluminescence output was reduced by nearly 2 log and it takes up to 8 hours for the cells to recover to steady state and again multiple treatments showed the same effect. The second treatment was carried out before the biofilm could recover to steady state. However, this did not show a significant increase in reduction in bioluminescence and there was quick recovery. Similarly the third APDT treatment showed reduction but showed quicker recovery than the first treatment (5 hours). The longer recovery time indicates that unlike ECAS treatment, APDT is biocidal. The biofilm population was reduced and takes longer time to recover to steady state levels. This indicates that even though APDT is able to reduce the biofilm

population to some extent, the remaining cells are able to regrow when supplied with fresh continuous media. Also it was found that APDT activity is dependent on the growth rate; with fast rate being the least sensitive and slow growth rate the most sensitive.

There are several explanations for the lowered APDT activity towards bacterial biofilm cells. First, reduced susceptibility of APDT to biofilms compared to planktonic cultures may be due to the reduced ability of MB to penetrate the full depth of the biofilm preventing damage to the bacterial cell targets. It has been suggested that the EPS traps the PS on the outside of the cell due to ionic or hydrophobic interactions (de Melo *et al.*, 2013). Second, it has been shown that MB are substrates of multidrug resistance pumps in bacteria (Tegos and Hamblin, 2006). Third, it has been shown that MB mediated APDT effects on biofilm (dental plaque bacteria) were affected by the presence of serum proteins present in brain–heart infusion broth (Fontana *et al.*, 2009).

Many studies have shown incomplete destruction of bacteria in biofilm after APDT (Fontana *et al.*, 2009; O'Neill *et al.*, 2002) in agreement with the findings of the current study. APDT carried out on saliva-derived biofilms observed using confocal scanning laser microscopy revealed that photodestruction occurred predominantly in the outer layers of the biofilm (O'Neill *et al.*, 2002). Therefore the reduced susceptibility of biofilms to APDT may be attributed to reduced penetration and retention of MB in the outer layer (Fontana *et al.*, 2009; O'Neill *et al.*, 2002). However, it has been shown that APDT mediated by cationic PS could overcome the protective effect of extracellular slime (Gad *et al.*, 2004). Various studies have shown APDT to be particularly effective against Gram-positive biofilm bacteria using different PS (de Melo *et al.*, 2013). It was also shown that APDT with MB reduced *S. mutans* and *S. aureus* biofilms by 2.81 log<sub>10</sub> and 3.29 log<sub>10</sub> respectively (Pereira *et al.*, 2011). Although MB was used to inactivate the biofilm, the target biofilm organisms, concentration of MB, light dose and biofilm model were different, making it difficult to compare to the present study.

Similarly, G-negative biofilm bacteria have also been shown to be sensitive to APDT (de Melo *et al.*, 2013). *P. aeruginosa* biofilms were exposed to APDT using 20 mM  $\delta$ -

ALA and 120 J/cm<sup>2</sup> light dose which eradicated the biofilm, although after 24 hours biofilms appeared to re-form thereafter and reached 7.2 log<sub>10</sub> CFU/ cm<sup>2</sup> after 48 hours of re-growth (Lee *et al.*, 2004). In addition to killing of cells a desirable feature of both APDT (Wainwright *et al.*, 2002) and ECAS (Thantsha and Cloete, 2006) are the ability of these agents to disrupt EPS via inducing oxidative damage of glucose and proteins, disrupting the biofilm stability.

APDT has been used in the treatment of several localized infections in animal models (Dai *et al.*, 2009; Demidova *et al.*, 2005; Hamblin *et al.*, 2002; Lambrechets *et al.*, 2005). Mice models with chronic biofilm infections caused by MRSA lux-bioluminescent strain were treated with APDT (Dai *et al.*, 2010). The bioluminescence signal disappeared when PS polyethylenimine chlorine (e6) (PEI-ce6) was topically applied to the infection followed by illumination with red light (up to 240 Jcm<sup>-2</sup>). However bioluminescence was observed after 24 h when bacteria regrow. There was accelerated wound healing (8.6 days) in comparison to the untreated infected wounds. It can be concluded that APDT has the potential to be an alternative treatment for localized infection. However the treatment needs to be optimized to reduce recurrence or regrowth of bacteria.

It has been reported that the slow growing bacteria survive adverse conditions compared to fast replicating cells (Gilbert *et al.*, 1990 ). Therefore a characteristic response by populations of replicating cells when in adverse environmental change is to reduce growth rate (Gilbert *et al.*, 1990). Therefore another mechanism of the protection of bacterial biofilms from antimicrobial agents might be related to the existence of bacteria in a slow growing or starved state (Gilbert and Brown, 1995). In this study it was found that the susceptibility of biofilm is influenced by growth rate. Interestingly it was found that fast growth rate was more susceptible to APDT compared to low growth rate. In contrast ECAS showed the opposite effect.

This study showed that growth rate is an important factor contributing to a cells susceptibility to treatments. To the author's knowledge it is the first time growth rate of biofilm and susceptibility to APDT and ECAS has been studied. To better understand the

growth rate effects of biofilm, further research need to be carried out where growth rate matched planktonic culture cells needs to be compared to growth rate matched biofilms.

The biofilm model system incorporated with a target bioluminescent organism *E. coli* Nissle 1917 pGLITE allowed for non invasive *in situ* monitoring of biofilm growth and enabled continuous monitoring of the effects of APDT and ECAS without disrupting the biofilm. These data shows that APDT and ECAS has the potential to rapidly reduce bacterial load in the biofilm. However, the treatments need to be optimised to prevent recurrence or regrowth of bacteria. The model could be slightly modified to incorporate serum to make it closer to the *in vivo* conditions. This system could then be used to assess the efficacy of new photosensitizers before testing them in animal models to give clinically relevant data or the model may be used as a replacement for animal model testing.

In conclusion this study has shown that bioluminescence could be utilized as a tool in the study of APDT and ECAS and is a robust system to use in the study of biofilms to better understand the activity of these treatments in real time. This study has opened up several interesting avenues of research which could be carried out to understand efficacy of these treatments against biofilms which may lead to applications of APDT and ECAS in clinical settings.

## **Chapter 8: General Discussion**

## 8.1 Discussion

This study was carried out in order to compare the effects of ROS killing by APDT and ECAS and predict the likelihood that the chosen treatments will be effective at killing microbes without significant harm to mammalian cells. The overall aims of this thesis was to develop appropriate reproducible rapid assays for studying APDT and ECAS (ROS generating systems) for microbial cell killing (chapter 3), to carry out comparative mechanistic study of the two systems (chapter 4), to assess potential of these agents to cause cytotoxicity to mammalian cells (chapter 5) and to measure DNA damage after exposure of mammalian cells (lymphocytes) to a specified dose of treatment (chapter 6) and to study the effects of treatments when applied to bacteria in the form of biofilms using an *in vitro* flat-bed perfusion model incorporated with bioluminescent target organism (chapter 7).

A rapid assay method was developed based on bioluminescent target organisms, allowing a comparison of the kill kinetics of APDT and ECAS (chapter 3). The assay was simple, rapid and sufficiently accurate to allow comparison of kill rates. It was found that viable count correlated closely with bioluminescence ( $r^2 > 0.9$ ) allowing replacement of the non-rapid viable count method with bioluminescence. Bioluminescence gave reproducible kill kinetic time plots for given conditions and it was found that compared to control, both APDT and ECAS at defined doses were effective in killing target organisms ( $>3 \log_{10}$  reductions) in a reasonable time frame (5 to 30 minutes). For both APDT and ECAS, there was dose dependent reduction in bioluminescence of the target organisms *E. coli* Nissle 1917-pGLITE and *P. aeruginosa* MCS5-lite.

Viable count methods were used to evaluate the efficacy of Gram-positive species since bioluminescent Gram-positive organisms giving sufficient light output were not available. For *S. aureus*, it was found that MRSA was more resistant compared to the methicillin sensitive strain. MRSA is considered a major threat to public health due to growing antibiotic resistance (Spellberg *et al.*, 2008). Using APDT, MRSA was reduced  $>3 \log_{10}$  in 30 minutes confirming previous studies (Demidova *et al.*, 2005) showing that both antibiotic resistant and non-resistant organisms could be targeted. The order of killing susceptibility (including non-lux targets) was *S. aureus*  $\gg$  *E. coli* Nissle 1917

pGLITE > *P. aeruginosa* MCS5-lite > MRSA. For ECAS (5% v/v), the antimicrobial activity against the *E. coli* Nissle 1917 pGLITE was several fold faster compared to APDT. At higher concentrations (10%, 25% and 50% v/v ECAS) the kill rate of target organism was very fast, reaching the limits of detection within 5 seconds. Compared to viable methods, the bioluminescence assay enabled accurate calculation of the kill rates of *E. coli* Nissle 1917 pGLITE, capturing initial kill rates even after exposure to fast acting agent.

With regard to the study of killing mechanisms, the standardised bioluminescence assay was used with incorporation of singlet oxygen enhancer (D<sub>2</sub>O), and addition of general or specific scavengers of ROS (tryptophan, azide, DMTU, mannitol). Previous work reported in the literature suggested that APDT could involve both type-I (mainly hydroxyl radical) and type-II (mainly singlet oxygen) killing mechanisms. The analysis of results obtained by comparing kill rates in the presence or absence of D<sub>2</sub>O and scavengers showed that APDT generated singlet oxygen (type-II reaction) since killing was enhanced with D<sub>2</sub>O and strongly inhibited by tryptophan, but not strongly inhibited by the specific hydroxyl scavengers, mannitol and DMTU suggesting that hydroxyl radical interactions (type-I reactions) were minimum. In contrast, for ECAS, mixed ROS mechanisms were clearly involved since azide and tryptophan inhibited killing, but D<sub>2</sub>O had little effect suggesting little contribution if any from singlet oxygen.

The use of fluorescent probes for ROS detection showed it to be a simple method in practice to determine ROS generation by APDT and ECAS. Overall the results using the fluorescence probes (SOSG, APF and HPF) in combination with specific scavengers, confirmed that the main ROS species produced in APDT are singlet oxygen (type II pathway) with a smaller contribution by hydroxyl radical (type I pathway). In contrast, ECAS inactivated SOSG and HPF but gave a clear fluorescence response with APF (inhibited by mannitol and DMSO), suggesting hydroxyl radical involvement with little or no singlet oxygen production with only slight increase with D<sub>2</sub>O and little inhibitory effect with azide. The main limitations of using fluorescent probes are their lack of selectivity towards one particular ROS (Kiesslich *et al.*, 2013) but this problem was ameliorated by the addition of specific scavengers at specified concentrations and

use of these probes was thus able to determine the portion of fluorescence ascribed to the ROS under study.

The regulatory authorities in Europe and the USA recommend that cytotoxicity, genotoxicity and carcinogenicity should be performed as a part of the application for marketing approval of pharmaceuticals. Both APDT and ECAS are effective at killing micro-organisms, thus they are both strong candidates for being used for treatment applications *in vivo*. In this case it is important to prove that they do not cause any side effects (cytotoxicity or genotoxicity) on host cells. For cytotoxicity, the concept of a protective index can be invoked. The protective index is a comparison of the amount of an agent or treatment that causes the therapeutic (antimicrobial) effect, to the amount that causes toxicity. Quantitatively, it is the ratio given by dividing the toxic dose by the therapeutic dose. A higher index is preferred since the therapeutic effect can be reached without eliciting damage to the host. Translated to *in vitro* testing, this would mean finding a dose that kills microbes effectively without damaging mammalian cells in culture. The data obtained in this thesis (chapters 5 and 6) suggests that for both APDT and ECAS, a level of treatment could be found whereby the kill rates of all the microbial test species were very much greater than those measured for mammalian cells, suggesting that a wide margin exists between an effective therapeutic dose and one that is likely to have cytotoxic or genotoxic effects on mammalian cells, suggesting that if applied in a clinical setting the treatments would have little damaging effects on the host.

It has been reported (George and Kishen, 2007) that *in vitro*, *Enterococcus faecalis* was killed at a much faster rate than normal fibroblasts after APDT treatment. In this study the rate of loss of fibroblast (measured as loss of mitochondrial activity in fibroblast cells) occurred at a mean rate constant of  $0.08 \text{ min}^{-1}$  which was significantly less compared to the kill rate of the *Enterococcus* (mean rate constant  $1.01 \text{ min}^{-1}$ ). Likewise, in this thesis, when *E. coli* Nissle 1917 pGLITE and keratinocytes were exposed to APDT simultaneously, the microbial kill rate was  $0.15 \text{ log RLU min}^{-1}$  and for keratinocytes was  $0.012 \text{ log cells min}^{-1}$  showing that the bacterial cells were much more susceptible to APDT compared to mammalian cells.

In addition to cytotoxicity it is important to ensure that these putative treatments do not cause any genotoxic effects to mammalian cells. Previous studies have shown that APDT is not genotoxic to keratinocytes (Zeina *et al.*, 2003). However, very few studies if any have reported on genotoxicity of these agents against lymphocytes in conditions relevant to APDT. Since both APDT and ECAS can be targeted to localised wound infections, and lymphocytes play an important role in wound healing (Schaffer and Barbul, 1998), it is important to determine that treatment is safe against these cells. For ECAS, the comet assay revealed only a very low level of genotoxicity towards lymphocytes whereas APDT showed a higher degree of DNA damage. However this was not as high as the positive control (100  $\mu$ M hydrogen peroxide). To test if the cells can repair the DNA damage after APDT, cells were incubated for 6 and 24 hours “recovery” time. However there was no reduction in tail moment as a measure of DNA damage; indeed, it appeared that DNA damage (increase in mean tail moment) was significantly increased ( $p < 0.05$ ) following the incubation period after treatment. These results indicate that some caution may need to be exercised when developing APDT protocols for deep seated wound infections where it is likely that lymphocytes are present and thus exposed to the treatment. In contrast, ECAS appears to be more favourable in terms of having lower potential damaging side effects towards mammalian cells.

In many cases of microbial infection and disease, the target micro-organisms are growing in a biofilm state and biofilms are reported to be many times more resistant to biocidal treatment than their planktonic counterparts (Costerton *et al.*, 1999). In this thesis (chapter 7), both ECAS and APDT were markedly less efficient at killing target cells when growing in biofilm mode even after multiple treatments, any of which would have caused a 3-log drop of bioluminescence in planktonic cells. For biofilms, the treatments only produced short term bacteriocidal or bacteriostatic effects characterised by a reduction of light output but only for a few hours before a slow or fast recovery back to normal (baseline) levels, depending on the flow rate/growth rate of the system. Slow flow rate/growth rate was associated with slow recovery whilst fast flow rate/growth rate gave a much quicker recovery when exposed to APDT.

In this thesis it was found that an *in vitro* flat-bed perfusion biofilm model integrated with a bioluminescent strain (target biofilm) was a suitable system to measure APDT and ECAS against biofilm cells. This model enabled continuous monitoring of bioluminescence output without the need to disrupt the biofilm for analysis. Therefore this model may be particularly suitable to study newly developed PS against biofilms. This model may more closely represent *in vivo* conditions and thus help to reduce the use of animal models in research.

## 8.2 Conclusions and further study

In conclusion this study showed that bioluminescence enabled accurate determinations of kill rates of target organisms after exposure to APDT and ECAS. The rapid assays enabled characterisation of the mechanisms of APDT and ECAS in terms of singlet oxygen and free radical mechanisms by using specific scavengers. This convenient simple assay approach together with specific ROS fluorescent probes was adequate in understanding the underlying mechanism of these agents and moreover was in agreement with the previously known mechanism of APDT. However for ECAS it was found that the mechanism was mainly hydroxyl radical rather than singlet oxygen. The ECAS mechanism appears to be more complex than previously thought. It was found that both agents were less damaging to mammalian cells (keratinocytes and lymphocytes) compared to bacterial cells. One possible reason for this observation could be the markedly different surface area to volume ratios possessed by eukaryotic and prokaryotic cells. Both APDT and ECAS are thought to damage membranes, and bacterial cells have much larger ratios of outer membrane to volume than do the much larger mammalian cells. A systematic study of species with increasing cell size (e.g. from small to large bacteria, small to large yeasts, and small to large mammalian cells) may support or rule out this hypothesis.

With regard to genotoxicity of treatments, then APDT produce higher levels of DNA damage compared to ECAS on lymphocytes. Therefore ECAS may be safer to use in a clinical setting. However, both these treatments were found to be less effective against biofilms compared to planktonic cultures. Since biofilms pose a significant challenge in treating persistent infections with conventional antibiotics, further studies are required to improve the efficacy of any new treatments against biofilms. There may be a number of reasons for the high resistance of biofilms to treatments including; lack of agent penetration into the biofilm, changes in the cell phenotype when growing in biofilm mode (e.g. up-regulation of drug efflux systems), or most likely, high production rates of agent neutralising material (slime, capsular material, proteins and other polymers). With regard to living biofilms, it should be noted that higher growth rates of the attached cells will produce higher numbers of exfoliating daughter cells which will also

react, neutralise or protect the attached living mother layers within the inner parts of the biofilm from agents. More research will be required in order to study these mechanisms of biofilm resistance.

Another important area that may require further investigation stems from the finding that APDT (in contrast with ECAS) could be genotoxic to lymphocytes. One way of minimising the damage is to have PS immobilised or using APDT conjugated to specific antibodies. In this form, production of ROS is external to the cell, where it is much less likely to interact with intracellular DNA and genotoxic damage would be avoided.

Indications for APDT and ECAS include the treatment of local, superficial skin and soft tissue infections or its use for the reduction of nosocomial colonization of the skin by multi-resistant bacteria. Topical treatments by conventional antimicrobial agents (e.g. antibiotics) can give rise to severe side effects such as allergic contact sensitization, development of resistance in the resident flora, or overgrowth of yeasts or superinfection by species resistant to the antibiotic (Fu *et al.*, 2013). Therefore alternatives such as APDT and ECAS are required. One advantage of topically applied PS with subsequent irradiation is the locally limited action of the photodynamic effect. In contrast, ECAS reacts with organic material including target microbes, but is soon neutralised. Therefore the mode of application of ECAS is different from that of APDT. For ECAS, an infected wound would be bathed, rinsed or irrigated using copious amounts of ECAS, which can be produced in large volumes. Only further research can show the advantages of this approach.

## References

- Abe, H., Ikebuchi, K., Wagner, S.J., Kuwabara, M., Kamo, N. and Sekiguchi, S. (1997) Potential Involvement of Both Type I and Type II Mechanisms in M13 Virus Inactivation by Methylene Blue Photosensitization *Photochemistry and Photobiology*. 66 (2), pp. 204-208.
- Ackroyd, R., Kelty, C., Brown, N. and Reed, M. (2001) The history of photodetection and photodynamic therapy *Photochemistry and Photobiology*. 74 (5), pp. 656-669.
- Agnez-Lima, L.F., Melo, J.T.A., Silva, A.E., Oliveira, A.H.S., Timoteo, A.R.S., Lima-Bessa, K.M., Martinez, G.R., Medeiros, M.H.G., Di Mascio, P., Galhardo, R.S. and Menck, C.F.M. (2012) DNA damage by singlet oxygen and cellular protective mechanisms. *Mutation Research/Reviews in Mutation Research*. 751 (1), pp. 15-28.
- Alanis, A.J. (2005) Resistance to antibiotics: are we in the post-antibiotic era? *Archives of Medical Research*. 36 (6), pp. 697-705.
- Al-Haq, M.I., Seo, Y., Oshita, S. and Kawagoe, Y. (2002) Disinfection effects of electrolyzed oxidizing water on suppressing fruit rot of pear caused by *Botryosphaeria berengeriana*. *Food Research International*. 35 (7), pp.657-664.
- Alloush, H.M., Salisbury, V., Lewis, R.J. and MacGowan, A.P. (2003) Pharmacodynamics of linezolid in a clinical isolate of *Streptococcus pneumoniae* genetically modified to express lux genes. *The Journal of Antimicrobial Chemotherapy*. 52 (3), pp. 511-513.
- Alves, E., Carvalho, C.M., Tome, J.P., Faustino, M.A., Neves, M.G., Tome, A.C., Cavaleiro, J.A., Cunha, A., Mendo, S. and Almeida, A. (2008) Photodynamic inactivation of recombinant bioluminescent *Escherichia coli* by cationic porphyrins under artificial and solar irradiation. *Journal of Industrial Microbiology & Biotechnology*. 35 (11), pp. 1447-1454.
- Alves, E., Costa, L., Carvalho, C.M., Tome, J.P., Faustino, M.A., Neves, M.G., Tome, A.C., Cavaleiro, J.A., Cunha, A. and Almeida, A. (2009) Charge effect on the photoinactivation of Gram-negative and Gram-positive bacteria by cationic meso-substituted porphyrins. *BMC Microbiology*. 9 pp.70-2180-9-70.
- Alves, E., Costa, L., Cunha, A., Faustino, M.A., Neves, M.G. and Almeida, A. (2011) Bioluminescence and its application in the monitoring of antimicrobial photodynamic therapy. *Applied Microbiology and Biotechnology*. 92 (6), pp. 1115-1128.
- Ammons, M.C. (2010) Anti-biofilm strategies and the need for innovations in wound care. *Recent Patents on Anti-Infective Drug Discovery*. 5 (1), pp. 10-17.
- Anderson, D., Yu, T.W. and McGregor, D.B. (1998) Comet assay responses as indicators of carcinogen exposure *Mutagenesis*. 13 (6), pp. 539-555.

- Bakand, S., Winder, C., Khalil, C. and Hayes, A. (2006) A novel in vitro exposure technique for toxicity testing of selected volatile organic compounds. *Journal of Environmental Monitoring*. 8 (1), pp. 100-105.
- Bakhr, V.M., Grishin, V.P., Panicheva, S.A. and Toloknov, V.I. (1999) Assessment of the effectiveness of medical instruments sterilization by electrochemically activated solutions and computer modeling of the dynamics of hospital infections. *Meditinskaja Tekhnika*. 2(2), pp.14-16.
- Banfi, S., Caruso, E., Buccafurni, L., Battini, V., Zazzaron, S., Barbieri, P. and Orlandi, V. (2006) Antibacterial activity of tetraaryl-porphyrin photosensitizers: An in vitro study on Gram negative and Gram positive bacteria. *Journal of Photochemistry and Photobiology B: Biology*. 85 (1), pp.28-38.
- Beard, S.J., Salisbury, V., Lewis, R.J., Sharpe, J.A. and MacGowan, A.P. (2002) Expression of lux Genes in a Clinical Isolate of *Streptococcus pneumoniae*: Using Bioluminescence To Monitor Gemifloxacin Activity. *Antimicrobial Agents and Chemotherapy*. 46 (2), pp. 538-542.
- Benhusein, G.M., Mutch, E., Aburawi, S. and Williams, F.M. (2010) Genotoxic effect induced by hydrogen peroxide in human hepatoma cells using comet assay. *The Libyan Journal of Medicine*. 5 pp.10.3402/ljm.v5i0.4637.
- Bertoloni, G., Rossi, F., Valduga, G., Jori, G. and van Lier, J. (1990) Photosensitizing activity of water- and lipid-soluble phthalocyanines on *Escherichia coli*. *FEMS Microbiology Letters*. 59 (1-2), pp. 149-155.
- Betti, C., Davini, T., Giannessi, L., Loprieno, N. and Barale, R. (1995) Comparative studies by comet test and SCE analysis in human lymphocytes from 200 healthy subjects. *Mutation Research*. 343 (4), pp. 201-207.
- Bhatti, M., MacRobert, A., Meghji, S., Henderson, B. and Wilson, M. (1998) A Study of the Uptake of Toluidine Blue O by *Porphyromonas gingivalis* and the Mechanism of Lethal Photosensitization. *Photochemistry and Photobiology*. 68 (3), pp. 370-376.
- Biel, M.A., Sievert, C., Usacheva, M., Teichert, M. and Balcom, J. (2011) Antimicrobial photodynamic therapy treatment of chronic recurrent sinusitis biofilms. *International Forum of Allergy & Rhinology*. 1 (5), pp. 329-334.
- Biel, M.A., Sievert, C., Usacheva, M., Teichert, M., Wedell, E., Loebel, N., Rose, A. and Zimmermann, R. (2011) Reduction of Endotracheal Tube Biofilms Using Antimicrobial Photodynamic Therapy. *Lasers in Surgery and Medicine*. 43 (7), pp. 586-590.
- Bjarnsholt, T., Kirketerp-Moller, K., Jensen, P.O., Madsen, K.G., Phipps, R., Krogh, K., Hoiby, N. and Givskov, M. (2008) Why chronic wounds will not heal: a novel hypothesis. *Wound Repair and Regeneration : Official Publication of the Wound Healing Society [and] the European Tissue Repair Society*. 16 (1), pp. 2-10.

- Boehncke, W.H., Elshorst-Schmidt, T. and Kaufmann, R. (2000) Systemic photodynamic therapy is a safe and effective treatment for psoriasis. *Archives of Dermatology*. 136 (2), pp. 271-272.
- Boehncke, W.H., Rück, A., Naumann, J., Sterry, W. and Kaufmann, R. (1996) Comparison of sensitivity towards photodynamic therapy of cutaneous resident and infiltrating cell types *in vitro*. *Lasers Surg Med*. 19 (4), pp. 451-457.
- Bonnett, R. (1995) Photosensitizers of the porphyrin and phthalocyanine series for photodynamic therapy. *Chemical Society Reviews*. 24 (1), pp.19.
- Borenfreund, E. and Puerner, J.A. (1985) Toxicity determined in vitro by morphological alterations and neutral red absorption. *Toxicology Letters*. 24 (2-3), pp.119-124.
- Bressler, N.M. and Bressler, S.B. (2000) Photodynamic therapy with verteporfin (Visudyne): impact on ophthalmology and visual sciences. *Investigative Ophthalmology & Visual Science*. 41 (3), pp. 624-628.
- Brown, S.B., Brown, E.A. and Walker, I. (2004) The present and future role of photodynamic therapy in cancer treatment. *The Lancet Oncology*. 5 (8), pp.497-508.
- Buchko, G.W., Wagner, J.R., Cadet, J., Raoul, S. and Weinfeld, M. (1995) Methylene blue-mediated photooxidation of 7,8-dihydro-8-oxo-2'-deoxyguanosine. *Biochimica Et Biophysica Acta* . 1263 (1), pp. 17-24.
- Calin, M.A. and Parasca, S.V. (2009) Light sources for photodynamic inactivation of bacteria. *Lasers in Medical Science*. 24 (3), pp. 453-460.
- Campbell, A. K. (1989) Living light: biochemistry, function and biomedical applications. *Essays Biochemistry*. 24, pp. 41-81.
- Castano, A.P., Demidova, T.N. and Hamblin, M.R. (2004) Mechanisms in photodynamic therapy: part one—photosensitizers, photochemistry and cellular localization. *Photodiagnosis and Photodynamic Therapy*. 1 (4), pp. 279-293.
- Chambers, H.F. and Deleo, F.R. (2009) Waves of resistance: *Staphylococcus aureus* in the antibiotic era *Nature Reviews.Microbiology*. 7 (9), pp. 629-641.
- Chatterjee, J. and Meighen, E.A. (1995) Biotechnological applications of bacterial bioluminescence (lux) genes. *Photochemistry and Photobiology*. 62 (4), pp. 641-650.
- Cloete, T.E., Thantsha, M.S., Maluleke, M.R. and Kirkpatrick, R. (2009) The antimicrobial mechanism of electrochemically activated water against *Pseudomonas aeruginosa* and *Escherichia coli* as determined by SDS-PAGE analysis. *Journal of Applied Microbiology*. 107 (2), pp. 379-384.
- Coates, A.R.M. and Hu, Y. (2007) Novel approaches to developing new antibiotics for bacterial infections. *British Journal of Pharmacology*. 152 (8), pp. 1147-1154.

Collins, A.R., Ma, A.G. and Duthie, S.J. (1995) The kinetics of repair of oxidative DNA damage (strand breaks and oxidised pyrimidines) in human cells. *Mutation Research*. 336 (1), pp. 69-77.

Collins, T.L., Markus, E.A., Hassett, D.J. and Robinson, J.B. (2010) The effect of a cationic porphyrin on *Pseudomonas aeruginosa* biofilms. *Current Microbiology*. 61 (5), pp. 411-416.

Contag, C.H., Contag, P.R., Mullins, J.I., Spilman, S.D., Stevenson, D.K. and Benaron, D.A. (1995) Photonic detection of bacterial pathogens in living hosts. *Molecular Microbiology*. 18 (4), pp. 593-603.

Costerton, J.W., Stewart, P.S. and Greenberg, E.P. (1999) Bacterial biofilms: a common cause of persistent infections. *Science*. 284 (5418), pp. 1318-1322.

Costerton, W., Veeh, R., Shirtliff, M., Pasmore, M., Post, C. and Ehrlich, G. (2003) The application of biofilm science to the study and control of chronic bacterial infections. *Journal of clinical investigation*. 112 (10), pp. 1466-1477.

Creagh, T.A., Gleeson, M., Travis, D., Grainger, R., McDermott, T.E. and Butler, M.R. (1995) Is there a role for *in vivo* methylene blue staining in the prediction of bladder tumour recurrence? *British Journal of Urology*. 75 (4), pp. 477-479.

Dai, T., Huang, Y. Y. and Hamblin, M. R. (2009) Photodynamic therapy for localized infections-State of the art. *Photodiagnosis and Photodynamic Therapy*. 6 (3-4), pp. 170-188.

Dai, T., Tegos, G.P., Zhiyentayev, T., Mylonakis, E. and Hamblin, M.R. (2010) Photodynamic therapy for methicillin-resistant *Staphylococcus aureus* infection in a mouse skin abrasion model. *Lasers in Surgery and Medicine*. 42 (1), pp. 38-44.

Daniell, M.D. And Hill, J.S. (1991) A history of photodynamic therapy. *The Australian and New Zealand Journal of Surgery*. 61(5), pp. 340-348.

Davies, D. (2003) Understanding biofilm resistance to antibacterial agents. *Nature Reviews Drug Discovery*. 2 (2), pp. 114-122.

de Kraker, M.E., Davey, P.G., Grundmann, H. and BURDEN study group (2011) Mortality and hospital stay associated with resistant *Staphylococcus aureus* and *Escherichia coli* bacteremia: estimating the burden of antibiotic resistance in Europe. *PLoS Medicine* [online]. 8 (10), pp.e1001104.

de Melo, W.C., Avci, P., de Oliveira, M.N., Gupta, A., Vecchio, D., Sadasivam, M., Chandran, R., Huang, Y.Y., Yin, R., Perussi, L.R., Tegos, G.P., Perussi, J.R., Dai, T. and Hamblin, M.R. (2013) Photodynamic inactivation of biofilm: taking a lightly colored approach to stubborn infection. *Expert review of anti-infective therapy*. 11(7), pp. 669-93.

Demidova, T.N. and Hamblin, M.R. (2004) Photodynamic therapy targeted to

pathogens. *International Journal of Immunopathology and Pharmacology*. 17 (3), pp. 245-254.

Demidova, T.N. and Hamblin, M.R. (2005) Photodynamic inactivation of *Bacillus* spores, mediated by phenothiazinium dyes. *Applied and Environmental Microbiology*. 71(11), pp. 6918-6925.

Demidova, T.N., Gad, F., Zahra, T., Francis, K.P. and Hamblin, M.R. (2005) Monitoring photodynamic therapy of localized infections by bioluminescence imaging of genetically engineered bacteria. *Journal of photochemistry and photobiology. B, Biology*. 81(1), pp. 15-25.

Di Poto, A., Sbarra, M.S., Provenza, G., Visai, L. and Speziale, P. (2009) The effect of photodynamic treatment combined with antibiotic action or host defence mechanisms on *Staphylococcus aureus* biofilms. *Biomaterials*. 30(18), pp. 3158-3166.

Dougherty, T.J. and Marcus, S.L. (1992) Photodynamic therapy. *European Journal of Cancer*. 28A (10), pp. 1734-1742.

Embleton, M.L., Nair, S.P., Cookson, B.D. and Wilson, M. (2002) Selective lethal photosensitization of methicillin-resistant *Staphylococcus aureus* using an IgG-tin (IV) chlorin e6 conjugate. *The Journal of Antimicrobial Chemotherapy*. 50 (6), pp. 857-864.

Embleton, M.L., Nair, S.P., Heywood, W., Menon, D.C., Cookson, B.D. and Wilson, M. (2005) Development of a Novel Targeting System for Lethal Photosensitization of Antibiotic-Resistant Strains of *Staphylococcus aureus*. *Antimicrobial Agents and Chemotherapy*. 49 (9), pp. 3690-3696.

Eming, S.A., Krieg, T. and Davidson, J.M. (2007) Inflammation in Wound Repair: Molecular and Cellular Mechanisms. *Journal of Investigative Dermatology*. 127 (3), pp.514-525.

Ergaieg, K., Chevanne, M., Cillard, J. and Seux, R. (2008) Involvement of both Type I and Type II mechanisms in Gram-positive and Gram-negative bacteria photosensitization by a meso-substituted cationic porphyrin. *Solar Energy*. 82 (12), pp. 1107-1117.

Evans, H.H., Horng, M.F., Ricanati, M., Deahl, J.T. and Oleinick, N.L. (1997) Mutagenicity of photodynamic therapy as compared to UVC and ionizing radiation in human and murine lymphoblast cell lines *Photochemistry and Photobiology*. 66 (5), pp.690-696.

Fairbairn, D.W., Olive, P.L. and O'Neill, K.L. (1995) The comet assay: a comprehensive review. *Mutation Research*. 339 (1), pp. 37-59.

Flors, C., Fryer, M.J., Waring, J., Reeder, B., Bechtold, U., Mullineaux, P.M., Nonell, S., Wilson, M.T. and Baker, N.R. (2006) Imaging the production of singlet oxygen in vivo using a new fluorescent sensor, Singlet Oxygen Sensor Green. *Journal of Experimental Botany*. 57 (8), pp. 1725-1734.

Fontana, C.R., Abernethy, A.D., Som, S., Ruggiero, K., Doucette, S., Marcantonio, R.C., Boussios, C.I., Kent, R., Goodson, J.M., Tanner, A.C and Soukos, N.S. (2009). The antibacterial effect of photodynamic therapy in dental plaque-derived biofilms. *Journal of Periodontal Research*. 44(6), pp. 751–759.

Foote, C.S. (1991) Definition of type I and type II photosensitized oxidation. *Photochemistry and Photobiology*. 54 (5), pp.659.

Foschi, F., Fontana, C.R., Ruggiero, K., Riahi, R., Vera, A., Doukas, A.G., Pagonis, T.C., Kent, R., Stashenko, P.P. and Soukos, N.S. (2007) Photodynamic inactivation of *Enterococcus faecalis* in dental root canals in vitro. *Lasers in Surgery and Medicine*. 39 (10), pp. 782-787.

Francis, K.P., Joh, D., Bellinger-Kawahara, C., Hawkinson, M.J., Purchio, T.F. and Contag, P.R. (2000) Monitoring bioluminescent *Staphylococcus aureus* infections in living mice using a novel luxABCDE construct. *Infection and Immunity*. 68 (6), pp. 3594-3600.

Fu, X.J., Fang, Y. and Yao, M. (2013) Antimicrobial photodynamic therapy for methicillin-resistant *Staphylococcus aureus* infection. *BioMed Research International*. 2013 pp. 159157.

Gad, F., Zahra, T., Francis, K.P., Hasan, T. and Hamblin, M.R. (2004) Targeted photodynamic therapy of established soft-tissue infections in mice. *Photochemical and photobiological sciences : Official journal of the European Photochemistry Association and the European Society for Photobiology*. 3(5), pp. 451-458.

Gad, F., Zahra, T., Hasan, T. and Hamblin, M.R. (2004) Effects of growth phase and extracellular slime on photodynamic inactivation of gram-positive pathogenic bacteria. *Antimicrobial Agents and Chemotherapy*. 48(6), pp. 2173-2178.

Ganz, R.A., Viveiros, J., Ahmad, A., Ahmadi, A., Khalil, A., Tolckoff, M.J., Nishioka, N.S. and Hamblin, M.R. (2005) *Helicobacter pylori* in patients can be killed by visible light. *Lasers in Surgery and Medicine*. 36 (4), pp. 260-265.

Garcez, A.S., Nunez, S.C., Lage-Marques, J.L., Hamblin, M.R. and Ribeiro, M.S. (2007) Photonic real-time monitoring of bacterial reduction in root canals by genetically engineered bacteria after chemomechanical endodontic therapy. *Brazilian Dental Journal*. 18 (3), pp. 202-207.

George, S. and Kishen, A. (2008) Influence of Photosensitizer Solvent on the Mechanisms of Photoactivated Killing of *Enterococcus faecalis*. *Photochemistry and Photobiology*. 84 (3), pp.734-740.

Gilbert, P. and Brown, M. R. W. (1995) *Mechanisms of the protection of bacterial biofilms from antimicrobial agents*. In: *Microbial biofilms*. Cambridge University Press, Cambridge.

Gilbert, P., Collier, P.J. and Brown, M.R. (1990) Influence of growth rate on susceptibility to antimicrobial agents: biofilms, cell cycle, dormancy, and stringent response. *Antimicrobial Agents and Chemotherapy*. 34 (10), pp. 1865-1868.

Gomes, A., Fernandes, E. and Lima, J.L. (2005) Fluorescence probes used for detection of reactive oxygen species. *Journal of Biochemical and Biophysical Methods*. 65 (2-3), pp. 45-80.

Gorman, A.A. and Rodgers, M.A., (1992) Current perspectives of singlet oxygen detection in biological environments. *Journal of Photochemistry and Photobiology. B, Biology*. 14(3), pp. 159-176.

Grahl, T. and Markl, H. (1996) Killing of micro-organisms by pulsed electric fields. *Applied Microbiology and Biotechnology*. 45(1-2), pp. 148-157.

Greenman., J. Saad., S Keith., H, Thorn, R.M. S. and Reynolds, D. M. (2013). Review: *In vitro* biofilm models for studying oral malodour. *Flavour and Fragrance Journal*. 28(4), pp. 212–222.

Gross, S., Brandis, A., Chen, L., Rosenbach-Belkin, V., Roehrs, S., Scherz, A. and Salomon, Y. (1997) Protein-A-mediated Targeting of Bacteriochlorophyll-IgG to *Staphylococcus aureus*: A Model for Enhanced Site-Specific Photocytotoxicity. *Photochemistry and Photobiology*. 66 (6), pp. 872-878.

Grune, T., Klotz, L.O., Gieche, J., Rudeck, M. and Sies, H. (2001) Protein oxidation and proteolysis by the nonradical oxidants singlet oxygen or peroxyxynitrite. *Free Radical Biology and Medicine*. 30 (11), pp. 1243-1253.

Gutierrez, A.A (2006) The science behind stable, super-oxidized water. *Wounds*. 18 (Suppl 1) pp. 7–10.

Hadjur, C., Wagnieres, G., Ihringer, F., Monnier, P. and van den Bergh, H. (1997) Production of the free radicals  $O_2^{\cdot-}$  and  $\cdot OH$  by irradiation of the photosensitizer zinc(II) phthalocyanine. *Journal of Photochemistry and Photobiology. B, Biology*. 38 (2-3), pp. 196-202.

Halliwell, B and Gutteridge J.M. (1990) Role of free radicals and catalytic metal ions in human disease: an overview. *Methods in Enzymology*. 186, pp. 1-197.

Halliwell, B. (2006) Reactive Species and Antioxidants. Redox Biology Is a Fundamental Theme of Aerobic Life. *Plant Physiology*. 141 (2), pp. 312-322.

Hall-Stoodley, L. and Stoodley, P. (2009) Evolving concepts in biofilm infections. *Cellular Microbiology*. 11 (7), pp. 1034-1043.

- Hamblin, M.R. and Hasan, T. (2004) Photodynamic therapy: a new antimicrobial approach to infectious disease? *Photochemical and Photobiological Sciences : Official Journal of the European Photochemistry Association and the European Society for Photobiology*. 3 (5), pp. 436-450.
- Hamblin, M.R. and Newman, L.E. (1994) New trends in photobiology. *Journal of Photochemistry and Photobiology B: Biology*. 23 (1), pp. 3-8.
- Hamblin, M.R., O'Donnell, D.A., Murthy, N., Contag, C.H. and Hasan, T. (2002) Rapid control of wound infections by targeted photodynamic therapy monitored by *in vivo* bioluminescence imaging. *Photochemistry and Photobiology*. 75(1), pp. 51-7.
- Hamblin, M.R., Viveiros, J., Yang, C., Ahmadi, A., Ganz R.A. and Tolkoff, M.J. (2005) *Helicobacter pylori* accumulates photoactive porphyrins and is killed by visible light. *Antimicrobial Agents and Chemotherapy*. 49(7), pp. 2822-2827.
- Hamblin, M.R., Zahra, T., Contag, C.H., Mcmanus, A.T. and Hasan, T. (2003) Optical monitoring and treatment of potentially lethal wound infections *in vivo*. *The Journal of Infectious Diseases*, 187(11), pp. 1717-1725.
- Hansch, A., Frey, O., Gajda, M., Susanna, G., Boettcher, J., Brauer, R. and Kaiser, W.A. (2008) Photodynamic treatment as a novel approach in the therapy of arthritic joints. *Lasers in Surgery and Medicine*. 40 (4), pp. 265-272.
- Hasting, J.W. (1996) Chemistries and colors of bioluminescent reactions : a review. *Gene*. 173, pp. 5-11.
- Hata, G., Uemura, M., Weine, F.S. and Toda, T. (1996) Removal of smear layer in the root canal using oxidative potential water. *Journal of Endodontics*. 22 (12), pp. 643-645.
- Henderson, B.W. and Miller, A.C. (1986) Effects of Scavengers of Reactive Oxygen and Radical Species on Cell Survival Following Photodynamic Treatment in Vitro: Comparison to Ionizing Radiation. *Radiation Research*. 108 (2), pp. 196.
- Hoiby, N., Ciofu, O., Johansen, H.K., Song, Z.J., Moser, C., Jensen, P.O., Molin, S., Givskov, M., Tolker-Nielsen, T. and Bjarnsholt, T. (2011) The clinical impact of bacterial biofilms. *International Journal of Oral Science*. 3 (2), pp. 55-65.
- Hongcharu, W., Taylor, C.R., Chang, Y., Aghassi, D., Suthamjariya, K. and Anderson, R.R. (2000) Topical ALA-photodynamic therapy for the treatment of acne vulgaris. *The Journal of Investigative Dermatology*. 115 (2), pp. 183-192.
- Hoyle, B.D. and Costerton, J.W. (1991) Bacterial resistance to antibiotics: the role of biofilms. *Progress in Drug Research.Fortschritte Der Arzneimittelforschung.Progres Des Recherches Pharmaceutiques*. 37 pp. 91-105.

Huang, L., Xuan, Y., Koide, Y., Zhiyentayev, T., Tanaka, M. and Hamblin, M.R. (2012) Type I and Type II mechanisms of antimicrobial photodynamic therapy: an in vitro study on gram-negative and gram-positive bacteria. *Lasers in Surgery and Medicine*. 44 (6), pp. 490-499.

Jassim, S.A., Ellison, A., Denyer, S.P. and Stewart, G.S. (1990) *In vivo* bioluminescence: a cellular reporter for research and industry. *Journal of Bioluminescence and Chemiluminescence*. 5(2), pp. 115-122.

Jori, G. (2006) Photodynamic therapy of microbial infections: state of the art and perspectives. *Journal of Environmental Pathology, Toxicology and Oncology : Official Organ of the International Society for Environmental Toxicology and Cancer*. 25 (1-2), pp. 505-519.

Jori, G. and Brown, S.B. (2004) Photosensitized inactivation of microorganisms. *Photochemical and Photobiological Sciences : Official Journal of the European Photochemistry Association and the European Society for Photobiology*. 3 (5), pp. 403-405.

Jori, G. and Spikes, J.D. (1990) Photothermal sensitizers: possible use in tumor therapy. *Journal of Photochemistry and Photobiology. B, Biology*. 6 (1-2), pp. 93-101.

Jori, G., Fabris, C., Soncin, M., Ferro, S., Coppellotti, O., Dei, D., Fantetti, L., Chiti, G. and Roncucci, G. (2006) Photodynamic therapy in the treatment of microbial infections: basic principles and perspective applications. *Lasers in Surgery and Medicine*. 38 (5), pp. 468-481.

Junqueira, J.C., Jorge, A.O., Barbosa, J.O., Rossoni, R.D., Vilela, S.F., Costa, A.C., Primo, F.L., Goncalves, J.M., Tedesco, A.C. and Suleiman, J.M. (2012) Photodynamic inactivation of biofilms formed by *Candida* spp., *Trichosporon mucoides*, and *Kodamaea ohmeri* by cationic nanoemulsion of zinc 2,9,16,23-tetrakis(phenylthio)-29H, 31H-phthalocyanine (ZnPc). *Lasers in Medical Science*. 27 (6), pp. 1205-1212.

Kadurugamuwa, J.L., Sin, L.V., Yu, J., Francis, K.P., Kimura, R., Purchio, T. and Contag, P.R. (2003) Rapid direct method for monitoring antibiotics in a mouse model of bacterial biofilm infection. *Antimicrobial Agents and Chemotherapy*. 47(10), pp. 3130-3137.

Kashef, N., Ravaei Sharif Abadi, G. and Djavid, G.E. (2012) Phototoxicity of phenothiazinium dyes against methicillin-resistant *Staphylococcus aureus* and multi-drug resistant *Escherichia coli* *Photodiagnosis and Photodynamic Therapy*. 9 (1), pp. 11-15.

Kharkwal, G.B., Sharma, S.K., Huang, Y., Dai, T. and Hamblin, M.R. (2011) Photodynamic therapy for infections: clinical applications. *Lasers in Surgery and Medicine*. 43(7), pp. 755-767.

Kiesslich, T., Gollmer, A., Maisch, T., Berneburg, M. and Plaetzer, K. (2013) A comprehensive tutorial on in vitro characterization of new photosensitizers for photodynamic antitumor therapy and photodynamic inactivation of microorganisms. *BioMed Research International*. 2013 pp. 840417.

Komerik, N., Wilson, M., Poole, S. (2000) The effect of photodynamic action on two virulence factors of gram-negative bacteria. *Journal of Photochemistry and Photobiology*. 72 (5), pp. 676-680.

Koseki, S., Yoshida, K., Isobe, S. and Itoh, K. (2004) Efficacy of acidic electrolyzed water for microbial decontamination of cucumbers and strawberries. *Journal of Food Protection*. 67 (6), pp.1247-1251.

Lambrechts, S.A., Demidova, T.N., Aalders, M.C., Hasan, T. and Hamblin, M.R. (2005) Photodynamic therapy for *Staphylococcus aureus* infected burn wounds in mice. *Photochemical and Photobiological Sciences : Official Journal of the European Photochemistry Association and the European Society for Photobiology*. 4 (7), pp. 503-509.

Lambrechts, S.A.G. Lambrechts, S.A., Schwartz, K.R., Aalders, M.C., Dankert, J.B. (2005) Photodynamic inactivation of fibroblasts by a cationic porphyrin. *Lasers in Medical Science*. 20 (2), pp. 62–67.

Lebeaux, D., Chauhan, A., Rendueles, O. and Beloin, C. (2013) From *in vitro* to *in vivo* Models of Bacterial Biofilm-Related Infections. *Pathogens*. 2(2), pp. 288–356.

Lee, C.F., Lee, C.J., Chen, C.T. and Huang, C.T. (2004) delta-Aminolaevulinic acid mediated photodynamic antimicrobial chemotherapy on *Pseudomonas aeruginosa* planktonic and biofilm cultures. *Journal of Photochemistry and Photobiology, B, Biology*. 75 (1-2), pp. 21-25.

Lee, Y., Park, H., Lee, J., Seo, H. and Lee, S. (2012) The photodynamic therapy on *Streptococcus mutans* biofilms using erythrosine and dental halogen curing unit. *International Journal of Oral Science*. 4 (4), pp. 196-201.

Lembo, A.J., Ganz, R.A., Sheth, S., Cave, D., Kelly, C., Levin, P., Kazlas, P.T., Baldwin, P.C.,3rd, Lindmark, W.R., McGrath, J.R. and Hamblin, M.R. (2009) Treatment of *Helicobacter pylori* infection with intra-gastric violet light phototherapy: a pilot clinical trial. *Lasers in Surgery and Medicine*. 41 (5), pp. 337-344.

Leonov, B.I. (1997) Electrochemical activation of water and aqueous solutions: past, present and future. In Proceedings of the First International Symposium on Electrochemical Activation, Moscow. pp. 11–27.

Levy, S.B. (2002) Factors impacting on the problem of antibiotic resistance. *Journal of Antimicrobial Chemotherapy*. 49 (1), pp. 25-30.

Lewis, K. (2001) Riddle of biofilm resistance. *Antimicrobial Agents and Chemotherapy*.

45 (4), pp. 999-1007.

Li, X.Y., Ding, F., Lo, P.S.Y. and Sin, S.H.P. (2002) Electrochemical Disinfection of Saline Wastewater Effluent. *Journal of Environmental Engineering*. 128 (8), pp. 697-704.

Liao, L.B., Chen, W.M. and Xiao, X.M. (2007) The generation and inactivation mechanism of oxidation–reduction potential of electrolyzed oxidizing water. *Journal of Food Engineering*. 78 (4), pp.1326-1332.

Liao, W., McNutt, M.A. and Zhu, W.G. (2009) The comet assay: a sensitive method for detecting DNA damage in individual cells. *Methods (San Diego, Calif.)*. 48 (1), pp. 46-53.

Lin, H.Y., Chen, C.T. and Huang, C.T. (2004) Use of merocyanine 540 for photodynamic inactivation of *Staphylococcus aureus* planktonic and biofilm cells. *Applied and Environmental Microbiology*. 70 (11), pp. 6453-6458.

Loshon, C.A., Melly, E., Setlow, B. and Setlow, P. (2001) Analysis of the killing of spores of *Bacillus subtilis* by a new disinfectant, Sterilox. *Journal of Applied Microbiology*. 91 (6), pp. 1051-1058.

Lyon, J.P., Pedroso e Silva Azevedo Cde, M., Moreira, L.M., de Lima, C.J. and de Resende, M.A. (2011) Photodynamic antifungal therapy against chromoblastomycosis. *Mycopathologia*. 172 (4), pp. 293-297.

Mah, T.F. and O'Toole, G.A. (2001) Mechanisms of biofilm resistance to antimicrobial agents. *Trends in Microbiology*. 9 (1), pp. 34-39.

Maisch, T. (2007) Anti-microbial photodynamic therapy: useful in the future? *Lasers in Medical Science*. 22 (2), pp. 83-91.

Maisch, T., Baier, J., Franz, B., Maier, M., Landthaler, M., Szeimies, R.M. and Baumler, W. (2007) The role of singlet oxygen and oxygen concentration in photodynamic inactivation of bacteria. *Proceedings of the National Academy of Sciences of the United States of America*. 104 (17), pp. 7223-7228.

Malakhov, S.F., Bautin, E.A., Paramonov, B.A. and Krasnopevtseva, O.S. (1994) The use of electrochemically activated solutions for treating burn wounds. *Voenno-meditsinskii Zhurnal*. 9 (9), 32-34.

Malik, Z., Ladan, H. and Nitzan, Y. (1992) Photodynamic inactivation of Gram-negative bacteria: problems and possible solutions. *Journal of Photochemistry and Photobiology. B, Biology*. 14 (3), pp. 262-266.

Mansfield, R. (2001) Photodynamic therapy: shedding light on restenosis *Heart*. 86 (6), pp. 612-618.

Marais J.T and Brözel, V.S (1999) Electro-chemically activated water in dental unit water lines. *British Dental Journal*. 187(3), 154–158.

Marais J.T. (2002) Biocompatibility of electrochemically aqueous activated solutions: an animal study. *Journal of South African Dental Association*. 57(1), pp. 12–16.

Marais, J.T. and Williams, W.P. (2001) Antimicrobial effectiveness of electro-chemically activated water as an endodontic irrigation solution. *International Endodontic Journal*. 34 (3), pp. 237-243.

Marais, J.T. and Williams, W.P. (2001) Antimicrobial effectiveness of electro-chemically activated water as an endodontic irrigation solution. *International Endodontic Journal*. 34 (3), pp. 237-243.

Marincs, F. (2000) On-line monitoring of growth of *Escherichia coli* in batch cultures by bioluminescence *Applied Microbiology and Biotechnology*. 53 (5), pp. 536-541.

Marques, C.N., Salisbury, V.C., Greenman, J., Bowker, K.E. and Nelson, S.M. (2005) Discrepancy between viable counts and light output as viability measurements, following ciprofloxacin challenge of self-bioluminescent *Pseudomonas aeruginosa* biofilms. *The Journal of Antimicrobial Chemotherapy*. 56 (4), pp. 665-671.

Martin, M., Showalter, R. and Silverman, M. (1989) Identification of a locus controlling expression of luminescence genes in *Vibrio harveyi*. *Journal of Bacteriology*. 171 (5), pp. 2406-2414.

Martinez-De Jesus, F.R., Ramos-De la Medina, A., Remes-Troche, J.M., Armstrong, D.G., Wu, S.C., Lazaro Martinez, J.L. and Beneit-Montesinos, J.V. (2007) Efficacy and safety of neutral pH superoxidised solution in severe diabetic foot infections. *International Wound Journal*. 4 (4), pp. 353-362.

Mashberg, A. (1983) Final evaluation of tolonium chloride rinse for screening of high-risk patients with asymptomatic squamous carcinoma. *Journal of the American Dental Association*. 106 (3), pp. 319-323.

Maskos, Z., Rush, J.D. and Koppenol, W.H. (1992) The hydroxylation of tryptophan. *Archives of Biochemistry and Biophysics*. 296 (2), pp.514-520.

Masuda, T., Oikawa, K., Oikawa, H., Sato, S., Sato, K. and Kano, A. (1995) Endoscope disinfection with acid electrolyzed water. *Digestive Endoscopy* 7(1) pp. 61–64.

McCaughan, J.S.,Jr (1999) Photodynamic therapy: a review. *Drugs & Aging*. 15 (1), pp. 49-68.

McNair, F.I., Marples, B., West, C.M. and Moore J.V. (1997) A comet assay of DNA damage and repair in K562 cells after photodynamic therapy using haematoporphyrin derivative, methylene blue and meso-tetrahydroxyphenylchlorin. *British Journal of Cancer*. 75 (12) pp. 1721–1729.

Meighen, E.A. (1991) Molecular biology of bacterial bioluminescence. *Microbiological Reviews*. 55(1), pp. 123-142.

Meighen, E.A. (1993) Bacterial bioluminescence: organization, regulation, and application of the lux genes. *FASEB journal : official publication of the Federation of American Societies for Experimental Biology*. 7(11), pp. 1016-1022.

Meire, M.A., Coenye, T., Nelis, H.J. and De Moor, R.J. (2012) Evaluation of Nd:YAG and Er:YAG irradiation, antibacterial photodynamic therapy and sodium hypochlorite treatment on *Enterococcus faecalis* biofilms. *International Endodontic Journal*. 45 (5), pp. 482-491.

Meisel, P. and Kocher, T. (2005) Photodynamic therapy for periodontal diseases: state of the art. *Journal of Photochemistry and photobiology.B, Biology*. 79(2), pp. 159-170.

Midden, W.R. and Dahl, T.A. (1992) Biological inactivation by singlet oxygen: distinguishing O<sub>2</sub>(<sup>1</sup>Δg) and O<sub>2</sub>(<sup>1</sup>Σg<sup>+</sup>). *Biochimica et Biophysica Acta*. 1117(2), pp. 216-222.

Millson, C.E., Wilson, M., MacRobert, A.J. and Bown, S.G. (1996) Ex-vivo treatment of gastric Helicobacter infection by photodynamic therapy. *Journal of Photochemistry and Photobiology.B, Biology*. 32 (1-2), pp. 59-65.

Minnock, A., Vernon, D.I., Schofield, J., Griffiths, J., Parish, J.H. and Brown, S.B. (2000) Mechanism of uptake of a cationic water-soluble pyridinium zinc phthalocyanine across the outer membrane of *Escherichia coli*. *Antimicrobial Agents and Chemotherapy*. 44 (3), pp. 522-527.

Moan, J. (1990) On the diffusion length of singlet oxygen in cells and tissues. *Journal of Photochemistry and Photobiology B, Biology*. 6 (3), pp. 343-344.

Moan, J. and Peng, Q. (2003) An outline of the hundred-year history of PDT. *Anticancer Research*. 23 (5A), pp. 3591-3600.

Moellering, R.C. (2011) Discovering new antimicrobial agents. *International Journal of Antimicrobial Agents*. 37(1), pp. 2-9.

Mohr, H., Bachmann, B., Klein-Struckmeier, A. and Lambrecht, B. (1997) Virus inactivation of blood products by phenothiazine dyes and light. *Photochemistry and Photobiology*. 65(3), pp. 441-445.

Morita, C., Nishida, T. and Ito, K. (2011) Biological toxicity of acid electrolyzed functional water: effect of oral administration on mouse digestive tract and changes in body weight. *Archives of Oral Biology*. 56 (4), pp. 359-366.

Nakae, H. and Inaba, H. (2000) Effectiveness of electrolyzed oxidized water irrigation in a burn-wound infection model. *The Journal of Trauma*. 49 (3), pp. 511-514.

- Nelson, S.M., Cooper, A.A., Taylor, E.L. and Salisbury, V.C. (2003) Use of bioluminescent *Escherichia coli* O157:H7 to study intra-protozoan survival of bacteria within *Tetrahymena pyriformis*. *FEMS Microbiology Letters*. 223 (1), pp. 95-99.
- Niemz M.H. (2007). *Laser-Tissue Interactions: Fundamentals and Applications*. 3rd ed. New York: Springer Berlin Heidelberg.
- Nitzan, Y., Gutterman, M., Malik, Z. and Ehrenberg, B. (1992) Inactivation of gram-negative bacteria by photosensitized porphyrins. *Photochemistry and Photobiology*. 55(1), pp. 89-96.
- Nitzan, Y., Shainberg, B. and Malik, Z. (1989) The mechanism of photodynamic inactivation of *Staphylococcus aureus* by deuteroporphyrin. *Current Microbiology*. 19 (4), pp. 265-269.
- Noodt, B.B., Kvam, E., Steen, H.B. and Moan, J. (1993) Primary DNA damage, HPRT mutation and cell inactivation photoinduced with various sensitizers in V79 cells. *Photochemistry and Photobiology*. 58 (4), pp. 541-547.
- Norden, B. and Tjerneld, F. (1982) Structure of methylene blue-DNA complexes studied by linear and circular dichroism spectroscopy. *Biopolymers*. 21 (9), pp. 1713-1734.
- O'Neill, J.F., Hope, C.K. and Wilson, M. (2002) Oral bacteria in multi-species biofilms can be killed by red light in the presence of toluidine blue. *Lasers in Surgery and Medicine*. 31 (2), pp. 86-90.
- Ochsner, M. (1997) Photophysical and photobiological processes in the photodynamic therapy of tumours. *Journal of Photochemistry and Photobiology B: Biology*. 39 (1), pp. 1-18.
- Olive, P.L. and Banáth, J.P. (2006) The comet assay: a method to measure DNA damage in individual cells. *Nature Protocols*. 1 (1), pp. 23-29.
- Olive, P.L., Banath, J.P. and Durand, R.E. (1990) Heterogeneity in radiation-induced DNA damage and repair in tumor and normal cells measured using the "comet" assay. *Radiation Research*. 122 (1), pp. 86-94.
- Olive, P.L., Frazer, G. and Banáth, J.P. (1993) Radiation-induced apoptosis measured in TK6 human B lymphoblast cells using the comet assay. *Radiation Research*. 136(1), pp. 130-6.
- Omar, G.S., Wilson, M. and Nair, S.P. (2008) Lethal photosensitization of wound-associated microbes using indocyanine green and near-infrared light. *BMC Microbiology* [online]. 8 pp. 111-2180-8-111.

Ostling, O. and Johanson, K.J. (1984) Microelectrophoretic study of radiation-induced DNA damages in individual mammalian cells. *Biochemical and Biophysical Research Communications*. 123 (1), pp. 291-298.

Oturan, M.A. (2000) An ecologically effective water treatment technique using electrochemically generated hydroxyl radicals for in situ destruction of organic pollutants: application to herbicide. *Journal of Applied Electrochemistry*. 30(4), pp. 475-482.

Park, H., Hung, Y.C. and Kim, C. (2002) Effectiveness of electrolyzed water as a sanitizer for treating different surfaces. *Journal of Food Protection*. 65 (8), pp. 1276-1280.

Patermarakis, G. and Fountoukidis, E. (1990) Disinfection of water by electrochemical treatment. *Water Research*. 24 (12), pp. 1491-1496.

Peng, C., Li, Y., Liang, H., Cheng, J., Li, Q., Sun, X., Li, Z., Wang, F., Guo, Y., Tian, Z., Yang, L., Tian, Y., Zhang, Z. and Cao, W. (2011) Detection and photodynamic therapy of inflamed atherosclerotic plaques in the carotid artery of rabbits. *Journal of Photochemistry and Photobiology, B, Biology*. 102 (1), pp. 26-31.

Pereira, C.A., Romeiro, R.L., Costa, A.C., Machado, A.K., Junqueira, J.C. and Jorge, A.O. (2011) Susceptibility of *Candida albicans*, *Staphylococcus aureus*, and *Streptococcus mutans* biofilms to photodynamic inactivation: an in vitro study. *Lasers in Medical Science*. 26 (3), pp. 341-348.

Pervaiz, S. and Olivo, M. (2006) Art and science of photodynamic therapy. *Clinical and Experimental Pharmacology & Physiology*. 33 (5-6), pp. 551-556.

Phillips, D. (1997) Chemical mechanisms in photodynamic therapy with phthalocyanines. *Progress Reactions Kinetics*. 22, pp. 175-300.

Phoenix, D.A. (2003) The phototoxicity of phenothiazinium derivatives against *Escherichia coli* and *Staphylococcus aureus*. *FEMS Immunology and Medical Microbiology*, 39, pp. 17-22.

Phoenix, D.A. and Harris, F. (2003) Phenothiazinium-based photosensitizers: antibacterials of the future? *Trends in Molecular Medicine*. 9 (7), pp. 283-285.

Price, M., Reiners, J.J., Santiago, A.M. and Kessel, D. (2009) Monitoring singlet oxygen and hydroxyl radical formation with fluorescent probes during photodynamic therapy. *Photochemistry and Photobiology*. 85 (5), pp.1177-1181.

Prilutskii, V.I., Bakhir, V.M. and Popov, A.I. (1996) The disinfection of water, water-supply systems, tanks and pools by using an electrochemically activated solution of a neutral anolyte. *Voprosy kurortologii, fizioterapii, i lechebnoi fizicheskoi kultury*, (4)(4), pp. 31-32.

Raab O. 1900. Ueber die Wirkung fluoreszierender Stoffe auf Infusorien. *Z Biol*, 39, pp. 524.

Ragas, X., Agut, M. and Nonell, S. (2010) Singlet oxygen in *Escherichia coli*: New insights for antimicrobial photodynamic therapy. *Free Radical Biology and Medicine*. 49 (5), pp. 770-776.

Repetto, G., del Peso, A. and Zurita, J.L. (2008) Neutral red uptake assay for the estimation of cell viability/cytotoxicity. *Nature Protocols*. 3 (7), pp. 1125-1131.

Robinson, G., Thorn, R. and Reynolds, D. (2012) The effect of long-term storage on the physiochemical and bactericidal properties of electrochemically activated solutions. *International Journal of Molecular Sciences*. 14 (1), pp. 457-469.

Robinson, G.M., Lee, S.W., Greenman, J., Salisbury, V.C. and Reynolds, D.M. (2010) Evaluation of the efficacy of electrochemically activated solutions against nosocomial pathogens and bacterial endospores. *Letters in Applied Microbiology*. 50 (3), pp. 289-294.

Robinson, G.M., Tonks, K.M., Thorn, R.M. and Reynolds, D.M. (2011) Application of bacterial bioluminescence to assess the efficacy of fast-acting biocides. *Antimicrobial Agents and Chemotherapy*. 55 (11), pp. 5214-5220.

Rocchetta, H.L., Boylan, C.J., Foley, J.W., Iversen, P.W., LeTourneau, D.L., McMillian, C.L., Contag, P.R., Jenkins, D.E. and Parr, T.R., Jr (2001) Validation of a noninvasive, real-time imaging technology using bioluminescent *Escherichia coli* in the neutropenic mouse thigh model of infection. *Antimicrobial Agents and Chemotherapy*. 45 (1), pp. 129-137.

Rodgers, J.D., Jedral, W. and Bunce, N.J. (1999) Electrochemical Oxidation of Chlorinated Phenols. *Environmental Science & Technology*. 33 (9), pp. 1453-1457.

Rosenthal, I. and Ben-Hur, E. (1995) Role of oxygen in the phototoxicity of phthalocyanines. *International journal of radiation biology*. 67 (1), pp. 85-91.

Ryskova, L., Buchta, V. and Slezak, R. (2010) Photodynamic antimicrobial therapy. *Central European Journal of Biology*. 5 (4), pp. 400-406.

Saad, S., Hewett, K. and Greenman, J. (2013) Use of an *in vitro* flat-bed biofilm model to measure biologically active anti-odour compounds. *Applied Microbiology and Biotechnology*. 97 (17), pp. 7865-7875.

Sabbahi, S., Alouini, Z., Jemli, M. and Boudabbous, A. (2008) The role of reactive oxygen species in *Staphylococcus aureus* photoinactivation by methylene blue. *Water Science and Technology : A Journal of the International Association on Water Pollution Research*. 58 (5), pp. 1047-1054.

Sakurai, Y., Ogoshi, K., Okubo, T., Kaku, M. and Kobayashi, I. (2002) Strongly acidic electrolyzed water: valuable disinfectant of endoscopes. *Digestive Endoscopy*. 14 (2), pp. 61-66.

Salisbury, V., Pfoestl, A., Wiesinger-Mayr, H., Lewis, R., Bowker, K.E. and MacGowan, A.P. (1999) Use of a clinical *Escherichia coli* isolate expressing lux genes to study the antimicrobial pharmacodynamics of moxifloxacin. *The Journal of Antimicrobial Chemotherapy*. 43 (6), pp. 829-832.

Schaffer and Barbul (1998) Lymphocyte function in wound healing and following injury. *British Journal of Surgery*. 85 (4), pp. 444-460.

Schierle, C.F., De la Garza, M., Mustoe, T.A. and Galiano, R.D. (2009) Staphylococcal biofilms impair wound healing by delaying reepithelialization in a murine cutaneous wound model. *Wound Repair and Regeneration*. 17 (3), pp. 354-359.

Sekiya S, Ohmori K, Harii K (1997) Treatment of infectious skin defects or ulcers with electrolyzed strong acid aqueous solution. *Artificial Organs*. 21(1) pp. 32-38

Selkon, J.B., Babb, J.R. And Morris, R., 1999. Evaluation of the antimicrobial activity of a new super-oxidized water, Sterilox, for the disinfection of endoscopes. *The Journal of Hospital Infection*, 41(1), pp. 59-70.

Setsukinai, K., Urano, Y., Kakinuma, K., Majima, H.J. and Nagano, T. (2003) Development of novel fluorescence probes that can reliably detect reactive oxygen species and distinguish specific species. *The Journal of Biological Chemistry*. 278 (5), pp. 3170-3175.

Sharma, M., Visai, L., Bragheri, F., Cristiani, I., Gupta, P.K. and Speziale, P. (2008) Toluidine Blue-Mediated Photodynamic Effects on Staphylococcal Biofilms. *Antimicrobial Agents and Chemotherapy*. 52 (1), pp. 299-305.

Sharma, S.K., Dai, T., Kharkwal, G.B., Huang, Y.Y., Huang, L., De Arce, V.J., Tegos, G.P. and Hamblin, M.R. (2011) Drug discovery of antimicrobial photosensitizers using animal models. *Current Pharmaceutical Design*. 17 (13), pp. 1303-1319.

Sharman, W.M., Allen, C.M. and van Lier, J.E. (1999) Photodynamic therapeutics: basic principles and clinical applications. *Drug Discovery Today*. 4 (11), pp. 507-517.

Sharman, W.M., Allen, C.M. and van Lier, J.E. (2000) Role of activated oxygen species in photodynamic therapy. *Methods in Enzymology*. 319 pp. 376-400.

Shetty, N., Srinivasan, S., Holton, J. and Ridgway, G.L. (1999) Evaluation of microbicidal activity of a new disinfectant: Sterilox 2500 against *Clostridium difficile* spores, *Helicobacter pylori*, vancomycin resistant *Enterococcus* species, *Candida albicans* and several *Mycobacterium* species. *The Journal of Hospital Infection*. 41 (2), pp. 101-105.

Shimabukuro, F., Neto, C.F., Sanches, J.A., Jr and Gattas, G.J. (2011) DNA damage and repair in leukocytes of melanoma patients exposed *in vitro* to cisplatin. *Melanoma Research*. 21 (2), pp. 99-105.

Shopova, M. And Gantchev, T., 1990. Comparison of the photosensitizing efficiencies of haematoporphyrin (HP) and its derivative (HPD) with that of free-base tetrasulphophthalocyanine (TSPC-H2) in homogeneous and microheterogeneous media. *Journal of Photochemistry and Photobiology.B, Biology*. 6(1-2), pp. 49-59.

Shraev, T.I., Legchilo, A.N., Kharlamov, A.T. And Legchilo, A.A. (1993) Sanitization of bronchial pathways by electrochemically activated solution of 0.8% potassium chloride. *Anesteziologiya i Reanimatologiya*. 1 (1), pp. 22-23.

Simões, M., Simões, L.C. and Vieira, M.J. (2010) A review of current and emergent biofilm control strategies. *LWT - Food Science and Technology*. 43 (4), pp. 573-583.

Singh, A. (1982) Chemical and biochemical aspects of superoxide radicals and related species of activated oxygen. *Canadian Journal of Physiology and Pharmacology*. 60 (11), pp. 1330-1345.

Singh, N.P., McCoy, M.T., Tice, R.R. and Schneider, E.L. (1988) A simple technique for quantitation of low levels of DNA damage in individual cells. *Experimental Cell Research*. 175 (1), pp. 184-191.

Soh, N. (2006) Recent advances in fluorescent probes for the detection of reactive oxygen species. *Analytical and Bioanalytical Chemistry*. 386 (3), pp. 532-543.

Solovyeva, A.M. and Dummer, P.M.H. (2000) Cleaning effectiveness of root canal irrigation with electrochemically activated anolyte and catholyte solutions: a pilot study. *International Endodontic Journal*. 33 (6), pp. 494-504.

Soukos, N.S. and Goodson, J.M. (2011) Photodynamic therapy in the control of oral biofilms. *Periodontology 2000*. 55 (1), pp. 143-166.

Soukos, N.S., Wilson, M., Burns, T. And Speight, P.M. (1996) Photodynamic effects of toluidine blue on human oral keratinocytes and fibroblasts and *Streptococcus sanguis* evaluated *in vitro*. *Lasers in Surgery and Medicine*, 18(3), pp. 253-259.

Soukos, N.S., Ximenez-Fyvie, L.A., Hamblin, M.R., Socransky, S.S. and Hasan, T. (1998) Targeted antimicrobial photochemotherapy. *Antimicrobial Agents and Chemotherapy*. 42 (10), pp. 2595-2601.

Souza, R.C., Junqueira, J.C., Rossoni, R.D., Pereira, C.A., Munin, E. and Jorge, A.O. (2010) Comparison of the photodynamic fungicidal efficacy of methylene blue, toluidine blue, malachite green and low-power laser irradiation alone against *Candida albicans*. *Lasers in Medical Science*. 25 (3), pp. 385-389.

Sparrow, J.R., Zhou, J. and Cai, B. (2003) DNA is a target of the photodynamic effects elicited in A2E-laden RPE by blue-light illumination. *Investigative Ophthalmology and Visual Science*. 44 (5), pp. 2245-2251.

Spellberg, B., Guidos, R., Gilbert, D., Bradley, J., Boucher, H.W., Scheld, W.M., Bartlett, J.G., Edwards, J., Jr and Infectious Diseases Society of America (2008) The epidemic of antibiotic-resistant infections: a call to action for the medical community from the Infectious Diseases Society of America. *Clinical Infectious Diseases : An Official Publication of the Infectious Diseases Society of America*. 46 (2), pp. 155-164.

Suzuki, T., Itakura, J., Watanabe, M., Ohta, M., Sato, Y., Yamaya, Y. (2002) Inactivation of staphylococcal enterotoxin-A with an electrolyzed anodic solution. *Journal of Agricultural and Food Chemistry*. 50(1), pp. 230–234.

Suzuki, T., Noro, T., Kawamura, Y., Fukunagami, K., Watanabe M., Ohta M, Sugiue, H, Sato, Y, Kohno M, Hotta K. (2002) Decontamination of aflatoxin-forming fungus and elimination of aflatoxin mutagenicity with electrolyzed NaCl anode solution. *Journal of Agricultural and Food Chemistry*. 50 (3), pp. 633–641.

Swain, U. and Rao, S.K. (2011). Study of DNA damage via the comet assay and base excision repair activities in rat brain neurons and astrocytes during aging. *Mechanisms of Ageing and Development*. 132(8-9), pp. 374–381.

Takemura, T., Ohta, N., Nakajima, S. and Sakata, I. (1989) Critical importance of the triplet lifetime of photosensitizer in photodynamic therapy of tumor. *Photochemistry and photobiology*. 50(3), pp. 339-344.

Tanaka, H., Hirakata, Y., Kaku, M., Yoshida, R., Takemura, H., Mizukane, R., Ishida, K., Tomono, K., Koga, H., Kohno, S. and Kamihira, S. (1996) Antimicrobial activity of superoxidized water. *Journal of Hospital Infection*. 34(1), pp. 43–49.

Tappeiner, H. V. and Jodlbauer, A. (1904) Über die Wirkung der photodynamischen (fluoreszierenden) Stoffe auf Infusorien Dtsch Arch Klin. Med. 80, pp. 427-487.

Tardivo, J.P., Del Giglio, A., de Oliveira, C.S., Gabrielli, D.S., Junqueira, H.C., Tada, D.B., Severino, D., de Fátima Turchiello, R. and Baptista, M.S. (2005) Methylene blue in photodynamic therapy: From basic mechanisms to clinical applications. *Photodiagnosis and Photodynamic Therapy*. 2 (3), pp. 175-191.

Tavares, A., Dias, S.R., Carvalho, C.M., Faustino, M.A., Tome, J.P., Neves, M.G., Tome, A.C., Cavaleiro, J.A., Cunha, A., Gomes, N.C., Alves, E. and Almeida, A. (2011) Mechanisms of photodynamic inactivation of a gram-negative recombinant bioluminescent bacterium by cationic porphyrins. *Photochemical and Photobiological Sciences : Official Journal of the European Photochemistry Association and the European Society for Photobiology*. 10 (10), pp. 1659-1669.

Tegos, G.P. and Hamblin, M.R. (2006) Phenothiazinium antimicrobial photosensitizers are substrates of bacterial multidrug resistance pumps. *Antimicrobial Agents and Chemotherapy*. 50 (1), pp. 196-203.

Thantsha, M.S. and Cloete, T.E. (2006) The effect of sodium chloride and sodium bicarbonate derived anolytes, and anolyte–catholyte combination on biofilms. *Water SA*. 32(2), pp. 237-242.

Thorn, R.M. and Greenman, J. (2009) A novel *in vitro* flat-bed perfusion biofilm model for determining the potential antimicrobial efficacy of topical wound treatments. *Journal of Applied Microbiology*. 107 (6), pp. 2070-2079.

Thorn, R.M., Lee, S.W., Robinson, G.M., Greenman, J. and Reynolds, D.M. (2012) Electrochemically activated solutions: evidence for antimicrobial efficacy and applications in healthcare environments. *European Journal of Clinical Microbiology & Infectious Diseases : Official Publication of the European Society of Clinical Microbiology*. 31 (5), pp. 641-653.

Thorn, R.M., Nelson, S.M. and Greenman, J. (2007) Use of a bioluminescent *Pseudomonas aeruginosa* strain within an *in vitro* microbiological system, as a model of wound infection, to assess the antimicrobial efficacy of wound dressings by monitoring light production. *Antimicrobial Agents and Chemotherapy*. 51(9), pp. 3217-3224.

Thorn, R.M (2009) *Development of in vitro microbiological systems for determining the antimicrobial potential of wound treatment*, PhD, University of the West of England.

Tsuji, S., Kawano, S., Oshita, M., Ohmae, A., Shinomura, Y., Miyazaki, Y., Hiraoka, S., Matsuzawa, Y., Kamada, T., Hori, M. and Maeda, T. (1999) Endoscope disinfection using acidic electrolytic water. *Endoscopy*. 31(7), pp. 528–535.

Usacheva, M.N., Teichert, M.C. and Biel, M.A. (2003) The role of the methylene blue and toluidine blue monomers and dimers in the photoinactivation of bacteria. *Journal of Photochemistry and Photobiology. B, Biology*. 71 (1-3), pp. 87-98.

Valduga, G., Breda, B., Giacometti, G.M., Jori, G. and Reddi, E. (1999) Photosensitization of wild and mutant strains of *Escherichia coli* by meso-tetra (N-methyl-4-pyridyl)porphine. *Biochemical and Biophysical Research Communications*. 256 (1), pp. 84-88.

Vatansever, F., de Melo, W.C., Avci, P., Vecchio, D., Sadasivam, M., Gupta, A., Chandran, R., Karimi, M., Parizotto, N.A., Yin, R., Tegos, G.P. and Hamblin, M.R. (2013) Antimicrobial strategies centered around reactive oxygen species--bactericidal antibiotics, photodynamic therapy, and beyond. *FEMS Microbiology Reviews*. 37 (6), pp. 955-989.

Venkitanarayanan, K.S., Ezeike, G.O., Hung, Y.C., Doyle, M.P., (1999) Inactivation of *Escherichia coli* O157:H7 and *Listeria monocytogenes* on plastic kitchen cutting boards by electrolyzed oxidizing water. *J Food Protection*. 62, pp. 857-860.

Vesterlund, S., Paltta, J., Laukova, A., Karp, M. and Ouwehand, A.C. (2004) Rapid screening method for the detection of antimicrobial substances. *Journal of Microbiological Methods*. 57 (1), pp. 23-31.

Vilela, S.F., Junqueira, J.C., Barbosa, J.O., Majewski, M., Munin, E. and Jorge, A.O. (2012) Photodynamic inactivation of *Staphylococcus aureus* and *Escherichia coli* biofilms by malachite green and phenothiazine dyes: an in vitro study. *Archives of Oral Biology*. 57 (6), pp.704-710.

Vivekanandan-Giri, A., Byun, J. and Pennathur, S. (2011) Quantitative analysis of amino Acid oxidation markers by tandem mass spectrometry. *Methods in Enzymology*. 491 pp. 73-89.

Vladimirov, Y.A., Osipov, A.N. and Klebanov, G.I. (2004) Photobiological principles of therapeutic applications of laser radiation. *Biochemistry.Biokhimiia*. 69 (1), pp. 81-90.

Wainwright, M. (1998) Photodynamic antimicrobial chemotherapy (PACT). *Journal of Antimicrobial Chemotherapy*. 42 (1), pp. 13-28.

Wainwright, M. (2000) Methylene blue derivatives--suitable photoantimicrobials for blood product disinfection? *International Journal of Antimicrobial Agents*. 16 (4), pp. 381-394.

Wainwright, M. (2005) The development of phenothiazinium photosensitisers. *Photodiagnosis and Photodynamic Therapy*. 2 (4), pp. 263-272.

Wainwright, M. and Crossley, K.B. (2004) Photosensitising agents—circumventing resistance and breaking down biofilms: a review. *International Biodeterioration and Biodegradation*. 53 (2), pp. 119 -126.

Wainwright, M., Mohr, H. and Walker W.H. (2007) Phenothiazinium derivatives for pathogen inactivation in blood products. *Journal of Photochemistry and Photobiology. B, Biology*. 86, pp. 45-58.

Wainwright, M., Phoenix, D.A., Laycock, S.L., Wareing, D.R. and Wright P.A. (1998) Photobactericidal activity of phenothiazinium dyes against methicillin-resistant strains of *Staphylococcus aureus*. *FEMS Microbiology Letters*. 160 (2), pp. 177-181.

Wainwright, M., Phoenix, D.A., Nickson, P.B. and Morton L.H.G (2002) The use of new methylene blue in *Pseudomonas aeruginosa* biofilm destruction. *Biofouling*. 18 (2002), pp. 247-249.

Webber, M.A., Alves, E., Faustino, M.A.F., Tomé, J.P.C., Neves, M.G.P.M.S., Tomé, A.C., Cavaleiro, J.A.S., Cunha, Â., Gomes, N.C.M. and Almeida, A. (2011) Photodynamic Antimicrobial Chemotherapy in Aquaculture: Photoinactivation Studies of *Vibrio fischeri* *Plos One* [online]. 6 (6), pp.e20970.

WHO (2014) Antimicrobial Resistance: Global Report on Surveillance. [online].

Wilson, M. (1993) Photolysis of oral bacteria and its potential use in the treatment of caries and periodontal disease. *The Journal of Applied Bacteriology*. 75 (4), pp. 299-306.

Wilson, M. and Yianni, C. (1995) Killing of methicillin-resistant *Staphylococcus aureus* by low-power laser light. *Journal of Medical Microbiology*. 42(1), pp. 62-66.

Wilson, M., Burns, T. and Pratten, J. (1996) Killing of *Streptococcus sanguis* in biofilms using a light-activated antimicrobial agent. *The Journal of Antimicrobial chemotherapy*. 37(2), pp. 377-81.

Winterbourn, C.C. (2014) The challenges of using fluorescent probes to detect and quantify specific reactive oxygen species in living cells. *Biochimica Et Biophysica Acta*. 1840 (2), pp. 730-738.

Winterbourn, C.C. and Kettle, A.J. (2000) Biomarkers of myeloperoxidase-derived hypochlorous acid. *Free Radical Biology & Medicine*. 29 (5), pp. 403-409.

Wong, T.W., Wang, Y.Y., Sheu, H.M. and Chuang, Y.C., (2005) Bactericidal effects of toluidine blue-mediated photodynamic action on *Vibrio vulnificus*. *Antimicrobial Agents and Chemotherapy*. 49(3), pp. 895-902.

Wood, S., Metcalf, D., Devine, D. and Robinson, C. (2006) Erythrosine is a potential photosensitizer for the photodynamic therapy of oral plaque biofilms. *Journal of Antimicrobial Chemotherapy*. 57 (4), pp. 680–684.

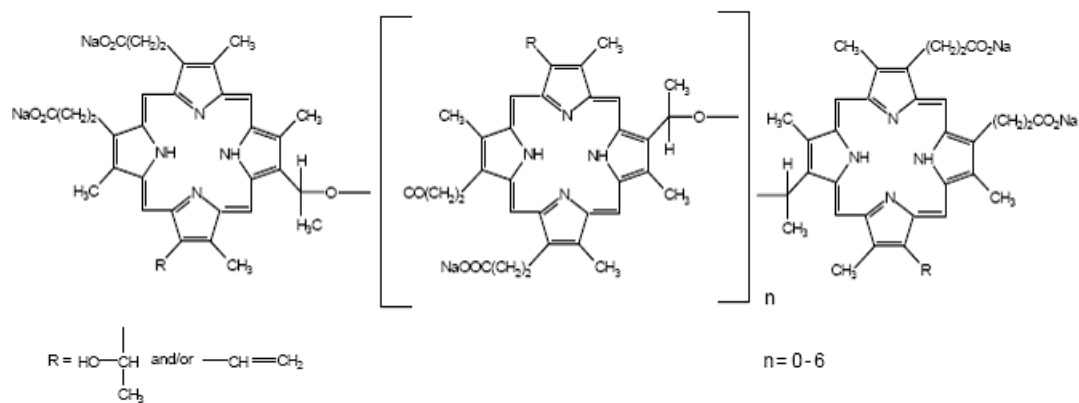
Xiong, K., Liu, H.J., Liu, R. and Li, L.T. (2010) Differences in fungicidal efficiency against *Aspergillus flavus* for neutralized and acidic electrolyzed oxidizing waters. *International Journal of Food Microbiology*. 137 (1), pp. 67-75.

Xu, Y., Young, M., Battaglinom R., Leslie, M., Fontana, C., Pagonis, T.C., Kent, R. and Soukos, N.S. (2009) Endodontics antimicrobial photodynamic therapy: safety assessment in mammalian cell cultures. *Journal of Endodontics*. 35 (11), pp. 1567–1572.

Yamakoshi, Y., Umezawa, N., Ryu, A., Arakane, K., Miyata, N., Goda, Y., Masumizu, T. and Nagano, T. (2003) Active oxygen species generated from photoexcited fullerene (C60) as potential medicines: O<sub>2</sub>-\* versus <sup>1</sup>O<sub>2</sub>. *Journal of the American Chemical Society*. 125 (42), pp. 12803-12809.

- Zanin, I.C., Goncalves, R.B., Junior, A.B., Hope, C.K. and Pratten, J. (2005) Susceptibility of *Streptococcus mutans* biofilms to photodynamic therapy: an *in vitro* study. *Journal of Antimicrobial Chemotherapy*. 56, pp. 324-330.
- Zeina, B., Greenman, J., Corry, D. and Purcell, W.M. (2002) Cytotoxic effects of antimicrobial photodynamic therapy on keratinocytes *in vitro*. *The British Journal of Dermatology*. 146 (4), pp. 568-573.
- Zeina, B., Greenman, J., Corry, D. and Purcell, W.M. (2003) Antimicrobial photodynamic therapy: assessment of genotoxic effects on keratinocytes *in vitro*. *The British Journal of Dermatology*. 148 (2), pp. 229-232.
- Zeina, B., Greenman, J., Purcell, W.M. and Das, B. (2001) Killing of cutaneous microbial species by photodynamic therapy. *The British Journal of Dermatology*. 144 (2), pp. 274-278.
- Zeina, B. (2001) *Killing of Cutaneous Microbial Species by Photodynamic Therapy*. PhD, University of the West of England.
- Zhao, B. and He, Y.Y. (2010) Recent advances in the prevention and treatment of skin cancer using photodynamic therapy. *Expert Review of Anticancer Therapy*. 10 (11), pp. 1797-1809.
- Zolfaghari, P.S., Packer, S. and Singer M., Nair, S.P., Bennett, J., Street, C. and Wilson, M. (2009) *In vivo* killing of *Staphylococcus aureus* using a light-activated antimicrobial agent. *BMC Microbiology*, (9), pp. 27.

## Appendix



Chemical structure of porfimer sodium (photofrin)